

Fingerprinting and Tracing the Signature of Basement-hosted Unconformity-type Uranium
Alteration through Thick Quaternary Tills: An Example from the Thelon Basin, Nunavut

by

Aaron Bustard

A thesis
presented to the University of Waterloo
in fulfilment of the
thesis requirement for the degree of
Master of Science
in
Earth Sciences

Waterloo, Ontario, Canada, 2016
© Aaron Bustard 2016

Author's Declaration

I hereby declare that I am the sole author of this thesis. This is a true copy of the thesis, including any required final revisions, as accepted by my examiners.

I understand that my thesis may be made electronically available to the public.

Abstract

The question of whether or not it is possible to trace the signature of alteration haloes surrounding deep-seated unconformity-type U mineralization through thick Quaternary tills is one of great importance for those conducting exploration in glaciated areas. The geochemical signals associated with alteration are often subtle and subject to numerous sources of noise, and multi-till stratigraphies can completely mask or truncate dispersal patterns. To study glacial dispersal from alteration zones surrounding unconformity-type uranium mineralization, this study focuses on a deep-seated (>100 m) basement-hosted unconformity-type U mineralized body known as Tatiggaq, which is located in the Thelon Basin of Nunavut. The Tatiggaq area presents an ideal opportunity to investigate this problem, since the area is blanketed by a thick (12-34 m) multi-till stratigraphy, mineralization does not intersect the bedrock-till interface, and the mineralization is surrounded by an extensive illitic alteration halo that reaches the bedrock surface. The recovery of till samples from diamond drill core from the multi-till stratigraphy overlying the subcropping alteration halo provides a unique opportunity to model glacial dispersal and identify whether the fingerprint of buried alteration can be traced through three dimensions to the modern day surface.

Sampling of till recovered during diamond drilling was combined with the sampling of surficial mudboils in the area surrounding Tatiggaq to trace the dispersal of alteration. The drill core samples were collected from four stratigraphic units that were deposited by early southwesterly and southerly ice flows, followed by a reversal in ice flow towards the northwest and west-northwest. Knowledge of the till stratigraphy directly above the Tatiggaq alteration zone was used to construct a three dimensional model of the sediments overlying bedrock to allow the tracing of alteration through the subsurface.

The geochemical fingerprint of the alteration halo at Tatiggaq was identified by applying univariate and multivariate statistical analysis, including principal component analysis, to geochemical data from altered and fresh rocks in the region. This analysis identified the enrichment of Fe_2O_3 , K_2O , Al_2O_3 , P_2O_5 , TiO_2 , B, Ni, U, Cr, and Sc, and depletion of CaO, MnO, Na_2O , Mo, Zn, Ba, and Sr in the altered rocks using total digestion of rock powders ($\text{HF-HClO}_4\text{-HNO}_3$). Partial digestion of the same rock powders using $\text{HNO}_3\text{-HCl}$ identified the enrichment of

U and depletion of V, Zn, Y, and Yb in the altered rocks. The observed trends in the bedrock data were then applied to the till geochemistry data to identify alteration signatures that were discernible across the till stratigraphy. These enrichment and depletion trends were used to generate four alteration indices (AI) for use in uranium exploration:

$$\begin{aligned}
 - \text{ AI1} &= \frac{K_2O + Al_2O_3}{(Na_2O + CaO) + (K_2O + Al_2O_3)} \text{ (Total Digestion)} \\
 - \text{ AI2} &= \frac{B + Ni + U}{(Zn + Sr) + (B + Ni + U)} \text{ (Total Digestion)} \\
 - \text{ AI3} &= \frac{Ni}{Zn + Ni} \text{ (Total Digestion)} \\
 - \text{ AI4} &= \frac{U}{V + U} \text{ (Partial Digestion)}
 \end{aligned}$$

A 3D model of the till sequence was constructed with GOCAD[®] and populated with interpolated values for the four alteration indices in order to trace alteration through the subsurface. Analysis of these trends revealed that alteration near the bedrock surface is pronounced, but rapidly attenuates moving up the stratigraphic sequence. Despite the rapid attenuation of the alteration signal in the subsurface, the signal is detectable at the surface down-ice from the main alteration zone with AI1 and AI2, and above the alteration zone with AI3. Although AI4 was successful at delineating alteration in the subsurface, no patterns were observed in the surficial mudboil data using AI4.

This study shows that despite a complex Quaternary stratigraphy and ice-flow history in a region, it is possible to trace glacial dispersal of subtle geochemical signatures related to subcropping alteration zones surrounding buried basement-hosted unconformity-type uranium deposits. However, the detection of such alteration signals requires a detailed knowledge of the alteration signal being sought out and an understanding of the depositional history and stratigraphy of Quaternary sediments. Continuing research into alteration systems surrounding basement hosted unconformity-type uranium deposits will help determine the applicability of the ratios developed here to other regions.

Acknowledgements

This project was funded primarily by Cameco Corporation and a Natural Science and Engineering Research Council Collaborative Research and Development grant (NSERC-CRD) to Dr. Martin Ross and Dr. Brian Kendall (UW). Funding was also provided by an Ontario Graduate Scholarship, a Society of Economic Geologists Canada Foundation Student Fellowship, and by NSERC in the form of a CGS-M grant. The Northern Scientific Training Program (NSTP) assisted with field travel expenses. Both of my supervisors, Dr. Martin Ross and Dr. Brian Kendall are thanked immensely for their patience, mentorship, and support over the course of this project. Members of the Quaternary team at Waterloo made my time enjoyable, namely Tyler, Cassia, Uly, Shawn, Jessey, Ying, Amanda, Pete, Ben, and Sam. Ryan, Dylan, and Jen made my time at Waterloo an even better experience. Tyler is especially thanked for extensive discussions about Quaternary geology and all other aspects of the project. Ying deserves special mention for her work on the Chemical Index of Alteration part of the project as part of her undergraduate thesis. Dr Shuhuan Li is thanked for her assistance with the X-ray diffraction analysis. My committee members, Dr. Lingling Wu and Dr. Shaun Frape, are thanked for their comments and involvement in the project. Cameco personnel provided a great deal of assistance with this project. Rebecca Hunter is thanked for her assistance, providing data, and her insight while in the field, and Gerard Zaluski is thanked immensely for his thought provoking reviews and comments on all aspects of the project.

Finally, I would like to thank both my parents and Heather for their support over the past three years. This wouldn't have been possible without it.

Table of Contents

Author's Declaration.....	ii
Abstract.....	iii
Acknowledgements.....	v
List of Figures.....	x
List of Tables.....	xiii
Chapter 1: Introduction.....	1
1.1. Research Problem.....	1
1.1.1. Study Location.....	2
1.2. Background Information.....	2
1.2.1. Bedrock Geology.....	2
1.2.2. Surficial Geology.....	6
1.2.3. Unconformity-type Uranium Deposits.....	10
1.2.4. Drift Prospecting.....	13
1.2.5. Mineral Exploration: Pathfinders and Data Analysis.....	16
1.3. Thesis Objectives.....	18
1.4. Methodology Overview.....	19
1.4.1. Sampling Procedures.....	19
1.4.2. Geochemical Analysis.....	19
1.4.3. Statistical Analysis.....	20
1.4.4. Data Visualization.....	20
1.5. Thesis Structure.....	20
Chapter 2: Fingerprinting the signature of subcropping alteration associated with unconformity-type uranium mineralization in glacial sediments, Part 1: Identification of the most effective pathfinders.....	21

2.1. Introduction.....	21
2.2. Geologic Setting.....	22
2.2.1. Bedrock Geology	22
2.2.2. Glacial History	24
2.3. Methods.....	25
2.3.1. Whole Rock Geochemistry	25
2.3.2. Sampling Procedures	26
2.3.3. Geochemical Analysis	28
2.3.4. Textural Analysis	29
2.3.5. Mineralogical Analysis	29
2.3.6. Principal Component Analysis	31
2.3.7. Chemical Index of Alteration.....	34
2.4. Results.....	35
2.4.1. Signature of Alteration in Bedrock.....	35
2.4.2. Geochemical Signature of Alteration in Tills	47
2.4.3. Mineralogical Signature of Alteration in Tills.....	61
2.5. Discussion	63
2.5.1. Identifying the Most Effective Pathfinders for Alteration.....	63
2.5.2. Potential Indices for Tracing Alteration	65
2.5.3. Principal Component Analysis as an Effective Tool for Exploratory Data Analysis.	72
2.5.4. Considerations for Geochemistry in Drift Prospecting.....	73
2.6. Conclusions.....	73
Chapter 3: Fingerprinting the Signature of Subcropping Alteration Associated with Unconformity-Type Uranium Mineralization in Glacial Sediments, Part 2: Dispersal Patterns through a Thick Multi-Till Succession	75
3.1. Introduction.....	75

3.2. Geologic Setting.....	77
3.2.1. Bedrock Geology	77
3.2.2. Glacial History	77
3.3. Methods.....	77
3.3.1. Alteration Indices.....	77
3.3.2. Three-Dimensional Modeling.....	78
3.4. Results and Interpretation	80
3.4.1. Three-Dimensional Stratigraphic Model	80
3.4.2. Three-Dimensional Dispersal Patterns of the Alteration Indices	82
3.4.3. Surficial Dispersal Patterns.....	89
3.5. Synthesis	98
3.5.1. Main Characteristics of Dispersal.....	98
3.5.2. Reconstruction of Dispersal.....	99
3.6. Conclusions.....	102
Chapter 4: Conclusions	103
4.1. Identifying and Tracing the Fingerprint of Unconformity-type Uranium Alteration in Tills	103
4.2. Thesis Contributions	103
4.3. Implications for Mineral Exploration	105
4.3.1. The Fingerprint of Unconformity-type Uranium Alteration Haloes.....	105
4.3.2. Drift Prospecting in Areas of Thick Till.....	105
References.....	106
Appendix A: Till drill core geochemistry.....	112
Appendix B: Surficial geochemistry.....	148
Appendix C: Whole rock PCA Results.....	192

Appendix D: Till drill core PCA Results	201
Appendix E: Clay mineralogy.....	210
Appendix F: Till drill core alteration index values.....	212
Appendix G: Surficial sample alteration index values	214

List of Figures

Figure 1-1: Geology of the Aberdeen Lake area.	3
Figure 1-2: Summary of the main ice flows recorded in the Tatiggaq area	10
Figure 2-1: A) Study location in Nunavut. B) Regional location of the study area, which occurs between Aberdeen Lake and Judge Sissons Lake, to the west of the Kiggavik-Sissons deposits. C) Map showing the locations of surficial mudboil samples (purple dots) in the vicinity of Gerhard Lake. D) Locations of diamond drill holes that were continuously cored and sampled at selected intervals (pink dots), and nearby locations of surficial samples.	23
Figure 2-2: Geological cross section of the Tatiggaq study area.....	24
Figure 2-3: Stratigraphy of the Tatiggaq area.....	25
Figure 2-4: Flow chart depicting the division of samples and analytical techniques used.....	28
Figure 2-5: Enrichment/depletion plot of the whole rock major oxide geochemistry.....	36
Figure 2-6: Enrichment/depletion plot of the whole rock trace element geochemistry.....	37
Figure 2-7: Enrichment/depletion plot of the whole rock trace element geochemistry.....	38
Figure 2-8: Principal component analysis of the major oxide data for the whole rocks	41
Figure 2-9: Principal component analysis of transition metal data for the whole rocks.....	42
Figure 2-10: Principal component analysis of transition metal data for the whole rocks.....	43
Figure 2-11: Principal component analysis of data (total digestion method) from elements expected to be good indicators of alteration for the whole rocks	44
Figure 2-12: Principal component analysis of data (partial digestion method) from elements expected to be good indicators of alteration for the whole rocks	45
Figure 2-13: CIA values for the whole rock data.	46
Figure 2-14: Histograms showing the distribution of the major oxides in tills associated with alteration zones.	49
Figure 2-15: Histogram showing the distribution of trace elements in tills (based on total digestion analyses)	50
Figure 2-16: Histogram showing the distribution of trace elements in tills (based on partial digestion analyses).....	51
Figure 2-17: Histograms for the clay % of the <63 µm fraction for the Tatiggaq drill core samples.....	51

Figure 2-18: Principal component analysis of the major oxide data for the till drill cores	55
Figure 2-19: Principal component analysis of transition metal concentrations determined by total digestion of the till drillcores.	56
Figure 2-20: Principal component analysis of transition metal concentrations determined by partial digestion of the till drillcores.....	57
Figure 2-21: Principal component analysis of the concentrations of elements (total digestion method) expected to be good indicators of alteration	58
Figure 2-22: Principal component analysis of the concentrations of elements (partial digestion method) expected to be good indicators of alteration.....	59
Figure 2-23: Ternary diagrams showing the CIA values for the various till lithologies sampled from the Tatiggaq drill holes.....	60
Figure 2-24: Results of X-Ray Diffraction (XRD) analysis of the clay fraction for both surface and drill core samples in the Tatiggaq study area.....	62
Figure 2-25: Dotplots for the various alteration indices for each rock type	68
Figure 2-26: Histograms showing the range in values of the different alteration indices for the four different till lithofacies from drill cores.	69
Figure 2-27: Histograms showing the range in values of the different alteration indices for the surficial till samples.	70
Figure 2-28: Figure comparing the alteration indices for all till samples collected in the Tatiggaq area	71
Figure 3-1: A) Study location in Nunavut. B) Regional location of the study area located between Aberdeen Lake and Judge Sissons Lake, to the west of the Kiggavik-Sissons deposits. C) Map showing the locations of surficial mudboil samples (purple dots). The red box indicates the location of surficial geochemistry maps presented in figures 3-7 through 3-12. D) Locations of diamond drill holes that were continuously cored and sampled at selected intervals	76
Figure 3-2: SGrids generated for the till units in the Tatiggaq study area (Dmm1, Dmm2, Dmm3, and Dmm4).	81
Figure 3-3: 3D model of the dispersal of Alteration Index 1.....	85
Figure 3-4: 3D model of the dispersal of Alteration Index 2 (using total digestion values) through the different till units.....	86
Figure 3-5: 3D model of the dispersal of Alteration Index 3 (using total digestion values)	87

Figure 3-6: 3D model of the dispersal of Alteration Index 4 (using partial digestion values)	88
Figure 3-7: Surficial dispersal of AI1.....	92
Figure 3-8: Surficial dispersal of AI2	93
Figure 3-9: Surficial dispersal of AI3l.....	94
Figure 3-10: Surficial dispersal of AI4	95
Figure 3-11: Surficial dispersal of Ni/Zn ratios determined by total digestion	96
Figure 3-12: Surficial dispersal of boron values in the study are.	97
Figure 3-13: Reconstruction of the dispersal history in the Tatiggaq area	101

List of Tables

Table 2-1: Number of whole rock samples for each rock type.....	26
Table 2-2: Minimums, maximums, and means of CIA data by rock type for the altered and fresh samples.....	47
Table 2-3: Summary table of the main features displayed in PCA for total digestion of till samples.....	54
Table 2-4: Summary table of the main features displayed in PCA for partial digestion of till samples.....	54
Table 2-5: Minimum, maximum, and mean CIA values for the different till lithofacies in the Tatiggaq drill core samples.....	61
Table 2-6: Summary statistics for the alteration indices of till samples.	72
Table 3-1: Formulas for the four alteration indices developed in chapter 2.....	78

Chapter 1: Introduction

1.1. Research Problem

Exploration for mineral deposits is becoming increasingly difficult. The large, near-surface deposits have largely been discovered in many districts and economical deposits in historical mining camps are being depleted (e.g. Doggett, 2013). One such example is unconformity-type uranium deposits. The Athabasca Basin of Saskatchewan is currently the sole Canadian producer of uranium from unconformity-type deposits (Kyser and Cuney, 2008), and at some point in the future the large highly profitable uranium deposits within the Athabasca Basin will be mined out. Looking toward other prospective areas and developing advanced mineral exploration techniques will help discover the next generation of large, high grade deposits when those in the Athabasca Basin are depleted.

The Thelon Basin, which straddles the border between Nunavut and the Northwest Territories, has great potential for the discovery of new unconformity-type uranium deposits. Exploration for uranium has been underway in and around the Thelon Basin since the 1970's (Hoeve and Sibbald, 1978; Fuchs et al., 1986; Fuchs and Hilger, 1989; Hasegawa et al., 1990; Jefferson et al, 2007; Kyser and Cuney, 2008). Exploration efforts in the Thelon Basin have been minor compared with other uranium-bearing basins, such as the Athabasca Basin of Saskatchewan and the McArthur Basin of northern Australia, chiefly due to the difficulty of exploration in the Thelon Basin but also because of higher uranium grades in the Athabasca Basin. Access to the Thelon Basin is difficult due to the remoteness of the area and the lack of roads. The eastern part of the basin, host to the majority of the known near-surface uranium deposits (e.g., Kiggavik), is characterized by permafrost terrain and many small lakes. Furthermore, most of the basin is covered by thick Quaternary sediments, including till, which can hinder the use of traditional mineral exploration techniques. For instance, gravity surveys will yield similar signatures for areas containing either thick tills or alteration zones because both geological materials have similar densities (Jefferson et al., 2007). Traditional geochemical surveys are complicated by the Quaternary stratigraphy (e.g., Hodder, 2014) and long permafrost history in the area. In addition, mineralization may not subcrop, and together with sediment cover and permafrost can leave a very subtle footprint of the underlying alteration and mineralization at the surface. Developing

exploration methods tailored for deeply-buried unconformity-type uranium deposits (like those in the Thelon Basin) that are specifically aimed at tackling the problems presented by thick glacial sediment cover will increase the likelihood of making new discoveries or at least optimize exploration strategies, such as prioritizing geophysical anomalies for drilling.

1.1.1. Study Location

The study area is located in central mainland Nunavut to the southeast of Aberdeen Lake in the Aberdeen Lake map area (NTS 66B, Figure 1-1). The study area is focused on mineral exploration targets held by Cameco on their Aberdeen and Turqavik projects (Hunter et al., 2011a and 2011b). The area under investigation is known as the Tatiggaq area, and is host to deep-seated uranium mineralization at a depth of approximately 100 m, and has a subcropping alteration halo (Hunter et al., 2011a). The Tatiggaq area is well delineated by diamond drilling, and is accessible by helicopter from a Cameco exploration camp located on the shore of Aberdeen Lake.

1.2. Background Information

1.2.1. Bedrock Geology

The bedrock geology of the area was first mapped by Patterson and LeCheminant (1985) at a 1:1,000,000 scale, and this work was later incorporated into a compilation by Paul et al. (2002). The area has been mapped at the property scale in more detail by Cameco as part of mineral exploration on the property (R. Hunter, pers. comm.; Hunter et al., 2011a, 2011b). The bedrock primarily consists of Archean basement gneisses that are overlain or intruded by Paleoproterozoic Trans-Hudsonian igneous rocks. To the north, the Archean gneisses are overlain by Paleoproterozoic quartz arenites of the Thelon Basin. The geology of the area, based on the compilation map produced by Paul et al. (2002), is shown in Figure 1-1.

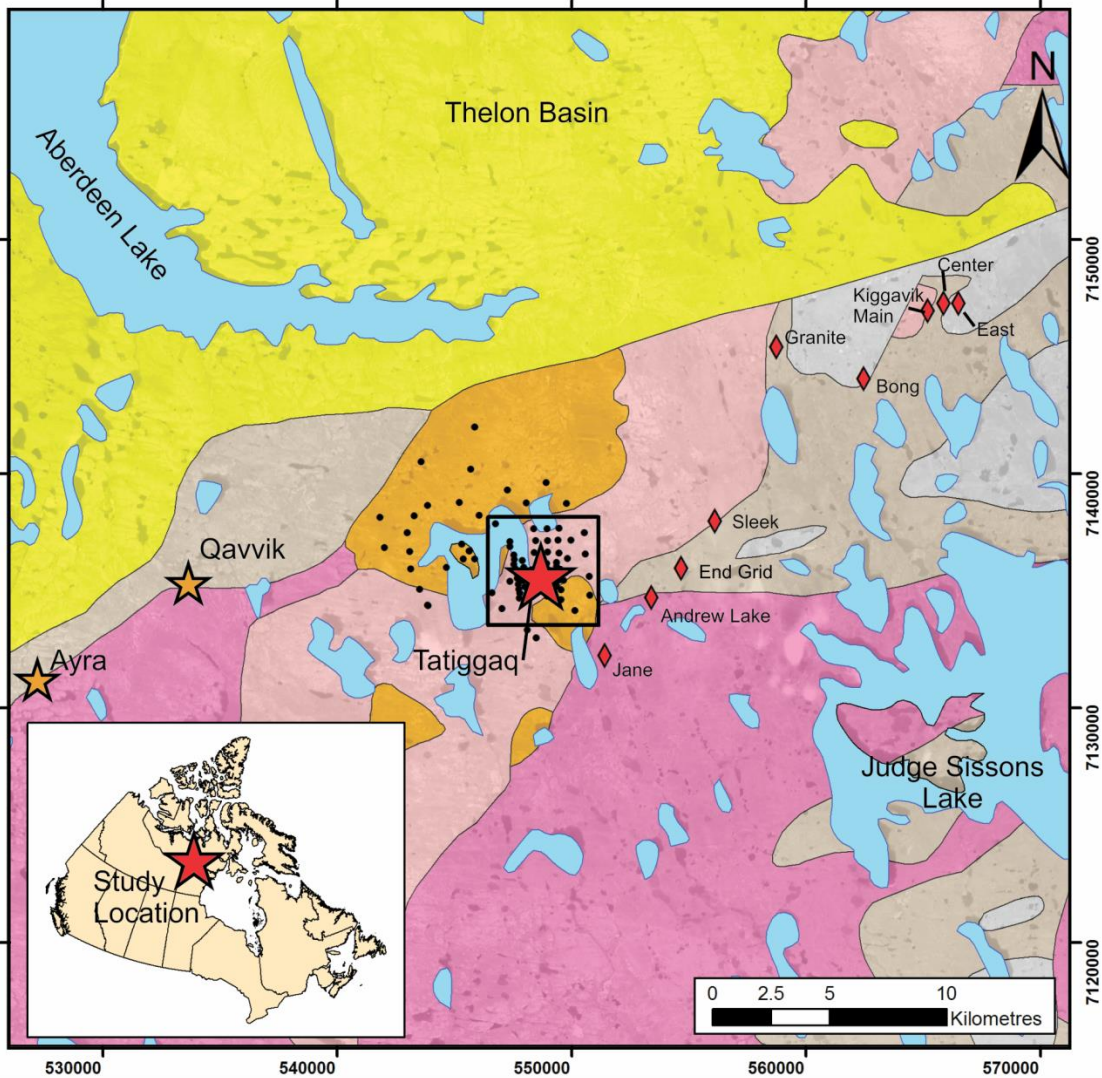


Figure 1-1: Geology of the Aberdeen Lake area showing the location of uranium occurrences (red diamonds) and the Tatiggaq study area for the present project (red star), as well as other local exploration targets (orange stars) discussed in the text. Surficial mudboil samples are the small black dots. Geology and hydrography from Paul et al. (2002) is overlain on SPOT 4/5 panchromatic imagery. The locations of the Kiggavik/Sissons deposits are from the NUMIN database (nunavutgeoscience.ca). See text for details of the geology.

The area to the southeast of Aberdeen Lake is characterized by five different rock types: 1- Thelon Formation sandstones and conglomerates; 2- volcanic rocks of the Wharton Group; 3- Hudson Suite intrusive igneous rocks; 4- meta-pelites and semi-pelites of the Woodburn Lake Group; and 5- a basement Mesoarchean granodiorite gneiss (Hunter et al., 2010a, 2010b). The lithologies are described as follows:

- Thelon Formation: The Thelon Formation is divided into four lithofacies by previous workers (Kyser et al., 2000; Rainbird et al., 2003; Hiatt et al., 2003, Hunter et al., 2010a, 2010b).
 - *Lithofacies 1* is divided into lithofacies 1a and 1b. Lithofacies 1a consists of trough cross-bedded, matrix-supported conglomerates and sublithic arenites interstratified with poorly to moderately sorted, medium- to coarse-grained sandstone. The depositional environment of lithofacies 1a is interpreted to be an alluvial fan. Lithofacies 1b is less common than 1a, and consists primarily of very fine sandstone to siltstone with clay. The flat-lying beds are 1-3 cm thick and commonly contain hematite alteration. Lithofacies 1b is interpreted as an overbank deposit.
 - *Lithofacies 2* is the main unit in the region surrounding the study area. It comprises a unit of feldspathic arenite with minor lithic clasts. It is massive to thickly-bedded and displays normal grading. Locally, clay and siltstone occur at the top of bedded sequences.
 - *Lithofacies 3* is known informally as “the platy sandstone unit”, and consists of a bedded, dark red to purple, medium- to coarse-grained, well-sorted quartz arenite. The unit contains 2-5% feldspar that is altered to clay in many cases. The unit also contains 1% interstitial clay, and displays asymmetric to symmetric ripples.
 - *Lithofacies 4* occurs locally throughout the region surrounding the study area, and consists of well-sorted medium- to coarse-grained quartz arenite. The unit also shows trough cross beds that are generally thin. The arenite locally contains quartz pebbles and cobbles.
- Wharton Group: Rocks belonging to the Wharton Group consist primarily of the Pitz Formation, which comprises porphyritic rhyolite to rhyodacite. The Pitz Formation

- contains 1-2 mm quartz phenocrysts and 1-8 mm sanidine phenocrysts (Hunter et al., 2010a, 2010b). The nearest occurrence of the Pitz formation is 55 km to the south and it is used to assist in determining the provenance of some till units (Hodder et al., 2016).
- Hudson Suite: The Hudson Suite consists of various intrusive phases that exhibit orange to pink weathering and range from fine-grained to pegmatitic in crystal size. Compositionally, rocks belonging to the Hudson Suite include lamprophyre dikes, mafic syenites, felsic quartz syenites, and subordinate monzogranites and granites. The compositional variations in the suite are related to magmatic evolution during emplacement (Hunter et al., 2010a, 2010b).
 - Lamprophyre dykes: The lamprophyre dykes are fine-grained and cross-cut the granites.
 - Hornblende syenite: The hornblende syenites are fine- to medium-grained and contain 5-25% hornblende. The most abundant mineral in the hornblende syenite is alkali feldspar.
 - Quartz syenite: The quartz syenites of the Hudson Suite are massive, fine- to medium-grained, and are composed primarily of microcline and orthoclase feldspar.
 - Woodburn Lake Group: Rocks of the Woodburn Lake Group are divided into pelitic, semi-pelitic, and metavolcanic gneisses (Zaleski et al., 2000). All three members in the area are characterized by fine-grained textures with local cm-scale melt segregations. The pelitic and semi-pelitic members locally contain disseminated pyrite and graphite, and the semi-pelitic member contains molybdenite. The semi-pelitic member is associated with iron formation. Semi-pelitic to arkosic gneisses in the area can contain 2-15% quartz veining (Hunter et al., 2010a, 2010b).
 - Mesoarchean granodiorite gneiss: The Mesoarchean granodiorite gneiss in the area is commonly medium- to coarse-grained, and ranges from granite to granodiorite in composition. The unit shows strong gneissic banding and is heavily deformed. Locally, the granodiorite gneiss contains thick pegmatitic units, and is commonly cut by cm-scale quartz veins and pegmatite dykes (Hunter et al., 2010a, 2010b).

1.2.2. Surficial Geology

The surficial geology of the study area was first investigated by Tyrrell (1897), and was followed by investigations by Aylsworth (1990) and remote sensing mapping by DeAngelis (2007). Most recently, Hodder (2014) provided the first detailed stratigraphy and ice flow history of the study area. Other studies of the Quaternary geology to the east of the study area were conducted by McMartin and Henderson (2004), McMartin et al. (2006), Robinson et al. (2014), and Robinson (2015).

Hodder (2014) investigated the ice flow history and Quaternary stratigraphy of the Aberdeen Lake area and developed a stratigraphic classification for the Tatiggaq study area. The study of Hodder (2014) is part of the same larger project as this work, and the samples collected by Hodder (2014) are the same for the present investigation. The detailed work conducted by Hodder (2014) in the Tatiggaq area led to the identification of four till units, which were discriminated predominantly by pebble lithological classification conducted on the 2-4 mm and 4-8 mm size fractions in addition to B:Rb geochemical ratios. The four units at Tatiggaq are named Dmm1, Dmm2, Dmm3, and Dmm4. Dmm1 is the oldest unit and thus occurs at the base of the stratigraphic column. By combining measured ice flow indicators, till fabric measurements, pebble lithology, and stratigraphy, Hodder (2014) developed a paleo-glaciological interpretation of the ice flow history in the region. In the Tatiggaq area, there was an early flow of unknown age responsible for the deposition of Dmm1, which he tentatively correlated to the oldest ice flow phase towards 255° based on the erosional record. Overlying Dmm1 is a thin (10 cm) and discontinuous, laminated, silty-clay bed of uncertain origin. This thin bed is in turn overlain by another diamicton (Dmm2), which was deposited by a southerly ice flow (180°) phase. This ice flow was followed by a sustained phase of till production (Dmm3) associated with ice flow towards the north-northwest (340°). The till stratigraphy suggests a reconfiguration of the Keewatin ice divide involving a north-south migration followed by counter-clockwise rotation. During deglaciation, a shift in the ice flow direction towards 270-300° resulted in the deposition of Dmm4 (Hodder, 2014).

Dmm1 occurs at the bottom of several diamond drill holes in the Tatiggaq area, and is described as a clast-rich massive till in which the clasts are predominantly locally derived with some Pitz Formation clasts. Dmm1 has a light red colour, which Hodder (2014) interprets as the result of

locally hematitized bedrock in the area. Dmm1 is overlain in several drill holes by thin (~10 cm thick) laminated clayey-silt sediments. The provenance of Dmm1 is uncertain due to the lack of diagnostic pebble clast lithology, but is thought to be the result of early ice flow events towards 255°.

Dmm2 overlies Dmm1 and the two units are locally separated by thin laminated sediments. Dmm2 is characterized by high contents of Thelon Formation clasts and a lack of Pitz Formation clasts, indicating that Dmm2 was likely derived from southerly ice-flows. Dmm2 is correlated with the second ice flow phase from the erosional record. Dmm2 is discontinuous across the Tatiggaq area and appears to be limited to bedrock lows. Visual discrimination of Dmm2 and younger Dmm3 is difficult and is thus better accomplished through pebble lithology or geochemically through the use of B:Rb ratios. Dmm2 has anomalously high B and low Rb contents due to its high abundance of Thelon Formation clasts (>60% sedimentary granules 2-4 mm; Hodder, 2014) compared with the other tills. The presence of anomalously high B contents in Dmm2 presents an important challenge for drift exploration at Tatiggaq because high B contents are also found in altered rocks associated with unconformity-type uranium deposits in the area. The maximum thickness of Dmm2 is inferred to be 6 m (Hodder, 2014).

Dmm3 is the prevalent till unit in the Tatiggaq area, and has a maximum thickness of 12 m. The pebble lithological makeup of Dmm3 is a mix of Thelon Formation, Pitz Formation, and basement clasts. Dmm3 was likely deposited as a result of northerly ice flows since the provenance of the material comprising the unit is from the south (Hodder, 2014).

Dmm4 is the youngest till unit deposited in the area and was only recovered in two drill holes because the first 5 m of drill core was rarely recovered. However, most surficial till samples collected are from Dmm4. The unit has a slightly paler colour than Dmm3 and was likely produced by northwest to westerly ice flow phases between 300° and 270°. The source of most pebbles in Dmm4 is the basement based on analysis of drill cores and surface samples.

The Quaternary geology of the Schultz Lake map area, located immediately to the east of the present study area, was described by McMartin et al. (2006). The study of McMartin et al. (2006) consisted of surficial mapping at a 1:100,000 scale with integrated ground observations, till sampling, paleo ice-flow indicator mapping, and regional till sampling. The Quaternary geology

of the Schultz Lake map area is similar to that of the Aberdeen Lake area. The Shultz Lake area was located under the Keewatin Ice Divide of the Laurentide Ice Sheet during the last glaciation (Aylsworth and Shilts, 1989; McMartin et al., 2006), and is characterized by near-continuous drift with a thickness greater than 5 m as well as rolling till plains over much of the map sheet. To the north of the Thelon River, the till is thinner and commonly less than 2 m thick. Glacio-fluvial sediments are not common in the Shultz Lake area (McMartin et al., 2006).

McMartin et al. (2006) identified four main ice flow sets with slight directional variations within each set. The earliest flows were west-southwest (striae at 227° -260°), with some measurements indicating south-southwesterly flows (striae at 188° -201°). The second flow set occurs in the centre of the Schultz Lake map area and consists of well-preserved southeasterly flows (159° - 178°), whereas in the southern part of the map area, there are striae measurements between 122° and 152°. The third flow was to the north-northwest (striae at 336° -348°) and occurred after a major ice flow reversal. The northwesterly flows are a regional phenomenon and are observed as far as 100 km south of the study area (McMartin et al., 2006). The northwesterly flows shifted counter clockwise (striae at 318° -334°) to become west-northwest flows (striae at 284° -315°). The fourth and final ice flow event is towards the west (striae at 268° -283°), and its record extends across the Aberdeen Lake area (Fig. 1-2) and continues further to the west (McMartin et al., 2006). The westerly flow indicators are truncated in the north by the onset region of the Dubawnt Ice Stream (McMartin et al., 2006). Most ice flow phases observed in both the Tatiggaq and Shultz Lake areas are interpreted to have occurred during the Late Wisconsinan, although the earliest southwesterly and southerly flows could have occurred during an earlier glaciation. The migration of flow patterns in the Shultz Lake area was interpreted by McMartin et al. (2006) to reflect rotation of the Keewatin Ice Divide from an east-west orientation to a northeast-southwest orientation, with a migration of 250 km to the south.

The landscape of the Shultz Lake area was heavily influenced by the last deglaciation of the area. During the retreat of the Laurentide Ice Sheet, the drainage of the Thelon River was blocked by ice, leading to flooding of the Thelon River Valley and the Princess Mary Lake Basin. The ice dam broke at approximately 6-7 ka BP (¹⁴C), giving a minimum deglaciation age for the area of 6 ka BP (McMartin et al., 2006). Following the breaching of the ice dam, marine waters flowed into the area, and marine reworking is observed below the marine limit in the Shultz Lake area

(McMartin et al., 2006) and in the Aberdeen Lake area (Hodder, 2014). The marine limit in the Schultz Lake area is marked by the preservation of shorelines at a present-day elevation between 180 m and 220 m (McMartin et al., 2006).

Regional-scale till sampling done by McMartin et al. (2006) allowed for the study of glacial dispersal in the area using both pebble lithologies and till geochemistry. The lithological and geochemical samples indicated that there is significant dispersal towards the northwest in the Schultz Lake study area. The northwesterly dispersal is dominant because the northwesterly flow in the area was long-standing and possibly fast (Hodder et al., 2016). In areas of thin drift, there is a strong correlation between the composition of the till and the underlying bedrock, and in areas of thicker till, the relationship is more complicated because of the presence of multiple till units. An interesting finding of McMartin et al. (2006) is that there is no conclusive evidence of westward dispersal in the clast lithology data, even though westward transport is evident in the landform record and from striae measurements.

Although McMartin et al. (2006) did not directly study the Aberdeen Lake area, the results of that study have implications for dispersal in the vicinity of Aberdeen Lake because of similarities in the glacial histories and the proximity of the two study areas. The primary implication, which was noted by McMartin et al. (2006), is that drift prospecting in areas of thick till will be difficult given the complex subsurface configurations of multiple till units. The identification of strong northwesterly dispersal patterns in the Schultz Lake area implies that similar dispersal patterns may be observed in the vicinity of Aberdeen Lake. The finding that strong westerly dispersal is not observed in the pebble lithological data may have implications on the shape of dispersal patterns.

The ice flow record developed by McMartin et al. (2006) was largely confirmed by the study of Robinson et al. (2014), which collected additional measurements in the vicinity of the Kiggavik uranium deposits. Robinson et al. (2014) summarized the ice flows in the area from oldest to youngest as follows: 1) flows towards 110-145°, 2) flows towards 325-345°, 3) flows towards 310-320°, and 4) flows towards 260-275°. A summary of the main ice flow directions recorded in the area is presented in Figure 1-2.













	Hodder et al., 2016	Robinson, 2015	McMartin et al., 2006
Youngest	 300°-270°	 270°	 268°-283°
	 340°	 320°	 336°-348°
	 180°	 340°	 159°-178°
Oldest	 255°	 110°	 227°-260°

Figure 1-2: Summary of the main ice flows recorded in the Tatiggaq area by Hodder et al. (2016), the Kiggavik area by Robinson (2015), and the Schultz Lake area by McMartin et al. (2006). Only the major ice flow events are presented in each case and minor transitory events are omitted.

1.2.3. Unconformity-type Uranium Deposits

Unconformity-type uranium deposits contain the highest grades of any known type of uranium deposit, and contain a significant portion of global uranium reserves. Sandstone-hosted roll front uranium deposits contain average grades of 0.04% to 0.1% U, whereas unconformity-type uranium deposits in the Athabasca Basin contain average grades of 2% U (Jefferson et al., 2007). Their exceptionally high grades make unconformity-type deposits desirable targets for exploration. Although the bulk tonnage of unconformity-type deposits is not as great as IOGC/Breccia-type deposits such as Olympic Dam in Australia, the high grades of unconformity-type deposits compensates for their smaller size. It is also important to note that Olympic Dam is not a primary uranium producer and uranium is recovered as a by-product (Kyser, 2014). Due to its numerous high grade deposits and operating mines, the Athabasca Basin has been subject to the most study (Kyser, 2014), and the following discussion focuses mainly on characteristics of the Athabasca Basin. Canadian Paleoproterozoic basins of interest for unconformity-type uranium include the Thelon, Elu, Hornby Bay, and Otish Basins (Kyser and Cuney, 2008). The Thelon Basin is host to several known deposits such as those found along the Kiggavik trend. Exploration and research in the Thelon Basin has increased over the past decade and has focused primarily on the eastern parts of the basin near Kiggavik (Kyser and Cuney, 2008; Uvarova et al., 2012), which is in close proximity to the Tatiggaq area. Although the predominant models for unconformity-type uranium deposits have been based on the Athabasca Basin, several characteristics can be extended to the Thelon Basin by analogy.

Unconformity-type uranium deposits are found at, above, or below unconformities separating Paleoproterozoic sedimentary basins from underlying metamorphosed basement rocks. The sedimentary basins associated with unconformity-type uranium are characterized by braided channel deposits composed primarily of sandstones and conglomerates (Kyser and Cuney, 2008). These highly permeable basins allowed for the widespread circulation of oxidizing diagenetic brines driven by large-scale tectonic adjustment. The oxidizing brines scavenged uranium because at low to moderate temperatures, the solubility of oxidized uranyl ions (U^{6+}) is much greater than reduced uranous (U^{4+}) ions and complexes (Kyser and Cuney, 2008). The uranium is deposited to form ore bodies when the oxidizing fluids come into contact with reducing conditions (Jefferson et al., 2007).

Unconformity-type deposits are structurally controlled by faults and other structures that focus fluid circulation. Deposits show different characteristics depending on their position relative to the unconformity (Jefferson et al., 2007; Kyser and Cuney, 2008). Deposits that are hosted at the unconformity tend to be polymetallic with elevated concentrations of Ni, Co, and As in addition to uranium, whereas basement-hosted deposits are more commonly monometallic and contain only uranium (Ruzicka, 1996). The main differences between basement-hosted and unconformity-contact hosted mineralization are the nature of the host rock and the fluid:rock ratio (Alexandre et al., 2005). The unconformity-type deposits found in the Thelon Basin tend to be monometallic (Fuchs et al, 1986; Fuchs and Hilger, 1989). Some unconformity-contact hosted deposits, such as the Boomerang prospect in the Western Thelon Basin, have elevated concentrations of Au (Kyser and Cuney, 2008). Sandstone-hosted deposits show predominantly illite and kaolinite alteration at both proximal and distal positions relative to the ore body, whereas basement-hosted deposits show distal illite alteration and proximal chlorite alteration (Figure 1-3).

Alteration styles for unconformity-type deposits occurring in the Athabasca Basin can be divided into two conceptual end-members: egress style and ingress style (Jefferson et al., 2007). Egress alteration haloes are the largest, and can extend for kilometers along strike and be 400 m wide at the unconformity. Egress alteration haloes can be further subdivided into two groups depending on the mineralogy involved. The first type of egress alteration is characterized by quartz dissolution with the formation of illite, whereas the second type includes silicification with later

illite and kaolinite formation and minor amounts of chlorite and dravite (Jefferson et al., 2007). Egress alteration envelops the structure hosting the mineralization, and the alteration halo is generally plume-shaped. Ingress alteration is associated with basement-hosted monometallic deposits, and the alteration is narrower due to the lower permeability of basement rocks relative to basinal rocks. Ingress alteration generally consists of an inner illite zone surrounded by an outer zone of Fe-Mg chlorite. Both inner and outer zones of ingress alteration systems may or may not contain sudoite. The egress and ingress alteration styles represent theoretical end-members of alteration, and characteristics of both styles are observed at many deposits (Jefferson et al., 2007). Ingress style is of primary interest in this study because the mineralization at Tatiggaq is basement-hosted, and the overlying Thelon Formation basinal rocks have been completely eroded (Hunter et al., 2010a, 2010b). Alteration within the Thelon Basin is also significantly simpler in mineralogy when compared to the deposits of the Athabasca Basin, since alteration surrounding deposits in the Thelon Basin is predominantly the illitization and sericitization of feldspar, with subordinate hematization and chloritization (Fuchs et al., 1986; Fuchs and Hilger, 1989; Hasegawa et al., 1990).

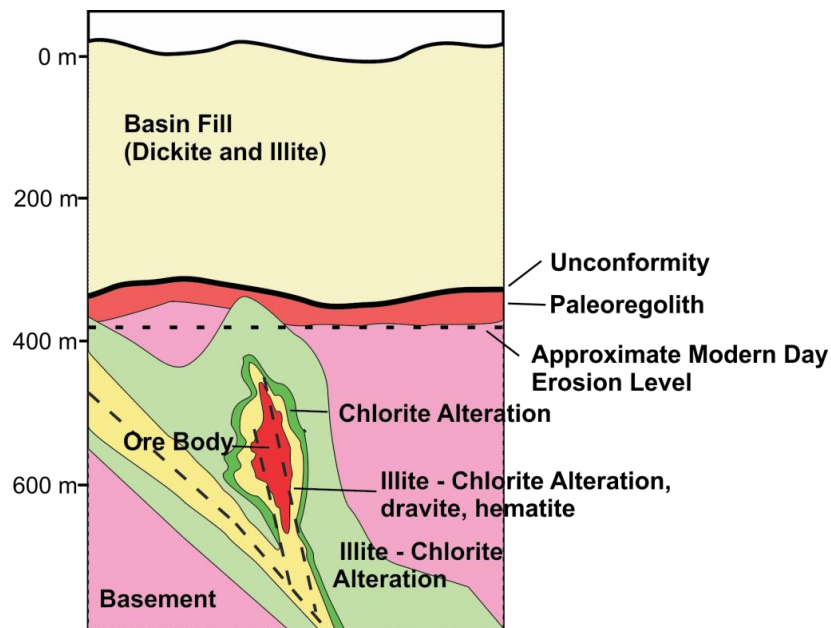


Figure 1-3: Sketch of the alteration surrounding basement-hosted unconformity-type uranium deposits typical of the Athabasca Basin. Alteration is general to unconformity-type deposits and the scale is approximate. Dotted line shows the level of erosion required to expose the alteration halo to glacial erosion similar to what is observed in the Aberdeen Lake area where the Thelon Formation basin fill has been entirely eroded. Alteration haloes in the Thelon Basin are of different character compared to those in the Athabasca Basin, and consist predominantly of illite with minor chlorite and hematite. Modified from Kyser (2014).

1.2.4. Drift Prospecting

The use of glacial sediment geochemistry is widely recognized as a valuable mineral exploration tool (e.g., Levson and Giles, 1995; Klassen, 1999, 2001). The most common glacial sediment to sample for mineral exploration is subglacial till, which is the material transported near or at the base of a glacier and is derived from material that the glacier is overriding. With knowledge of the ice flow history of an area, the origin of the till can be traced back to its bedrock source (McMartin and Paulen, 2009). Through eroding and incorporating material from mineralization or alteration zones, geochemical characteristics of the bedrock source are incorporated into the till. However, the signal of a source (alteration or mineralization) in till decays with distance from the source as more material is entrained by the glacier (Klassen, 2001). Dispersal patterns observed in surficial till are commonly referred to as a “dispersal train”. These dispersal patterns can be kilometres long and hundreds of metres wide (Levson and Giles, 1995).

Drift prospecting is the process of tracing mineralogical, lithological, or geochemical indicators back to their bedrock source (Klassen, 2001). Since till is a product of the mechanical erosion of bedrock (Klassen, 2001), the erosion of previous till units, or the deformation of previous till units (Stea and Finck, 2001), indicators dispersed in till can be traced back to their source by using knowledge of the ice flow history of an area (Klassen, 2001; Stea and Finck, 2001; McMartin and Paulen, 2009). Material can be entrained by deformation at the base of the glacier or by incorporation into the ice (Hooke et al., 2010). At the interface between the glacier and the substrate, material is comminuted to smaller grain sizes. By contrast, material incorporated into the ice undergoes little grain size modification (Stea and Finck, 2001).

The concentration of an indicator element or mineral in till is expected to be highest close to the interface between the till and the bedrock source. The area of high concentration at the source is known as the “head”, and concentrations decrease down-ice towards the “tail” of the dispersal train. In relatively thick till, the subsurface part of a dispersal ‘train’ conceptually takes the shape of a dispersal ‘plume’ rising through the till to the surface (Miller, 1984) (Figure 1-4). This conceptual model is based on the assumption of one ice flow event and a single till sheet. The concentration of material down-ice from the last occurrence of the bedrock source will decrease in different ways depending on a number of factors. Classic dispersal curves fit exponential decay or linear decrease functions relatively well (e.g., Klassen, 1997), although other dispersal

curves may exist due to sediment re-entrainment and other complicating factors (Parent et al., 1996).

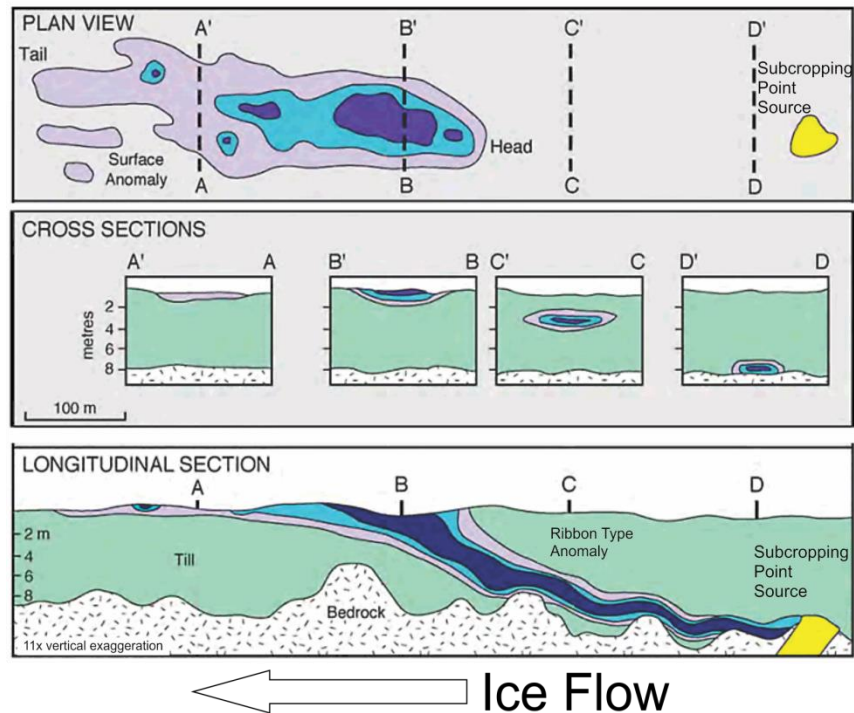


Figure 1-4: Conceptual model of glacial dispersal in till from a point source due to one ice flow event. Modified from McClenaghan (2007) after Miller (1984).

In the simplest case of one ice flow event, the surface of a dispersal train will have a linear or ribbon shape parallel to the dominant ice flow direction (Miller, 1984; Parent et al., 1996). If an area has experienced more than one significant ice flow event, re-entrainment of material from the first event by the second event will result in a fan-shaped composite dispersal pattern (Parent et al., 1996), with the angle between the outer bounds of the fan being controlled by the ice flow directions. When tracing back from an inferred tail, this area is called the “provenance envelope” (Finck and Stea, 1995; Stea and Finck, 2001; Plouffe et al., 2011). Fan-shaped dispersal trains typically have a main branch resulting from the latest ice flow event, and a palimpsest portion that is the result of re-entrainment of the pre-existing dispersal by the older ice flow event(s) (Parent et al., 1996). Amoeboid dispersal trains commonly occur in core regions of the Laurentide Ice Sheet due to the migration of warm-based ice divides or ice saddles that led to ice flow reversals (Parent et al., 1996; Stea and Finck, 2001; Trommelen et al., 2013). Amoeboid dispersal trains are irregular in shape and will display limited dispersal in multiple directions

related to ice flow history (Parent et al., 1996). A generalized illustration of the different types of dispersal patterns observed at surface is presented in Figure 1-5 below.

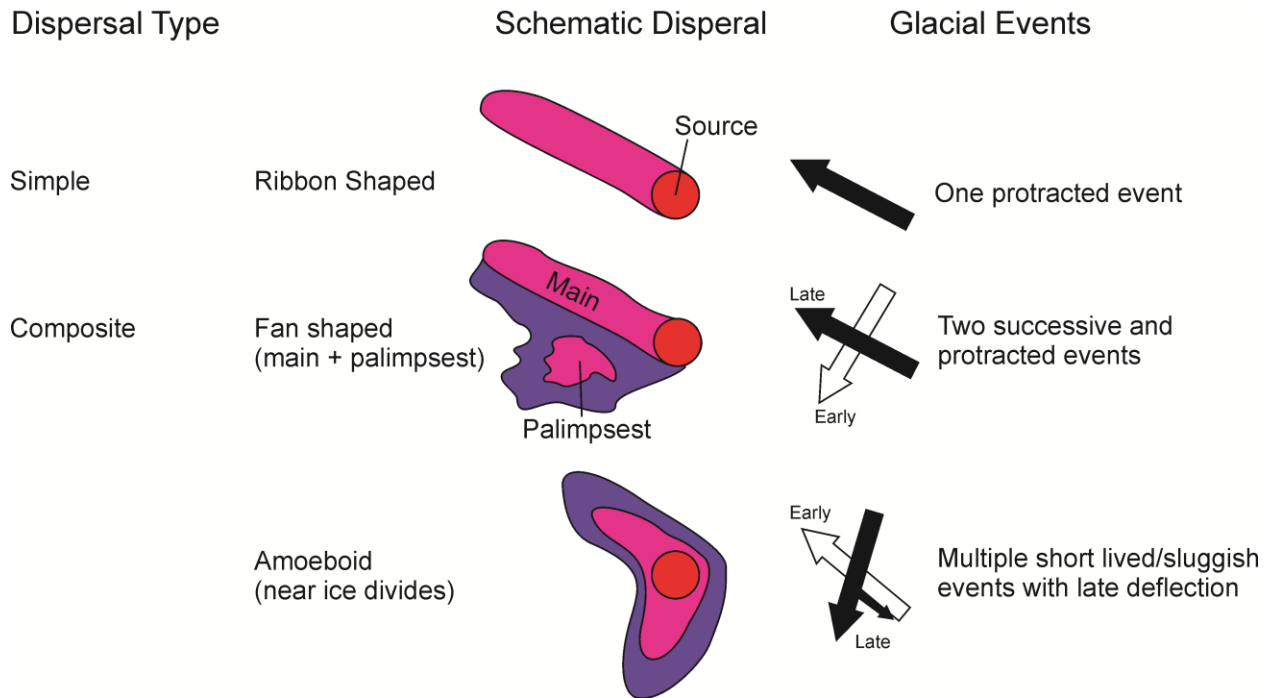


Figure 1-5: Plan view of ribbon-shaped, fan-shaped, and amoeboid dispersal patterns that can form as a result of different ice flow histories. Modified from Parent et al. (1996).

Recognizing geochemical dispersal in areas of thick drift can be challenging. In many cases, the patterns exhibited by dispersal trains are not ideal (Parent et al., 1996; Stea and Finck, 2001; Klassen, 2001). The tail of a dispersal train can be eroded and capped by distal material that has no relation to the dispersal train, and will therefore not be observed at the surface (Hooke et al., 2010). Deposition of indicators may also periodically stop over an area due to changing subglacial conditions or because the source is no longer available for erosion, thus resulting in a “skip zone” where an indicator is not observed (Stea and Finck, 2001). Furthermore, successive glacial episodes and shifts in subglacial regimes result in a continuum of potential till stratigraphies. Possible end members that can occur include the complete preservation of a pre-existing till unit if the subglacial conditions shift to a cold-based regime, hybrid tills that result from mixing and overprinting, and layered stratigraphy that occurs when sediment supplies are high (Trommelen et al., 2013). All of these factors result in complicated dispersal patterns that require a knowledge of the glacial conditions at the time of deposition to trace back to the source (Stea and Finck, 2001; McMartin and Paulen, 2009; Trommelen et al., 2013).

Till sampling is used in many exploration programs in areas where glaciations have occurred, although in many parts of Canada, A and B horizon soil sampling is often preferred by exploration companies (Levson and Giles, 1995). In permafrost terrains, such as the Thelon Basin, well-developed soil horizons are absent due to the formation of mudboils and thus till represents the best media to sample (McMartin and McClenaghan, 2001). Till sampling is often only carried out by surficial sampling, and much of the research conducted on dispersal patterns in till has focused on their surficial two-dimensional shape. Some studies, such as those conducted at the Huckleberry mine in British Columbia (Ferbey and Levson, 2009; Ferbey et al., 2012), have employed drilling and sampling of till in the subsurface to investigate the nature of dispersal in three dimensions. The studies at Huckleberry sampled till in the subsurface using a Becker Hammer to identify the influence of ice flow reversals on dispersal patterns. The till units overlying the Huckleberry mineralized zones were deposited over the course of several ice flow phases including several reversals. The work of Ferbey et al. (2012) determined that the signal of mineralization in till can be transmitted upwards through 30 m, and geochemical anomalies at the surface can occur 500-1000 m away from ore zones. The signature of mineralization was transmitted through the till even with ice flow reversals, and where the mineralized body was not re-exposed to erosion between ice flow events. Hence, dispersal plumes can continue to form through the reworking of earlier tills in areas of thick drift (Ferbey et al., 2012). In areas that have experienced one or more ice flow event(s), the observed direction of dispersal at the surface may differ from the last ice flow direction in an area if earlier flows were of longer duration and were characterized by larger dispersal distances (Ferbey et al., 2012). A similar situation was also described in northeastern Manitoba by Trommelen et al. (2013), whereby one particular dispersal train is related to an earlier ice flow event that is opposite in direction to the latest ice flow that drumlinized the surface.

1.2.5. Mineral Exploration: Pathfinders and Data Analysis

Exploration for unconformity-type uranium deposits in the Thelon Basin using till was studied by Robinson et al. (2014), where a till geochemistry sampling program was carried out in the vicinity of the Kiggavik trend of deposits that consists of the Kiggavik Main Zone (KMZ), Centre Zone (CZ), and East Zone (EZ), as well as other minor deposits along the trend. Mineralization at Kiggavik intersects the bedrock surface, and the mineralized zones were

exposed to erosion, which allowed for glacial dispersal of mineralized material. The study of Robinson et al. (2014) included the geochemical analysis of the <63 µm and <2 µm size fractions of mudboils. The sampling program identified a small irregularly-shaped dispersal fan emanating from the KMZ, and identified several pathfinder elements (U, Au, Mo, Ag, Bi, Cu, Co, W, Pb, and Cs). Dispersal was found to continue for up to 1 km to the west and down-ice from the deposit. A mudboil directly over the subcropping Kiggavik ore body was found to contain anomalous values of Pt, Pb, B, Hg, and Te, but these elements suffered from censored values and variable values near the detection limit with increasing distance down-ice, and were thus determined to be inappropriate pathfinder elements. Nickel concentrations were also elevated near Kiggavik. The geochemical signature associated with the KMZ ore body was strongest within 250 m of mineralization, and was dispersed in the main ice flow direction (Robinson et al., 2014). Robinson et al. (2014) recommends the use of the <2 µm fraction of till when conducting till sampling surveys because the clay-sized fraction of tills is known to preferentially host higher contents of some trace elements (Shilts, 1995).

Although the tracing of elements related to ore zones at the subcropping Kiggavik deposit has its applications, it is not necessarily applicable to the exploration for deep-seated ore bodies such as those at Tatiggaq. In cases where mineralized zones do not intersect the bedrock-till interface, it is necessary to explore for the alteration zones which surround unconformity-type uranium deposits. The exploration for alteration zones surrounding ore deposits using drift prospecting techniques is not new (see Earle, 2001; Normandeaux et al., 2012; Plouffe et al., 2012; Plouffe and Ferbey, 2015), but it has rarely been applied to basement-hosted unconformity-type uranium deposits and in three dimensions. Exploration for porphyry Cu-Mo deposits in the Canadian Cordillera has seen some success by looking for the large alteration haloes that surround porphyry systems. These studies focused on searching for the mineralogical signature of alteration zones (e.g., apatite) (Plouffe et al., 2012; Plouffe and Ferbey, 2015).

For unconformity-type deposits in the Athabasca Basin of Saskatchewan, Earle (2001) developed techniques for determining normative clay mineralogy from boulder trains at the surface. The methods developed by Earle (2001) were specifically for determining the normative quantities of dravite, chlorite (sудоite), illite, and kaolin (kaolinite/dickite) from B, MgO, K₂O, and Al₂O₃ concentrations. For this method, Earle (2001) used data from samples collected from sandstone

boulders that originated from basinal rocks in the Athabasca Basin. Only basinal boulders were sampled because their mineralogy is much simpler than that of basement rocks, which would not allow normative mineralogy to be used due to the presence of multiple aluminosilicate phases. Altered sandstones can easily be picked out based on their normative mineralogy, specifically high concentrations of illite and dravite (Earle, 2001).

Earle (2001) states that clasts below pebble size are not suitable for normative clay analysis due to the difficulty of separating clast lithologies, a requirement for normative clay mineralogy analysis. The method was not deemed as suitable for use on the <63 μm size fraction because in the Athabasca Basin situation, the till matrix is a complex mixture with a component of extrabasinal debris that makes it more challenging to interpret than the locally-derived (and abundant) sandstone boulders at the surface (Earle, 2001). However, given that till geochemistry is in essence a micro-variation of boulder tracing (Klassen, 2001), there is no reason why sufficiently developed methods could not detect alteration in the <63 μm size fraction.

Statistical analysis in mineral exploration has traditionally been limited to examining one element at a time (univariate analysis) through tools like box-plots, histograms, and maps, or through examining two elements at a time (bivariate analysis) using tools like scatter-plots (Grunsky, 2010). These methods are the least time-consuming to perform and require less advanced statistical skills. In recent years, exploration of large geochemical data sets has trended towards the use of multivariate statistical techniques for data analysis, specifically Principal Component Analysis (PCA) (Drew et al., 2007; Grunfeld, 2007; Grunsky, 2010; Normandeaux et al., 2012; Grunsky, 2013). PCA provides a way to reduce the dimensionality of large geochemical data sets and examine the relationship between multiple elements at the same time. Hence, PCA can be very useful for discriminating different geological processes, each of which can be identified by the relationships between the concentrations of elements in a sample set. However, PCA is a technique sensitive to variations in users input (e.g. number of samples or elements), and careful execution must be applied to reduce the potential for spurious results that occur due to excessive degrees of freedom (Reimann et al., 2008; Grunsky, 2010).

1.3. Thesis Objectives

The aims of this thesis are as follows:

1. Characterize the fine fraction of different till units identified in the Tatiggaq drilling target, Aberdeen Lake area, Nunavut
2. Identify in till the geochemical footprint of alteration for basement-hosted unconformity-type uranium alteration haloes in the Thelon Basin
3. Identify the surficial footprint of alteration emanating from the alteration halo
4. Develop geochemical indices to map the alteration footprint through tills in 2D and 3D

1.4. Methodology Overview

1.4.1. Sampling Procedures

Both mudboils and till drill core were sampled. The sampling of mudboils was carried out in accordance with standard procedures for northern terrain as set out by McMartin and McClenaghan (2001). The silty “cap” of the mudboil (Shilts, 1978) was avoided and samples were collected at depths greater than 10 cm. Oxidized material and biological material such as roots were avoided. At each mudboil sample location, two samples were collected: one 2-3 kg sample for grain size, clast count (cf. Hodder, 2014), and mineralogical analysis, and one 3-5 kg sample for geochemical analysis. Till drill core samples were taken from drill core collected during diamond drilling to delineate the mineralization at depth. Two samples were collected for each sample of core: one sample between 10-20 cm long for grain size, clast count, and mineralogical analysis; and one sample 20-30 cm long for geochemical analysis.

1.4.2. Geochemical Analysis

Geochemical analysis of the <63 μm size fraction was carried out at the Saskatchewan Research Council Geoanalytical lab in Saskatoon, Saskatchewan, using the analytical package ICPMS2 “Basement Exploration”. Both total digestion ($\text{HF-HClO}_4\text{-HNO}_3$) and partial digestion (modified aqua regia; 1 part HNO_3 to 1 part HCl) was carried out for each sample, and was followed by measurement of a suite of major and trace elements using Inductively Coupled Plasma-Optical Emission Spectrometry (ICP-OES) and Inductively Coupled Plasma-Mass Spectrometry (ICP-MS), respectively. Boron concentrations were determined using fusion followed by dissolution and ICP-OES analysis. Analysis was conducted using Perkin Elmer ICP-OES instruments (models DV4300 and DV5300), and a Perkin Elmer Sciex Elan DRC II ICP-MS (Saskatchewan Research Council, 2012). Grain size analysis was conducted at the University of Waterloo by laser diffraction using a Frisch Analysette 22 to complement the geochemical data.

Mineralogical information for the <4 µm fraction was determined by X-ray diffraction following grain size separation by settling and decantation (Poppe et al., 2001). The < 4 µm fraction was analyzed for clay mineralogy as the alteration haloes associated with unconformity-type uranium deposits are clay-rich (Kyser and Cuney, 2008). A full description of analytical techniques can be found in Chapter 2.

1.4.3. Statistical Analysis

Statistical analysis of the geochemical data ranged from exploratory data analysis (Grunsky, 2010) to more advanced techniques (Reimann et al., 2008). Exploratory data analysis included the construction of histograms, probability plots, scatter-plot matrices, and Tukey box-plots. Advanced statistical analysis included PCA. All statistical analysis was conducted in the R Statistical Environment (R Core Team, 2015), and was supported by the ‘rgr’ package developed by the Geological Survey of Canada (Garrett, 2013).

1.4.4. Data Visualization

Visualization of the geochemical data was carried out with several programs. Plots for basic geochemical data (e.g., scatter-plots, box-plots, histograms) and PCA results were constructed using the ggplot2 package (Wickham, 2009) of the R Statistical Environment (Grunsky, 2002; R Core Team, 2015). Ternary diagrams were created using the ‘ggtern package’ (Hamilton, 2015). The ‘reshape2’ package was used extensively for data manipulation (Wickham, 2007). For the production of maps, including 2D geochemical maps, ArcGIS® (ESRI) was used. Finally, GOCAD® (Paradigm) was used for the construction of the 3D models.

1.5. Thesis Structure

This thesis is divided into four chapters. Chapter 1 provided an introduction to the overall topic with more background literature. Chapters 2 and 3 are designed as papers to be submitted to an academic journal as a two-part paper. Chapter 2 details the geochemical footprint of alteration zones surrounding unconformity-type uranium deposits. Chapter 3 focuses on tracing the dispersal of the alteration signature in both surface and subsurface tills. Chapter 4 summarizes the results of Chapters 2 and 3, and discusses the implications of this study.

Chapter 2: Fingerprinting the signature of subcropping alteration associated with unconformity-type uranium mineralization in glacial sediments, Part 1: Identification of the most effective pathfinders

2.1. Introduction

The alteration haloes surrounding basement-hosted unconformity-type uranium deposits are typically large (Jefferson et al., 2007) and present promising targets for mineral exploration. The nature of the alteration haloes varies from deposit to deposit, but the general characteristics remain similar. One area of particular interest for the discovery of new basement-hosted unconformity-type uranium deposits is the Thelon Basin of Nunavut, which has been underexplored when compared with the Athabasca Basin of Saskatchewan. Exploration in the Thelon Basin is complicated by several factors, including its remote access. However, perhaps one of the largest obstacles to exploration for unconformity-type uranium deposits in the Thelon Basin is its near continuous cover by Quaternary sediments (e.g., Hodder 2014). These sediments can complicate the identification of geophysical signatures of low density alteration zones that are commonly identified by gravity surveys. Furthermore, the Quaternary cover can mask the geochemical signature of alteration or mineralized zones by capping them with distally derived materials. However, the presence of till cover in an area can be overcome and may even present several advantages to exploration. Although the alteration haloes associated with many unconformity-type deposits are generally large relative to the size of the deposit itself, the footprint of the alteration zone is very small relative to the sample spacing of 4 to 10 kilometres typically used in regional geochemical surveys, although more localized surveys may have a spacing of 1 to 2 kilometers (McMartin and McClenaghan, 2001). Glacial dispersion can lead to the creation of dispersal patterns that are orders of magnitude larger than the bedrock target (Levson and Giles, 1995; Klassen, 2001; Hooke et al., 2013). This means that although unconformity-type ore bodies may have sizes on the order of 20-50 metres wide by more than 1000 metres strike length, the footprint of dispersal from alteration haloes can present a target that extends for kilometres.

The goals of this study are threefold: 1) Determine the geochemical signature of the alteration zones surrounding a known example of unconformity-type uranium mineralization near Aberdeen Lake, Nunavut, Canada; 2) determine if the signature of alteration is transferred to the

tills; and 3) determine if the signature in the subsurface tills is also observed in the surficial till unit. To achieve these goals, a combination of geochemical and statistical analysis was used. The first part of the study presented in this chapter focuses on identifying the geochemical fingerprint of alteration haloes by comparing altered bedrock to unaltered bedrock in the area, and looking for this fingerprint in tills. Modelling of the dispersal pattern is presented in Chapter 3 below.

The area under investigation is located in the Thelon Basin of central mainland Nunavut. The area is host to several known uranium deposits, such as the Kiggavik deposit. The deposits in the area lie along a generally northeast to southwest trend, and are hosted along a series of faults. The mineralized area under investigation is known as the Tatiggaq prospect (Hunter et al., 2011b), and is located directly to the south of Gerhard Lake, which is located approximately 100 km west of the hamlet of Baker Lake (Figure 2-1).

2.2. Geologic Setting

2.2.1. Bedrock Geology

In the Tatiggaq study area, there are three primary rock units present: 1) syenite, consisting of both hornblende and quartz syenites, which belong to the Hudson Suite; 2) pelite to semipelite belonging to the Woodburn Lake Group; and 3) a lamprophyre dyke crosscutting the other rocks in the area (Hunter et al., 2011a, 2011b). The ore body itself is located at a depth of > 100 m, and is hosted along various faults in the subsurface (Figure 2-2). The bedrock surrounding the ore body is heavily altered such that many of the primary textures in the host rocks are entirely destroyed (Hunter et al., 2011a, 2011b). Other rock types in the area include sandstones of the Paleoproterozoic Thelon Formation, pegmatites, and Archean gneisses (Paul et al., 2002; Hunter et al., 2011a, 2011b). A more complete description of the various rock types was provided in section 1.2.1.

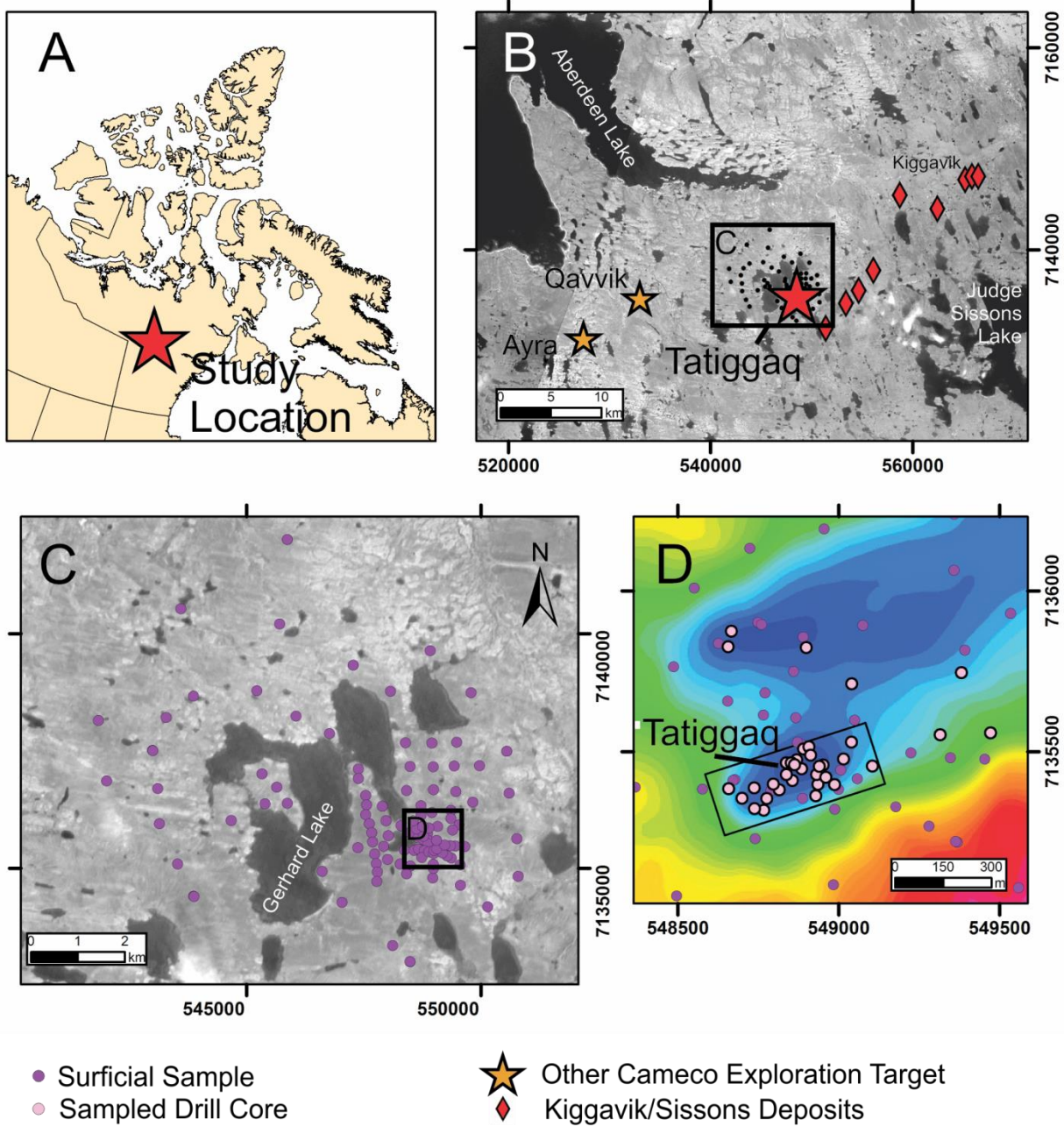


Figure 2-1: A) Study location in Nunavut. B) Regional location of the study area, which occurs between Aberdeen Lake and Judge Sissons Lake, to the west of the Kiggavik-Sissons deposits. C) Map showing the locations of surficial mudboil samples (purple dots) in the vicinity of Gerhard Lake. D) Locations of diamond drill holes that were continuously cored and sampled at selected intervals (pink dots), and nearby locations of surficial samples. The coloured background is gravity data, where blue represents gravity lows and red represents gravity highs. Gravity lows can correspond with areas of higher clay alteration or with areas of thicker sedimentary cover. The black rectangle surrounding the highest density of drill holes in D is the 3D modelled area discussed in chapter 3.

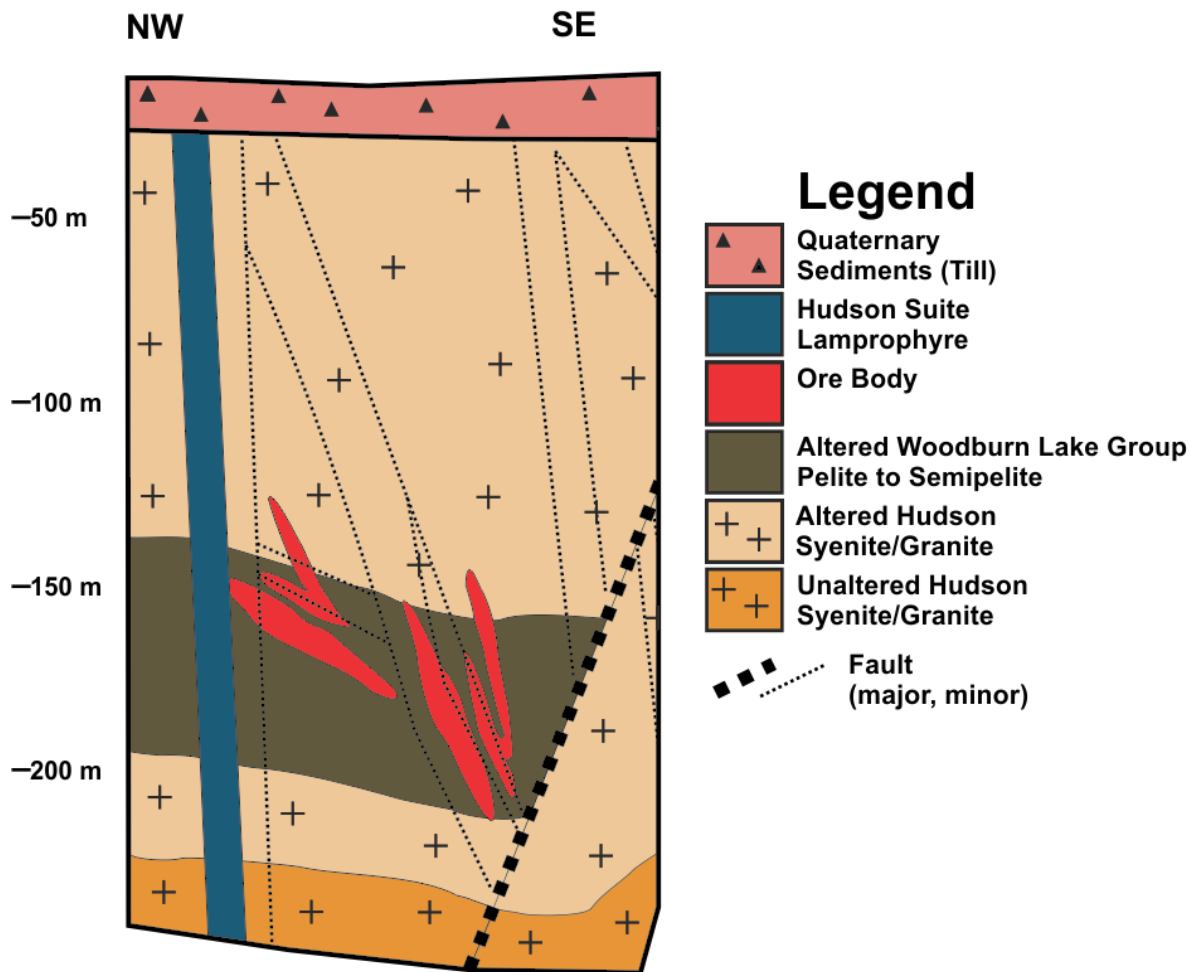


Figure 2-2: Geological cross section of the Tatiggaq study area. Note that the ore body is located more than 100 m below the ground surface, but alteration continues to the bedrock surface. The different till units are not depicted in this illustration due to scale. Modified from Hunter (2013).

2.2.2. Glacial History

The glacial history of the Tatiggaq area was studied in detail by Hodder (2014). Samples analyzed for geochemistry in this study were also examined by Hodder (2014) to determine provenance. Hodder (2014) identified four diamicton units interpreted to be subglacial tills in the Tatiggaq study area (Figure 2-2). The diamicton units are named Dmm1 (oldest) through Dmm4 (youngest). In the Tatiggaq area, Dmm4 is the unit observed at the surface and the other units are only observed in drill cores.

The depositional record of diamicton in the Tatiggaq area is depicted in Figure 2-3. Dmm1 was deposited over the bedrock surface due to ice flows that were possibly towards 255° as suggested

by the unit's stratigraphic position and the ice flow history of the area. Dmm1 is characterized by a siltier matrix than many of the other units in the area, contains numerous altered clasts, and no clasts derived from the Thelon Formation. The deposition of Dmm1 was followed by the deposition of thinly laminated sediments of uncertain origin (Hodder, 2014). Dmm2 is interpreted to be the product of a southerly (180°) ice flow event due to its high content of Thelon Formation rocks derived from north of the study area. Dmm3 was deposited by ice flow towards 340° following an ice flow reversal. It is distinguished from Dmm2 by its lower content of Thelon Formation clasts, its higher abundance of Pitz Formation clasts, and a lower B:Rb ratio (Hodder, 2014). Dmm4 was produced by ice flow between 270° and 300° (Hodder, 2014). The ice flow history in the region was driven by changes in the configuration of the Keewatin Ice Divide during the last glaciation (McMartin et al., 2006; Hodder, 2014). A more detailed description of the Quaternary stratigraphy and glacial history of the Tatiggaq study area can be found in section 1.2.2.

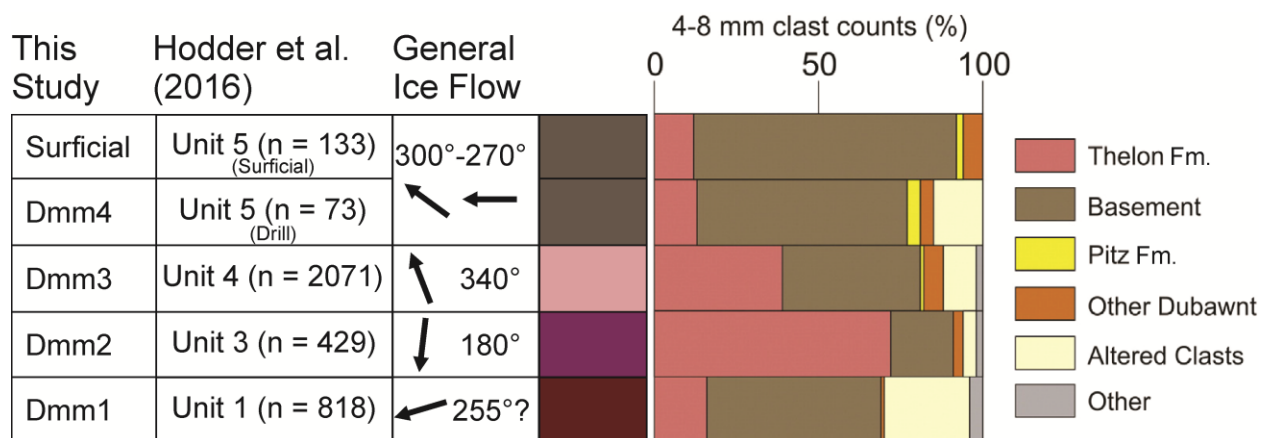


Figure 2-3: Stratigraphy of the Tatiggaq area. The nomenclature used in this study and Hodder et al. (2016) is shown for each till unit. For each unit, the ice flow direction responsible for deposition and composite clast counts showing provenance are shown. Modified from Hodder (2014) and Hodder et al. (2016).

2.3. Methods

2.3.1. Whole Rock Geochemistry

Whole rock geochemical data for altered and unaltered rocks in the study area was provided by Cameco Corporation from the company's geochemical database for the area. Several altered and fresh samples of rock types representative of the area were provided to facilitate the fingerprinting of alteration. The number of samples of each rock type is presented in Table 2-1

below. Fingerprinting of the geochemical signature of alteration is a critical first step when attempting to trace alteration through tills, because although there have been many studies on the geochemical characteristics of alteration zones in other areas, alteration signatures can be deposit- or region-specific (Jefferson et al., 2007; Kyser, 2014).

Table 2-1: Number of whole rock samples for each rock type

Rock Type	Fresh	Altered	Total
Archean Gneiss	6	5	11
Hornblende Syenite	6	7	13
Quartz Syenite	7	5	12
Thelon Formation (Sandstone)	4	6	10
Woodburn Lake Group (Metapelite)	8	10	18
Pegmatite	6	4	10

As a first order characterization of single element signatures of alteration in the whole rock data, an “Enrichment Factor” (EF) was calculated for each rock type, where $EF = \frac{\bar{x}(\text{altered rock})}{\bar{x}(\text{fresh rock})}$ where \bar{x} is the arithmetic mean of the rock type. An $EF > 1$ indicates relative enrichment and an $EF < 1$ indicates relative depletion of an element for a given rock type. The calculated EF’s for oxides and trace elements are subdivided on the basis of rock type.

2.3.2. Sampling Procedures

Sampling was carried out over two field seasons, 2012 and 2013, with 2013 sampling done to follow up on areas of interest identified following the 2012 program. The sampling program integrated both surficial mudboil samples and diamond drill core samples of till. Surficial samples were collected from mudboils because mudboils are the preferred sampling media in permafrost terrain (McMartin and McClenaghan, 2001). Mudboils form in the active layer of clay-rich sediments (such as till) in permafrost terrains. Convection cells in mudboils constantly cycle material within the active layer (Shilts, 1978). Therefore, a mudboil sample collected at several tens of centimetres of depth represents an aggregate sample of the active layer. The

thickness of the active layer within the study area was measured to be approximately 0.75 m from digging by hand in sand. It is estimated to be similar in till, although drill core recovery data suggest the active layer could be thicker (1-4 m) in places. Mudboils were sampled at depths greater than 10 cm and care was taken to avoid organic or oxidized material. At each surficial sampling site, two samples were collected: one 2-3 kg sample for grain size, clast count, and mineralogical analysis, and one 3-5 kg sample for geochemical analysis. Clast count data was described in detail by Hodder (2014). A total of 92 samples from drill core and 123 surficial samples, including duplicates, were collected at the Tatiggaq study area. The locations of the sampled drill holes and mudboil samples are shown in Figure 2-1.

For drill core, 67 samples were collected in 2012 and 25 samples were collected in 2013, including duplicates. Drill core was stored in racks outdoors and thus was exposed to the elements. The majority of the drill cores sampled were recovered in 2012, and the samples collected in 2012 were less weathered. For older drill cores and samples collected in 2013, care was taken to avoid material that had been exposed to the atmosphere at the ends of core boxes. Material that had been modified by standing water in the core boxes was not sampled for geochemical analysis due to potential contamination. In line with procedures for surficial sampling, two samples were collected for each section of core: one sample between 10-20 cm long for grain size, clast count, and mineralogical analysis; and one sample 20-30 cm long for geochemical analysis. The diamond drill core sampled was NQ sized (core diameter of 47.6 mm). Field duplicate samples were collected approximately every 10 samples for both surficial and drill core sampling and several tie-in samples were collected at the same locations during both field seasons to confirm consistency between the sampling programs. The processing and analytical procedures applied to each sample are presented in Figure 2-4.

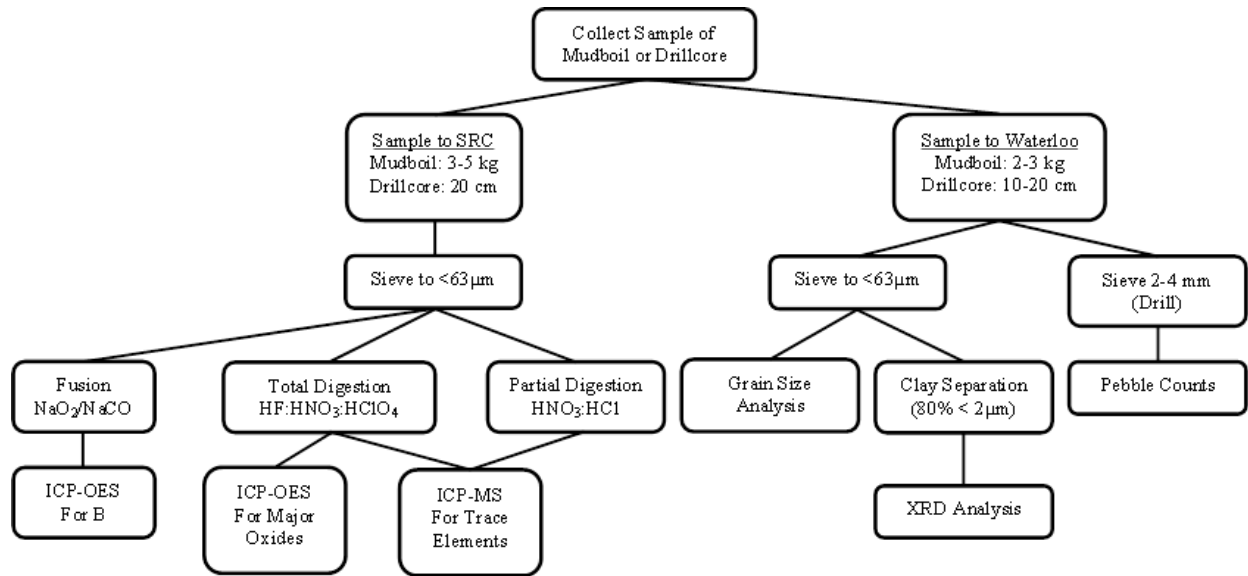


Figure 2-4: Flow chart depicting the division of samples and analytical techniques used. SRC = Saskatchewan Research Council.

2.3.3. Geochemical Analysis

Geochemical analysis was conducted at SRC Geoanalytical Laboratories and was carried out on the <63 µm size fraction of the till. The ICPMS2 “Basement Exploration” package was used (Saskatchewan Research Council, 2012). The analytical package consisted of three different analytical techniques: partial digestion followed by ICP-MS analysis for trace elements, total digestion followed by ICP-MS analysis for trace elements, and total digestion followed by ICP-OES analysis for major and minor elements. The two digestion methods are used as they provide information on different proportions of elements. The partial digestion is commonly used in uranium exploration since it does not digest some refractory detrital heavy minerals, thus allowing the detection of more subtle U anomalies. The total digestion was conducted by dissolution in concentrated HF:HNO₃:HClO₄, followed by drying and the re-dissolution of the residue in dilute HNO₃ for analysis. The partial digestion was done with a 1:1 mixture of concentrated HNO₃:HCl. Boron was analyzed separately by ICP-OES following fusion with a Na₂O/NaCO₃ mixture (Saskatchewan Research Council, 2012).

Data quality was monitored by the inclusion of field duplicates approximately every 9 samples, and the inclusion of analytical duplicates, internal Cameco standards, and lab standards. Field duplicates yielded values that reproduced to within 10% for most elements, and the element concentrations of standards fell within 5-10% of their known values.

2.3.4. Textural Analysis

Grain size analysis was carried out at the University of Waterloo by laser diffractometer. Samples were first sieved to $< 63 \mu\text{m}$ and 2-3 g of material was dispersed in 4% sodium hexametaphosphate overnight to deflocculate the clay fraction. Samples were then stirred on a magnetic stir plate as a small aliquot was pipetted into the laser diffractometer to determine grain size distribution. Output from the diffractometer was then converted to percentages of silt and clay in the sample.

The grain size of a sample is known to influence geochemical results, and should be taken into account when interpreting geochemical data for unconsolidated materials (Shilts, 1995). Even when analyzing the $< 63 \mu\text{m}$ size fraction, the amount of clay ($< 2 \mu\text{m}$) relative to silt (2-63 μm) will influence element concentrations. This is due in part to the terminal grades of various minerals. Some elements will be preferentially enriched in silt-sized minerals, whereas certain elements will favour clay-sized minerals. This is also due in part to the larger surface area of clay-sized minerals, creating more available area for the adsorption of elements, such as Cu, Zn, Fe, Mn, and U, which are released during the breakdown of sulfides (Lett, 1995). For this study, increased clay content may amplify the signature of alteration in tills because the alteration zones surrounding unconformity-type deposits are clay-rich (Kyser, 2014).

2.3.5. Mineralogical Analysis

Mineralogical analysis of the clay fraction was conducted by X-ray diffraction (XRD) on a PANalytical Empyrean II at the University of Waterloo's Ecohydrology research group's Environmental Particle Analysis Laboratory. Separation of the clay fraction was conducted using a slightly modified version of the decantation method outlined by Poppe et al. (2001). To separate the clay fraction ($< 4 \mu\text{m}$), an aliquot of $< 63 \mu\text{m}$ material was dispersed in a wide-mouth jar with approximately 250 ml of de-ionised water and approximately 1 ml of 4 wt% sodium hexametaphosphate solution. Sodium hexametaphosphate was added to prevent the flocculation of clays during settling since flocculated clays settle slower. The jar containing each sample was then shaken for 1 minute to mix the sample, placed in an ultrasonic bath for 1 minute to disperse the clays, and then shaken for 30 seconds before commencing settling. Samples were then allowed to settle for 3 hours and 54 minutes at 24°C , during which time all material $> 4 \mu\text{m}$ is expected to settle more than 5 cm. Following the completion of settling, the liquid above 5 cm

was extracted using a plastic syringe. The removed liquid was placed in open sample bags and dried for 48 hours at 60°C. For at least 1 in 12 samples, approximately 15 ml of liquid was taken from the aliquot to be dried and analyzed by laser diffractometer to ensure limited extraction of silt-sized particles. Laser diffractometer analysis indicated that less than 1% of the material extracted was larger than 4 µm, and less than 19% was larger than 2 µm. Following drying, the samples were disaggregated using a mortar and pestle and placed into glass vials for XRD analysis. The ratio of the <63 µm to <4 µm fraction by weight was compared to the expected total amount of clay in the <63 µm fraction based on laser diffractometer measurements of clay content. On average, 72% of the potential clay was recovered in a single decantation procedure. The 72% recovery may be an underestimate as the laser diffractometer does not measure the abundance of silt and clay by weight. The amount of <63 µm material used for separation depended on the clay content of the sample, and for subsurface samples, between 10 and 15 g of material was used. For surficial mudboil samples, as much as 100 g of <63 µm material was used in order to obtain enough clay for analysis. Approximately 1.2 g of clay was required for XRD analysis with a 1 hour scan due to the size of the sample holder.

XRD analysis was conducted on all samples for 1 hour with a 2θ angle between 10° and 70°. Initially, mineral phases of interest were identified by the analysis of the peaks from one sample (TUR022-SA) analyzed with a 12-hour scan. A 12-hour scan is better for the detection of phases present in small quantities due to higher resolution, but the higher resolution comes at a cost that is prohibitive for examining numerous samples. Eleven phases were identified from this 12-hour scan: quartz, illite, chlorite, albite, dravite, orthoclase, hematite, muscovite, crandallite, montmorillonite, and dickite. The clay-sized phases identified to the east of the area at Kiggavik by Robinson et al. (2014), minerals expected to be formed in alteration zones (Jefferson et al., 2007; Kyser and Cuney, 2008), and common mineral phases were all used to determine the likely phases that match the XRD peaks observed (since XRD analysis is semi-quantitative and requires some interpretation as to what phases are reasonable). The suite of 11 phases was then applied to the data collected from the 1-hour scans of each sample. Reanalysis of TUR022-SA with a 1-hour scan identified the same phases, and confirmed that a 1-hour scan was suitable to identify the phases present. Where the semi-quantitative percent of a phase was 0 in a given sample, the proportions of phases in the sample were recalculated without the absent phases.

2.3.6. Principal Component Analysis

Principal component analysis (PCA) is a useful tool for exploratory analysis of geochemical data sets (Grunsky, 2010), and has been used to identify the geochemical signatures associated with mineralization in tills (Normandeaux et al., 2012; Grünfeld, 2007).

The goal of PCA is dimension reduction. PCA is computed based on the covariance and correlation matrices of a data set, and the technique produces several variables called principal components that explain as much of the variance in the data as possible. PCA generates as many principal components as elements entered into the calculation, but the majority of information is contained in the first few principal components. Individual principal components can identify geological processes that affect several elements. For example, the first principal component could represent the enrichment of one element and depletion of another due to alteration processes, whereas the second principal component could represent lithological variations (Reimann et al., 2008).

PCA is conducted by sequentially determining the direction of maximum variance through the geochemical data set in multi-dimensional space. The direction through multivariate space with the most variability is the first principal component, and the line along the maximum variability is called the first principal component axis. The second principal component is determined by finding the direction in multidimensional space showing the second highest variance that is perpendicular to the first component. Subsequent components are determined in a similar manner with each component being orthogonal to the previous component (Reimann et al., 2008). PCA generates two outputs of primary interest: principal component scores and loadings. Principal component scores are generated by projecting the sample points in multi-dimensional space onto each principal component axis. Each sample gets a score for each principle component, and the score represents the position of the sample on the axis. Loadings represent the relationship of each principal component to the original variables (elements), and indicate how much each variable contributes to a particular component. Loadings and scores are often presented together on an x-y scatter-plot called a bi-plot, which allows for easy interpretation of the data. Bi-plots are commonly constructed for PC-1 vs PC-2, PC-2 vs PC-3, and PC-1 vs PC-3 to visualize structures in the data. The amount of variability accounted for by each component will sum to

100%, and more than 80% of the variability in the data should be explained by the first 4 or 5 components (Reimann et al, 2008).

To prepare data for PCA, all data must be in the same units. All data in ppm must be converted to weight percent or vice versa before analysis is conducted, although in certain cases it is advisable to treat major and trace elements separately due to the different geochemical processes affecting them (Reimann et al., 2008). Censored values must not be included as negative values for mathematical reasons. In this study censored values were replaced by a value of one half the detection limit. Data normality is not strictly required to conduct PCA, although the data should be transformed to be as close to normally distributed as possible, and it is recommended to log-transform data before analysis. Log-transformations are recommended as they help normalize and open the data. Outliers in the data set will severely influence the results of PCA, and should either be removed or robust statistical methods should be applied. However, outliers should not be ignored completely because they may identify geological features of interest such as mineralization (Reimann et al., 2008). Robust PCA methods attempt to fit most of the data points and are therefore insensitive to outliers, but the centered log-ratio (CLR) transform cannot be used in robust methods due to mathematical reasons. It is therefore necessary to apply an isometric log-ratio (ILR) transformation and back-transform the results for presentation (Egozcue et al., 2003; Filzmoser et al., 2009; Garret, 2013).

Dimensionality also limits the number of elements that can be examined. There are several rules that can be used to determine the maximum number of elements to be examined and still return stable results. For the present study the rule $n > 9p$ is generally applied, where n is the number of samples, and p is the number of elements. The use of this rule dictates that if 90 samples are available, the approximate number in the Tatiggaq drill core geochemical data set, a maximum of 10 elements should be used for PCA. Due to this limitation, several subsets of elements will be analyzed separately. Certain groups of elements, such as the rare earth elements, do not need to be included individually because they have similar geochemical behavior (Reimann et al, 2008). For the whole rock PCA, the rule of $n > 9p$ is broken in order to retain the same set of elements used on the till drill core samples. Since a total of 74 rock samples were used for PCA and at most 9 elements were included in each grouping, there was a ratio of 8.2 samples to 1 element

for the total digest data. The rule of $n > 9p$ was maintained for PCA of partial digest data since fewer elements were included.

To identify potential multi-element anomalies associated with unconformity-type uranium alteration, PCA was carried out on the data. Given the rule of one variable can be analyzed for every nine samples (Reimann et al., 2011), analysis had to be carried out on different geochemical groups. The groups were selected on the basis of geochemical properties, elements identified during previous studies, and based on variability observed during single-element exploratory analysis of the whole rock data set (discussed below).

To identify potential multi-element anomalies associated with unconformity-type uranium alteration, PCA was carried out on the data from rock samples and till drill core samples. The first group of elements used for PCA was the major oxides (K_2O , Al_2O_3 , MgO , Fe_2O_3 , Na_2O , P_2O_5 , MnO , CaO , and TiO_2). The major oxides were chosen based on their ability to show variations in the data that were related to mineralogical changes since they are more likely to be integral structural components of minerals. The second group analyzed was a subset of the transition metals, and included Ni, Cr, Co, Cu, Zn, V, Mo, Y, and Sc. The transition metal grouping was used to monitor the behaviour of some metals without B present as B was observed to dominate the alteration signature for some rock types. PCA was carried out separately for the total digest and partial digest data, and the two data sets were not mixed (Cr and Y concentrations were not obtained for partial digests). The third group analyzed is considered to comprise the “alteration elements”, as these include elements identified during single element analysis (see below), and by the work of prior researchers investigating unconformity-type uranium deposits (e.g., Ruzicka, 1996; Robinson, 2014). The “alteration elements” include Ni, Cr, B, V, Sc, Zn, Mo, U, and Sr (Cr, B, and Sr concentrations were not obtained for partial digests).

The PCA was carried out using the “rgr” package (Garret, 2013) in the R Statistical Environment (R Core Team, 2015), and the results were plotted using a custom script and the “ggplot2” package (Wickham, 2009).

2.3.7. Chemical Index of Alteration

The chemical index of alteration (CIA) provides a means to quantify the degree to which rocks have been chemically weathered. The index relies on the removal of Na and Ca during the breakdown of feldspars to clay minerals, and the resulting relative enrichment in Al. In addition, K is used in the index, and K is typically not removed during the breakdown of feldspars as it can be incorporated into some weathering products such as illite. CIA is calculated for the whole rock data as described by Fedo et al. (1995). The CIA is calculated using Equation 1 below, where each element is in molar proportions. Ideally, the CaO term should be corrected to account for contributions from carbonates and apatite using CO₂ and P₂O₅ concentrations (Fedo et al., 1995). The lack of CO₂ data prevented this correction, but has minimal impact on CIA values because carbonates are scarce in the area. The CIA value for a given sample is between 0 and 100, and unaltered rocks will have values of approximately 50. Values greater than 50 indicate progressively greater degrees of chemical weathering due to the removal of Na and Ca along with the relative enrichment of Al.

$$\text{Equation 1: } \frac{Al_2O_3}{Al_2O_3 + CaO + Na_2O + K_2O} \times 100$$

One downside to the chemical index of alteration is that it is sensitive to K-metasomatism or other alteration processes that result in K enrichments. Illitization, which is observed in the alteration zones surrounding unconformity-type uranium deposits, will result in K enrichment. The K enrichment will result in a lowering of the CIA value for a given sample. This process can be useful, however, because samples that plot below the expected chemical weathering trend on the ternary diagram could be indicative of alteration related to mineralization. Other indices of alteration have been proposed to account for K enrichment during weathering, such as the chemical index of weathering (CIW), but these indices have been criticized for having greater variability, relative to CIA, in the starting values for unaltered rocks with different lithologies (Fedo et al., 1995).

2.4. Results

2.4.1. Signature of Alteration in Bedrock

2.4.1.1. Single Element Anomalies

Diagrams showing the enrichment factors for major oxides determined by total digestion, trace elements determined by total digestion, and trace elements determined by partial digestion are presented in Figure 2-5, Figure 2-6, and Figure 2-7, respectively. For the major oxides, the elements showing the strongest enrichment in altered rocks are Al_2O_3 and K_2O . The strongest depletions in the major oxides of altered rocks are MnO , CaO , and Na_2O , although it is noted that the values for MnO and Na_2O are generally close to the detection limit. For trace element analyses derived from total digests, B shows the strongest enrichment, and Ni, U, and Be show variable enrichment across the different altered rock types. By contrast, Sr and Zn are depleted. For trace element analyses derived from partial digests, U shows enrichment, whereas Zn and V show depletion in the altered rocks.

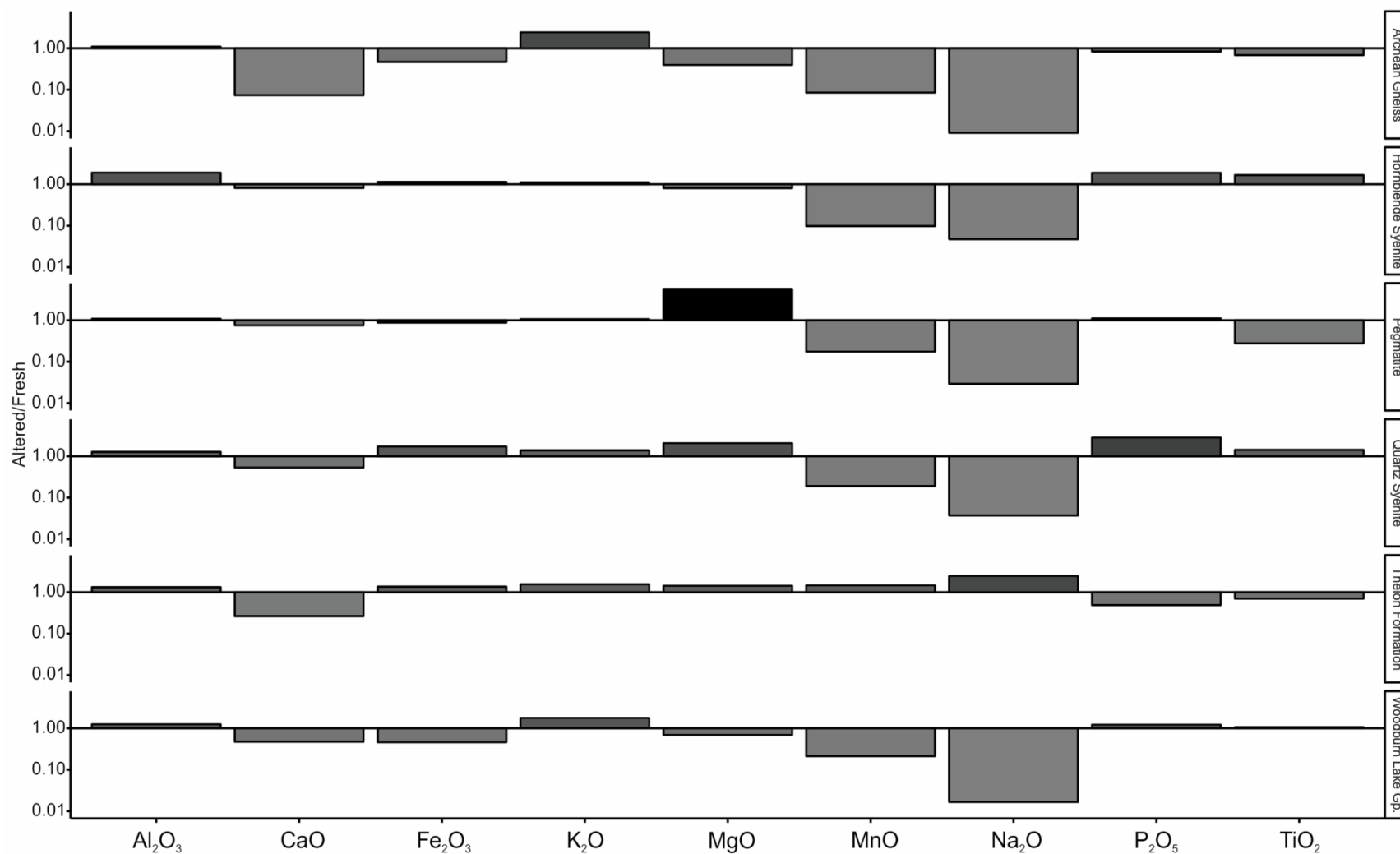


Figure 2-5: Enrichment/depletion plot of the whole rock major oxide geochemistry (expressed as oxide concentration of altered rocks divided by oxide concentration of unaltered rocks), subdivided by rock type. Al₂O₃ and K₂O show minor enrichment across all rock types, and MgO shows variable enrichment/depletion. MnO, CaO and Na₂O are depleted across all rock types except for Na₂O and MnO in the case of the Thelon Formation.

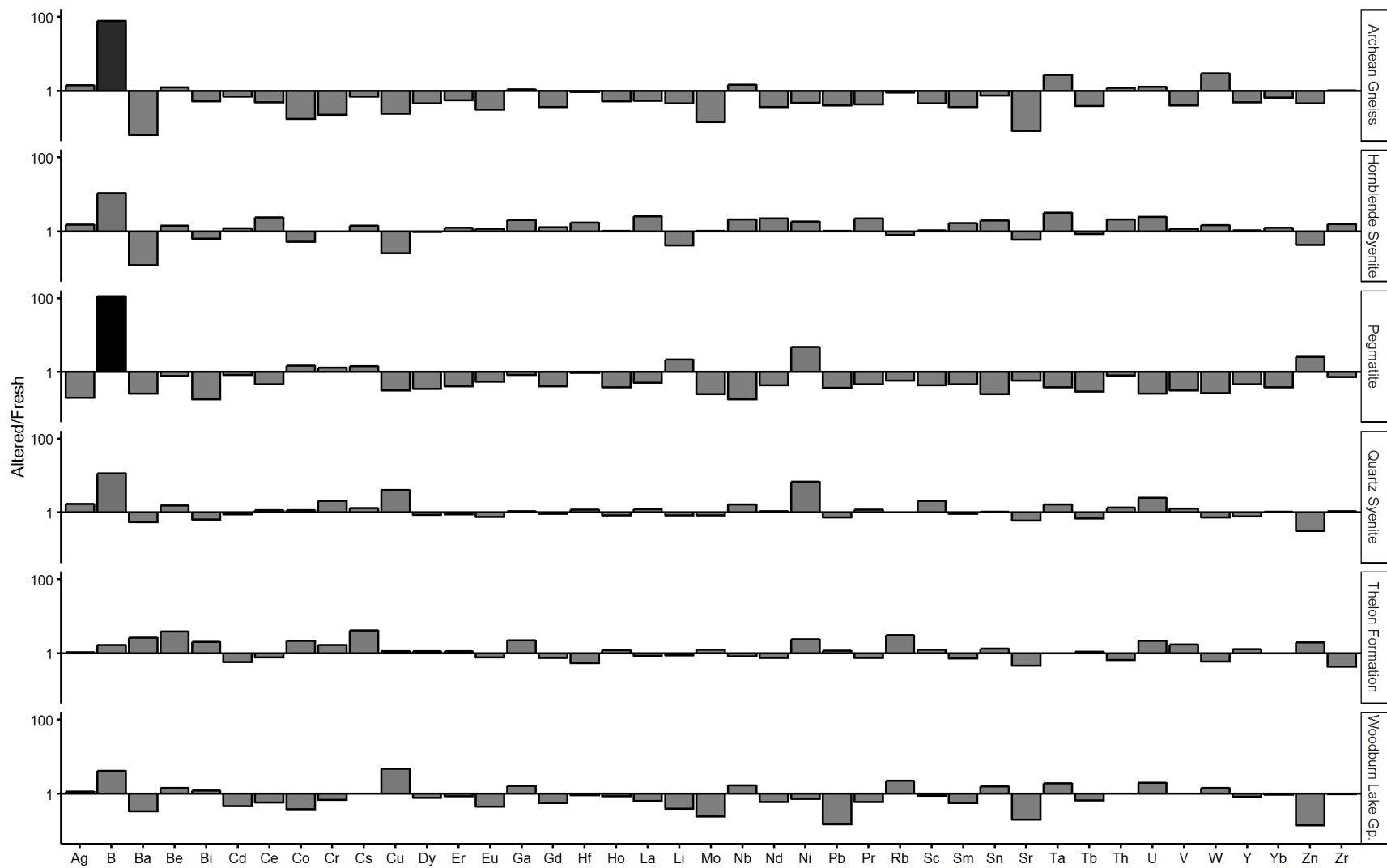


Figure 2-6: Enrichment/depletion plot of the whole rock trace element geochemistry (expressed as trace element concentration of altered rocks divided by trace element concentration of unaltered rocks) by total digestion, subdivided by rock type. B shows the highest enrichment of all elements, whereas Ni, U, and Be show variable enrichment. Sr and Zn show more consistent depletion relative to the other elements analyzed.

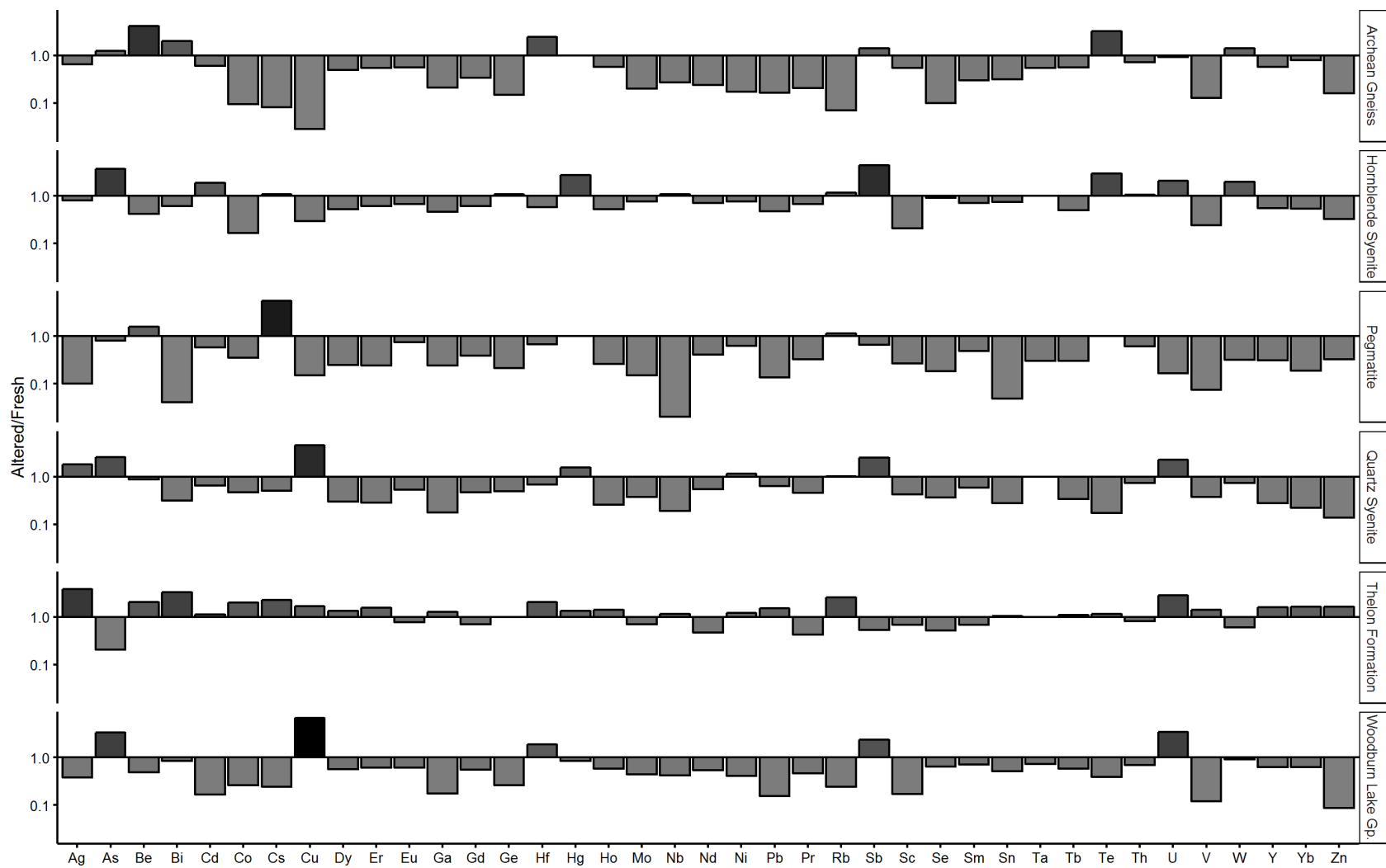


Figure 2-7: Enrichment/depletion plot of the whole rock trace element geochemistry (expressed as trace element concentration of altered rocks divided by trace element concentration of unaltered rocks) by partial digestion, subdivided by rock type. U shows enrichment in most cases. The loss of U in the pegmatite is likely due to the differences in mineralogy compared to other rock types. Many elements show consistent depletion with alteration, with the strongest and most consistent depletions occurring for Zn, V, and many of the rare earth elements.

2.4.1.2. Multi-element anomalies

In the PCA of whole rock major oxides (Figure 2-8), discrimination between the altered and fresh rocks is apparent in the 1st principal component. K₂O, TiO₂, and P₂O₅ are associated with negative 1st principal component loadings, and negative scores are associated with the altered rocks. MgO, Fe₂O₃, Na₂O, and MnO are associated with positive 1st principal component values, and the fresh rocks have positive scores. Lithological variations appear to be associated with the 2nd principal component, where pegmatite has the highest PC2 values, and hornblende syenite and Archean gneiss have the lowest PC2 values. Other lithologies appear to fall within similar clusters along the PC2 axis. K₂O and Na₂O are associated with positive 2nd principal component values, whereas CaO, MgO, P₂O₅, and TiO₂ are all associated with negative values. The 3rd principal component for the major oxides accounts for only 9% of the variability in the data set. Altered rocks as well as several unaltered rocks from the Thelon Formation are associated with positive PC3 values.

Principal component analysis of Sc, V, Cr, Co, Ni, Cu, Zn, Y, and Mo concentrations determined from total digestion of the whole rocks is presented in Figure 2-9 (transition metal grouping). The bi-plot of PC1 vs PC2 shows less pronounced discrimination between the altered and fresh rocks compared with the major oxide PCA shown in Figure 2-8, but several trends can still be derived. Positive PC1 values are generally associated with fresh rocks, and negative PC1 values are generally associated with altered rocks. Exceptions to this trend include rocks of the Thelon Formation and the quartz syenite, although the altered quartz syenite samples have lower PC1 values than fresh syenite samples. Positive PC1 values are associated with Mo, Zn, V, Co, and Cu, whereas negative PC1 values are associated with Ni, Cr, and Sc. PC2 shows an association with lithology, where pegmatite samples have the lowest PC2 scores and Woodburn Lake Group samples have the highest PC2 scores. Positive PC2 values are associated with Ni, Cr, Co, Cu, and Zn. Negative PC2 values are associated with Sc, Y, Mo, and V. PC3 shows significant scatter and does not display any significant trends.

Principal component analysis of Sc, V, Co, Ni, Cu, Zn, Y, and Mo concentrations determined from partial digestion of the whole rocks is shown in Figure 2-10 (transition metal grouping). In this case, discrimination between altered and fresh rocks is not as obvious compared with the total digestion method shown in Figure 2-9. PC1 is characterized primarily by positive values for

Co, Ni, V, and Cu, and by negative values for Sc, Y, and Zn. PC1 appears to be associated primarily with lithology, in contrast to the association of PC1 with alteration for the total digestion data on the same transition metals. Negative PC2 values are associated with Ni, Sc, and Y. Positive PC2 values are associated with Cu and Mo. PC3 does not show an obvious pattern.

For samples analyzed following total digestion, PCA of elements expected to be good indicators of alteration based on exploratory data analysis as part of this research and previous research (Ruzicka, 1996; Jefferson et al., 2007; Robinson, 2015) included Ni, Cr, B, V, Sc, Zn, Mo, U, and Sr. The results of PCA for these “alteration elements” are presented in Figure 2-11. PC1 is associated with lithology, whereas PC2 is associated with alteration for most rock types. Positive PC1 values are associated with B, U, and Mo, and negative PC1 values are associated with V, Cr, and Ni. Altered rocks have positive PC2 values, and are associated with B, Ni, and Cr. Negative PC2 values are associated with Sr, Zn, Mo, Sc, and V. The third principal component does not show any obvious trends.

For samples analyzed following partial digestion, PCA of elements expected to be good indicators of alteration based on exploratory data analysis as part of this research and previous research (Ruzicka, 1996; Jefferson et al., 2007; Robinson, 2015) included Ni, V, Sc, Zn, Mo, and U. The results of this analysis are presented in Figure 2-12. PC1 appears to be mainly associated with elevated U and low Mo concentrations of the pegmatites. Negative PC1 values are associated with Zn and V. PC2 is associated with alteration for most rock types. Positive PC2 values are associated primarily with Ni, and negative PC2 values are associated with V, Zn, Sc, and Mo.

The main trends observed in the PCA results for whole rock data is that alteration is responsible for the largest geochemical differences in the data set, which is why altered and fresh rocks are commonly distributed on opposite ends of the PC1 axis (c.f. Figure 2-8A, 2-9A). The other main source of geochemical variability in the PCA results is rock type, which can be seen in PC2 in Figures 2-8A and 2-9A. In the analysis of alteration elements by total digestion (Figure 2-11), it appears that rock type is the dominant source of variation in the data set and is thus associated with PC1, whereas PC2 is associated with alteration.

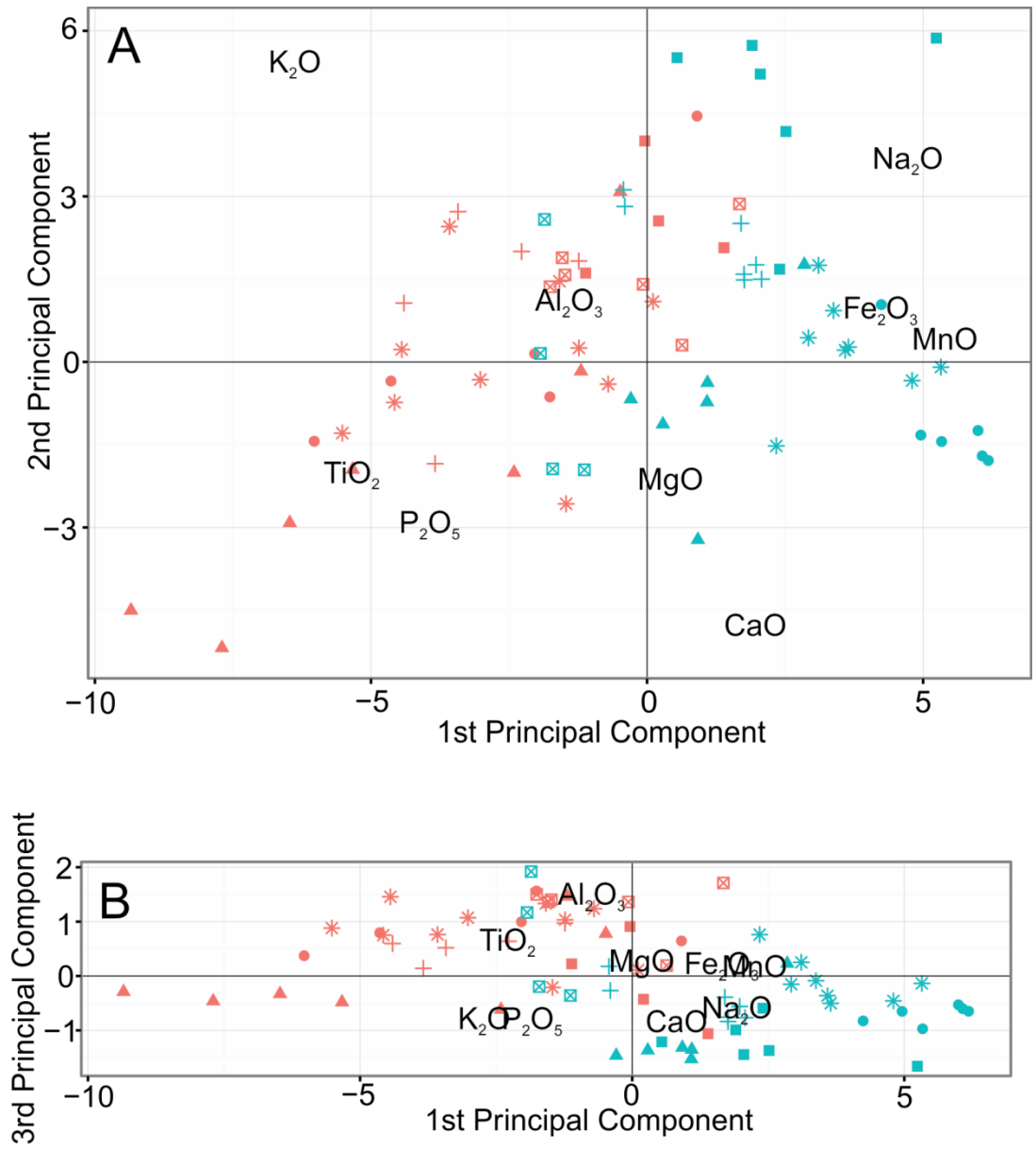


Figure 2-8: Principal component analysis of the major oxide data for the whole rocks (K_2O , Al_2O_3 , MgO , Fe_2O_3 , Na_2O , P_2O_5 , MnO , CaO , and TiO_2). A) 1st and 2nd principal components. B) 1st and 3rd principal components.

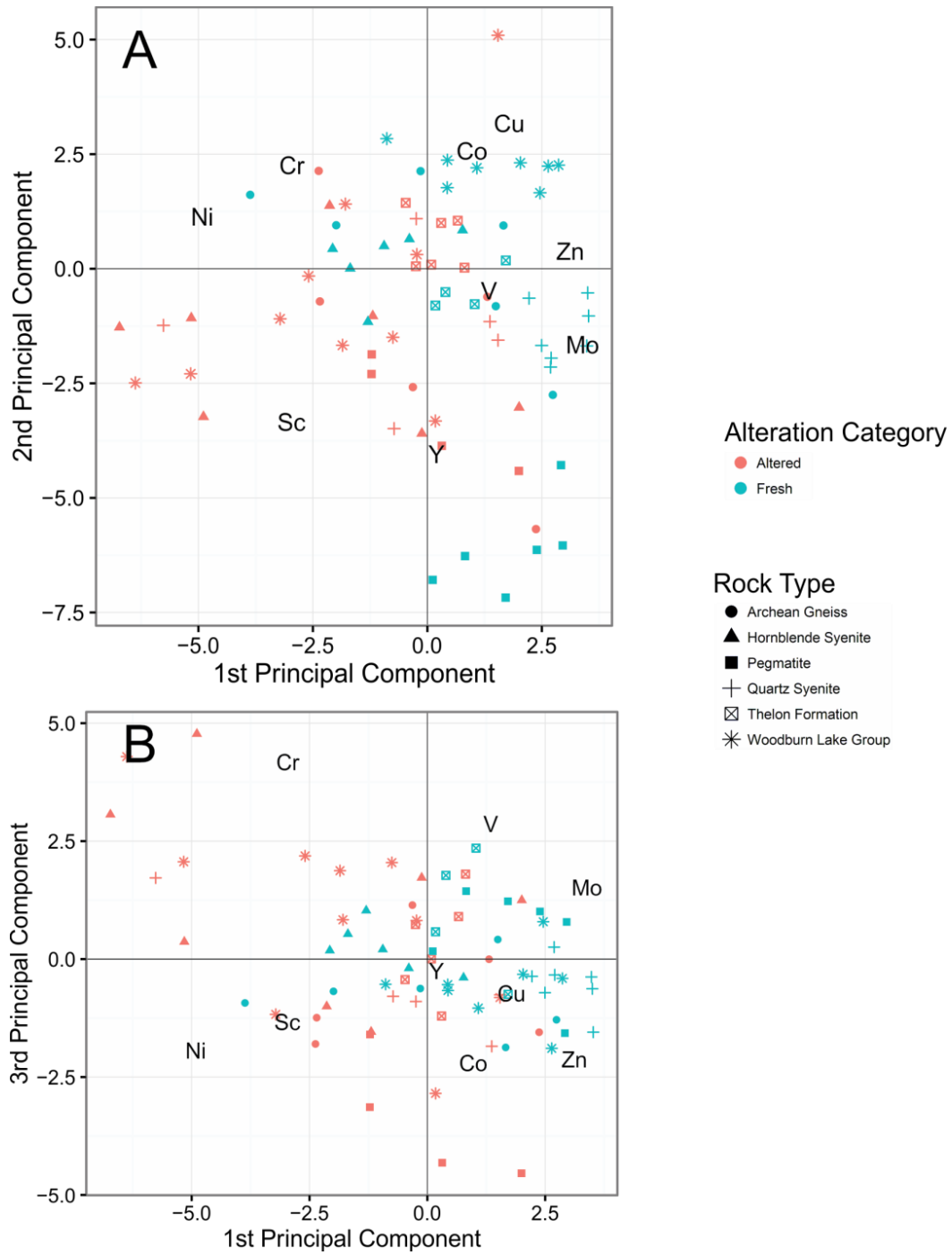


Figure 2-9: Principal component analysis of transition metal data (Sc, V, Cr, Co, Ni, Cu, Zn, Y, and Mo) determined by total digestion of the whole rocks. A) 1st and 2nd principal components. B) 1st and 3rd principal components.

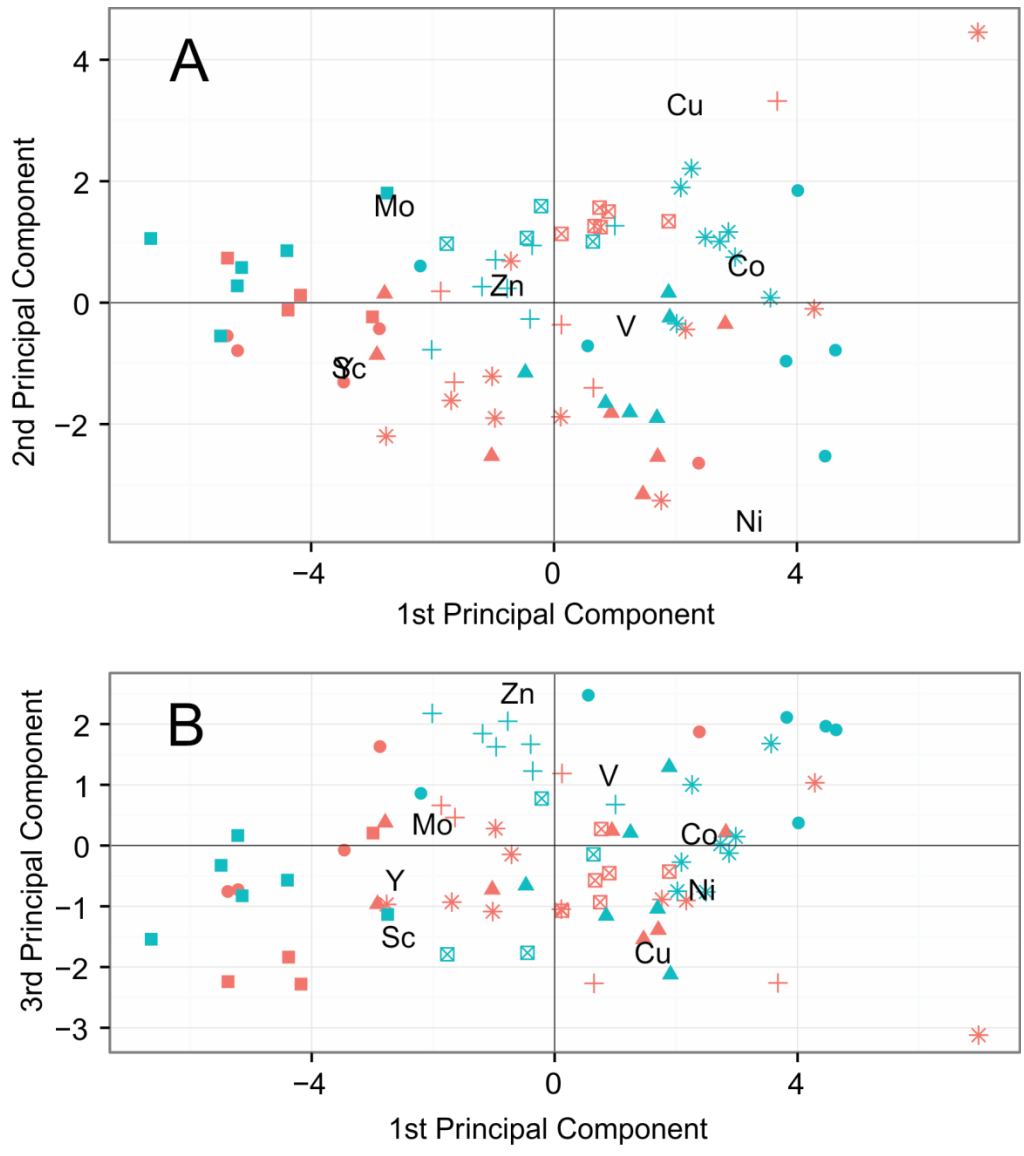


Figure 2-10: Principal component analysis of transition metal data (Sc, V, Co, Ni, Cu, Zn, Y, and Mo) determined by partial digestion of the whole rocks. A) 1st and 2nd principal components. B) 1st and 3rd principal components.

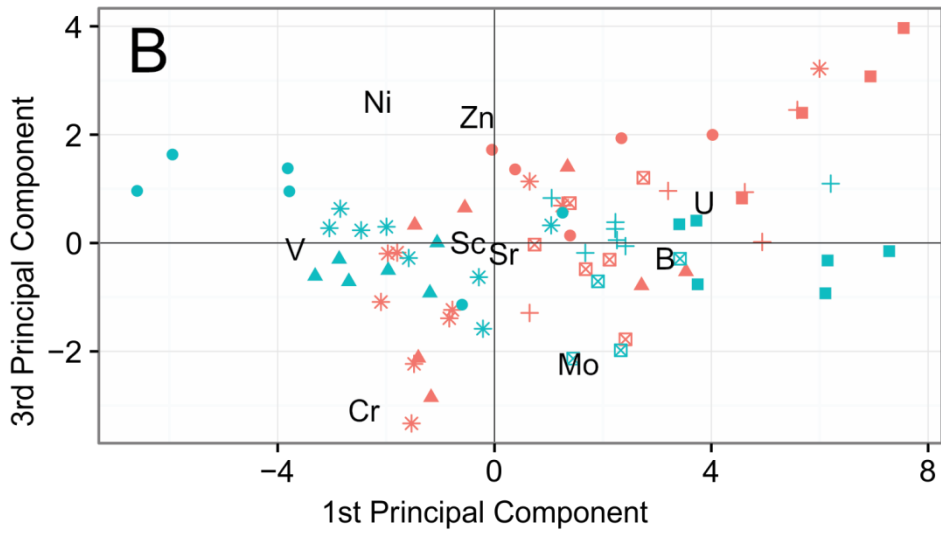
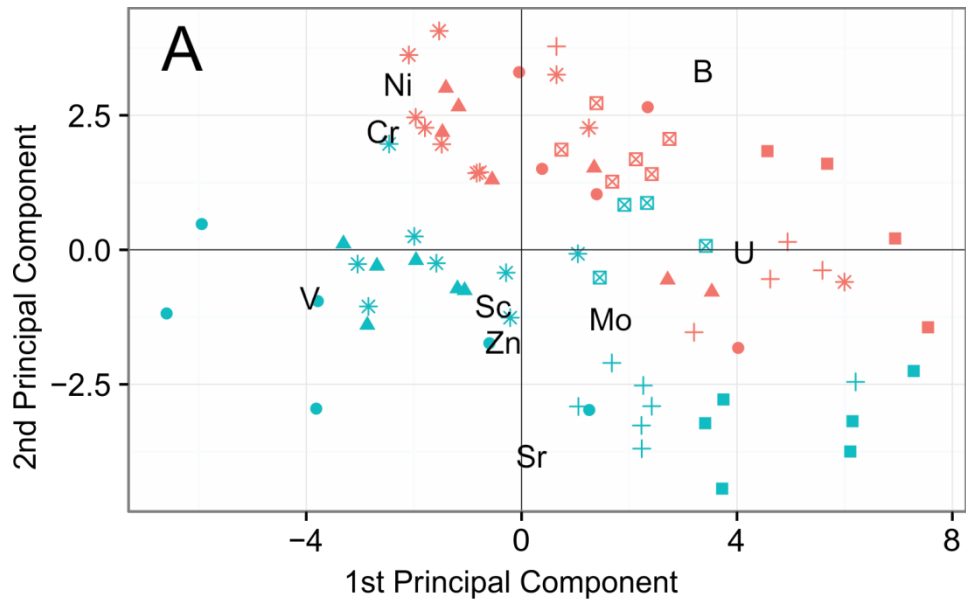


Figure 2-11: Principal component analysis of data (total digestion method) from elements expected to be good indicators of alteration (Ni, Cr, B, V, Sc, Zn, Mo, U, and Sr) based on this work and previous research (Ruzicka, 1996; Jefferson et al., 2007; Robinson, 2015). A) 1st and 2nd principal components. B) 1st and 3rd principal components.

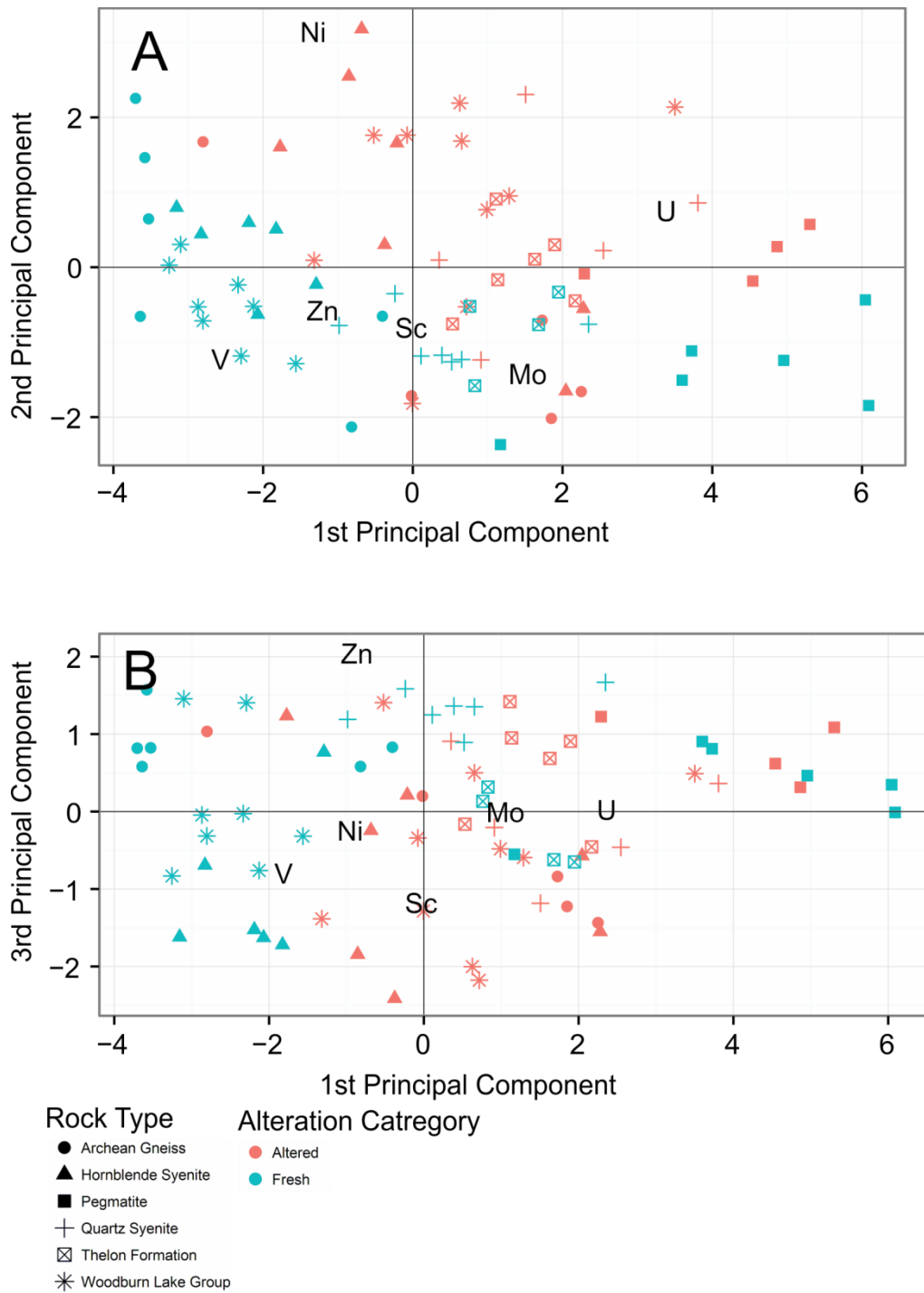


Figure 2-12: Principal component analysis of data (partial digestion method) from elements expected to be good indicators of alteration (Ni, V, Sc, Zn, Mo, and U) based on this work and previous research (Ruzicka, 1996; Jefferson et al., 2007; Robinson, 2015). A) 1st and 2nd principal components. B) 1st and 3rd principal components.

2.4.1.3. Chemical Index of Alteration

The chemical index of alteration (described in section 2.3.7) was applied to the whole rock data to identify whether the CIA is a useful geochemical vector for the exploration of unconformity-type uranium deposits. CIA was investigated as a potential tool for drift prospecting using till data in the Tatiggaq area by Wang (2014). The CIA values for each rock type are plotted in Figure 2-13. A summary of the numeric CIA values is presented in Table 2-2. For each rock type, the altered rocks show higher CIA values than their unaltered counterparts. However, for the Thelon Formation, the averages of altered and fresh samples differs by only 2.6, and the similarities between the altered and fresh samples can be clearly observed when the samples are plotted on a ternary diagram (Figure 2-13, middle of bottom row). Other rock types show good separation between altered and unaltered samples, and are clearly discernible from one another when plotted.

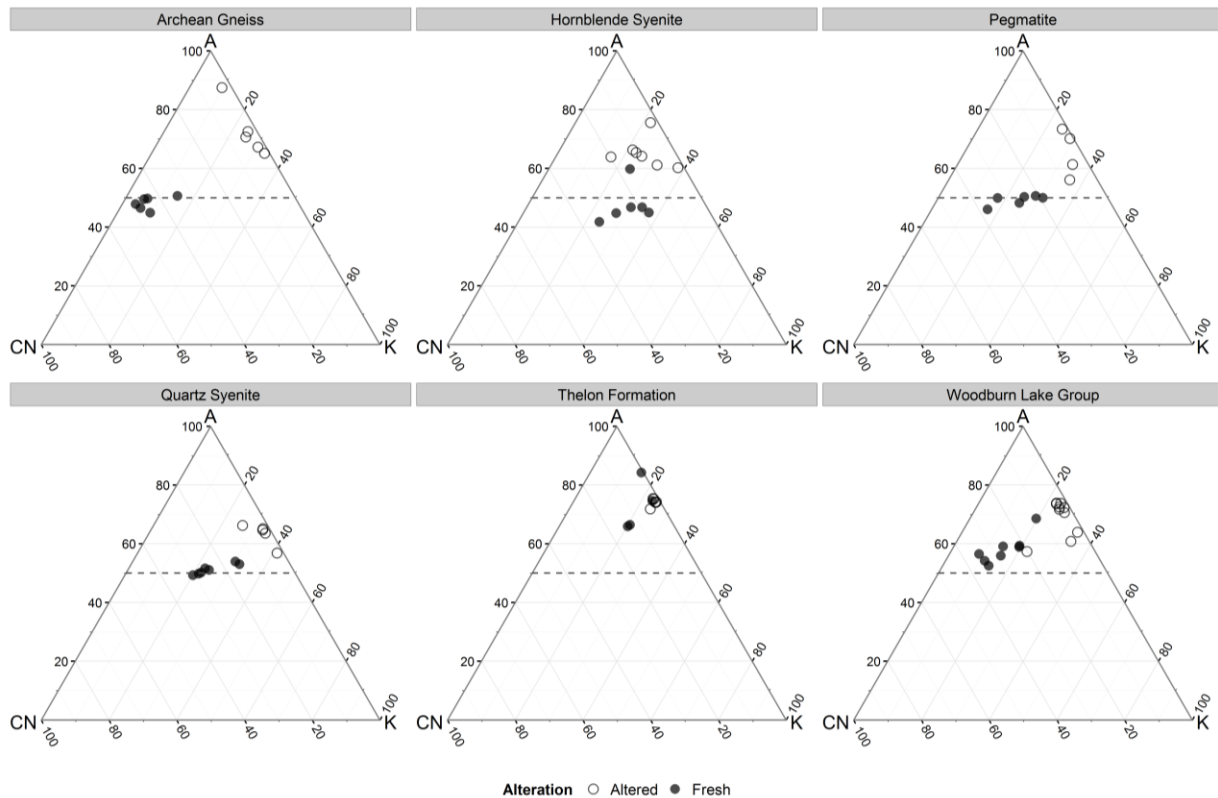


Figure 2-13: CIA values for the whole rock data, subdivided by rock type. Altered and fresh samples are represented by hollow circles and solid circles, respectively. For the majority of rock types, with the exception of the Thelon Formation sandstones, the CIA values are around 50 (dashed line) for fresh rocks, as is expected.

Table 2-2: Minimums, maximums, and means of CIA data by rock type for the altered and fresh samples. Note that with the exception of Thelon Formation samples, the altered rocks have a higher CIA value.

	Fresh CIA			Altered CIA		
	Minimum	Mean	Maximum	Minimum	Mean	Maximum
Archean Gneiss	44.9	48.2	50.7	65.1	72.6	87.5
Hornblende Syenite	41.8	47.5	59.8	60.2	65.3	75.6
Pegmatite	46.1	49.2	50.6	56.1	65.2	73.4
Quartz Syenite	49.3	51.3	54.0	56.8	63.3	66.2
Thelon Formation	65.9	72.8	84.3	71.8	74.2	75.4
Woodburn Lake Group	52.5	58.2	68.6	57.4	69.1	73.9

2.4.2. Geochemical Signature of Alteration in Tills

2.4.2.1. Single Element Anomalies

Identification of the alteration signatures in the tills focused primarily on the drill core samples rather than the surficial samples, since several drill core samples are known to be in very close proximity to altered bedrock and contain altered clasts (Hodder, 2014), and therefore are expected to contain some signature related to alteration. Signals identified in the drill core data guided the search for alteration signatures in the surficial samples. The subdivision of tills in the Tatiggaq area by Hodder (2014) is partially related to alteration signatures, as the B:Rb ratio of samples together with counts of Thelon Formation clasts were used in part to differentiate the units. Elevated B concentrations were shown in section 2.4.1 to be related to alteration processes, and B anomalies are expected to be observed in tills proximal to the alteration zones. In the following, reference to till units Dmm1, Dmm2, Dmm3, and Dmm4 follows the classification outlined by Hodder (2014).

To identify the signature of alteration in the till, the elements determined to be enriched or depleted in altered rocks in section 2.4.1 were plotted for the different drill core samples. The concentration of an indicator is expected to be highest closest to its source (Klassen, 2001). Hence, it is expected that Dmm1, the lowest stratigraphic unit, should exhibit the strongest signature of alteration since it contains the highest proportion of altered clasts (Hodder, 2016), and is in contact with the altered bedrock surface.

The major oxides associated with alteration in the drill core samples are plotted in Figure 2-14. Dmm1 shows elevated major oxide concentrations for most elements, including Al_2O_3 , CaO,

Fe₂O₃, K₂O, and TiO₂. The elevated values for the major oxides may be related to the higher silt content of Dmm1 relative to Dmm2 and Dmm3 (Figure 2-17).

For the trace elements analyzed following total digestion (Figure 2-15), the two samples belonging to Dmm4 have relatively low B concentrations. The general trends in the trace element data are that Dmm1 and Dmm2 often occur at opposite ends of the population with the exception of B, where B shows the highest values in Dmm2 but B concentrations in Dmm1 are highly variable. Dmm1 has the highest concentrations of Ba, Cr, Ni, Sc, V, and Zn, and the lowest concentrations of Sr. Dmm2 has the lowest concentrations of Ba, Cr, Mo, Ni, Sc, V, and Zn, and has the highest concentrations for Sr. Dmm3 generally shows intermediate concentrations for most elements. Dmm4, with only two samples in the drill core data, generally plots alongside Dmm3, with the exception of B and Sr (very low concentrations), and V and Ba (slightly higher concentrations).

Histograms for select trace elements analyzed following partial digestion are shown in Figure 2-16. Similar to the total digestion data, Dmm1 and Dmm2 tend to plot at opposite ends of the population in terms of elemental concentrations. Dmm1 has the highest concentrations of U, V, Y, and Zn. Dmm2 tends to have the lowest concentrations for all elements displayed in Figure 2-16. As with the elements analyzed by total digestion, Dmm3 shows an intermediate concentration for most elements. The total digest analysis shows clearer differences between the till units than the partial digest for most elements.

Figure 2-17 shows the clay percent of the < 63 µm fraction for all of the drill core samples. Dmm1 has the lowest clay content of all the tills in the study area, and Dmm2 and Dmm3 show a similar range of higher values.

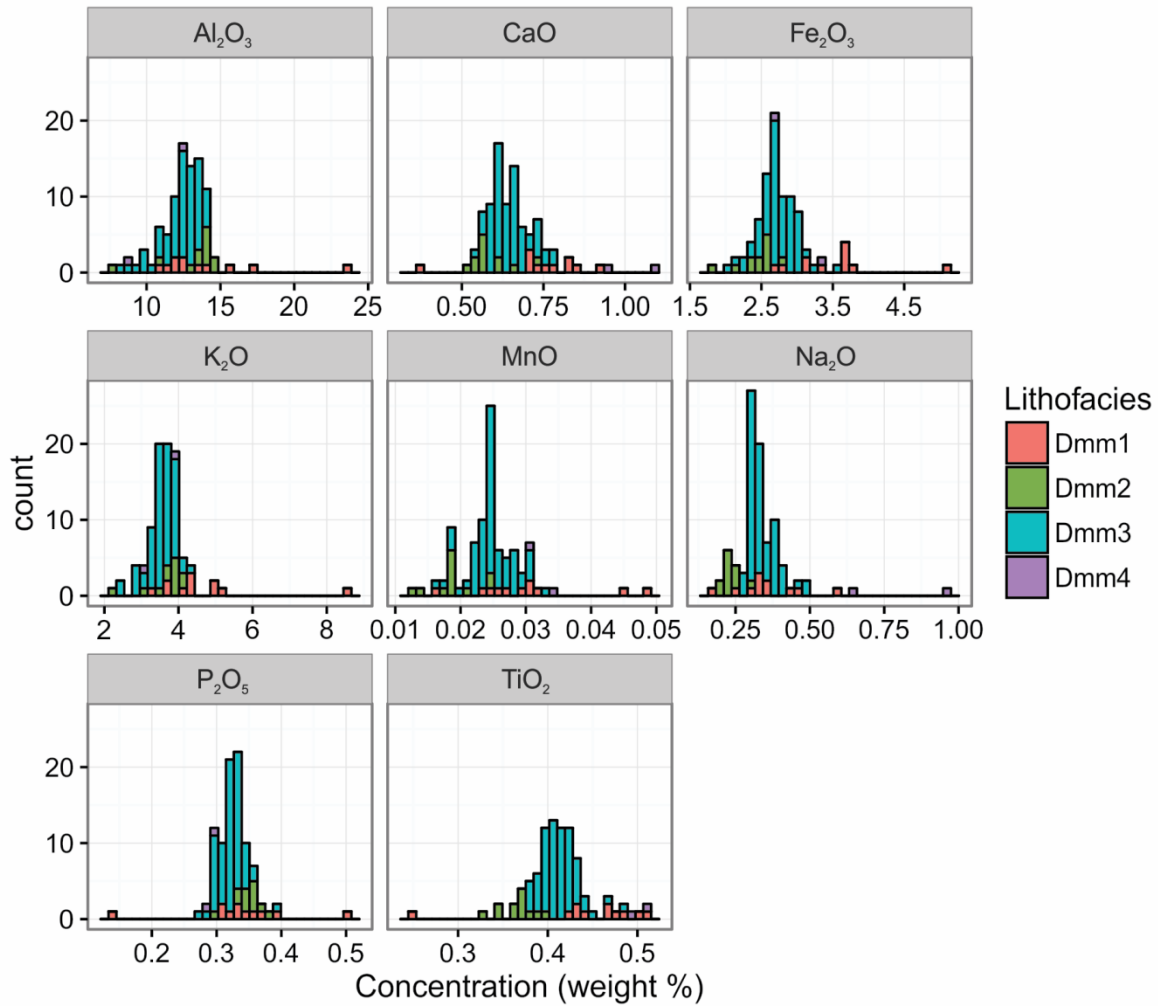


Figure 2-14: Histograms showing the distribution of the major oxides in tills associated with alteration zones. Dmm1 has higher concentrations of CaO , Fe_2O_3 , K_2O , MnO , and TiO_2 . Dmm2 has high Al_2O_3 , K_2O , and P_2O_5 concentrations, and low CaO , Fe_2O_3 , MnO , Na_2O , and TiO_2 concentrations.

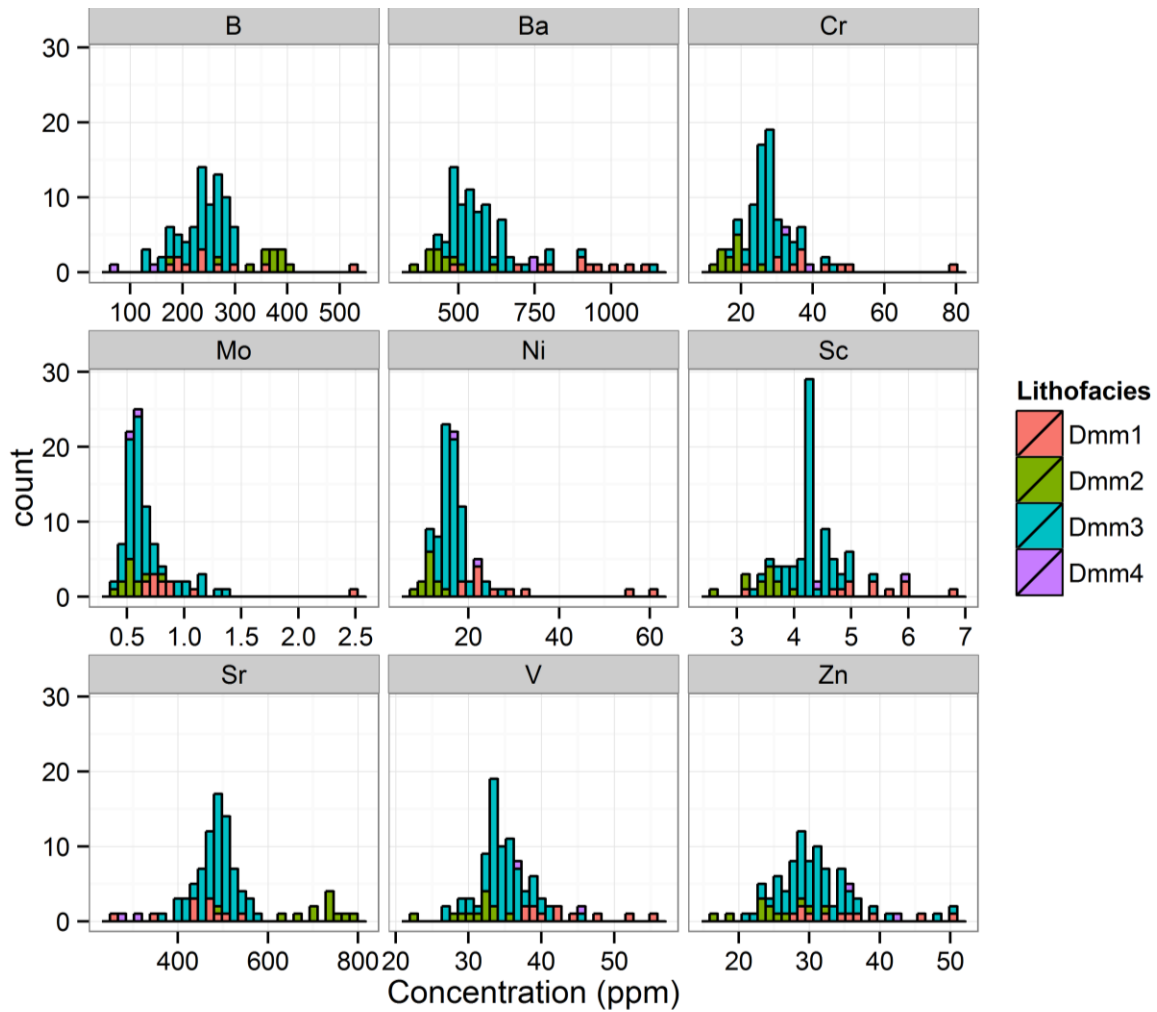


Figure 2-15: Histogram showing the distribution of trace elements in tills (based on total digestion analyses) that are associated with alteration processes. Dmm1 has high concentrations of Ba, Cr, Ni, Sc, and V, and low Sr concentrations. Dmm2 shows very high B and Sr concentrations, but has lower concentrations of most other elements.

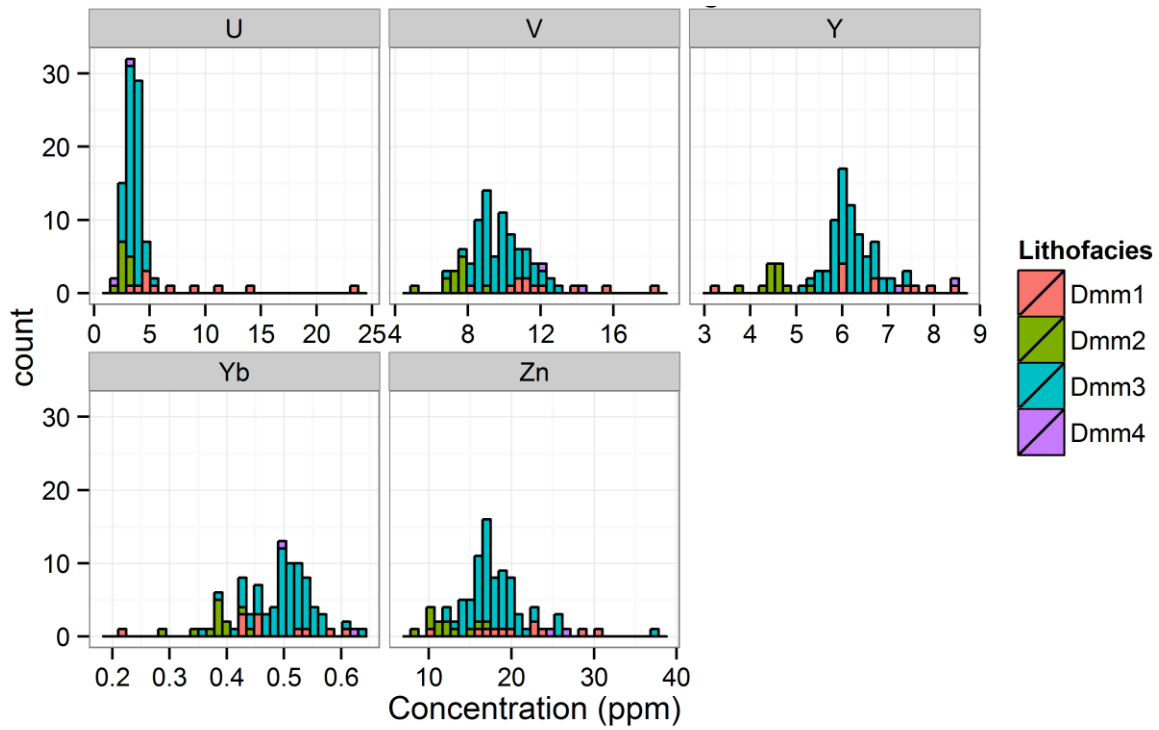


Figure 2-16: Histogram showing the distribution of trace elements in tills (based on partial digestion analyses) that are associated with alteration processes. Dmm1 has the highest concentrations of all elements except for Yb and Zn. Dmm2 has low concentrations of all elements.

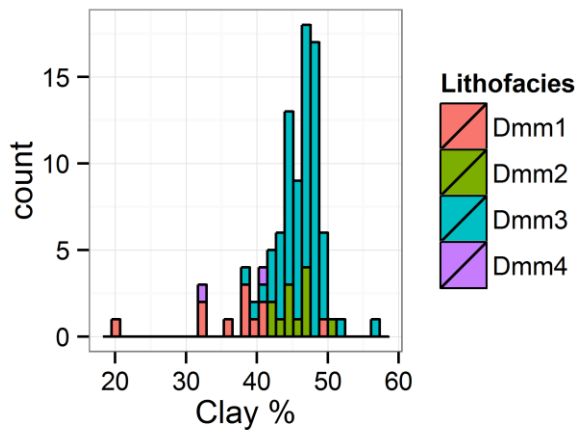


Figure 2-17: Histograms for the clay % of the <63 μm fraction for the Tatiggaq drill core samples. Dmm1 and Dmm4 generally contain less clay than Dmm2 and Dmm3.

2.4.2.2. Multi-Element Anomalies

Principal component analysis was carried out on the drill core samples to assist in the detection of multi-element signatures of alteration in the tills. The resulting bi-plots are shown in Figure 2-18 through Figure 2-22 and the results are summarized in Table 2-3 and Table 2-4.

The PCA of major oxides (K_2O , Al_2O_3 , MgO , Fe_2O_3 , Na_2O , P_2O_5 , MnO , CaO , and TiO_2) shows strong discrimination between Dmm2 and the other lithofacies, whereas Dmm1, Dmm3, and Dmm4 are not discriminated as easily (Figure 2-18). This discrimination is primarily based on PC1. Positive PC1 values are associated with CaO , Fe_2O_3 , Na_2O , and MnO . Negative PC1 values are primarily associated with Al_2O_3 , with lesser influence from K_2O , TiO_2 , and P_2O_5 . PC2 is characterized by positive MnO , MgO , K_2O , Na_2O , and Al_2O_3 values, and negative CaO , TiO_2 , and P_2O_5 values. PC3 shows considerably less variation than PC1 or PC2, but still discriminates Dmm2 from the other units.

Principal component analysis of Sc, V, Cr, Co, Ni, Cu, Zn, Y, and Mo concentrations determined by total digestion of the tills is presented in Figure 2-19 (transition metal grouping). As with the major oxide PCA for till, Dmm2 plots as a separate group from the other units. A combination of positive PC1 and PC2 values, as well as Ni and Cr, discriminate Dmm1 from Dmm2 and Dmm4. Positive PC1 values are associated with Ni, Cr, Mo, Co, Cu, and Zn, whereas negative PC1 values are associated with V, Sc, and Y. Positive PC2 values are associated with Ni, Cr, Sc, and Y, whereas negative values are associated with Zn, Cu, and Co. PC3 shows less of a discrimination between Dmm1 and the other units, and is primarily associated with negative values of Mo.

Principal component analysis of Sc, V, Co, Ni, Cu, Zn, Y, and Mo concentrations determined by partial digestion of the tills is shown in Figure 2-20 (transition metal grouping). PC1 discriminates between the different units, with Dmm2 being associated with negative values. Discrimination of Dmm1 is less pronounced using the partial digest data compared with the total digest data. Positive PC1 values are associated with Ni, Co, and Zn, whereas Y, V, and Mo are associated with negative values. PC2 is associated with positive Sc, Ni, and Y values, and negative Cu, Zn, Co, and Mo values. PC3 discriminates Dmm1 somewhat from the other till units, and negative values are associated with Ni, Mo, V, and Co.

Principal component analysis for the concentrations of “alteration elements” (Ni, Cr, B, V, Sc, Zn, Mo, U, and Sr) determined by total digestion are presented in Figure 2-21. Dmm2 is strongly associated with positive PC1 values and negative PC2 values, whereas Dmm1 is associated with negative PC1 values and positive PC2 values. Dmm2 is associated with B, Sr, and Zn. Positive PC1 values are associated with V, Sc, Zn, Sr, and B. Negative PC1 values are associated with U, Ni, Cr, and Mo. Positive PC2 values are associated with U, V, Ni, and Sc, whereas negative PC2 values are associated with Mo, Cr, Zn, Sr, and B. PC1 and PC2 are both strongly controlled by the geochemical differences between Dmm1 and Dmm2. PC3 shows similar discrimination between Dmm1 and Dmm2 and many of the same elemental associations. However, in PC3, B is associated with positive values.

Principal component analysis for the concentrations of “alteration elements” (Ni, V, Sc, Zn, Mo, and U) determined by partial digestion are presented in Figure 2-22. In the PC1 versus PC2 bi-plot, Dmm2 is discriminated less clearly from the other units based on the partial digest data compared with the total digest data. Positive PC1 values are associated with V, Sc, and Mo, whereas negative PC1 values are associated with Zn, U, and Ni. Positive PC2 values are associated with V, Sc, and Zn, whereas negative values are associated with U, Ni, and Mo. PC3 discriminates Dmm2 from the other units, primarily on the basis of U, but the inclusion of only six elements weakens any interpretation.

The main features observed in the PCA of till drill core is the separation of the various till lithofacies. PCA results for all of the groupings, with the exception of the partial digestion of the transition metals, distinguish Dmm1 and Dmm2 along the PC1 axis which indicates that the geochemical differences between these two lithofacies is responsible for the greatest amount of variability within the data set. Dmm3 tends to occur between Dmm1 and Dmm2, indicating either an intermediate source or a mixing of the two end members.

Table 2-3: Summary table of the main features displayed in PCA for total digestion of till samples.

Group	Dmm1	Dmm2
Major Oxides	+ve PC1, PC2 MgO, MnO, Na ₂ O, Fe ₂ O ₃	-ve PC1, PC2; +ve PC3 P ₂ O ₅ , TiO ₂
Transition Metals	+ve PC1, PC2 Ni, Cr Mo	-ve PC1, PC2, PC3 V, Sc, Y
Alteration Elements	-ve PC1; +ve PC2, PC3 U, Ni, Cr	+ve PC1; -ve PC2, PC3 B, Sr, V, Sc

Table 2-4: Summary table of the main features displayed in PCA for partial digestion of till samples.

Group	Dmm1	Dmm2
Transition Metals	-ve PC3 Ni, Mo	-ve PC1, PC3 V, Mo, Y
Alteration Elements	-ve PC1, PC2, PC3 U	+ve PC1, -ve PC3 Sc, V,

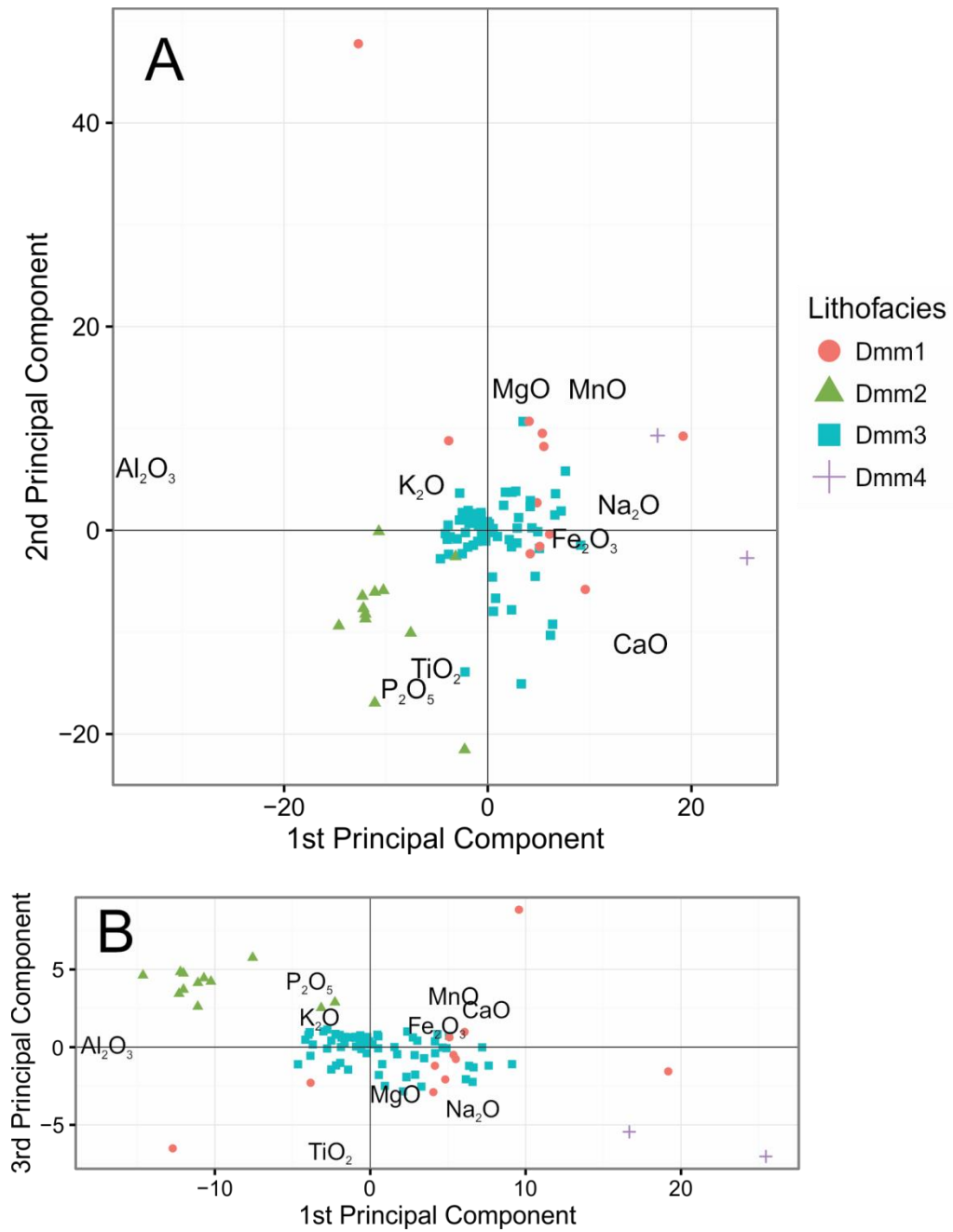


Figure 2-18: Principal component analysis of the major oxide data for the till drill cores (K_2O , Al_2O_3 , MgO , Fe_2O_3 , Na_2O , P_2O_5 , MnO , CaO , and TiO_2). A) 1st and 2nd principal components. B) 1st and 3rd principal components.

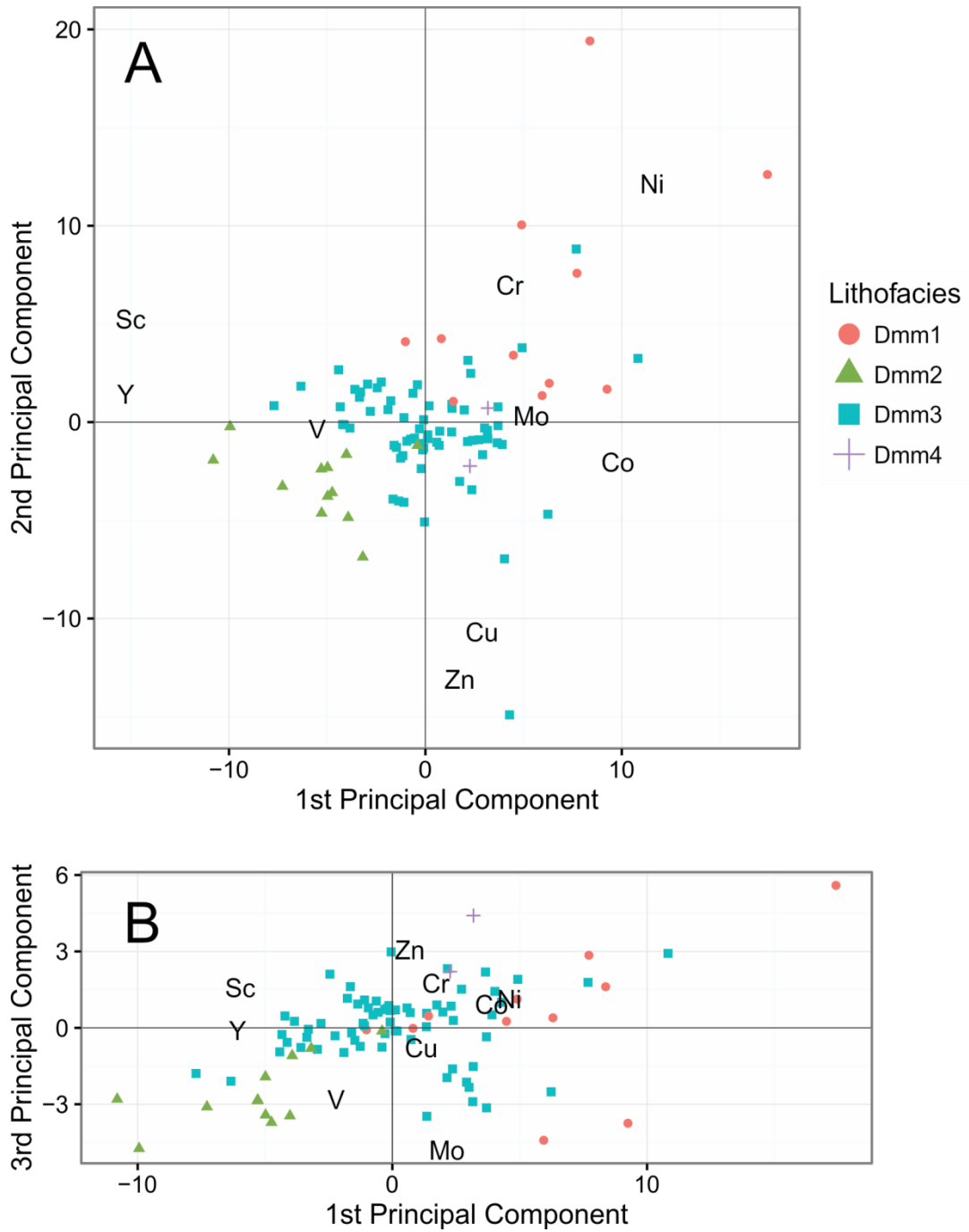


Figure 2-19: Principal component analysis of transition metal concentrations (Sc, V, Cr, Co, Ni, Cu, Zn, Y, and Mo) determined by total digestion of the till drill cores. A) 1st and 2nd principal components. B) 1st and 3rd principal components.

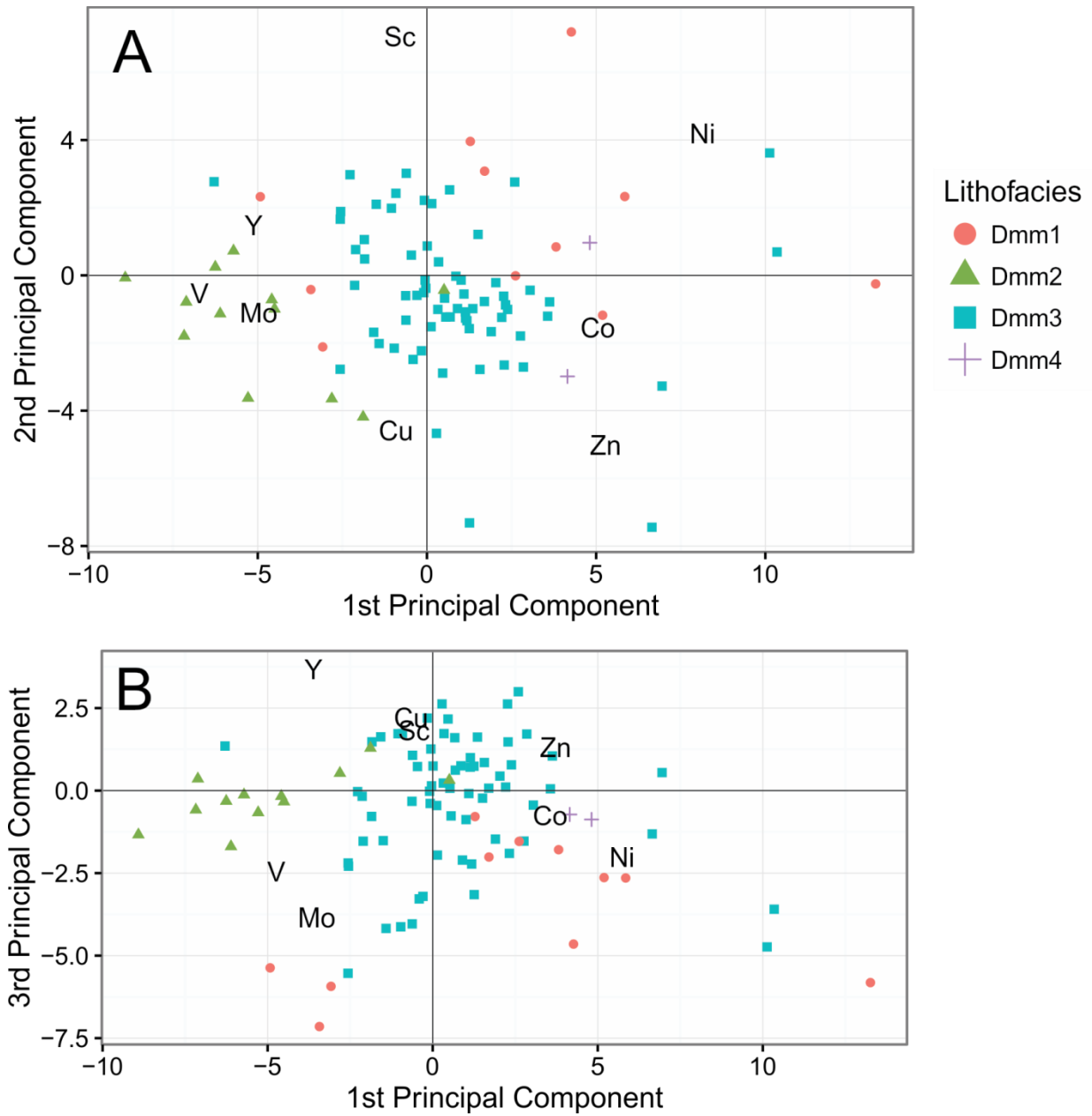


Figure 2-20: Principal component analysis of transition metal concentrations (Sc, V, Co, Ni, Cu, Zn, Y, and Mo) determined by partial digestion of the till drill cores. A) 1st and 2nd principal components. B) 1st and 3rd principal components.

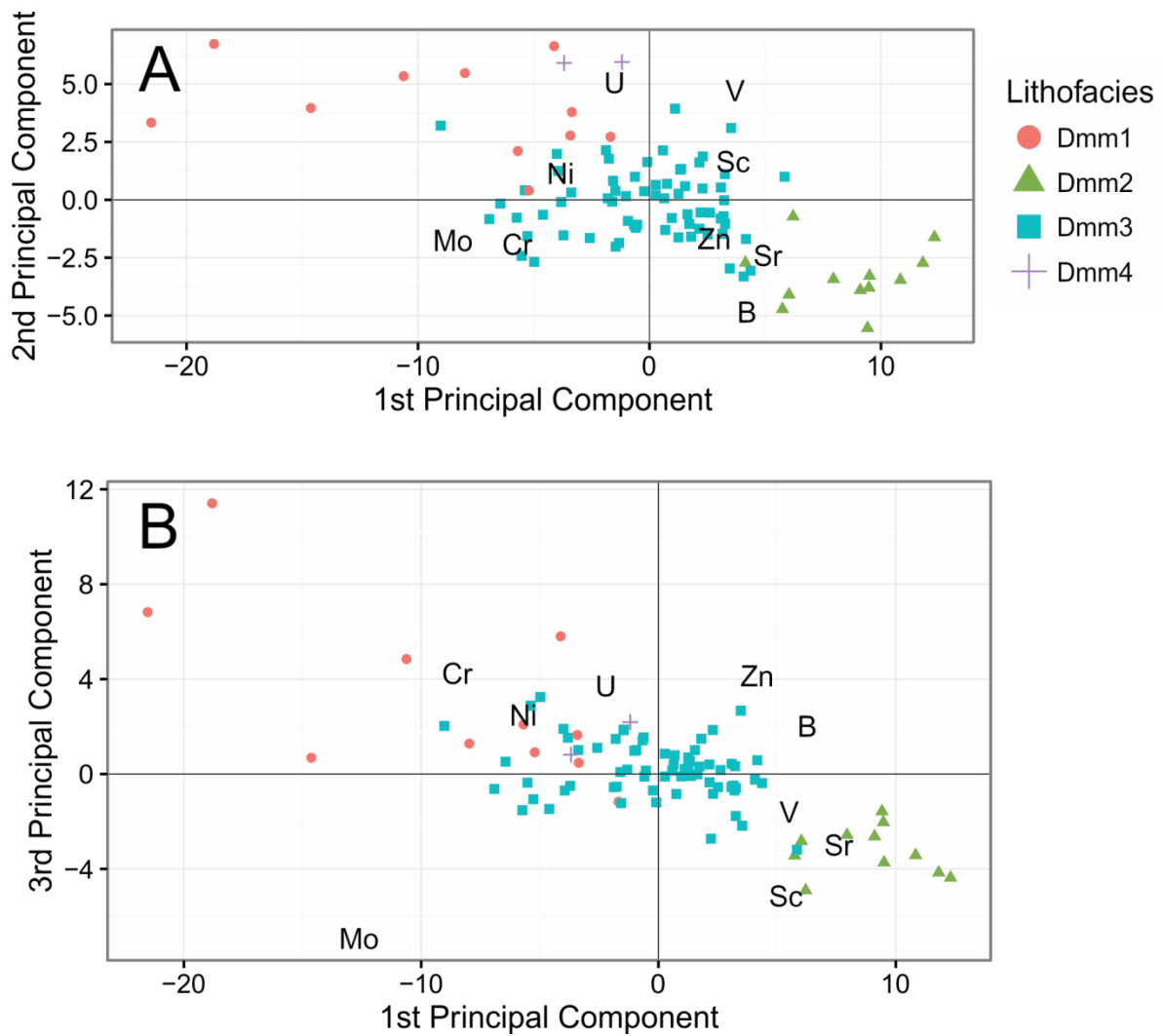


Figure 2-21: Principal component analysis of the concentrations of elements (total digestion method) expected to be good indicators of alteration (Ni, Cr, B, V, Sc, Zn, Mo, U, and Sr) based on this work and previous research (Ruzicka, 1996; Jefferson et al., 2007; Robinson, 2015). A) 1st and 2nd principal components. B) 1st and 3rd principal components.

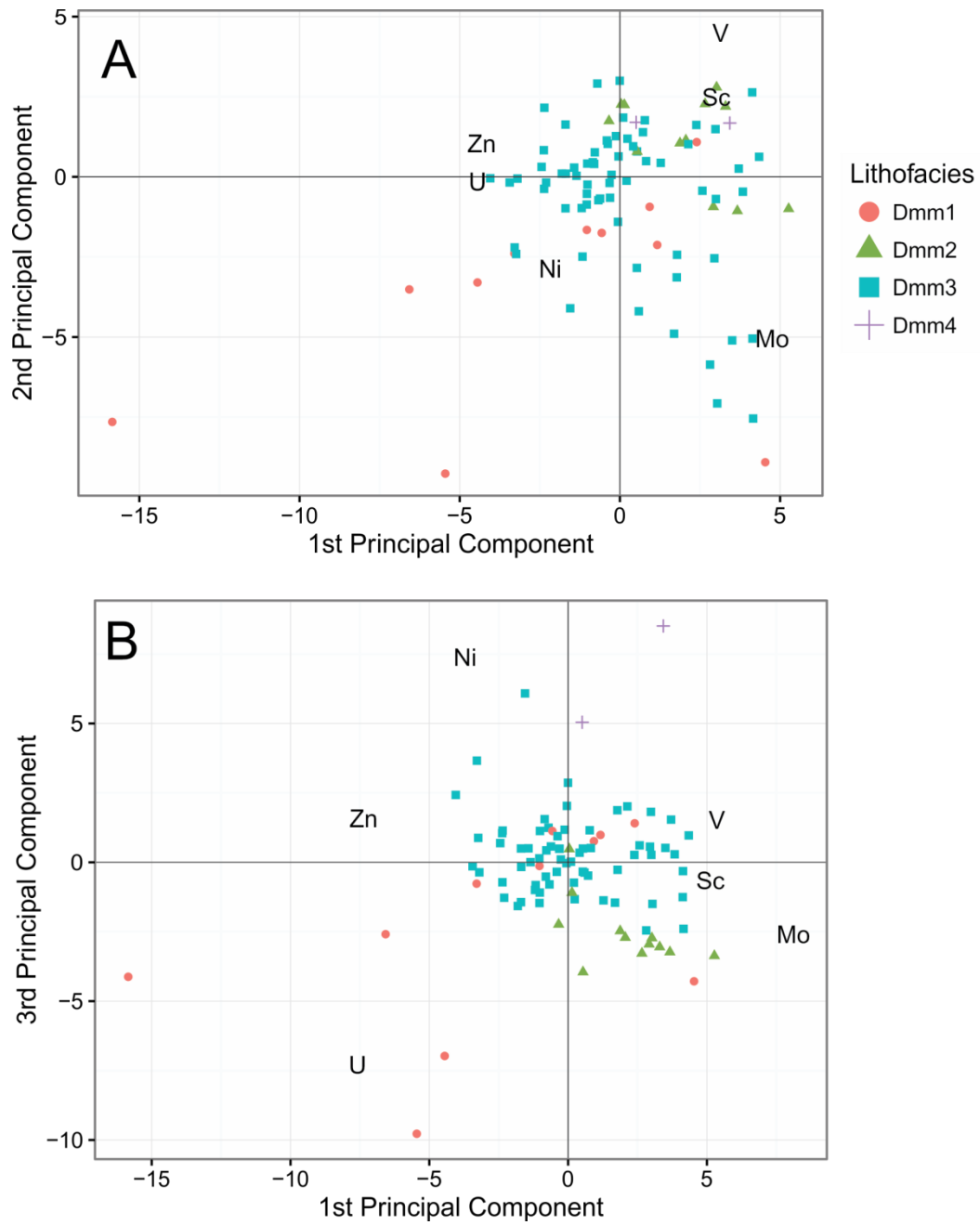


Figure 2-22: Principal component analysis of the concentrations of elements (partial digestion method) expected to be good indicators of alteration (Ni, V, Sc, Zn, Mo, and U) based on this work and previous research (Ruzicka, 1996; Jefferson et al., 2007; Robinson, 2015). A) 1st and 2nd principal components. B) 1st and 3rd principal components.

2.4.2.3. Chemical Index of Alteration

The CIA was calculated for the till drill core samples at the Tatiggaq study area and ternary diagrams presenting the data are shown in Figure 2-23. The minimum, maximum, and mean CIA values for the different till units are presented in Table 2-5. The CIA values for the different tills (~ 70) are generally higher than those of fresh bedrock (~ 50). Two distinct groupings are clearly visible in the CIA data for Dmm1 and Dmm3, where one group for each till unit plots closer to the Al_2O_3 vertex, indicating a higher degree of alteration/weathering. Otherwise, the CIA data for Dmm1 are rather homogenous and follow a short but uniform alteration trend away from the $CaO + Na_2O$ apex. An undergraduate thesis by Wang (2014) at the University of Waterloo did not identify any major dispersal trends associated with CIA in the study area, and thus concluded that CIA is not a useful tool for tracing dispersal from unconformity-type uranium deposits at Tatiggaq.

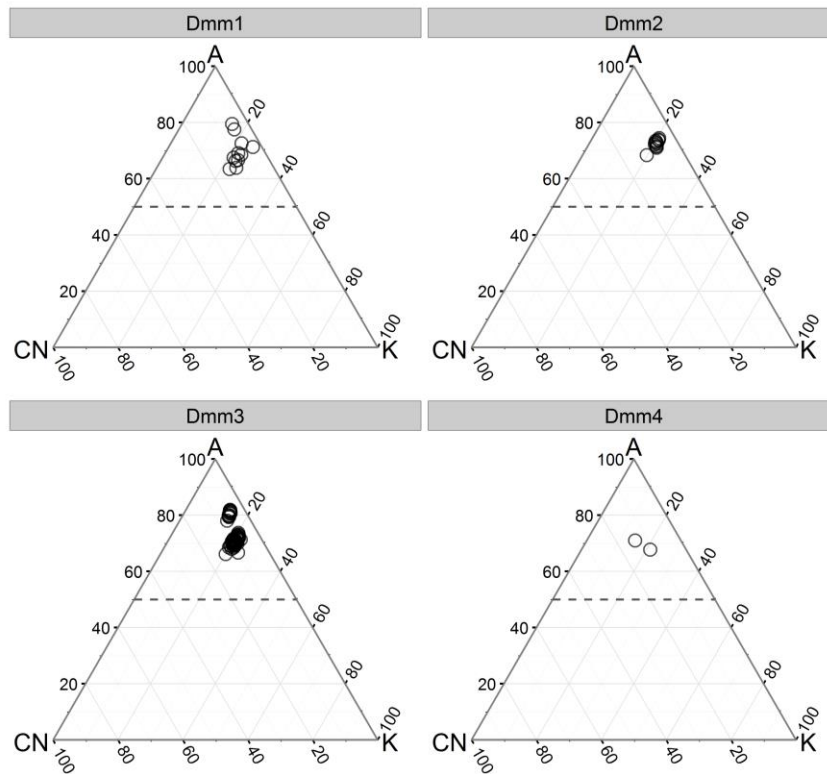


Figure 2-23: Ternary diagrams showing the CIA values for the various till lithologies sampled from the Tatiggaq drill holes. The majority of the samples exhibit high CIA values and distinct groupings can be seen in the Dmm1 and Dmm3 data. The theoretical “unaltered” line where the CIA is equal to 50 is represented by the dashed line.

Table 2-5: Minimum, maximum, and mean CIA values for the different till lithofacies in the Tatiggaq drill core samples

	Minimum	Mean	Maximum
Dmm1	63.5	69.7	79.5
Dmm2	68.4	72.4	74.5
Dmm3	66.2	72.8	82.0
Dmm4	67.8	69.4	71.0

2.4.3. Mineralogical Signature of Alteration in Tills

Clay mineralogy was examined on the clay fraction (<4 µm) of 44 drill core samples and 10 surface samples collected in the Tatiggaq area. The samples were chosen based on their location relative to the subcropping alteration and are arranged along the dominant ice flow direction running from southeast to northwest.

Eleven mineral phases were identified in the clay fraction of the samples with XRD. The phases are: quartz, hematite, muscovite, orthoclase, dickite, albite, dravite, montmorillonite, illite, crandallite, and chlorite. Illite, muscovite, quartz, and montmorillonite were the most common minerals observed. Hematite was only detected in 5 samples. Results from XRD analysis fail to discriminate any major trends within the drill core samples, however, trends can be observed when comparing surficial samples to drill core samples (Figure 2-24), which is essentially comparing Dmm4 to Dmm1, Dmm2, and Dmm3. Montmorillonite is more abundant in the drill core samples compared with the surficial samples. Some minerals, such as crandallite and hematite, consistently occur at or near the detection limit and may be artifacts.

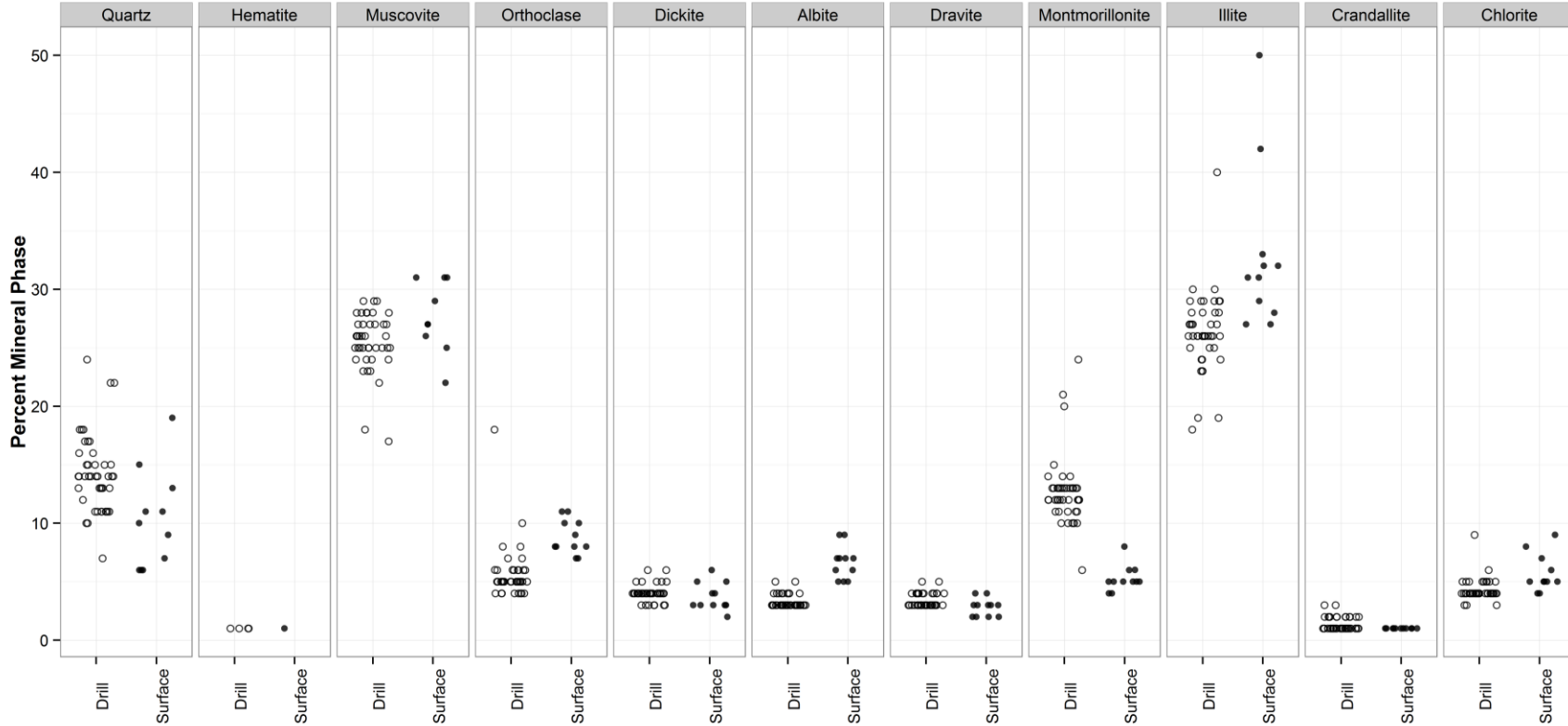


Figure 2-24: Results of X-Ray Diffraction (XRD) analysis of the clay fraction for both surface and drill core samples in the Tatiggaq study area. The most abundant phases are illite, muscovite, quartz, and montmorillonite, which normally have concentrations higher than 10%. Non-detects (numerous for hematite) are not plotted. The surface and drill core samples have similar abundances of chlorite, crandallite, dravite, dickite, muscovite, and hematite. Differences exist between the surface and drill core samples primarily with respect to the abundance of montmorillonite. Differences between surface and drill core samples may be due to different provenances of the tills.

2.5. Discussion

2.5.1. Identifying the Most Effective Pathfinders for Alteration

The identification of alteration zones using geochemical data requires a different set of elements than those used while exploring for subcropping ore bodies since elements that are concentrated in mineralized zones are not the same as the elements concentrated in alteration zones. Based on the single element and multi-element analysis of the fresh and altered whole rocks presented in section 2.4.1 above, the best pathfinders for detecting unconformity-type alteration in the Tatiggaq area can be divided into several groups that are defined by various geological processes.

The first group of pathfinders for unconformity-type uranium alteration consists of the major oxides that are either enriched or depleted during the alteration process. As observed in Figure 2-5 and Figure 2-8, enrichments in Fe_2O_3 , K_2O , Al_2O_3 , P_2O_5 , and TiO_2 are observed in the altered rocks, whereas depletions in CaO , MnO , and Na_2O are evident. Many of these enrichment and depletion patterns can likely be explained by the changes in mineralogy associated with the alteration haloes. During intense illitic alteration of feldspars and other minerals in the host rocks, Ca and Na would be liberated because these elements are not compatible with the structure of illite, $(\text{K}, \text{H}_3\text{O})(\text{Al}, \text{Mg}, \text{Fe})_2(\text{Si}, \text{Al})_4\text{O}_{10}[(\text{OH})_2, \text{H}_2\text{O}]$. However, K, Al, Mg, and Fe are all incorporated into the illite structure and could be preserved. Furthermore, in the study of some alteration zones in the Athabasca Basin, it has been observed that K can be carried by the ore-forming fluid and deposited during alteration (Alexandre et al., 2005). The presence of slightly enriched P_2O_5 in the alteration zone likely reflects the presence of phosphates. Elevated TiO_2 in the alteration zones is likely due to the resistive nature of many Ti-bearing phases, and the low mobility of Ti, on the order of metres, in many hydrothermal settings (Van Baalen, 1993). The depletion of MnO in alteration zones relative to fresh rocks is likely due to the redox-sensitive nature of Mn, since the ore-forming fluids associated with unconformity-type uranium deposits are extremely oxidizing (Kyser and Cuney, 2008).

The second group of elements consists of the trace elements whose concentrations were determined by total digestion of the whole rocks. The total digestion process ensures that most of

the sample is digested for analysis with the exception of the most refractory minerals (Saskatchewan Research Council, 2012). As seen in Figure 2-6 and the PCA results, several elements show clear elevation/depletion trends in the whole rock data. The elements that show the greatest amount of enrichment include B, Ni, U, Cr, and Sc, whereas Mo, Zn, Ba, and Sr show the most significant depletions. Boron shows the greatest level of enrichment in the alteration zones, which has been documented in other areas such as the Athabasca Basin. This is not necessarily expected in the Thelon Basin since dravite, $\text{NaMg}_3\text{Al}_6(\text{BO}_3)_3\text{Si}_6\text{O}_{18}(\text{OH})_4$, is not thought to be present in the alteration zones surrounding the deposits in the region even though small amounts of dravite are observed in the clay fraction of samples analyzed by XRD.

The third group, trace elements whose concentrations were determined by partial digestion of the whole rocks, predominantly shows depleted values in the altered rocks. The depletion in the partially digested rocks compared with the totally digested rocks may be due to the enriched elements identified in the total digest being hosted in refractory phases that are not readily dissolved by the partial digestion method. The primary trends observed within the partially digested whole rock data is the enrichment of U, whereas V, Zn, Y, and Yb all show strong depletion.

XRD analysis of the clay-sized fraction of tills at Tatiggaq failed to detect any significant dispersal related to clay mineralogy. Interestingly, illite dispersal was expected to be observed emanating from the alteration halo since illite is the primary alteration mineral, but the highest illite values are observed in the surficial till units. There are several potential explanations for this result. Firstly, the XRD method used did not have a high capacity for discriminating similar mineral phases such as illite and muscovite. Secondly, tills in the study area are known to have incorporated material originating from the sedimentary rocks of the Thelon Formation (Hodder, 2014), which are known to contain high proportions of illite (Hiatt et al., 2010). High background values of illite in the tills due to the influence of the Thelon Formation, combined with the poor resolution in separating illite from muscovite in the XRD procedure, could explain the ambiguous patterns observed. The occurrence of high background values of illite in the surficial till unit (Dmm4) may also be related to the Kiggavik-Sissons deposits to the east of the Tatiggaq area given that this large group of unconformity-type deposits have illitic alteration

haloes (Robinson et al., 2014), and Dmm4 is interpreted by Hodder (2014) to be derived from westerly ice flows.

Identifying the same geochemical signatures of alteration in the till samples as in the altered whole rocks is critical for the development of a suite of suitable pathfinder elements for tracing the dispersal of alteration in tills. Elements may not provide the same signal-to-noise contrast as they do in the bedrock. This is because till geochemistry will represent a mixture of different geochemical signatures as it is composed of material originating from a number of sources (Stea and Finck, 2001; Klassen, 2001). For this study, Dmm1 of the Tatiggaq drill core samples contains the highest alteration signal since Dmm1 is the lowest stratigraphic unit, is in contact with the altered bedrock surface, and contains the highest proportion of altered clasts. Dmm2 is known to contain abundant clasts from the Thelon Formation (Hodder, 2014), which may result in a higher background level for certain elements, such as B, and a lower background level for other elements, such as Na. Hence, it is important to consider the origin of different till units when identifying potential pathfinders. The selection of less ambiguous pathfinders is desirable.

2.5.2. Potential Indices for Tracing Alteration

Due to the differences in background levels of elements in different parent lithologies, it can be helpful to use element ratios to determine geochemical trends instead of relying on individual elements as pathfinders. By using element ratios, the effect of grain size on controlling the geochemical patterns observed in tills (Shilts, 1995) can also be reduced or eliminated (Mäkinen, 1995). An example of an element ratio is the CIA (Nesbitt and Young, 1982; Fedo et al., 1995). However, given the influence of weathering on the CIA and the effects of K-metasomatism on reducing CIA values (Fedo et al., 1995), it is preferable that indices other than the CIA be developed that are specifically designed for detecting alteration signatures associated with unconformity-type uranium deposits in the Thelon Basin. To highlight the fingerprint of alteration processes, it is effective to divide the elements which are enriched during alteration by those that are depleted. When generating such alteration indices, it is unlikely that one index will definitively discriminate altered versus fresh rocks across the various rock types. It may therefore be useful to apply more than one index in exploration for alteration haloes.

Alteration indices were determined by comparing elements enriched during alteration to those that were depleted, and the ability of the indices to discriminate altered from fresh rocks across the different rock types was compared. The four most promising elemental ratios identified, named alteration index (AI) 1 through 4, are discussed below. The various alteration indices are evaluated based on their ability to discriminate altered and fresh rocks not only within a single rock type, but between fresh and altered rocks of other lithologies as well. This is because till is commonly sourced from multiple lithologies that are present in a region, and false positives due to a local unaltered lithology are undesirable. A closed ratio is used in these indices to ensure that the values fall between 0 and 1. Closed ratios are beneficial in situations where background is variable because it will reduce the noise in the signal related to differing source lithologies at the cost of lowering the maximum signal. Closed ratios take the form of $Ratio_{closed} = \frac{enriched}{depleted+enriched}$, whereas an open ratio would be of the form $Ratio_{open} = \frac{enriched}{depleted}$. Several other alteration indices, such as the Chemical Index of Alteration (CIA) (Fedo et al, 1995), also use closed ratios. A comparison of altered versus fresh rocks using these indices subdivided by rock type is presented in Figure 2-25.

The first proposed index of alteration for identifying unconformity-type uranium is based on using major oxide data and is presented in Equation 2. Alteration index (AI) 1 is generated by using elements enriched for most rock types during alteration (K_2O and Al_2O_3) and elements that which are removed during illitic alteration of minerals such as feldspar and hornblende (Na_2O and CaO).

AI1 succeeds at discriminating between fresh and altered rocks for most of the rock types with the exception of the Thelon Formation, and is very successful at discriminating between the Archean gneiss and the pegmatite.

$$\text{Equation 2: Alteration Index 1} = \frac{K_2O + Al_2O_3}{(Na_2O + CaO) + (K_2O + Al_2O_3)}$$

The second proposed alteration index (Equation 3), utilizes trace elements that show the greatest degree of enrichment during alteration (B, Ni and U), and the elements that show the most consistent depletion (Zn + Sr) (based on total digestion analyses). Alteration index 2 values are higher for altered rocks of each rock type, although there is some overlap between the different rock types. The second index is particularly effective at detecting alteration in the Archean

gneiss, pegmatite, Thelon Formation, and Woodburn Lake Group rocks. Fresh rocks of the Thelon Formation have elevated values as high as those of the altered syenite units, which is due to elevated B levels in the Thelon Formation compared with other fresh rock types.

$$\text{Equation 3: } \textit{Alteration Index 2} = \frac{B + Ni + U}{(Zn+Sr)+(B + Ni + U)} \textit{ (Total Digestion Values)}$$

Alteration index 3 (Equation 4) was derived by examining only the most consistently enriched (Ni) and depleted (Zn) elements based on total digestion and ICP-MS analyses. Although B shows the greatest enrichment overall, it was omitted due to its analysis with a different technique, fusion, and the fact that background B concentrations in the Thelon Formation are higher than in the other rock types. Alteration index 3 is particularly effective at separating altered from unaltered rocks for the hornblende syenite, the quartz syenite, and the Woodburn Lake Group. The ability to differentiate alteration in these three rock types is of particular interest in this study area since the bedrock is predominantly syenite.

$$\text{Equation 4: } \textit{Alteration Index 3} = \frac{Ni}{Zn+Ni} \textit{ (Total Digestion Values)}$$

Alteration index 4 (Equation 5) uses the most enriched element (U) and the most depleted element (V) based on the partial digestion analyses. Alteration index 4 is able to discriminate between altered and unaltered rocks for each rock type except for the pegmatite. This alteration index is not ideal for pegmatite because of the high U concentrations in fresh pegmatite.

$$\text{Equation 5: } \textit{Alteration Index 4} = \frac{U}{V+U} \textit{ (Partial Digestion Values)}$$

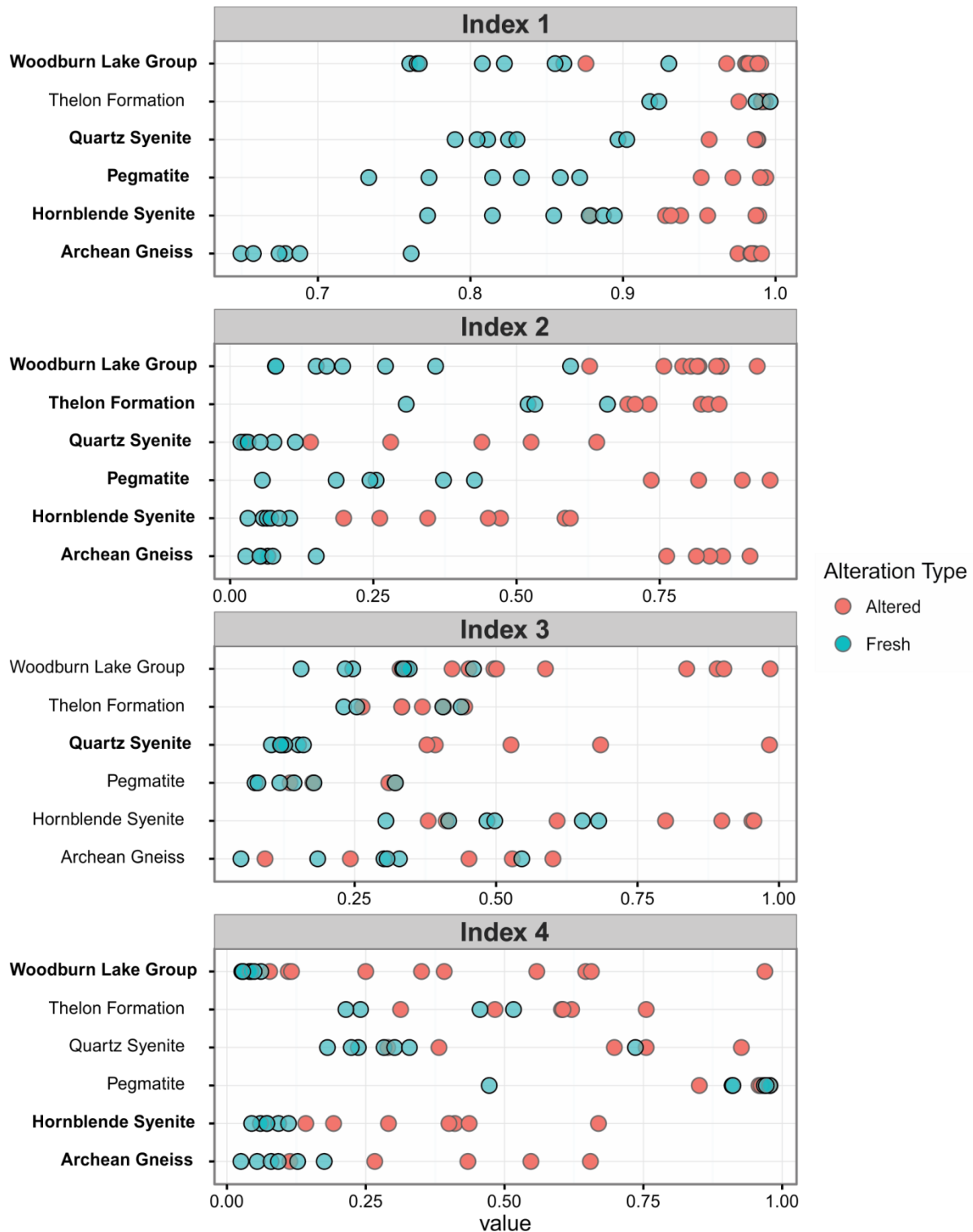


Figure 2-25: Dotplots for the various alteration indices for each rock type. Rock types are bolded where the index is successful at discriminating altered from unaltered rocks (i.e. less than one sample overlap between the two groups). See text for definitions of the alteration indices.

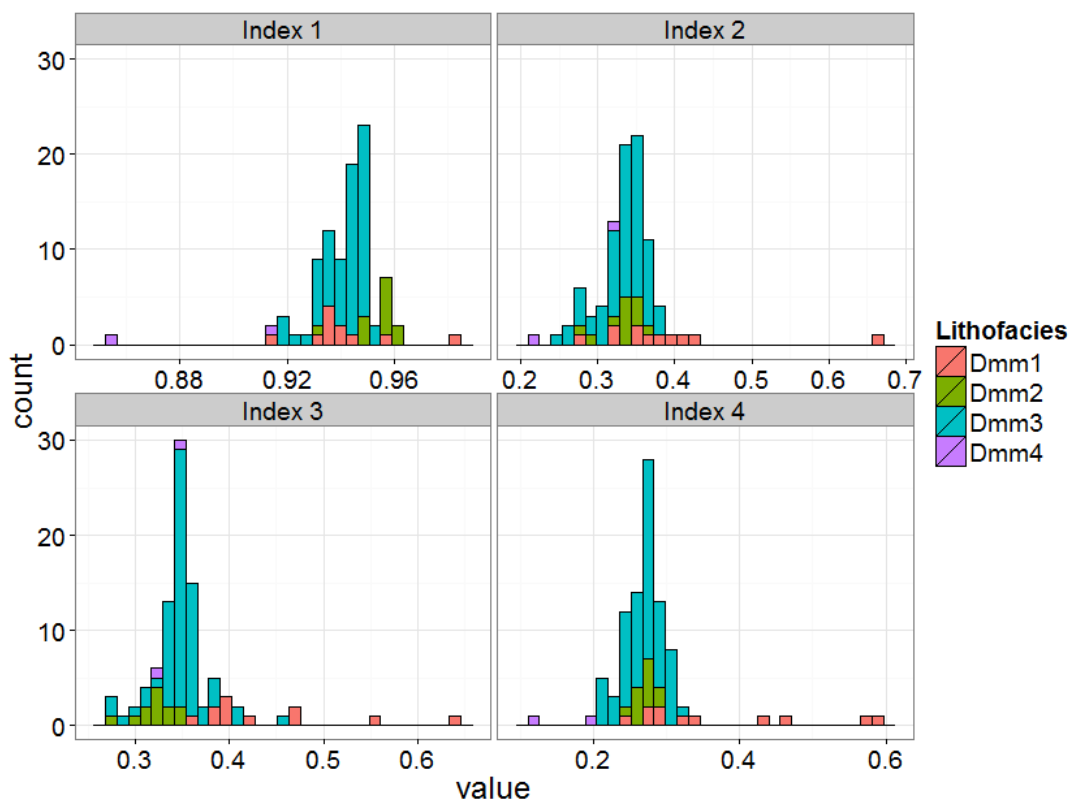


Figure 2-26: Histograms showing the range in values of the different alteration indices for the four different till lithofacies from drill cores.

The surficial samples show significantly smaller values for all of the alteration indices developed with the exception of AI3. In the case of AI1, a distinct population of samples have higher values of around 0.84 (Figure 2-27), which may be indicative of samples with an altered material component. AI2 shows a skewed distribution. AI3 shows a more bimodal distribution. AI4 displays several small populations in the surficial geochemistry data. The distributions of the alteration indices for surficial samples are plotted and discussed in Chapter 3 below.

A graphical comparison between the surficial and drill core samples is presented in Figure 2-28 and summary statistics are presented in Table 2-6. For AI1, the surficial samples have considerably lower values with Dmm4 bridging the gap between the surficial samples and the other drill core lithofacies. Alteration indices 2 and 4 are both similar to AI1 in that surficial samples have consistently lower values than the drill core samples. The pattern of lower overall values for surficial samples is not observed in AI3, however, where there is considerable overlap between drill core and surficial data, with two samples in the surficial dataset having the highest

values in the area outside of Dmm1. The reason for the higher surficial AI3 values in Dmm3 is not well understood, although it may be due to a surficial process that results in a disruption of the proportions of Ni and Zn in the samples.

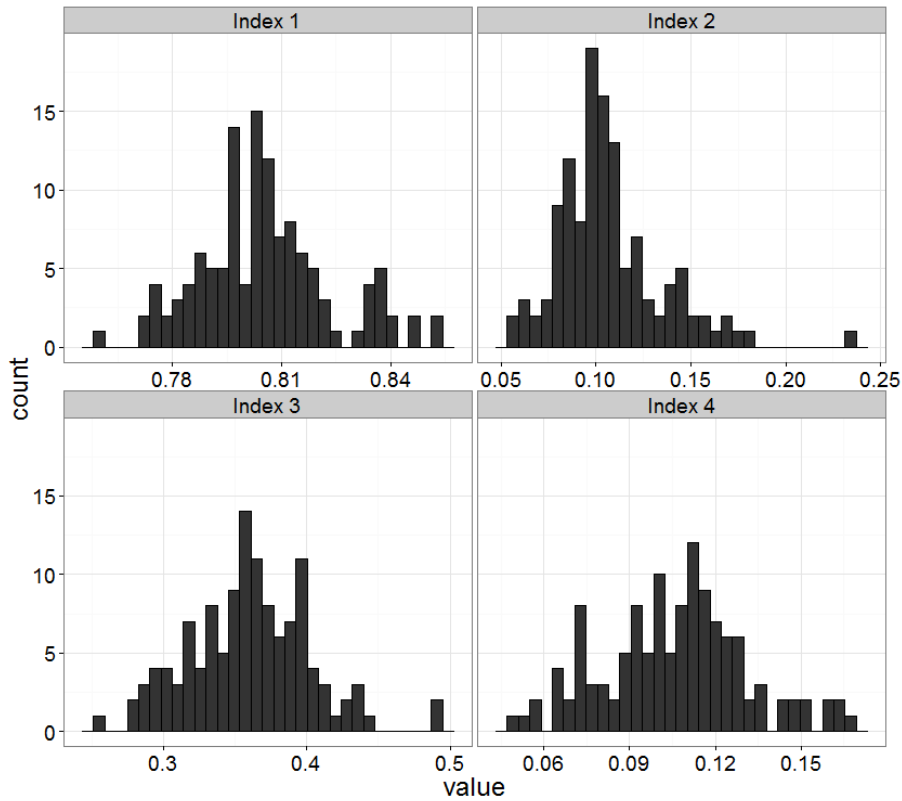


Figure 2-27: Histograms showing the range in values of the different alteration indices for the surficial till samples.

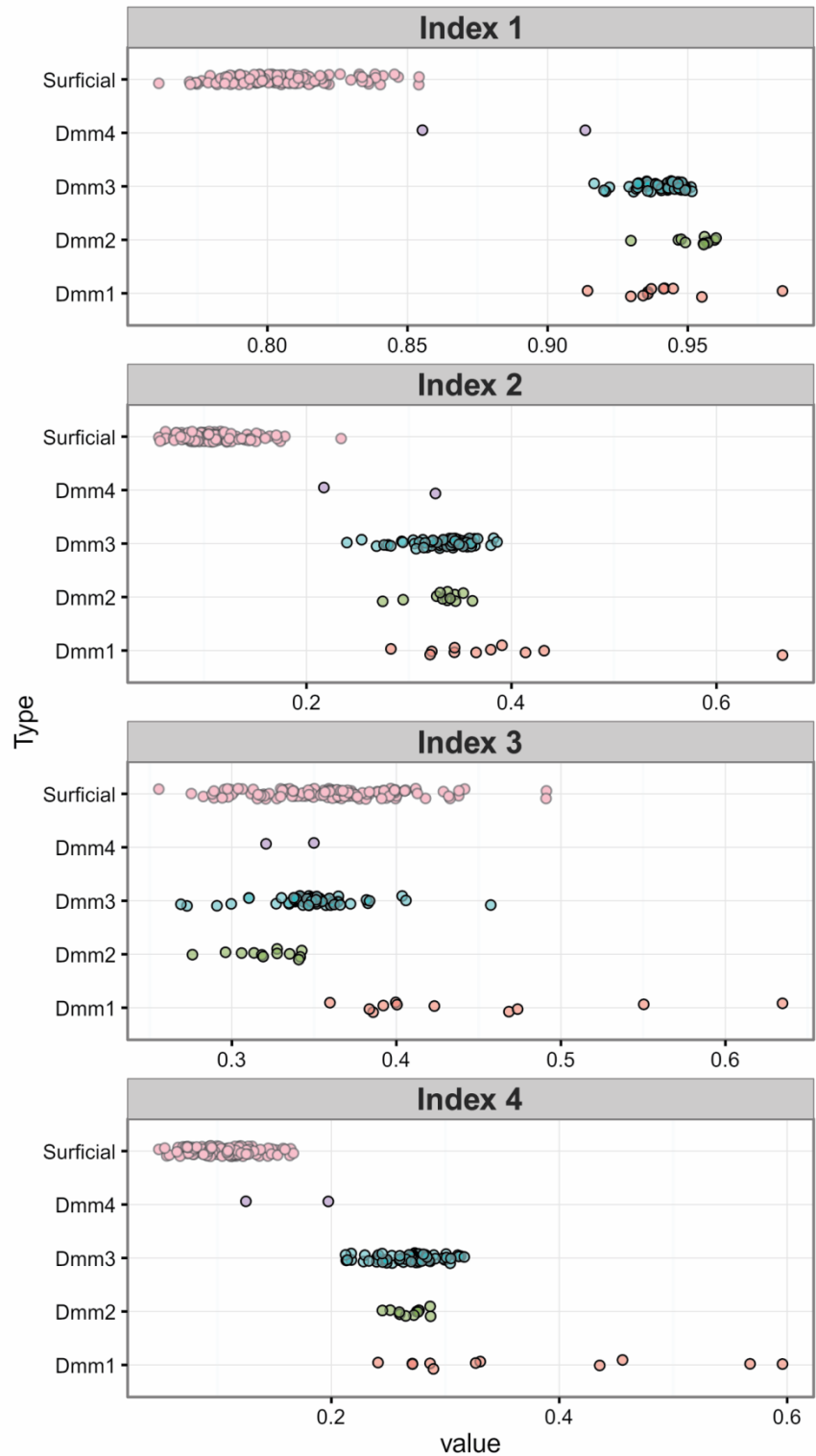


Figure 2-28: Comparison of the alteration indices for all till samples collected in the Tatiggaq area. Note the generally lower values in the surficial samples and the generally higher values in Dmm1.

Table 2-6: Summary statistics for the alteration indices of till samples. Only minimum and maximum values are included for Dmm4 since it only contains two values.

Dmm1	Index 1	Index 2	Index 3	Index 4
Minimum	0.914	0.282	0.360	0.241
Median	0.937	0.366	0.400	0.327
Maximum	0.984	0.664	0.635	0.596
Mean	0.941	0.387	0.443	0.370
Standard Deviation	0.017	0.102	0.084	0.124

Dmm2	Index 1	Index 2	Index 3	Index 4
Minimum	0.930	0.274	0.276	0.245
Median	0.956	0.338	0.323	0.274
Maximum	0.960	0.362	0.342	0.287
Mean	0.953	0.332	0.320	0.269
Standard Deviation	0.008	0.024	0.020	0.013

Dmm3	Index 1	Index 2	Index 3	Index 4
Minimum	0.917	0.239	0.269	0.212
Median	0.943	0.340	0.348	0.271
Maximum	0.951	0.386	0.457	0.317
Mean	0.941	0.333	0.349	0.268
Standard Deviation	0.008	0.030	0.027	0.026

Dmm4	Index 1	Index 2	Index 3	Index 4
Minimum	0.855	0.217	0.321	0.125
Maximum	0.913	0.326	0.350	0.197

Surficial	Index 1	Index 2	Index 3	Index 4
Minimum	0.761	0.056	0.256	0.049
Median	0.804	0.102	0.361	0.109
Maximum	0.854	0.234	0.491	0.167
Mean	0.805	0.107	0.360	0.106
Standard Deviation	0.018	0.028	0.042	0.025

2.5.3. Principal Component Analysis as an Effective Tool for Exploratory Data Analysis

The PCA presented in sections 2.4.1 and 2.4.2 is an effective tool for conducting exploratory data analysis even with data sets that limit the number of elements that can be analyzed.

Traditionally, PCA is conducted on data sets containing hundreds to thousands of samples (Grunsky et al., 2009; Drew et al., 2010; Johnson, 2014), and is mathematically limited by smaller datasets (Reimann et al., 2008). By making informed choices about the elements to

include when conducting the analysis, PCA, and specifically PCA bi-plots, provide a useful tool for the discrimination of different geochemical groupings. PCA of the whole rock data in this study assisted in the visual discrimination of altered and unaltered samples and the elements most strongly associated with alteration. Visualizing expected pathfinder elements in the context of known altered rocks in an area allows for the determination of which pathfinder elements will be most useful. This is because each mining camp is different, and the geochemical and mineralogical nature of ore zones, alteration zones, and host rocks will all influence the geochemical signature of alteration observed in an area.

Principal component analysis has also been shown to be of use when discriminating different phases of till in an area as seen with the drill core geochemical data at Tatiggaq. Although their physical appearance in drill core is similar, Dmm2 and Dmm3 are immediately discernible in many PCA bi-plots (e.g., Figure 2-18). This provides a valuable tool for quickly discriminating till units based on multivariate geochemistry.

2.5.4. Considerations for Geochemistry in Drift Prospecting

The recognition of the alteration signal in tills is not necessarily straightforward, as many types of noise will interfere with its occurrence and there is overlap in expression of alteration in the local rock types. Although not straightforward, the signal of alteration associated with unconformity-type uranium deposits has been demonstrated to be observable in tills. Each alteration index developed has its own weaknesses at discriminating various types of altered and fresh rocks which complicates recognition of alteration. The most promising indices are AI1 and AI2 for the Tatiggaq study area since they show the greatest discrimination between altered and fresh rocks. The lack of overlap between the surficial and drill core samples for most of the indices initially appears discouraging for applications in mineral exploration, however it must be remembered this discrepancy may be chiefly due to differing provenance of the till units. In addition, the signal of alteration is expected to attenuate as it moves upwards through till. Whether the spatial patterns of these alteration indices allow for the tracing of altered material from the surface to the source will be examined in detail in Chapter 3.

2.6. Conclusions

This chapter has identified several pathfinders and indices that can be used in the exploration for deep-seated unconformity-type uranium deposits. It has also been shown that the signals related

to alteration can be observed in till units directly overlying alteration, and that there is potential for the dispersal of these anomalies. The dispersal of these pathfinders and indices will be discussed further in Chapter 3. This study highlights that in areas where more than one lithology is present, it is difficult to identify unambiguous vectors towards alteration based on single minerals or single elements. It is therefore best to use an index of alteration or series of indices that are each suitable for detecting different features related to alteration. Ideally, alteration indices should be constructed by dividing elements that are enriched by alteration processes by those that are depleted, and the use of closed ratios can reduce the effects of geological background variability. The alteration indices identified to detect alteration in the Tatiggaq area are:

$$\begin{aligned}
 - \text{ AI1} &= \frac{K_2O + Al_2O_3}{(Na_2O + CaO) + (K_2O + Al_2O_3)} \text{ (Total Digestion)} \\
 - \text{ AI2} &= \frac{B + Ni + U}{(Zn + Sr) + (B + Ni + U)} \text{ (Total Digestion)} \\
 - \text{ AI3} &= \frac{Ni}{Zn + Ni} \text{ (Total Digestion)} \\
 - \text{ AI4} &= \frac{U}{V + U} \text{ (Partial Digestion)}
 \end{aligned}$$

In the Tatiggaq area, total digestion geochemistry has been observed to show the greatest alteration signal, which is why three of the four alteration indices use total digestion values, and only one (AI4) uses partial digestion data. AI1 and AI2 show the greatest discrimination between altered and fresh bedrock, and AI2 is preferred to AI1 since AI2 is less influenced by input from the Thelon Formation as seen in Dmm2.

The use of multivariate statistical analysis has also proven to be of use in detecting multi-element anomalies associated with alteration processes, and in recognizing these anomalies when they are transmitted to tills. Multivariate statistics such as PCA can also discriminate between different till lithologies.

Both the chemical index of alteration and the mineralogical analysis of the clay fraction of till by X-ray diffraction provide ambiguous results for the detection of alteration zones in this study area. Clay mineralogy may prove to be of use for exploration in some terrains, but the ubiquitous presence of illite in tills restricts its use as an exploration tool in the Thelon Basin.

Chapter 3: Fingerprinting the Signature of Subcropping Alteration Associated with Unconformity-Type Uranium Mineralization in Glacial Sediments, Part 2: Dispersal Patterns through a Thick Multi-Till Succession

3.1. Introduction

Mineral exploration in glaciated terrains often involves the tracing of mineral indicators and geochemical pathfinders that form distinctive dispersal patterns in glacial sediments at the surface. However, identifying dispersal patterns can be a complicated task in areas characterized by a thick multi-till succession and complex ice flow history. Shifting ice flow and associated till production phases are unlikely to generate the classical conceptual dispersal pattern that gently climbs from a buried source towards the surface (cf. Fig. 1-6; Miller 1984). Complex three-dimensional patterns are predicted in areas where multi-till stratigraphy records shifting ice flow directions. An important exploration question is whether the dispersal “plume” is relatively continuous through the till succession and intersects the surface at some distance from its buried source and at a detectable concentration. Few studies have looked into this problem (e.g. Ferbey and Levson, 2009; Ferbey et al, 2012), even though several prospective regions are characterized by multi-till stratigraphy and complex ice flow records.

The Aberdeen Lake area in Nunavut is a prospective region for uranium and is known to have a complex glacial history that resulted in the deposition of at least 4 till units (Hodder, 2014; Hodder et al. 2016), thus complicating the detection of a buried source of interest. In this case, the exploration target is deep-seated unconformity-type uranium mineralization. An additional complication is that mineralization does not subcrop. Instead, a large alteration halo surrounding mineralization intersects the buried bedrock surface. Therefore, it is the mineral products of the alteration that are expected to be traceable in the glacial sediments. Combining the alteration signatures determined in Chapter 2 with the stratigraphic knowledge of the subsurface may make it possible to trace the dispersal of alteration and identify the geochemical signature of alteration at the surface, if it is present.

The aim of this chapter is to use the alteration indices developed in Chapter 2 to visualize and map dispersal of the alteration signature in tills located in the study area (Figure 3-1). The first objective is to determine the spatial extent of the dispersed alteration footprint in the older

subsurface tills. The second objective is to assess the net effect of subsequent ice flow shifts and related till production on the footprint within an area of interest (an exploration drilling target). The third and final objective is to determine whether there is a detectable alteration footprint in the youngest surficial till in the larger study area.

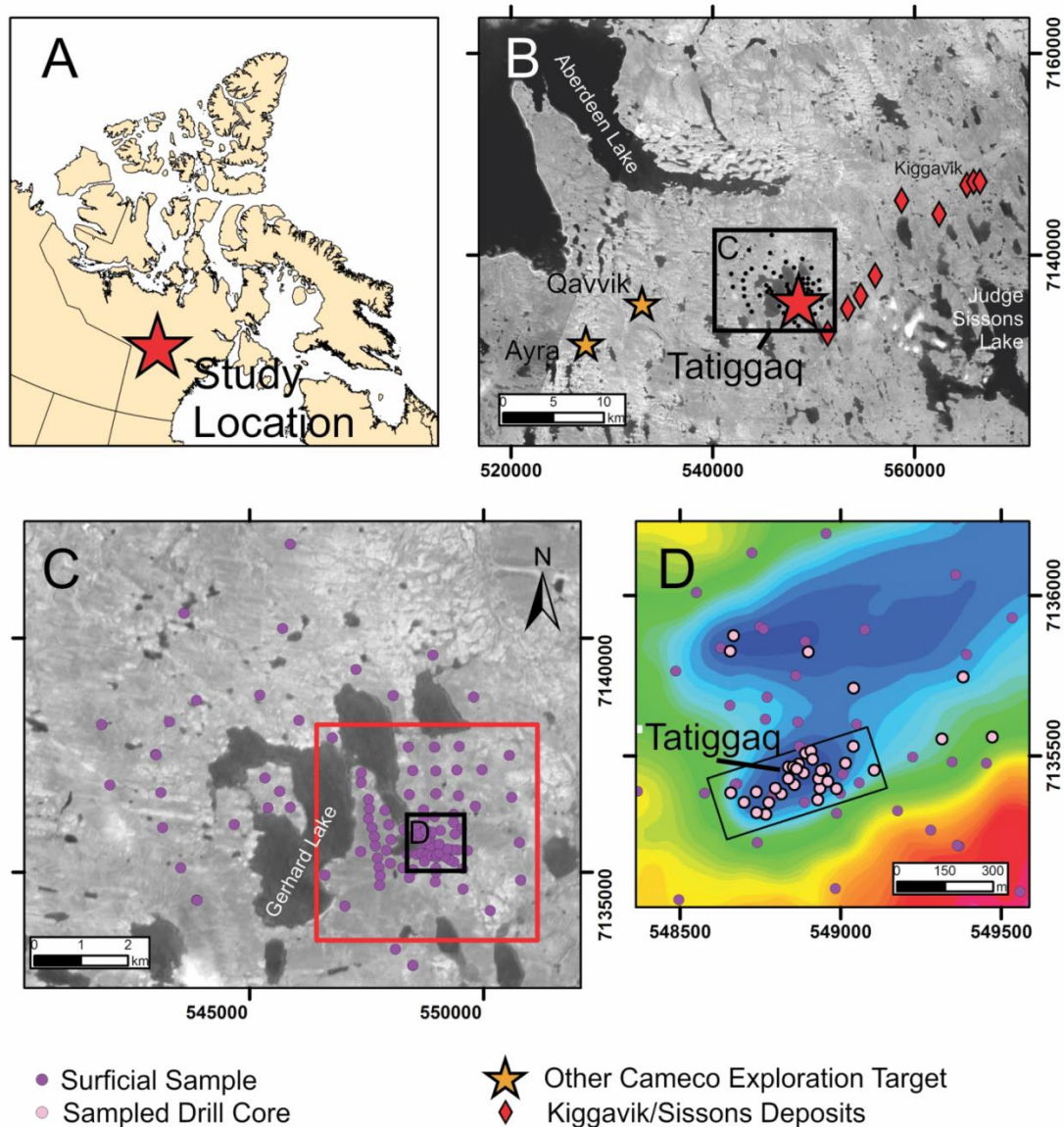


Figure 3-1: A) Study location in Nunavut. B) Regional location of study area, which is located between Aberdeen Lake and Judge Sissons Lake, to the west of the Kiggavik-Sissons deposits. C) Map showing the locations of surficial mudboil samples (purple dots). The red box indicates the location of surficial geochemistry maps presented in figures 3-7 through 3-12. D) Locations of diamond drill holes that were continuously cored and sampled at selected intervals (pink dots) and the locations of nearby surficial samples. The coloured background is gravity data, where blue represents gravity lows and red represents gravity highs. Gravity lows can be associated with areas of higher clay alteration or with areas of thicker sedimentary cover. The black rectangle surrounding the highest density of drill holes in D is the 3D modelled area discussed in this chapter.

3.2. Geologic Setting

3.2.1. Bedrock Geology

The bedrock geology in the study area is comprised predominantly of intrusive rocks belonging to the Hudson Suite (Hunter et al., 2010a, 2010b). The rocks are chiefly quartz syenites and hornblende syenites. Members of the metamorphic Woodburn Lake Group, consisting of pelites and metavolcanic gneisses, are also present at depth. The Thelon Formation is completely absent in the Tatiggaq area and is interpreted to have been eroded. The area is cut by several large faults, and is also intruded by lamprophyre dykes. The rocks surrounding the mineralization, hosted at approximately 100 m depth, are heavily altered and in some places retain little of their primary texture. A more complete description of the rock types in the study area is presented in Chapter 1 (cf. section 1.2.1).

3.2.2. Glacial History

The glacial history and Quaternary stratigraphy of the study area was studied in detail by Hodder (2014). The ice flow history of the area is divided into 4 phases that resulted in the deposition of the 4 till units. The oldest ice flow phase recorded in the area was towards 255°, and the deposition of Dmm1 is correlated to that phase. Subsequently, Dmm2 was deposited by ice flow towards 180°. A migration of the Keewatin Ice Divide resulted in ice flow towards 340°, which deposited Dmm3. The final ice flow event in the area varied from 270° to 300° and was responsible for capping the area with Dmm4 (Hodder, 2014). A more complete description of the Quaternary stratigraphy and glacial history of the study area and surrounding region is presented in Chapter 1 (cf. section 1.2.2).

3.3. Methods

3.3.1. Alteration Indices

Four alteration indices were constructed to trace the dispersal of alteration products through the till succession. These alteration indices are described in detail in Chapter 2 above and were developed by comparing element abundances in altered and unaltered bedrock samples (using total acid digestion and partial digestion methods) collected from drilling programs in the region. Their formulas are listed in Table 3-1.

Table 3-1: Formulas for the four alteration indices developed in Chapter 2.

Alteration Index	Formula
1	$\frac{K_2O + Al_2O_3}{(Na_2O + CaO) + (K_2O + Al_2O_3)} \text{ (Total Digestion)}$
2	$\frac{B + Ni + U}{(Zn + Sr) + (B + Ni + U)} \text{ (Total Digestion)}$
3	$\frac{Ni}{Zn + Ni} \text{ (Total Digestion)}$
4	$\frac{U}{V + U} \text{ (Partial Digestion)}$

3.3.2. Three-Dimensional Modeling

The extent and shape of three-dimensional geological models are often determined by the distribution of borehole data. In this study, the boreholes are concentrated over geophysical targets (i.e., low gravity anomalies). Several boreholes intersected altered bedrock. In this context, it is expected that the full three-dimensional dispersal patterns away from the source extend beyond the area that can be modeled using existing subsurface data. In addition, most boreholes occur along an ENE-WSW trend (Fig. 3-1) that follows the main bedrock structures of interest. This orientation matches relatively closely two of the known ice flow directions in the study area (Dmm1 and Dmm4), but the ice flow direction responsible for producing the thickest till (Dmm3) is nearly perpendicular to that orientation. The spatial distribution of boreholes was thus an important factor that had to be taken into account in the design of this research and, specifically, for the questions that could be addressed.

The three-dimensional model of till dispersal was constructed using GOCAD[®] (Paradigm), which is an object-based geomodelling software program. The locations and drill paths (azimuth and dip) of sampled drill holes were loaded into the program as “wells” and samples were placed along the drill paths using measured depths as “horizons” at the center of the sampled interval. The “horizons” were converted to a “point set” in the software, which allows the extraction of X, Y, and Z (UTM easting, northing, and elevation above sea level). The X, Y, and Z data was then aggregated with its corresponding geochemical information for each sample. In addition to the geochemical samples, a “point set” was also generated for each lithological contact. Markers for the contacts between the 4 till units were determined based on drill core logs (Hodder, 2014), and

where no obvious contact was observed between the different till lithologies that were discriminated geochemically, the contact was interpreted to be at the midpoint between the two samples of different lithologies. The upper surface of Dmm1 was determined based on laminations or related sediments in the drill core as described by Hodder (2014). The contact between Dmm2 and Dmm3 was not obvious in the drill core and relied entirely on taking the midpoint between two samples. The lower boundary of Dmm4 was determined by where lithological changes were observed in the till core, but in the absence of any obvious contact, as was the case with many of the logged drill holes, the contact was interpreted as the end of poor recovery. Point sets for the bedrock and modern day ground surface were generated by using the starts and ends of the drill holes.

GOCAD allows the construction of surfaces using point sets, and a surface was generated for the modern day ground surface, the bedrock surface, and each till lithological contact. Surfaces representing the lithological boundaries as well as the bedrock and ground surface were generated by direct interpolation between points at the contact. Triangular Irregular Network (TIN) surfaces were generated directly from the points. This technique was selected to ensure that each data point was included as a node in the surface. Since the points along the near-vertical boreholes are very close in their XY position, the multiple TIN surfaces would not have crossover issues. The TIN method assumes that the minimum and maximum elevations are sampled in the point data, which may not be true. However, the study area is relatively flat, which makes this assumption reasonable.

Following the generation of surfaces representing lithological contacts, stratigraphic grids (SGrids) were constructed for each lithological unit and the SGrids were made to be conformable between their upper and lower lithological contacts. The generated SGrids do not contain all of the drill holes sampled at Tatiggaq in order to avoid interpolating data with large separation distances. The area modeled in GOCAD is outlined by the black box in Figure 3-1. Cells with a thickness smaller than 15 cm were not displayed. The only units that are not continuous throughout the study area are Dmm1 and Dmm2. The SGrids constructed to represent the till units are each modelled to be 20 cells in the x direction and 10 cells in the y direction. Dmm1, Dmm2, and Dmm4 were each modelled to be 1 cell thick, and Dmm3 was modelled to be 2 cells thick (2 grid layers) since it has more complete sampling and is the thickest unit.

The SGrids were populated by geochemical, lithological, and grain size data of interest by lithofacies. Data for each lithofacies was then interpolated one layer at a time using the discrete smooth interpolation technique (Mallet, 1989) built into GOCAD to map geochemical values continuously across each section of the SGrid. Following the assignment of each property to the individual lithofacies and the interpolation step, the SGrids for the four lithofacies were merged to form a single SGrid. Merging the four lithofacies into a single SGrid allows for the use of a uniform colour scale for presenting the geochemical data. By creating and interpolating within the SGrids separately, it can be ensured that dispersal patterns within an individual unit are maintained. Dmm4 is not displayed in the geochemical interpolations because the unit was represented by only 2 drill core samples. This unit is better analyzed using surface samples, which are discussed separately due to the differing sample media.

3.4. Results and Interpretation

3.4.1. Three-Dimensional Stratigraphic Model

The three-dimensional model constructed using SGrids in GOCAD is presented in Figure 3-2. The location of this modelled block is shown in Figure 3-1D. The model contains five layers of SGrids with one layer for each diamicton unit with the exception of Dmm3, which contains two modelled layers due to its thickness.

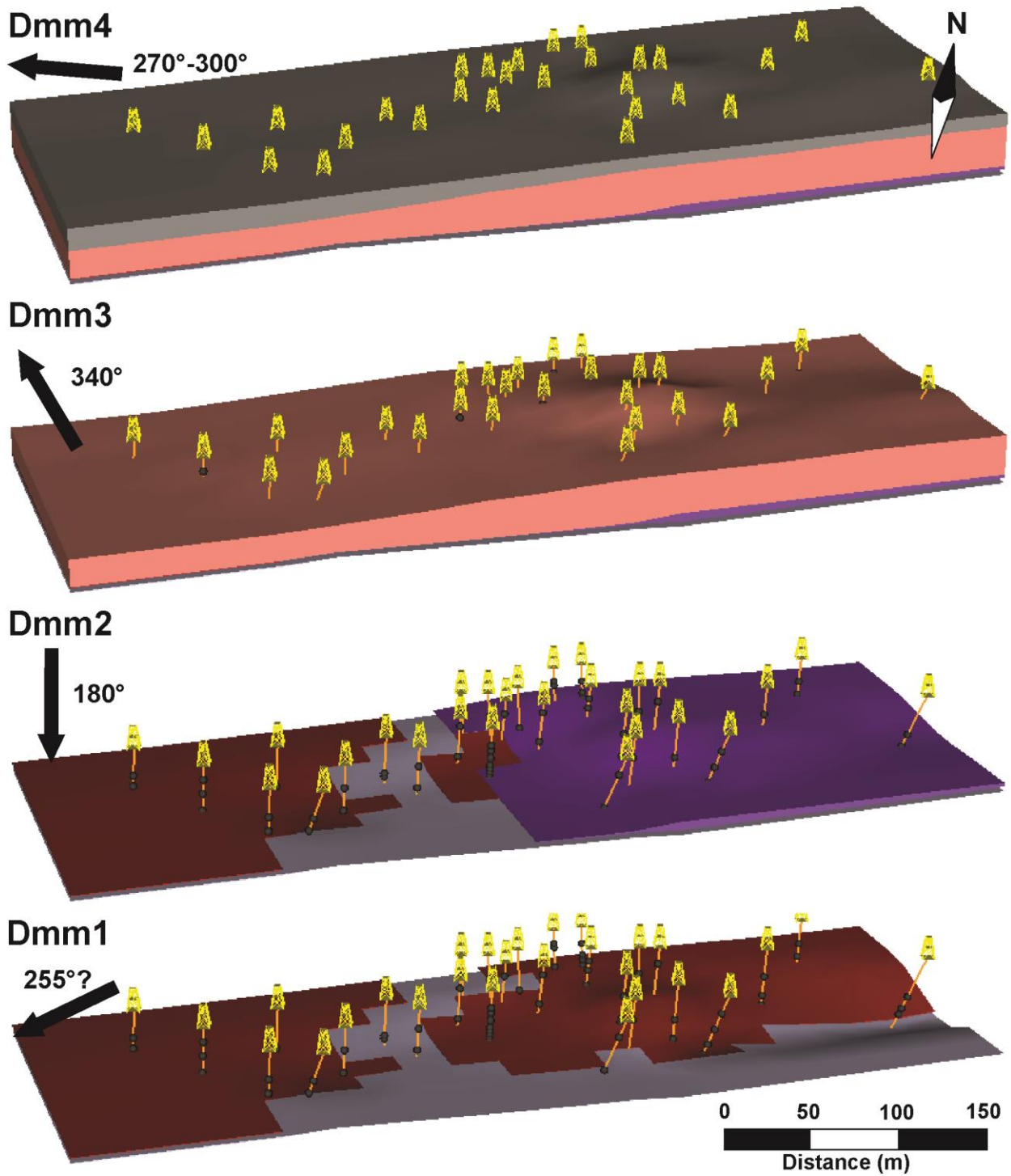


Figure 3-2: SGrids generated for the till units in the Tatiggaq study area (Dmm1, Dmm2, Dmm3, and Dmm4). Also shown are the ice flow phases responsible for their deposition (from Hodder, 2014). Drill holes included for creating the grids are represented by the orange lines and the collars are represented by the yellow derricks. The modelled bedrock surface is shown as grey. Samples are represented by dark grey spheres. The view is looking north, 2x vertical exaggeration.

3.4.2. Three-Dimensional Dispersal Patterns of the Alteration Indices

Mapping of the alteration indices in three dimensions revealed complex spatial patterns that appear to be strongly controlled by the till stratigraphy. The values of AI1 in drill core (Figure 3-3) display several patterns. In Dmm1, the highest values are observed in the boreholes from the southwest of the modelled block, and the DSI interpolation suggests further increase in the SW direction, although it is not well-constrained because it is close to the boundary of the grid. Nonetheless, a southwest high zone (AI1 of about 0.96) is clear from the borehole data alone. In contrast, the lowest values occur in the northern part of the grid. It is important to note that this old till (Dmm1) covers the main bedrock alteration zone and that values of AI1 are low directly above the main zone.

In Dmm2, high values for AI1 are observed in the north/northeast, with moderate values occurring elsewhere. In the lower Dmm3a layer, low values (<0.923) in the middle of the grid are surrounded by relatively higher values (>0.940). In the upper layer (Dmm3b), moderate values (0.940-0.960) dominate, with sporadic low values in the middle and in the north and west corners.

Higher values of AI1 are characteristic of Dmm2 (see Chapter 2). In the 3D model, high values of AI1 are observed in the northeastern corner, consistent with dispersal originating from the north, as determined by Hodder (2014). The high AI1 values in Dmm2 in the northeastern part of the grid are the product of far-traveled Thelon Formation clasts. Overprinting of the already high background values of the Thelon clast-rich till by incorporating altered material amplifies the observed signal in Dmm2.

Dmm3 shows more subtle trends than Dmm1 and Dmm2 and thus is more difficult to interpret. In the lower portion of Dmm3, the high values in the eastern part of the grid may be the result of re-entrainment of material previously transported southward. This is partially consistent with the ice flow history, but it is unclear how the material would have been dispersed eastward towards the main alteration zone. It is possible that these higher values in the eastern portions of Dmm3 originated from the known deposits to the east along the Kiggavik trend, although a local source of the alteration is more probable. This source could potentially be towards the northeast. The alteration signal observed in the upper portions of Dmm3 are easier to reconcile with the ice flow

history in the area, as the high values observed along the bottom edge of the modeled area can be explained by the re-entrainment of material originally dispersed during the southerly flows.

AI2 shows high values in the southwestern portion of Dmm1 (Figure 3-4), which is similar to the pattern observed with AI1. In Dmm2, the high AI1 values in the northeast are not accompanied by similarly high AI2 values. In contrast, high AI2 values are located in the western portion of the layer, which corresponds to the middle of the grid. In the lower Dmm3a layer, the trend is moderate values towards the southwestern part of the grid. In the upper Dmm3b layer, the distribution is patchy, with moderate values in the central and western portions.

The dispersal of AI2 is in many ways similar to the dispersal of AI1. In the drill core model, high values occur in the west end of the modelled grid, which is again consistent with an early flow towards 255° as per Hodder (2014). However, there is a difference in the Dmm2 samples in that there is less evidence of flows towards the south. This is likely because AI2 is superior at discriminating altered from fresh Thelon Formation rocks (Chapter 2). AI2 shows similar trends as AI1 in Dmm3 except for the lack of distinctive high values in the eastern part of the layer. The absence of high values in the eastern portion of the lower layer of Dmm3, together with higher levels being found in the western part of the layer, is supportive of northwesterly ice flows being responsible for the deposition of Dmm3. A slight increase in AI2 values in the upper part of Dmm3 also suggests re-entrainment of southerly transported material by the dominant northwesterly flows in the area.

AI3 shows a different pattern than either AI1 or AI2 (Figure 3-5). The highest AI3 values are within Dmm1, whereas the overlying units have significantly lower values. Within Dmm2, slightly higher values occur to the west, and high values in Dmm3 occur in the central and western portions of the modelled area. AI4 shows a similar pattern as AI3, with the highest values occurring in the western portions of Dmm1 (Figure 3-6). Dmm2 and Dmm3 show little differentiation.

AI3 shows trends very different from those displayed by AI1 and AI2. In the drill core model, the values for Dmm1 are significantly higher than values for any other lithofacies. Nevertheless, the highest values of AI1 in Dmm1 occur to the west of the modelled area, which again is

consistent with early flows towards 255°. In Dmm2, the trend is to higher AI3 values in the western part of the area, indicating some inheritance from Dmm1, although the contrast between Dmm1 and Dmm2 is higher than what is seen in other alteration indices. No evidence of high alteration values associated with southerly dispersal of till rich in Thelon Formation clasts with a high alteration signal is observed in Dmm2. The lower and upper portions of Dmm3 have the highest values in the middle and north/northwest edge of the grid, respectively. The dispersal of AI3 within the modelled area is consistent with dispersal towards 340° being responsible for deposition. In Dmm4, low values are typically observed, with the highest values occurring to the west. AI4 shows the simplest patterns in the subsurface. The highest values are found in Dmm1 to the west of the modelled area, whereas in Dmm2 and Dmm3, there is no obvious structure to the dispersal.

In general, the oldest till (Dmm1) shows patterns for all indices that are oriented to the southwest. These patterns are consistent with the old ice flow phase towards 255° associated with that till (Hodder et al., 2016). Dmm1 partly covers the main alteration zone, which means that after deposition of Dmm1, the main zone became largely protected from further glacial erosion. It is unclear with the current subsurface data coverage whether altered debris from partial erosion of Dmm1 were dispersed southward in Dmm2 because the gridded model is too small to capture any southward dispersion. Moving up the till stratigraphy, the patterns quickly become more elusive. It is possible that Dmm3 re-entrained altered material from Dmm1 in the southwest corner of the grid and transported it in the northwest direction. Similarly, altered debris in Dmm2 dispersed to the south could have been brought back over the study area by Dmm3, but this cannot be verified.

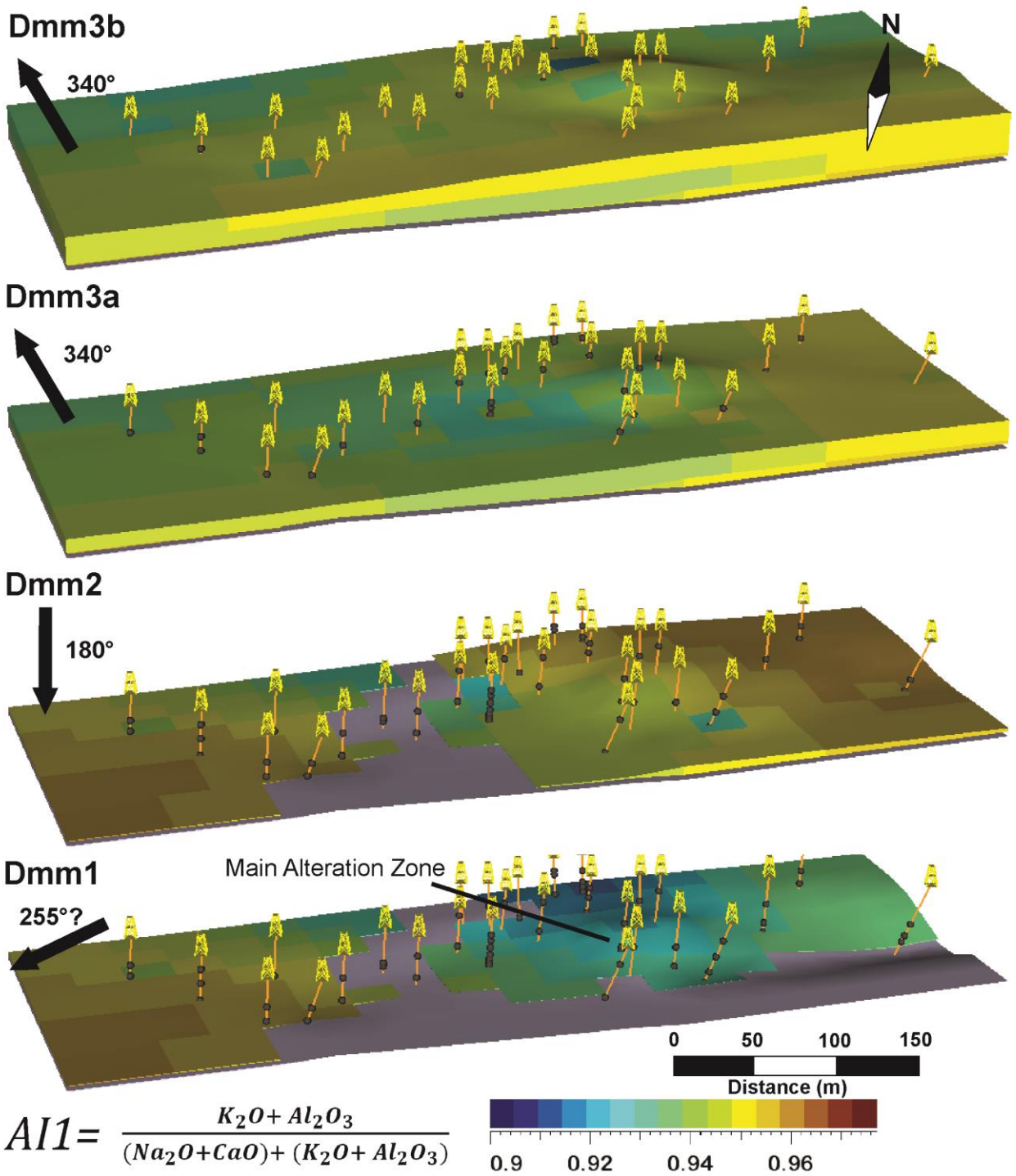


Figure 3-3: 3D model of the dispersal of Alteration Index 1 (using total digestion values) through the different till units. Dmm4 is not modeled as it only contained 2 samples. Arrows on the left show the ice flow direction responsible for deposition of the respective unit (from Hodder, 2014).

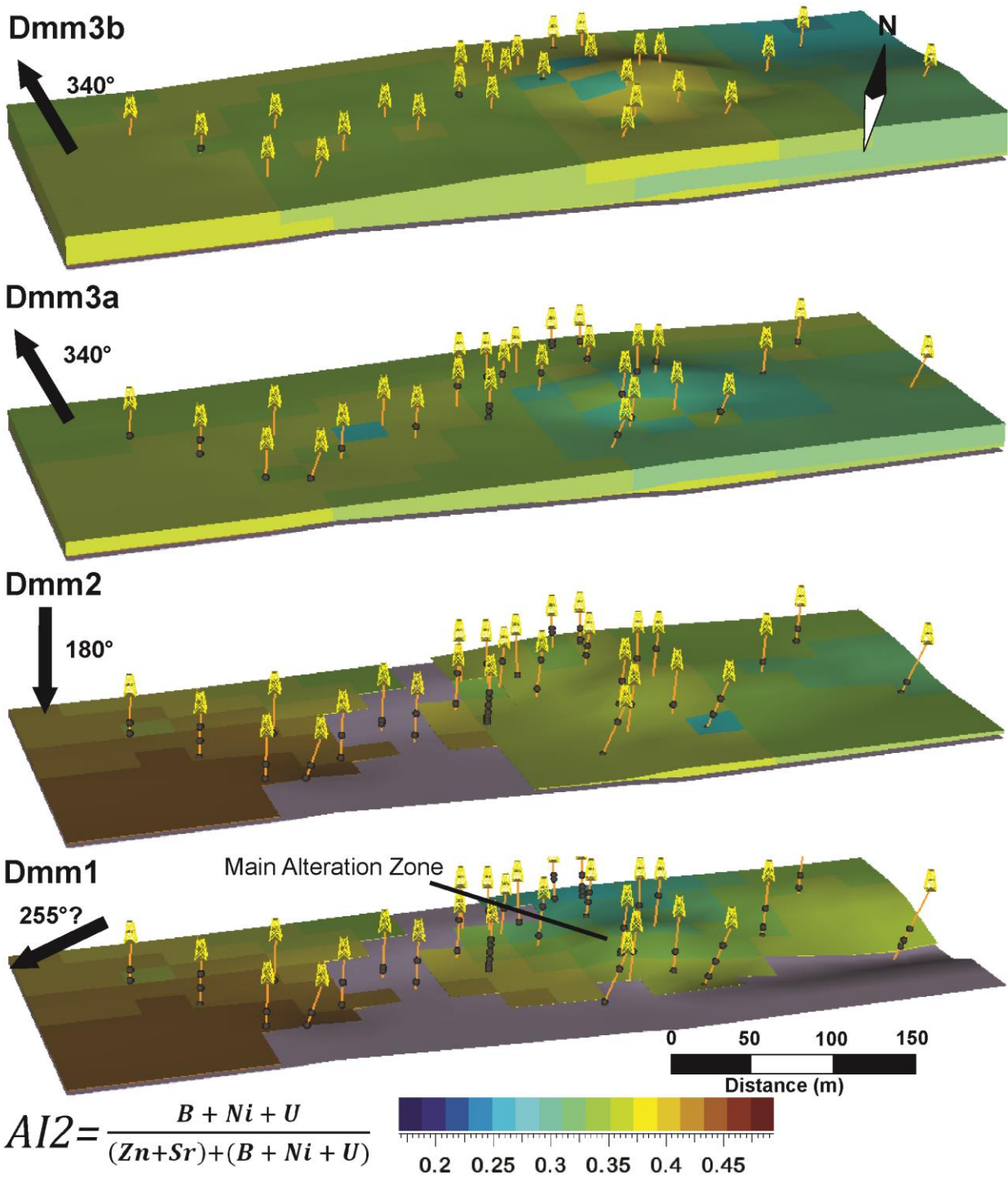


Figure 3-4: 3D model of the dispersal of Alteration Index 2 (using total digestion values) through the different till units. Dmm4 is not modeled as it only contained 2 samples. Arrows on the left show the ice flow direction responsible for deposition of the respective unit (from Hodder, 2014).

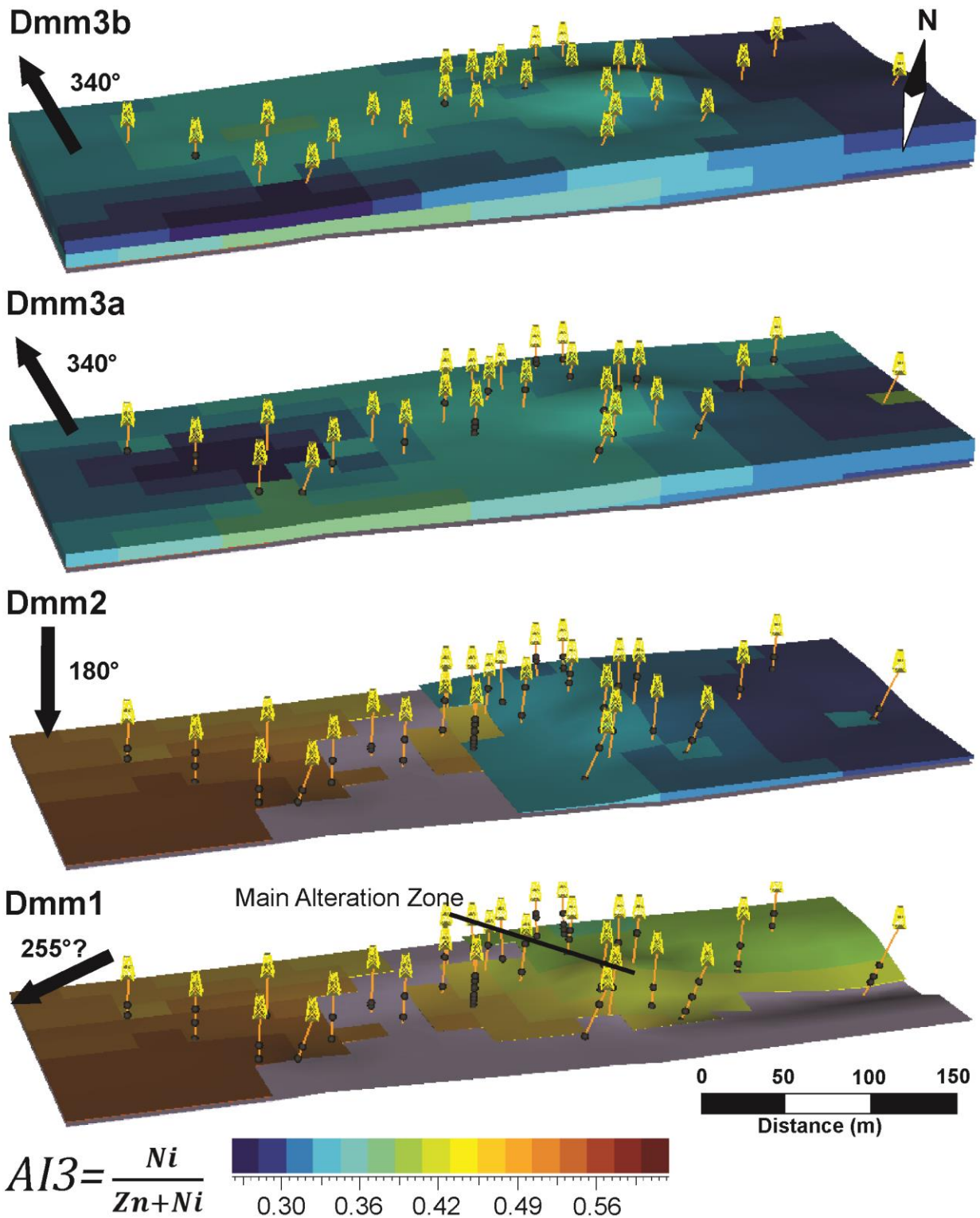


Figure 3-5: 3D model of the dispersal of Alteration Index 3 (using total digestion values) through the different till units. Dmm4 is not modeled as it only contained 2 samples. Arrows on the left show the ice flow direction responsible for deposition of the respective unit (from Hodder, 2014).

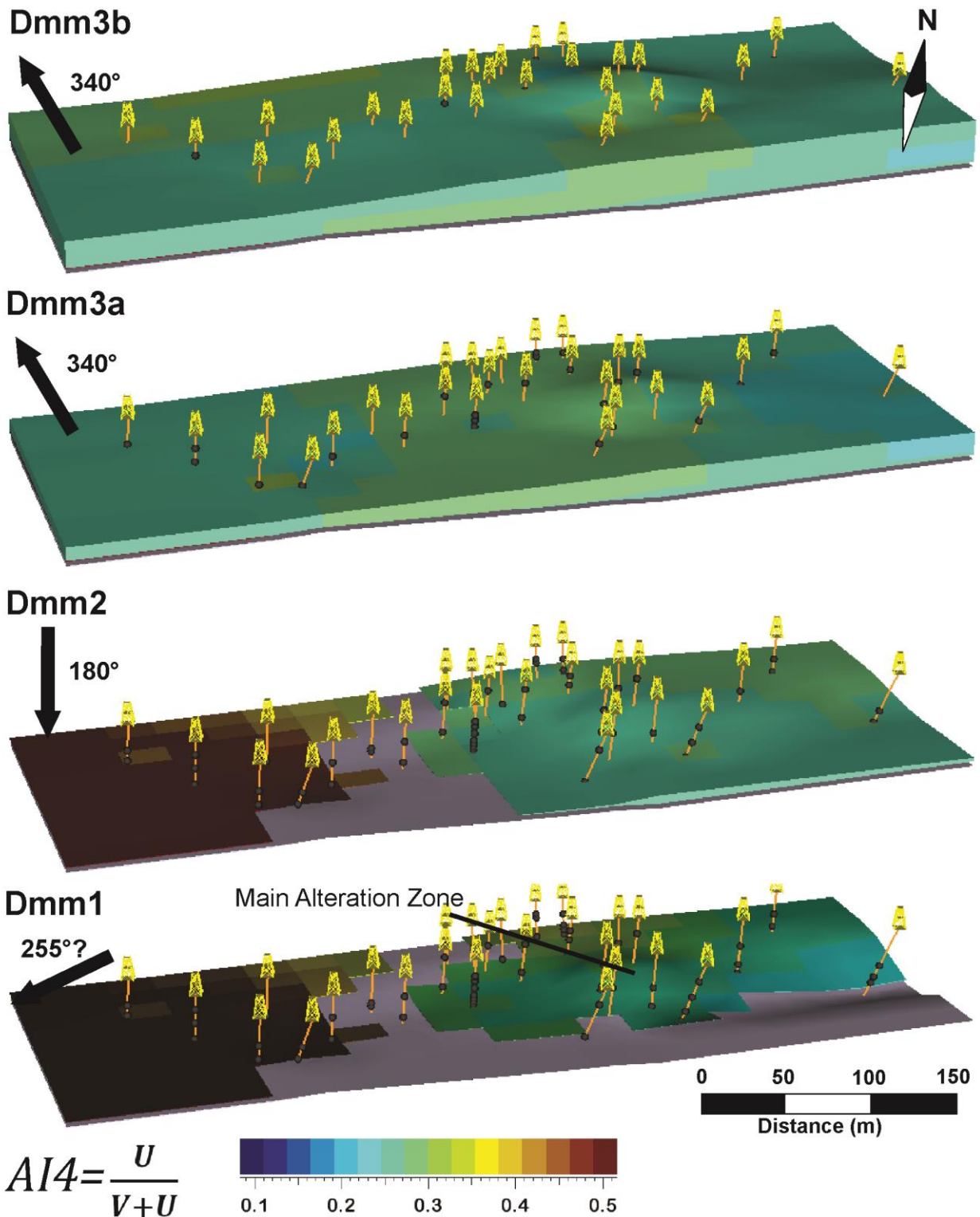


Figure 3-6: 3D model of the dispersal of Alteration Index 4 (using partial digestion values) through the different till units. Dmm4 is not modeled as it only contained 2 samples. Arrows on the left show the ice flow direction responsible for deposition of the respective unit (from Hodder, 2014).

3.4.3. Surficial Dispersal Patterns

The spatial distribution of the surficial alteration indices is shown on Figures 3-7 to 3-10. For AI1, most values are below 0.83 (Figure 3-7). However, at about 1 km northwest of the main subcropping alteration zone, there is a cluster of five surface samples with higher values ranging from 0.835 to 0.854. Two isolated samples with values around 0.85 occur northwest of the main zone. A few more isolated samples with values >0.835 occur to the south and southeast of the main zone, with one occurring less than 500 m to the south and another approximately 2 km to the southeast (Figure 3-7).

AI2 shows similar patterns as AI1, in that the >90 th percentile samples (i.e., high values) appear to mostly occur northwest of the main alteration zone (Figure 3-8). A few isolated samples with similar values occur to the south/southeast. The high AI1 value observed approximately 2 km to the southeast is not accompanied by a high AI2 value.

Surficial dispersal of AI1 is consistent with a composite dispersal pattern as described by Parent et al. (1996). The dispersal appears as fan-shaped. The relatively higher values observed directly to the south and southeast of the primary alteration zone are likely related to compositional inheritance in Dmm4 from older southward phases. The highest values in the surficial dispersal lie along a line oriented towards the west and northwest, which is coincident with the predominant ice flow phase in the area. The two samples on this line, falling within the 90th percentile, are likely the result of re-entrainment related to the late westerly ice flows in the area. One sample in the study area, located approximately 2.5 km to the southeast, is interpreted to be related to dispersal originating from the Andrew Lake deposit. The predominance of high values in close vicinity to the Tatiggaq alteration zone, and down-ice from it in the predominant ice flow direction (340°), strongly suggests that the surficial expression of AI1 is related to dispersal originating from the Tatiggaq alteration zone. In summary, Dmm4 was deposited by westward-flowing ice, but it shows weak compositional inheritance from the two previous ice flow phases due to re-entrainment and incorporation in Dmm4 of debris from Dmm2 and Dmm3.

In terms of surficial dispersal, AI2 again shows similar features as AI1. For the most part, the highest values fall along a line trending towards the northwest, with 2 samples occurring to the south/southeast of the main alteration zone. The interpretation for AI2 dispersal is the same as for AI1, namely that the dispersal of AI2 is related primarily to the dominant 340° flows in the

area following early southerly dispersal, and later minor re-entrainment by late westerly flows. In the case of AI2, there are high values in the area that are not related to the alteration zone at Tatiggaq. The source of these two anomalous samples is uncertain but may also be due to the presence of farther-traveled material originating from deposits along the Kiggavik trend.

As with the drill core data, AI3 shows an entirely different expression at the surface than AI1 and AI2 (Figure 3-9). The highest values (>90th percentile) occur almost exclusively within 1 km of the alteration zone, with the exception of two samples located approximately 6 km northwest and ~2 km north of the main alteration zone. Other than these two exceptions, the high AI3 values occur in a much smaller region compared with the high AI1 and AI2 values, which suggests that AI3 is influenced by different processes. Unlike the other alteration indices, AI3 values are higher in the surficial samples than in Dmm3b. This increase could be due to the differing provenance of the surficial unit, although the localized highs in the surface make this possibility unlikely. Another possibility is that some surficial process has enhanced the signal over the alteration zone.

The surficial dispersal pattern for AI3 is more similar to the amoeboid pattern of Parent et al. (1996) than the fan/palimpsest pattern observed with AI1 and AI2. The dispersal at surface is constrained to within 1 km of the alteration zone and appears to be the result of south/southeasterly flow followed by dispersal towards the northwest. The anomalous value occurring several km to the north of the alteration zone is not interpreted to be related to dispersal originating from the alteration zone.

In addition to AI3, total digestion values for Ni divided by Zn are plotted (Figure 3-11) to determine the effectiveness of a closed ratio versus an open ratio as a pathfinder [$\text{Ni}/(\text{Ni}+\text{Zn})$ vs Ni/Zn]. Again, the Ni/Zn ratios are highest directly over the main alteration zone. However, the signal of the alteration zone is not as obvious as it is in the AI3 plot which leads to a smaller exploration footprint. This difference could be linked to the increased noise caused by using an open ratio versus a closed ratio, as discussed in Chapter 2.

The difference in dispersal pattern of AI3 compared with AI1 and AI2 is most likely due to the differences in geochemical characteristics of the indices, even though both Zn and Ni are used in AI2 and AI3. AI1 is at one end of the spectrum, as it consists entirely of major elements that are

likely to be important structural components of the alteration minerals and are unlikely to be mobilized by processes other than strong chemical weathering, whereas the behavior of Zn and Ni is entirely different as evidenced by AI3 dispersal patterns. This indicates that Ni may be hosted within a refractory phase that is either emplaced during alteration or resistant to alteration.

AI4 does not show any obvious patterns at the surface in terms of the distribution of high values (Figure 3-10). A high value is located directly over the main alteration zone although this is likely a coincidence given that the other high values in the study area appear to be randomly distributed.

Since B is enriched in altered bedrock samples (cf. Section 2.4.1) and is included in AI2, surficial geochemistry values for B are also shown (Figure 3-12). No obvious surficial B patterns are observed, with just one high value occurring directly west of the alteration zone. Boron values in the surficial unit are significantly lower compared with drill core values.

A comparison of ratios to single elements, such as B in AI2 (Figure 3-8) compared with just B alone (Figure 3-12) indicates that using a combination of enriched elements and depleted elements in closed ratios produces a clearer picture of dispersal. For B, this is magnified by the low values observed in the surficial mudboils compared with the drill core samples.

The dispersal of the CIA was also tested in this project. The results are described in Wang (2014). Dispersal of the CIA in the subsurface did not show clear dispersal trends due to the influence of K-rich illite in Thelon Formation sandstone. Wang (2014) did identify high values to the west of the alteration zone, but other high values in the area and a lack of coincident geochemical trends in the subsurface resulted in the conclusion that the CIA is not a reliable index for tracing the dispersal of alteration from unconformity-type uranium deposits.

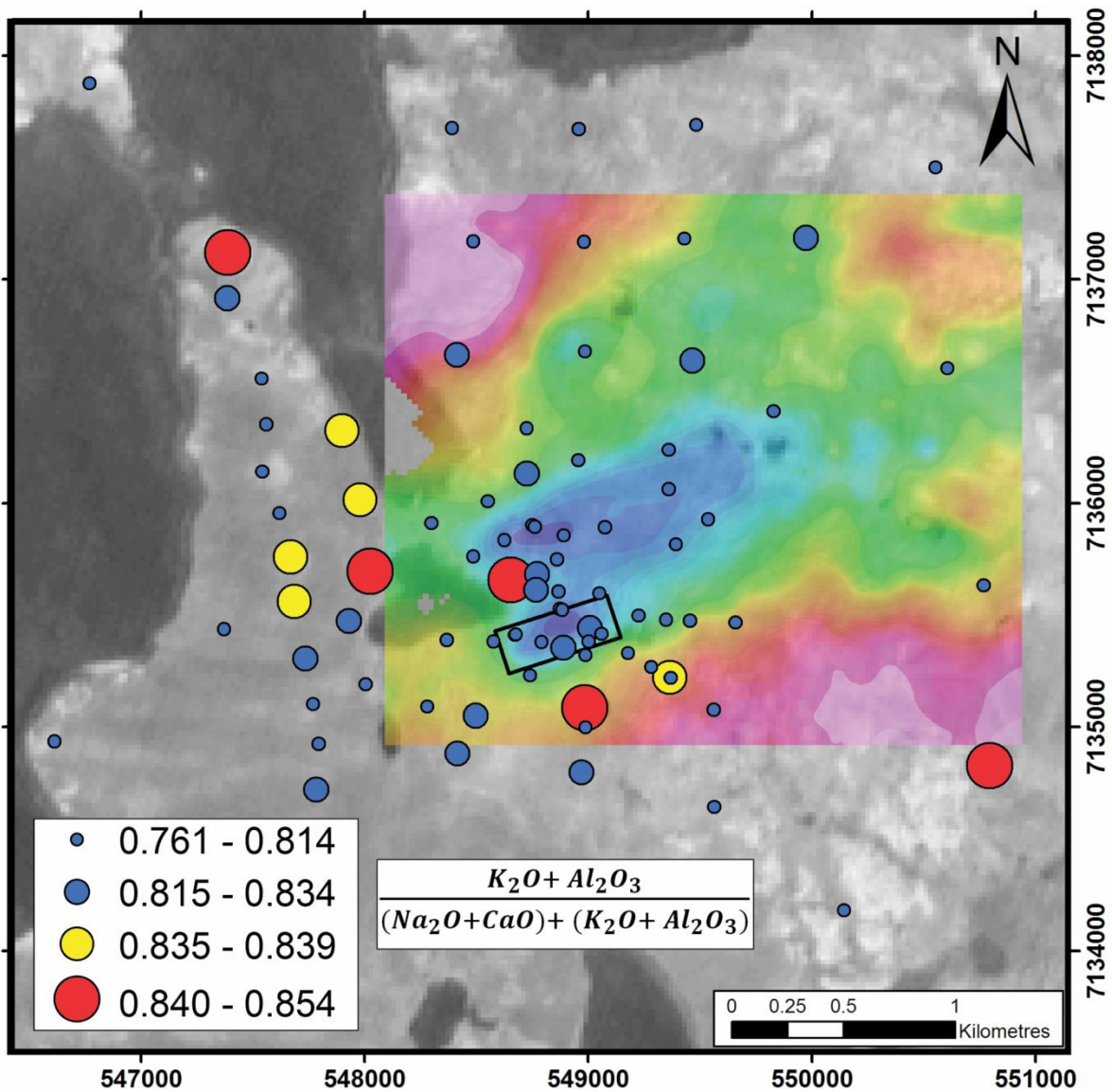


Figure 3-7: Dispersal of AlI. The index shows a fairly strong dispersal towards the northwest, with possible slight entrainment to the south. The high values located to the south and to the east may be the result of dispersal originating from the other deposits in the region (Jane and Andrew Lake). Colour and size graduations are based on the 75th, 90th, and 95th percentiles. The black box represents the extent of the 3D model.

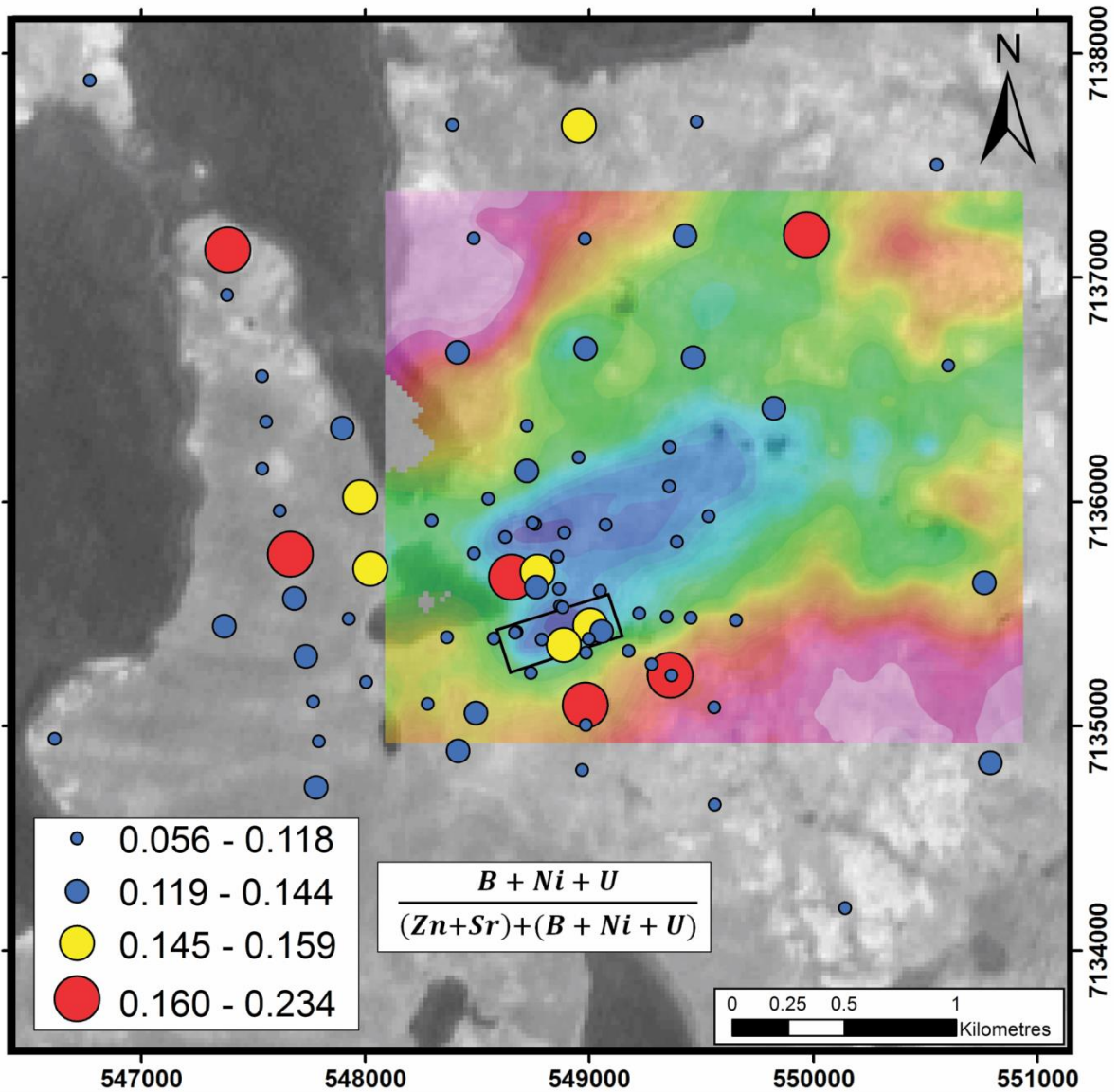


Figure 3-8: Dispersal of AI2. The second index displays patterns similar to AI1, but the sample shown in Figure 3-7 that is thought to show alteration related to the Andrew Lake deposit is not anomalous. The black box represents the extent of the 3D model.

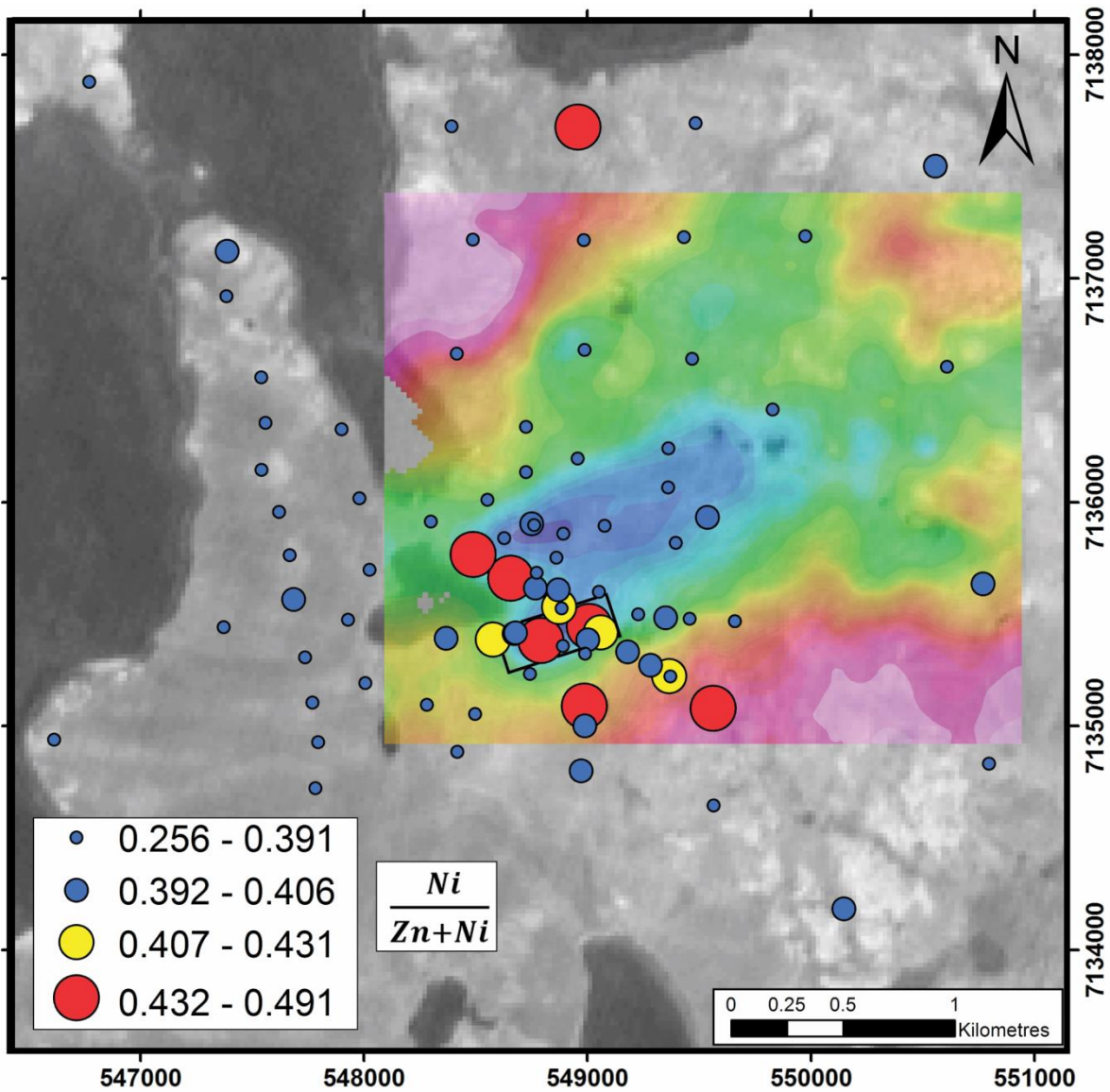


Figure 3-9: Dispersal of AI3. The third index shows the highest values directly over the alteration zone at Tatiggaq, and appears to be an amoeboid dispersal pattern with slight dispersal to the south. The anomalous sample directly to the north of the alteration zone was collected in a slightly swampy environment, which may explain its elevated value. The black box represents the extent of the 3D model.

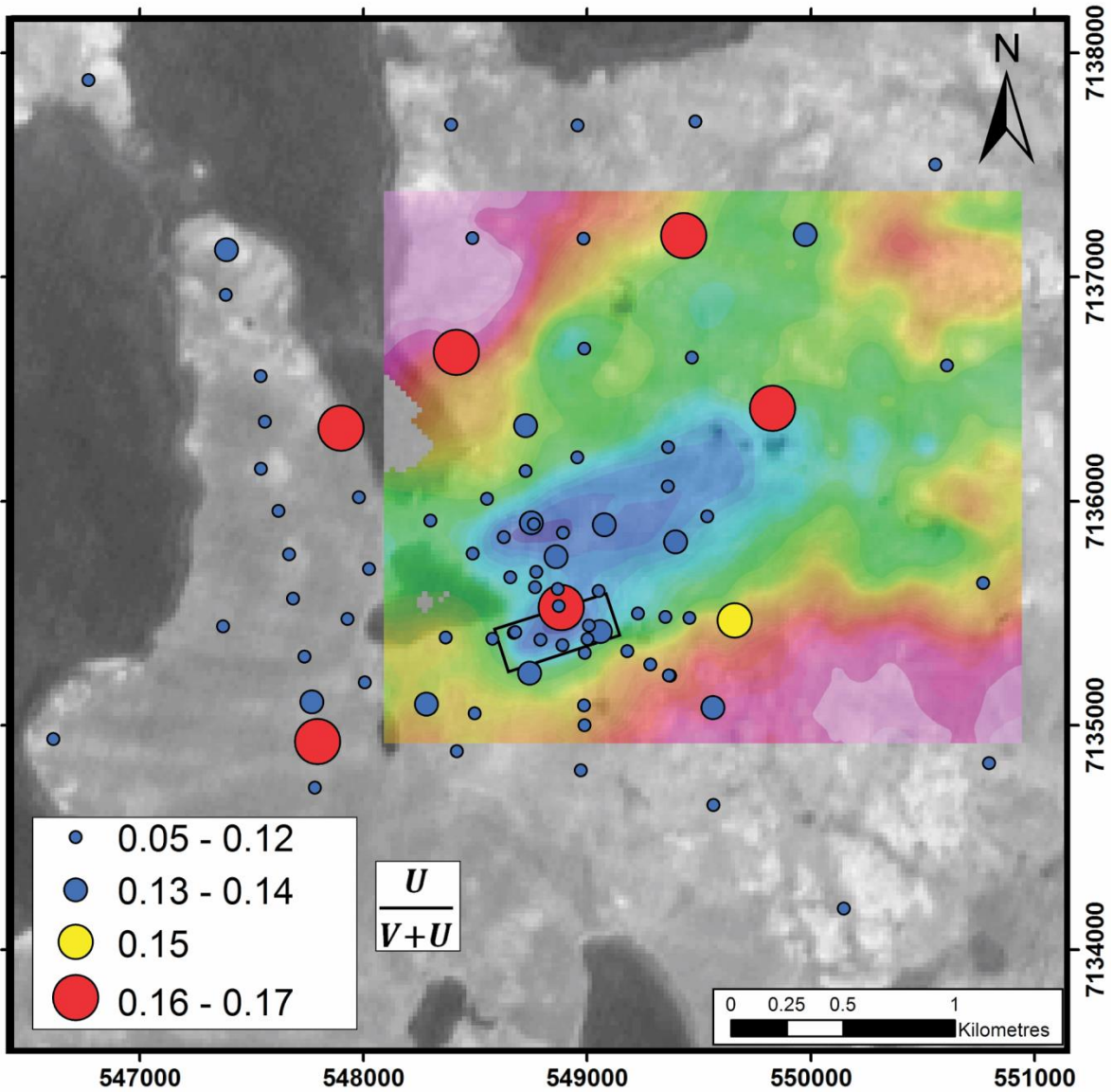


Figure 3-10: Surficial dispersal of AI4. The fourth index shows a random distribution of high values in the area, which may be due to high uranium values in some of the unaltered source rocks. Dispersal is not evident using AI4. The black box represents the extent of the 3D model.

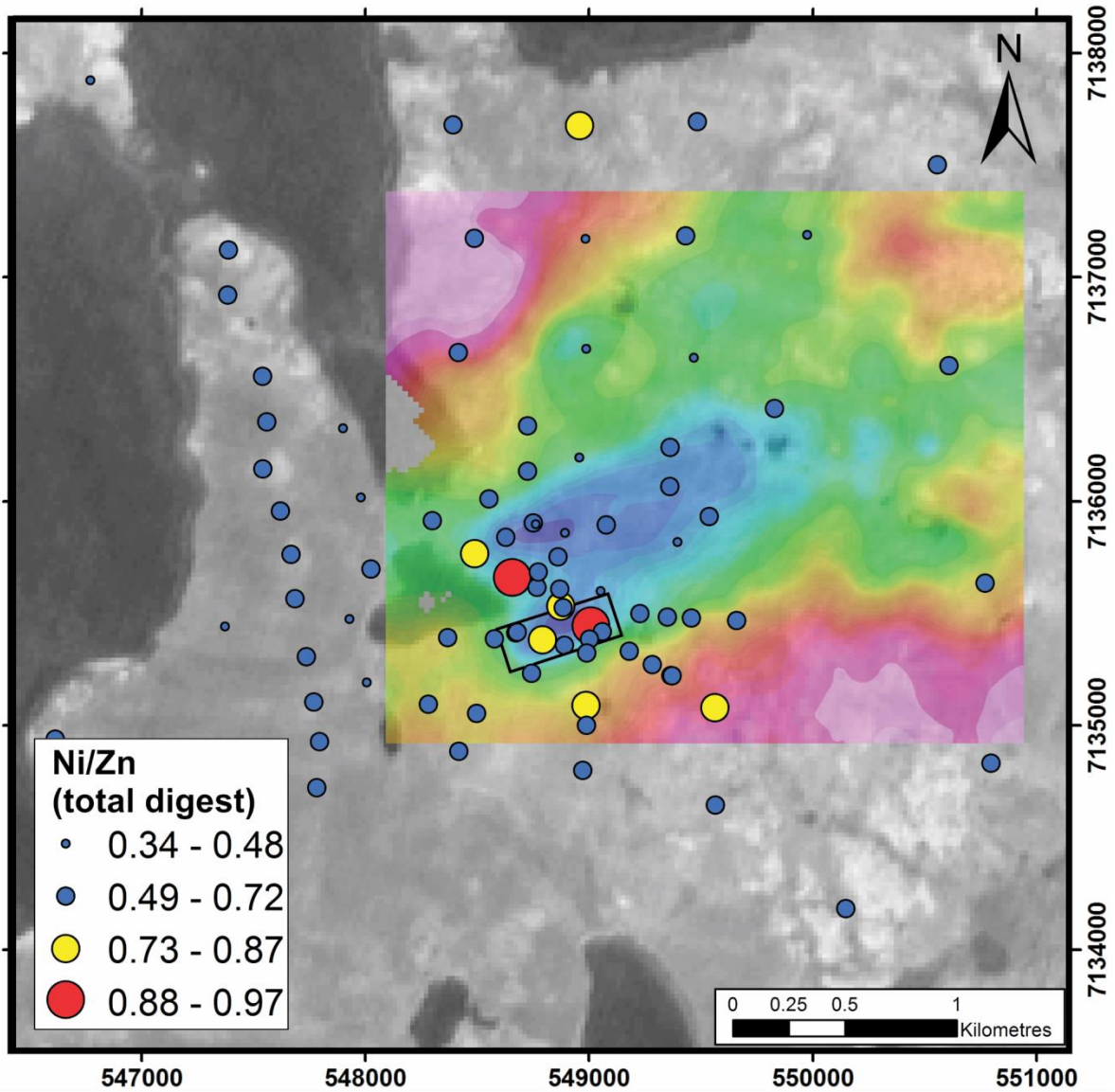


Figure 3-11: Ni/Zn ratios determined by total digestion. The highest values lie in close proximity to the zone of strongest alteration at Tatiggaq. Alteration index 3, which is $Ni/(Ni+Zn)$, yields a clearer alteration signature compared with Ni/Zn ratios (Figure 3-9). The black box represents the extent of the 3D model.

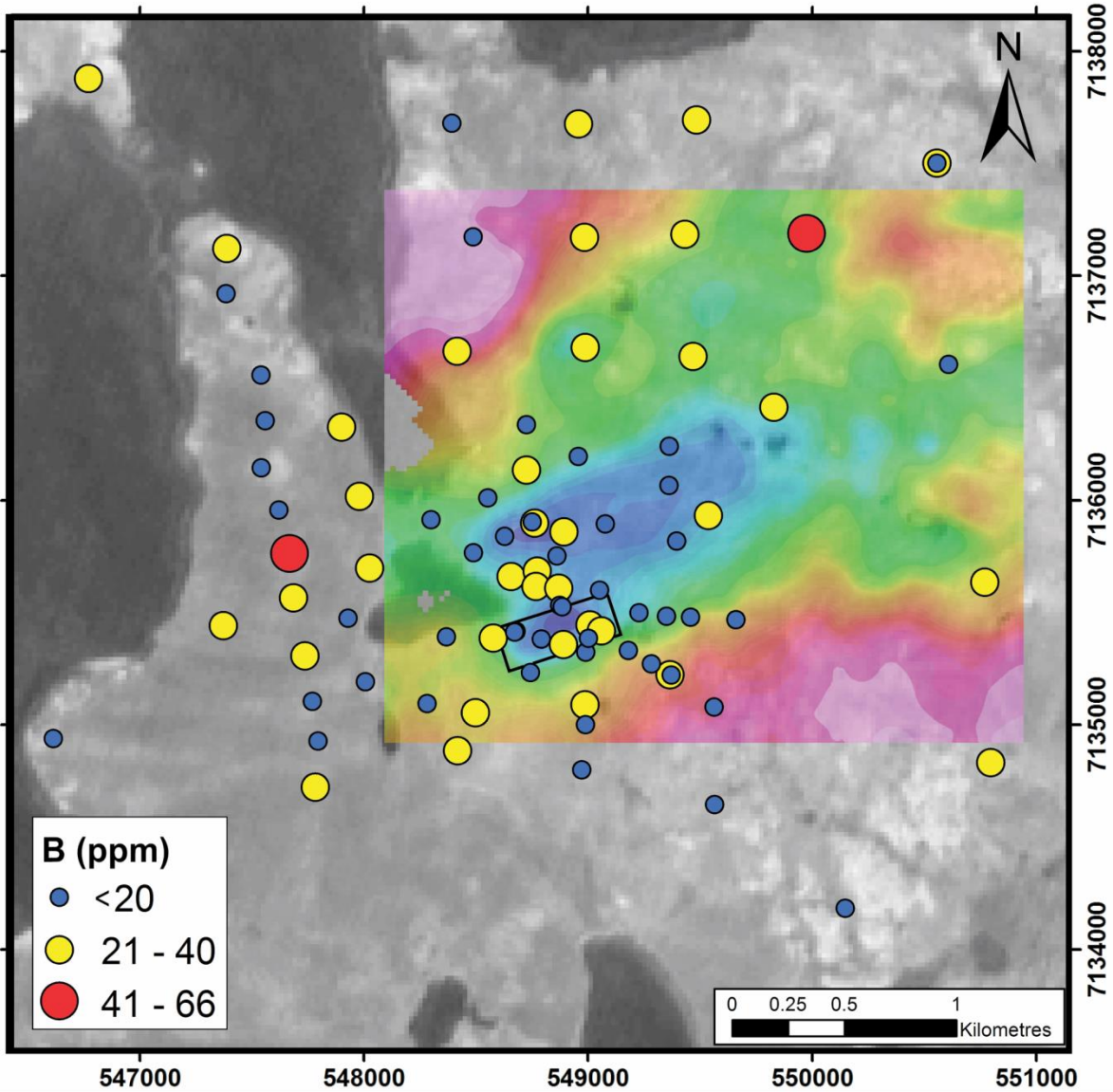


Figure 3-12: Surficial dispersal of boron values in the study area. No obvious dispersal patterns are observed, and the highest boron value is located directly to the west of the alteration zone although other samples with high boron enrichment also occur to the northeast and south (southern anomaly not pictured). The black box represents the extent of the 3D model.

3.5. Synthesis

3.5.1. Main Characteristics of Dispersal

Both AI1 and AI2 show reworked fan-shaped down-ice dispersion from the alteration zone with re-entrainment of previously deposited material. This interpretation is based on the decrease in values directly over the alteration zones moving up the stratigraphy, and with the displacement of the surficial anomaly down-ice but not directly in the direction of the dominant ice flow in the region. This pattern is the result of multiple episodes of re-entrainment of altered material over the course of multiple ice flow events in the area with the introduction of some far travelled material such as the Thelon Formation clasts observed in Dmm2. Tracing the dispersal of altered material in the area is partially limited by the lack of drill holes to the southwest.

The suitability of the different alteration indices for exploration use varies depending on the situation. For instance, AI4 does not provide a strong footprint at the surface in the Tatiggaq area, but it does provide a strong footprint at the bottom of the drill holes and thus could serve as an effective exploration vector in areas of thin till if modified material is avoided. Both AI1 and AI2 can be effective pathfinders towards alteration zones if several elevated values occur in close proximity and along a reasonable ice flow trend. As with any drift exploration method, individual anomalies may indicate an anomalous bedrock source, but the anomalies with the highest priority should be those that appear in sample clusters. AI1 and AI2 are effective at tracing alteration for approximately 2.5 km, and the inferred maximum width of the fan is 1 km. Accurate measurement of this fan is difficult due to the presence of lakes in the area where sampling was not possible. However, the presence of the dispersal fan observed with AI1 is not continuous, and there is considerable noise in the data that complicates the application of regional till surveys in the recognition of dispersal of this magnitude while sampling the fan more than once. Since AI1 and AI2 provide similar results in delineating dispersal, but AI2 is not affected as much by noise related to the occurrence of samples with abundant Thelon Formation clasts, AI2 is recommended above AI1.

In contrast to AI1 and AI2, the dispersal observed with AI3 is more constrained and occurs within 1 km of the alteration zone, which provides a clearer and more focused footprint. As discussed above, the difference in size of dispersal may be related to the different geochemical characteristics of Ni and Zn. If the elements associated with mineralization are hosted in

different mineral or size fractions, the character of dispersal will differ since different phases have different residence times in till (Klassen, 2001). As with AI1 and AI2, it would be challenging to recognize the footprint of the alteration zone using a typical regional till survey sample spacing of 4 to 10 km (McMartin and McClenaghan, 2001). However, given the constrained nature of the dispersal in relation to the alteration zone, AI3 used in conjunction with the larger AI1 or AI2 footprint would allow for the confirmation of the presence of alteration at depth.

For AI4, the geochemical characteristic that U is highly mobile in oxidizing systems (Kyser and Cuney, 2008) results in a ratio that is highly susceptible to later modification during interaction with water, although the effects of this modification would likely be limited given the time since deglaciation. This is seen in the lack of dispersal for AI4 beyond Dmm1. The noisy signal of AI4 at the surface is the result of two main factors: the signal not being transmitted effectively upwards through till, and excessive noise at the surface. Since U and V are both redox sensitive compared to many other elements, even a small extent of contamination from reducing organic matter when collecting a mudboil sample could alter the measured ratio.

3.5.2. Reconstruction of Dispersal

The complex patterns shown in previous sections are interpreted to capture the net effect of sediment dispersion events related to multiple ice flow shifts and till production phases. A single till can retain compositional inheritance from the re-entrainment of a previous till and its incomplete homogenization within the newly produced till (Parent et al., 1996; Stea and Finck, 2001). Multi-till stratigraphy, however, is a special case or end-member in the till continuum that is caused by relatively high sediment supply and net deposition (preservation) of sediment layers (Trommelen et al., 2013). Compositional inheritance preserved through the till succession may still exist, but is expected to be diluted by abundant new debris introduced into the mix during the production of the younger tills. The compositional makeup of a young till can even partially overprint the top part of an underlying till. It is thus expected that debris re-entrained multiple times from a source now covered by a succession of till units will be considerably diluted in the youngest till at the surface.

A reconstruction of dispersal of altered material is presented in Figure 3-13. The reconstruction is an attempt at reproducing the patterns produced by the analysis of compositional data (cf. chapter 2) using what is known of the glacial history in the area (Hodder et al., 2016). This exercise provides a means to visually and critically assess the overall interpretation.

The first ice flow event (Figure 3-13A, E) would have resulted in a linear or ribbon-shaped dispersal train towards 255° and is hosted within Dmm1. The shift of ice flow towards the south (180°) would have resulted in a composite dispersal pattern (Figure 3-13B, F). Dispersal from the ice flow towards the south would have involved both the re-entrainment of altered material from the previously existing dispersal train, as well as the alteration zone since the margins of the alteration zone were partially re-exposed to the base of the glacier. The alteration signal in Dmm2 at the alteration zone would also be elevated by till rich in Thelon Formation clasts (i.e., elevated concentrations of elements such as B). Dispersal within Dmm3 (Figure 3-13C, G) would consist entirely of re-entrainment of material contained within Dmm2, and Dmm1 where Dmm2 is missing, since Dmm3 is not observed in contact with the alteration zone. However, Dmm1 and Dmm2 are likely not continuous everywhere, and the alteration zone may have been exposed to minor erosion by Dmm3 in places. Dispersal of altered material in Dmm3 is expected to be the farthest travelled since Dmm3 is the dominant ice flow event in the region. Distal transport for Dmm3 is supported by its thick till succession, large coincident drumlins, and its content of distally sourced Pitz Formation clasts (Hodder, 2014). However, the deposition and concentration of re-entrained altered material by the flows to the northwest is highly dependent on the subglacial dynamics at play during deposition (Klassen, 2001; Trommelen et al, 2013).

The last ice flow event in the region (Figure 3-13D, H) resulted in slight re-entrainment of altered material towards the west (270-300°). This signal is manifested in the surficial till and in Dmm4. The marked difference in the geochemical and textural compositions of material in the surficial till compared with the drill cores suggests that this last ice flow phase produced a new till with material from an eastern source, which would have further diluted the already diluted altered debris at the top of Dmm3. The lower alteration indices observed in the mudboil samples, with the exception of AI3, suggests that the signal is the result of re-entrainment and mixing rather than of a skip zone or window into the underlying till units such as Dmm3.

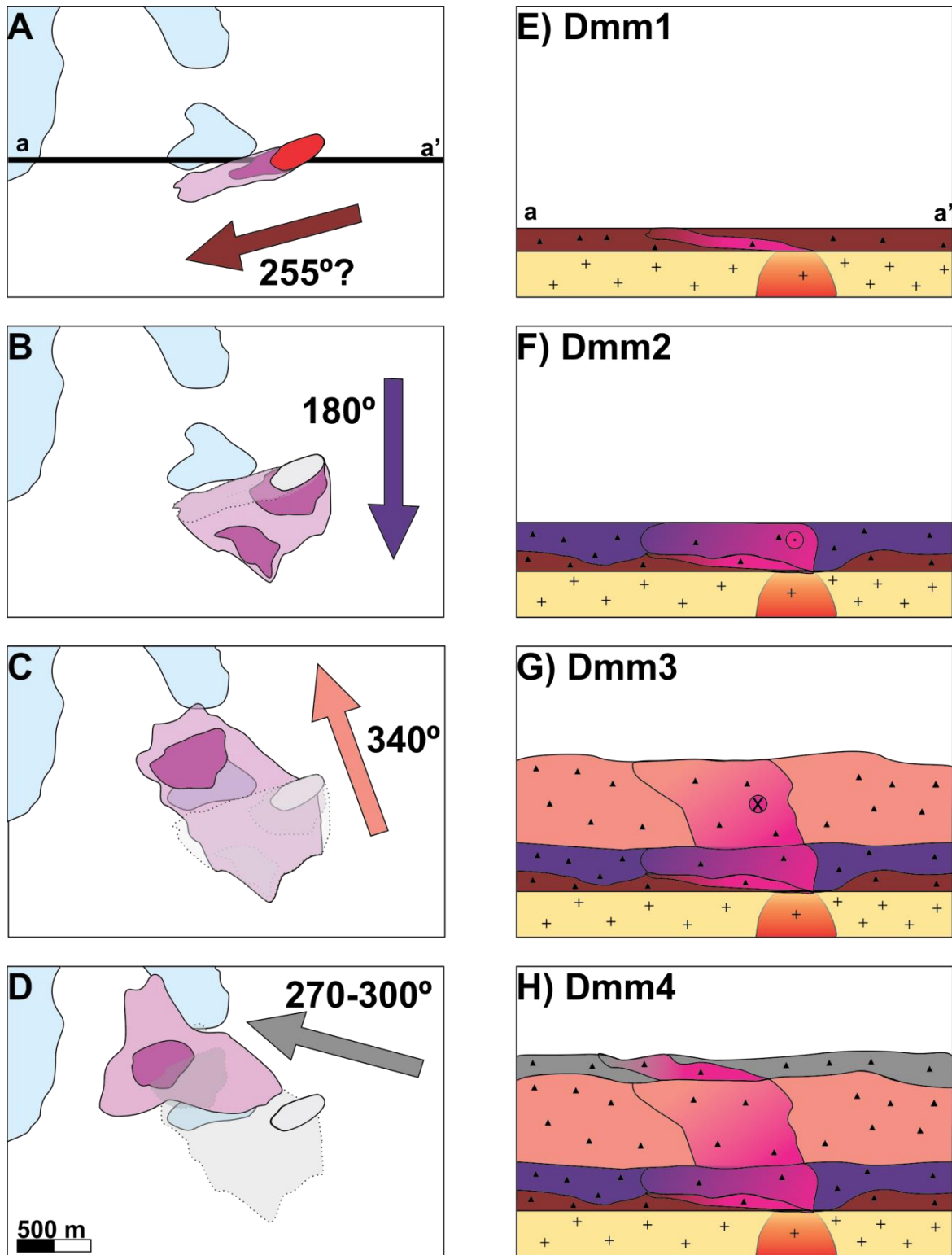


Figure 3-13: Reconstruction of the dispersal history in the Tatiggaq area. Panels A-D show plan views of the modelled dispersal with purple representing the hypothetical surficial expression at the end of the associated ice flow phase. Grey shading represents the extent of dispersal during the previous ice flow phase. Panels E-H show vertically exaggerated cross-sections of the dispersal as it rises through the till.

3.6. Conclusions

Identifying and tracing compositional evidence of a bedrock source at surface in an area covered by multiple tills is a major challenge. If a detrital signature from a buried source is present, it is possible for this signature to extend to the surface, but this may not occur due to several factors. Firstly, the signal may become too diluted by mixing with detritus from other sources and thus may reach a low enough level that it is not detectable. Secondly, the signal of the source may be compositionally similar to other distally derived sources that are not altered or mineralized. Lastly, the presence of multi-till stratigraphy in an area may truncate dispersal by capping it with material that incorporates little to no material from the source being sought out. Through careful analysis of compositional data, together with knowledge of the glacial geology history of an area, it is possible to address these barriers and inform exploration geologists of what type of detrital signature may be found at the surface.

In the case of the buried alteration zones near Aberdeen Lake, Nunavut, all three barriers to exploration are encountered to some extent. Nevertheless, the dispersed signature can be traced in the subsurface tills, and it appears to be detectable at surface despite considerable dilution. The occurrence of a considerable amount of Thelon Formation input in one of the till units makes the use of single elemental indicators (e.g., B) impractical, but this obstacle has been addressed by the use of multi-element alteration indices (involving elements enriched and depleted in altered material) that amplify the signal associated with alteration. An understanding of the subsurface stratigraphy and depositional history significantly assists with the creation of a model for the dispersal of altered material through the multiple tills of the study area and its surficial expression.

The generation of alteration indices combined with the study of the subsurface at Tatiggaq has greatly enhanced the capacity to recognize and map patterns that represent the signature of dispersed detritus from the alteration zone while mitigating the effect of false anomalies. These indices may potentially be applicable at other similar targets in the Thelon Basin, and they may be applicable to other prospective zones where similar alteration assemblages are known or predicted.

Chapter 4: Conclusions

4.1. Identifying and Tracing the Fingerprint of Unconformity-type Uranium Alteration in Tills

This work developed several indices that can be used in the exploration for unconformity-type uranium deposits. The use of multi-element ratios, developed with the aid of multi-variate statistics, is preferable to relying on tracing the dispersal using a single element. This is clearly demonstrated in the dispersal of B in the Tatiggaq area, since B is clearly elevated in the altered bedrock but is scarcely observed in high quantities in the surficial tills. However, when B is combined with other elements that are elevated or depleted in altered material, as in AI2, the signal is magnified at the surface and a clear dispersal pattern of alteration products is observed.

Principal component analysis was shown to be a useful tool in identifying geochemical trends associated with alteration processes and in discriminating different till units. PCA can be used to test many pathfinder elements against one another if geochemical data is available for fresh and altered rocks in a district. This allows for the early determination of which elements in an area will provide meaningful exploration vectors.

4.2. Thesis Contributions

This thesis has added to the understanding of both mineral exploration in areas covered by thick multi-till successions and the exploration for unconformity-type uranium deposits by using till geochemistry. The most significant findings and contributions are as follows:

- 1) This study identified the geochemical characteristics associated with alteration surrounding basement-hosted unconformity-type uranium deposits in the Thelon Basin of Nunavut. These characteristics have been applied to generate four alteration indices that can be applied to mineral exploration in the region. These indices are as follows:

$$- AI1 = \frac{K_2O + Al_2O_3}{(Na_2O + CaO) + (K_2O + Al_2O_3)} \text{ (Total Digestion)}$$

$$- AI2 = \frac{B + Ni + U}{(Zn + Sr) + (B + Ni + U)} \text{ (Total Digestion)}$$

$$- AI3 = \frac{Ni}{Zn + Ni} \text{ (Total Digestion)}$$

$$- AI4 = \frac{U}{V + U} \text{ (Partial Digestion)}$$

- 2) The use of multi-variate statistical techniques, specifically PCA has been shown to be an effective exploratory technique for use with local scale geochemical data sets. Limitations on the technique can be overcome by grouping elements based on prior geological knowledge, especially comparison of geochemical data for fresh versus altered rocks in the area.
- 3) The geochemical signature of altered bedrock was successfully observed in subsurface tills. The level of alteration observed in the tills is variable. Specifically, the degree of alteration is observed to be higher in lithofacies that are lower in the till stratigraphy and are closer to the altered source.
- 4) Three-dimensional models of dispersal have been created that show the dispersal of altered products in the subsurface. These models highlight the stratigraphic controls that are exerted on till dispersal, and the influence of having the source of alteration being buried by the earliest ice flow event in the area. This capping prevents further direct erosion and incorporation of the altered bedrock into younger tills, and hence any observed alteration signal must be from the re-entrainment of older tills.
- 5) The dispersal of altered material has been successfully traced to the surface with three of the four alteration indices developed. Two of these indices (AI1 and AI2) show down-ice dispersal with evidence of re-entrainment whereas a third index (AI3) shows a targeted geochemical high over the alteration zone.
- 6) This study highlights that it is critical to understand the till stratigraphy and ice flow history of an area while performing till geochemical surveys since one or more distally derived units may truncate or bury dispersal from a buried source. By carefully examining the geochemistry of the sediments, it may be possible to detect geochemical inheritance in these units.
- 7) A conceptual model for the development of alteration patterns in the Tatiggaq area has been created by combining knowledge of the ice flow history of the area with observed geochemical patterns. The reconstruction of dispersal is a good test that strengthens the interpretations of the study.

4.3. Implications for Mineral Exploration

4.3.1. The Fingerprint of Unconformity-type Uranium Alteration Haloes

Multi-element signatures provide strong fingerprints for unconformity-type uranium deposits that are more robust for use in heterogeneously sourced sample media such as subglacial tills. The most effective of these fingerprints are based on known alteration processes such as illitization, which results in the enrichment of Al_2O_3 , the relative enrichment of K_2O , and the depletion of Na_2O and CaO . B acts a useful pathfinder element in many districts but is less useful in the Thelon Basin because it is elevated in rocks of the Thelon Formation. By combining B with other elements, such as Ni, Zn, U, and Sr, the signal associated with the alteration halo can be amplified and traced from the surface back to the bedrock source.

4.3.2. Drift Prospecting in Areas of Thick Till

This work showed that tracing alteration through thick tills is possible in the Thelon Basin, and hence that vectors to mineralization can be developed for areas with complex ice flow histories. Although the occurrence of multiple ice flow directions creates complex ice flow patterns in the till stratigraphy, the transmission of altered material upwards through 15 m of till is still possible. However, it is also possible that surficial units with no relation to underlying sediments can mask the expression of a dispersal train at the surface. This masking is partly seen in the study area, as evidenced by the lower values of the alteration indices in the surficial samples. The tracing of alteration through these thick till sheets requires having knowledge of both the local and regional ice flow history. Identifying different till units in an area is also critical for mineral exploration since differing provenance can strongly influence the magnitude of the alteration signature in till.

References

- Alexandre, P., Kyser, K., Polito, P., Thomas, D., 2005. Alteration mineralogy and stable isotope geochemistry of Paleoproterozoic basement-hosted unconformity-type uranium deposits in the Athabasca Basin, Canada. *Economic Geology* 100, 1547–1563.
- Aylsworth, J.M., 1990. Surficial Geology, Aberdeen Lake, District of Keewatin, Northwest Territories. Geological Survey of Canada, Map 43-1989, scale 1:125 000.
- De Angelis, H., 2007. Glacial geomorphology of the east-central Canadian Arctic. *Journal of Maps* 3, 323-341.
- Drew, L., Grunsky, E., Sutphin, D., and Woodruff, L., 2010. Multivariate analysis of the geochemistry and mineralogy of soils along two continental-scale transects in North America. *Science of the total environment* 409 (1) pp: 218-27.
- Doggett, M.D., .Global Mineral Exploration and Production – the Impact of Technology. *in* Proceedings, Workshop on Deposit Modeling, Mineral Resource Assessment, and Sustainable Development. 31st International Geological Congress, August 18-19, 2000, Rio de Janeiro, Brazil, pages 19-21
- Garret, R.G., The ‘rgr’ package for the R Open Source statistical computing and graphics environment - a tool to support geochemical data interpretation *Geochemistry: Exploration, Environment, Analysis*, November 2013, v. 13, p. 355-378, First published on November 15, 2013, doi:10.1144/geochem2011-106
- Grunsky, E.C., 2010. The interpretation of geochemical survey data. *Geochemistry: Exploration, Environment, Analysis*. 10, 27–74.
- Grunsky, E., Drew, L., and Sutphin D., 2009. Process recognition in multi-element soil and stream-sediment geochemical data. *Applied Geochemistry* 24 (8) 1602-1616
- Grunsky, E., 2002. R: a data analysis and statistical programming environment—an emerging tool for the geosciences. *Computers & Geosciences* 28 (10) 1219-1222.
- Earle, S., 2001. Application of composite glacial boulder geochemistry to exploration for unconformity-type uranium deposits in the Athabasca Basin, Saskatchewan, Canada. Geological Society, London, Special Publications 185, 225-235.
- Egozcue, J.J., Pawlowsky-Glahn, V., Mateu-Figueras, G., Barceló-Vidal, C., 2003. Isometric Logratio Transformations for Compositional Data Analysis. *Mathematical Geology* 35, 279–300.
- Fayek, M., Kyser, T.K., 1997. Characterization of multiple fluid-flow events and rare-earth-element mobility associated with formation of unconformity-type uranium deposits in the Athabasca Basin, Saskatchewan. *Canadian Mineralogist* 35, 627–658.

- Fedo, C.M., Nesbitt, H.W. and Young, G.M. 1995. Unraveling the effects of potassium metasomatism in sedimentary rocks and paleosols, with implications for paleoweathering 115 conditions and provenance. *Geology* 23, 921-924.
- Ferbey, T., Levson, V.M., and Lett, R.E., 2012. Till geochemistry of the Huckleberry Mine area, west-central British Columbia (NTS 093E/11); BC Ministry of Energy, Mines, and Petroleum Resources, Open File 2012-2, 52 pages.
- Ferbey, T. and Levson, V.M., 2009. The influence of ice flow reversals on the vertical and horizontal distribution of trace metals in tills, Huckleberry Mine area, west-central British Columbia; in *Application of Till and Stream Sediment Heavy Mineral and Geochemical Methods to Mineral Exploration in Western and Northern Canada*; Paulen, R.C. and McMartin, I., (eds.). Geological Association of Canada, GAC Short Course Notes 18, pages 145-151.
- Filzmoser, P., Hron, K., Reimann, C., 2009. Principal component analysis for compositional data with outliers. *Environmetrics* 20, 621–632.
- Finck, P.W. and Stea, R.R., 1995. The compositional development of tills overlying the South Mountain Batholith, Nova Scotia. Nova Scotia Department of Natural Resources. Paper 95-1, 52 pages.
- Fuchs, H., Hilger, W., and Prosser, E. 1986. Geology and exploration history of the Lone Gull property. *Uranium Deposits of Canada*: 286–292.
- Fuchs, H.D., and Hilger, W. 1989. Kiggavik (Lone Gull): an unconformity related uranium deposit in the Thelon Basin, Northwest Territories, Canada. *Uranium Resources and Geology of North American*: International Atomic Energy Agency, Tech. Doc. 500: 429–454.
- Grünfeld, K., 2007. The separation of multi-element spatial patterns in till geochemistry of southeastern Sweden combining GIS, principal component analysis and high-dimensional visualization. *Geochemistry: Exploration, Environment, Analysis* 7, 303–318.
- Hamilton, N., 2015. ggtern: An Extension to 'ggplot2', for the Creation of Ternary Diagrams. Rpackage version 1.0.6.0. <http://CRAN.R-project.org/package=ggtern>
- Hasegawa, K., Davidson, G.I., Wollenberg, P., Yoshimasa, I., 1990. Geophysical exploration for unconformity-related uranium deposits in the northeastern part of the Thelon Basin, Northwest Territories, Canada. *Mining Geology*, 40(2), 83-95.
- Hecht, L., Cuney, M., 2000. Hydrothermal alteration of monazite in the Precambrian crystalline basement of the Athabasca Basin (Saskatchewan, Canada): implications for the formation of unconformity-related uranium deposits. *Mineralium Deposita* 35, 791–795.
- Hiatt, E.E., Palmer, S.E., Kyser, T.K., O'Connor, T.K. 2010. Basin evolution, diagenesis and uranium mineralization in the Paleoproterozoic Thelon Basin, Nunavut, Canada. *Basin Research* 22, 302-323.

- Hoeve, J., Sibbald, T.I.I., 1978. On the genesis of Rabbit Lake and other unconformity-type uranium deposits in northern Saskatchewan, Canada. *Economic Geology* 73, 1450–1473.
- Hodder, T.J., 2014. Quaternary Stratigraphy and Glacial Dynamics from a Core Region of the Laurentide Ice Sheet, Aberdeen Lake, Kivalliq, Nunavut. Unpublished MSc Thesis, University of Waterloo. 245 pages.
- Hodder, T.J., Ross, M., and Menzies, J., 2016. Sedimentary record of ice divide migration and ice streams in the Keewatin core region of the Laurentide Ice Sheet, *Sedimentary Geology* 338, 97-114.
- Hooke, R. LeB., Cummings, D.I., Lesemann, J.-E., Sharpe, D.E. 2013. Genesis of dispersal plumes in till. *Canadian Journal of Earth Sciences*, 50, 847-855.
- Hunter, R., Black, R., Zaluski, G. 2011a. Cameco Corporation 2010 Geological, Geophysical, Geochemical & Diamond Drilling Exploration Report. Aberdeen Project, Nunavut (NTS 66B-1, 2, 3, 6, 7, 8, 9, 10).
- Hunter, R., Black, R., Lesperance, J., Zaluski, G. 2011b. Cameco Corporation 2010 Geological, Geophysical, Geochemical & Diamond Drilling Exploration Report. Turqavik Project, Nunavut (NTS 66A-5, 12 & 66B-8, 9, 15, 16).
- Hunter, R. 2013. Turqavik and Aberdeen Projects – 2012 Exploration update. oral presentation, Nunavut Mining Symposium, April 9, 2013, Iqaluit, NU. URL <http://2013.nunavutminingsymposium.ca/wp-content/uploads/2013/04/9-Hunter-Cameco.pdf>
- Jefferson, C., Thomas, D., Quirt, D., Mwenifumbo, C., Brisbin, D., 2007. Empirical models for Canadian unconformity-associated uranium deposits, in: *Proceedings of Exploration 07: Fifth Decennial International Conference on Mineral Exploration*. pp. 741–769.
- Johnson, C.L., 2014. Fingerprinting Quaternary Subglacial Processes on Hall Peninsula, Baffin Island, using Multiproxy Data. Unpublished MSc Thesis, University of Waterloo. 174 pages.
- Klassen, R.A., 1999. The application of glacial dispersal models to the interpretation of till geochemistry in Labrador, Canada. *Journal of Geochemical Exploration*, 67, 245-269.
- Klassen, R. A., 2001. A Quaternary geological perspective on geochemical exploration in glaciated terrain. *Geological Society of London, Special Publication* 185, 1–17.
- Kyser, K., 2014. Uranium Ore Deposits, in: *Treatise on Geochemistry*. Elsevier, pp. 489–513.
- Kyser, K. and Cuney, M., 2008. Unconformity-related uranium deposits. In: Cuney, M. and Kyser, K., (eds.) *Recent and not-so-recent developments in uranium deposits and implications for exploration*, Mineralogical Association of Canada Short Course Series, vol. 39, pp. 161–220. Quebec, Mineralogical Association of Canada.

- Mäkinen, J., 1995. Effects of grinding and chemical factors on the generation and composition of the till fine fraction: and experimental study. *Journal of Geochemical Exploration*, 54, 49-62.
- Levson, V.M. and Giles, T.R., 1995. Glacial Dispersal Patterns of Mineralized Bedrock: With Examples from the Nechako Plateau, Central British Columbia. in: Bobrowsky, P.T., Sibbick, S.J., Newell, J.M., Matysek, P.F. (eds.) *Drift exploration in the Canadian Cordillera*. British Columbia Ministry of Energy, Mines and Petroleum Resources, Paper 1995-2, pages 67-76.
- Mallet, J.L., 1989. Discrete smooth interpolation. *ACM Transactions on Graphics (TOG)*, 8(2), pp.121-144.
- McMartin, I., and Paulen, R.C., 2009. Ice flow indicators and the importance of ice flow mapping for drift prospecting; in *Application of Till and Stream Sediment Heavy Mineral and Geochemical Methods to Mineral Exploration in Western and Northern Canada*; Paulen, R.C. and McMartin, I., (eds.). Geological Association of Canada, GAC Short Course Notes 18, pages 15-34.
- McMartin, I., Dredge, L.A., Ford, K.L., and Kjarsgaard, I.M., 2006. Till composition, provenance and stratigraphy beneath the Keewatin Ice Divide, Schultz Lake area (NTS 66A), mainland Nunavut. Geological Survey of Canada, Open File 5312, 79 pages.
- McMartin, I., McClenaghan, M.B., 2001. Till geochemistry and sampling techniques in glaciated shield terrain: a review. Geological Society, London, Special Publications 185, 19–43.
- Miller, J.K., 1984. Model for clastic indicator trains in till; in *Prospecting in Areas of Glaciated Terrain*, Institute of Mining and Metallurgy, London, pages 69-77.
- Nesbitt H.W. and Young G.M. 1982. Early Proterozoic climates and plate motions inferred from major element chemistry of lutites. *Nature* 299(5885): 715-717.
- Normandeaux, P.X., McMartin, I., Paquette, J., Corriveau, L., and Montreuil, J-F., 2012. Geochemical signatures of IOCG mineralization and alteration in till. *Mineralogical Magazine*, 76, 2173
- Parent, M., Paradis, S.J., Doiron, A., 1996. Palimpsest glacial dispersal trains and their significance for drift prospecting. *Journal of Geochemical Exploration* 56, 123–140.
- Patterson, J., LeCheminant, A.N. 1985. A preliminary geological compilation of the northeastern Barrens Grounds, parts of the Districts of Keewatin and Franklin. Geological Survey of Canada, Open File 1138, Scale 1:1 000 000.
- Paul, D., Hanmer, S., Tella, S., Peterson, T.D., LeCheminant, A.N. 2002. *Geology, Compilation, bedrock geology of the Western Churchill Province, Nunavut-Northwest Territories*. Geological Survey of Canada, Open File 4236, Scale 1:1 000 000.
- Plouffe, A. and Ferbey, T. (2015): Till composition near Cu-porphyry deposits in British Columbia: highlights for mineral exploration; in: TGI 4 - Intrusion Related

- Mineralisation Project: new vectors to buried porphyry-style mineralisation, Rogers, N. Editor, Geological Survey of Canada, Open File 7843, pages 15-37.
- Plouffe, A., Ferbey, T., Levson, V.M., and Bond, J.D., 2012. Glacial history and drift prospecting in the Canadian Cordillera: recent developments; Geological Survey of Canada, Open File 7261, 51 p.
- Plouffe, A., Anderson, R.G., Gruenwald, W., Davis, W.J., Bednarski, J.M., and Paulen, R.C., 2011. Integrating ice-flow history, geochronology, geology, and geophysics to trace mineralized glacial erratics to their bedrock source, an example from south central British Columbia; *Canadian Journal of Earth Sciences*, v.48, pages 1113-1129.
- Poppe, L.J., Paskevich, V.F., Hathaway, J.C., Blackwold, D.S., 2001. A Laboratory Manual for X-Ray Powder Diffraction. U. S. Geological Survey Open-File Report 01-041. URL: <http://pubs.usgs.gov/of/2001/of01-041/index.htm>, accessed April 14, 2014.
- R Core Team, 2015. R: A language and environment for statistical computing. R Foundation for Statistical Computing, Vienna, Austria. URL <http://www.R-project.org/>.
- Reimann, C., Filmozer, P., Garrett, R.G., Dutter, R., 2008. Statistical data analysis explained. Applied environmental statistics with R. Chichester, John Wiley and Sons Ltd, 343p
- Reimann, C., Filzmoser, P., 2000. Normal and lognormal data distribution in geochemistry: death of a myth. Consequences for the statistical treatment of geochemical and environmental data. *Environmental Geology* 39, 1001–1014.
- Robinson, S.V.J, Paulen, R.C., Jefferson, C.W., McClenaghan, M.B., Layton-Matthews, D., Quirt, D., Wollenberg, P., 2014. Till geochemical signatures of the Kiggavik uranium deposit, Nunavut. Geological Survey of Canada, Open File 7550, 2014; 168 pages.
- Ruzicka, V., 1996. Unconformity-associated uranium. In: Eckstrand, O.R., Sinclair, W.D., and Thorpe, R.I. (eds.), *Geology of Canadian Mineral Deposit Types*. Geological Survey of Canada, *Geology of Canada*, no. 8, pages 197-210.
- Saskatchewan Research Council, 2012. Geoanalytical laboratories 2012 fee schedule. Saskatoon.
- Shilts, W., 1978. Nature and genesis of mudboils, central Keewatin, Canada. *Canadian Journal of Earth Sciences*, 15 (7) 1053-1068.
- Shilts, W.W., 1995. Geochemical partitioning in till. in: Bobrowsky, P.T., Sibbick, S.J., Newell, J.M., Matysek, P.F. (eds.) *Drift exploration in the Canadian Cordillera*. British Columbia Ministry of Energy, Mines and Petroleum Resources, Paper 1995-2, pages 149-163.
- Stea, R.R., Finck, P.W. 2001. An evolutionary model of glacial dispersal and till genesis in Maritime Canada. In: *Drift Exploration in Glaciated Terrain*. McClenaghan, M.B., Bobrowsky, P.T., Hall, G.E.M., Cook, S.J. (eds.). Geological Society Special Publication 185, p. 237-265.
- Tyrrell, J.B., 1897. Report on the Doobaunt, Kazan, and Ferguson rivers and the northwest coast of Hudson Bay. Geological Survey of Canada, Annual Report 618: 1F-218F.

- Trommelen, M.S., Ross, M., Campbell, J.E., 2013. Inherited clast dispersal patterns: Implications for palaeoglaciology of the SE Keewatin Sector of the Laurentide Ice Sheet. *Boreas*, Vol. 42, pp. 693–713.
- Uvarova, Y. a., Kyser, T.K., Lahusen, L., 2012. The uranium potential of the north-eastern part of the Paleoproterozoic Thelon Basin, Canada. *Journal of Geochemical Exploration* 119-120, 76–84.
- Van Baalen, M.R., 1993. Titanium mobility in metamorphic systems: A review. *Chemical Geology* , 110(1-3): 233-249.
- Wang, Y., 2014. Testing the Chemical Index of Alteration as a tracer in glacial sediments of buried alteration zones. Unpublished BSc thesis, University of Waterloo, 27 pages.
- Wickham, H., 2009. *ggplot2: elegant graphics for data analysis*. Springer New York, 2009.
- Wickham, H., 2007. Reshaping Data with the reshape Package. *Journal of Statistical Software*, 21(12), 1-20. URL <http://www.jstatsoft.org/v21/i12/>

Appendix A: Till drill core geochemistry

Sample_ID	Prefix	Number	Year	WellName	X	Y	Z	Meas_dep_m	pctClay	pctSilt	Nclay_pct	NSilt_pct	Ag_p_ppm
TUR020-SA	TUR	020-SA	2012	TUR020	548871	7135474	-175.2	12.8	56.8	43.2	56.8	43.2	0.12
TUR021-SA	TUR	021-SA	2012	TUR021	548891	7135509	-182.3	5.7	48.6	51.2	48.7	51.3	0.1
TUR021-SB	TUR	021-SB	2012	TUR021	548892	7135508	-176.3	11.8	45.3	54.4	45.4	54.6	0.1
TUR021-SC	TUR	021-SC	2013	TUR021	548891	7135509	-183.5	4.5	44.4	55.5	44.4	55.6	0.03
TUR022-SA	TUR	022-SA	2012	TUR022	548908	7135515	-182.5	5.6	48.5	51.4	48.5	51.5	0.15
TUR022-SB	TUR	022-SB	2012	TUR022	548908	7135515	-178.9	9.1	46.2	53.4	46.4	53.6	0.1
TUR022-SC	TUR	022-SC	2012	TUR022	548909	7135515	-175.8	12.2	50.3	49.7	50.3	49.7	0.14
TUR022-SD	TUR	022-SD	2012	TUR022	548909	7135515	-172.4	15.7	32.7	67.2	32.7	67.3	0.11
TUR022-SE	TUR	022-SE	2013	TUR022	548908	7135515	-177.4	10.6	46.9	53.1	46.9	53.1	0.04
TUR022-SF	TUR	022-SF	2013	TUR022	548909	7135515	-174.4	13.6	31.6	68.2	31.7	68.3	0.06
TUR024-SA	TUR	024-SA	2012	TUR024	548838	7135465	-181.6	6.5	48.3	51.6	48.3	51.7	0.13
TUR025-SA	TUR	025-SA	2012	TUR025	548853	7135465	-180.6	7.4	47.2	52.6	47.3	52.7	0.07
TUR029-SA	TUR	029-SA	2012	TUR029	548656	7135826	-177.8	10.2	42.8	56.9	42.9	57.1	0.15
TUR031-SA	TUR	031-SA	2012	TUR031	548666	7135874	-182.6	5.9	43.8	54.9	44.4	55.6	0.1
TUR031-SB	TUR	031-SB	2012	TUR031	548666	7135873	-171.4	17.1	41.0	58.6	41.1	58.9	0.06
TUR031-SC	TUR	031-SC	2013	TUR031	548666	7135874	-177.1	11.3	47.4	52.6	47.4	52.6	0.03
TUR031-SD	TUR	031-SD	2013	TUR031	548666	7135873	-174.2	14.3	40.7	59.2	40.8	59.2	0.03
TUR031-SF	TUR	031-SF	2013	TUR031	548665	7135873	-168.4	20.1	39.8	60.1	39.8	60.2	0.04
TUR032-SA	TUR	032-SA	2012	TUR032	548911	7135490	-178.6	7.7	49.7	50.2	49.7	50.3	0.04
TUR032-SB	TUR	032-SB	2012	TUR032	548910	7135491	-173.8	12.5	44.6	54.9	44.8	55.2	0.06
TUR032-SC	TUR	032-SC	2013	TUR032	548912	7135490	-181.5	4.6	38.9	60.9	39.0	61.0	0.04
TUR034-SA	TUR	034-SA	2012	TUR034	548884	7135447	-184.9	3.2	47.5	52.1	47.7	52.3	0.05
TUR034-SB	TUR	034-SB	2012	TUR034	548882	7135449	-175.8	12.6	47.2	52.6	47.3	52.7	0.06
TUR035-SA	TUR	035-SA	2012	TUR035	549041	7135710	-183.0	6.3	46.1	53.8	46.1	53.9	0.05
TUR035-SB	TUR	035-SB	2012	TUR035	549040	7135710	-177.0	12.3	49.3	50.7	49.3	50.7	0.05
TUR036-SA	TUR	036-SA	2012	TUR036	548862	7135460	-182.1	4.9	45.5	54.4	45.6	54.4	0.04
TUR038-SA	TUR	038-SA	2012	TUR038	548934	7135400	-180.4	6.9	47.6	52.2	47.7	52.3	0.04
TUR039-SA	TUR	039-SA	2012	TUR039	548928	7135431	-173.6	15.9	20.1	79.6	20.2	79.8	0.08
TUR039-SB	TUR	039-SB	2012	TUR039	548928	7135431	-174.5	15.0	42.8	57.1	42.8	57.2	0.06
TUR039-SC	TUR	039-SC	2013	TUR039	548930	7135430	-181.7	7.5	48.7	51.2	48.7	51.3	0.04
TUR040-SA	TUR	040-SA	2012	TUR040	548950	7135460	-186.1	5.6	48.2	51.6	48.3	51.7	0.04
TUR041-SA	TUR	041-SA	2012	TUR041	548939	7135457	-183.6	9.1	46.6	53.0	46.8	53.2	0.04
TUR041-SB	TUR	041-SB	2012	TUR041	548939	7135458	-178.1	14.8	47.0	52.9	47.1	52.9	0.05

p: partial digest

t: total digest

Appendix A: Till drill core geochemistry

Sample_ID	Prefix	Number	Year	WellName	X	Y	Z	Meas_dep_m	pctClay	pctSilt	Nclay_pct	NSilt_pct	Ag_p_ppm
TUR042-SA	TUR	042-SA	2012	TUR042	548983	7135401	-182.0	7.8	48.0	51.9	48.0	52.0	0.04
TUR042-SB	TUR	042-SB	2012	TUR042	548980	7135403	-176.9	14.5	47.1	52.8	47.1	52.9	0.04
TUR042-SC	TUR	042-SC	2012	TUR042	548974	7135407	-168.6	25.3	46.4	53.4	46.5	53.5	0.04
TUR042-SD	TUR	042-SD	2013	TUR042	548976	7135405	-172.0	20.9	45.0	55.0	45.0	55.0	0.02
TUR043-SA	TUR	043-SA	2012	TUR043	548925	7135366	-181.8	7.8	48.4	51.4	48.5	51.5	0.04
TUR043-SB	TUR	043-SB	2012	TUR043	548917	7135372	-171.0	22.3	41.1	58.3	41.4	58.6	0.04
TUR044-SA	TUR	044-SA	2012	TUR044	548761	7135323	-177.8	12.3	47.4	52.5	47.5	52.5	0.05
TUR044-SB	TUR	044-SB	2012	TUR044	548758	7135325	-173.8	17.8	43.2	56.5	43.3	56.7	0.27
TUR045B-SA	TUR	045B-SA	2012	TUR045B	549096	7135463	-175.3	18.1	45.8	54.1	45.9	54.1	0.08
TUR045B-SB	TUR	045B-SB	2012	TUR045B	549092	7135466	-169.3	26.3	46.9	53.0	46.9	53.1	0.08
TUR045B-SC	TUR	045B-SC	2013	TUR045B	549093	7135465	-171.4	23.5	42.8	57.0	42.9	57.1	0.03
TUR046-SA	TUR	046-SA	2012	TUR046	549471	7135560	-177.6	7.4	47.3	52.5	47.4	52.6	0.05
TUR046-SB	TUR	046-SB	2013	TUR046	549472	7135559	-181.0	4.0	47.8	52.1	47.8	52.2	0.03
TUR046-SC	TUR	046-SC	2013	TUR046	549471	7135560	-172.4	12.7	41.8	58.1	41.8	58.2	0.07
TUR047-SA	TUR	047-SA	2012	TUR047	549317	7135553	-180.8	4.6	49.1	50.8	49.2	50.8	0.05
TUR047-SB	TUR	047-SB	2012	TUR047	549317	7135552	-174.9	10.6	42.1	57.3	42.4	57.6	0.09
TUR048-SA	TUR	048-SA	2012	TUR048	549014	7135478	-178.7	9.1	48.3	51.5	48.4	51.6	0.1
TUR048-SB	TUR	048-SB	2012	TUR048	549013	7135479	-172.8	15.2	42.2	57.7	42.2	57.8	0.09
TUR048-SC	TUR	048-SC	2012	TUR048	549013	7135479	-169.9	18.2	43.9	55.5	44.2	55.8	0.05
TUR049-SA	TUR	049-SA	2012	TUR049	548698	7135356	-178.2	8.9	39.4	48.5	44.8	55.2	0.04
TUR049-SB	TUR	049-SB	2012	TUR049	548698	7135357	-173.2	14.0	38.0	62.0	38.0	62.0	0.05
TUR049-SC	TUR	049-SC	2013	TUR049	548699	7135356	-182.3	4.7	40.8	59.1	40.8	59.2	0.05
TUR050-SA	TUR	050-SA	2012	TUR050	549038	7135531	-175.6	11.9	48.9	50.9	49.0	51.0	0.88
TUR050-SB	TUR	050-SB	2012	TUR050	549038	7135531	-171.8	15.7	38.5	61.3	38.6	61.4	0.15
TUR050-SC	TUR	050-SC	2013	TUR050	549039	7135531	-179.6	7.7	46.1	53.8	46.1	53.9	0.57
TUR051-SA	TUR	051-SA	2012	TUR051	548737	7135324	-177.9	8.8	47.0	52.8	47.1	52.9	0.07
TUR051-SB	TUR	051-SB	2012	TUR051	548736	7135324	-173.8	13.1	46.0	53.8	46.1	53.9	0.05
TUR052-SA	TUR	052-SA	2012	TUR052	548775	7135355	-180.1	7.4	48.7	51.2	48.7	51.3	1.49
TUR052-SB	TUR	052-SB	2012	TUR052	548774	7135356	-173.4	14.2	42.0	57.8	42.1	57.9	0.58
TUR053-SA	TUR	053-SA	2012	TUR053	548657	7135386	-177.7	8.7	44.7	55.1	44.8	55.2	0.07
TUR053-SB	TUR	053-SB	2012	TUR053	548656	7135386	-174.5	11.9	44.8	54.9	44.9	55.1	0.06
TUR053-SC	TUR	053-SC	2012	TUR053	548656	7135386	-172.4	14.0	36.1	63.5	36.2	63.8	0.06
TUR054-SA	TUR	054-SA	2012	TUR054	548959	7135422	-176.2	11.3	48.7	51.1	48.8	51.2	0.05

p: partial digest

t: total digest

Appendix A: Till drill core geochemistry

Sample_ID	Prefix	Number	Year	WellName	X	Y	Z	Meas_dep_m	pctClay	pctSilt	Nclay_pct	NSilt_pct	Ag_p_ppm
TUR054-SB	TUR	054-SB	2012	TUR054	548958	7135422	-170.2	17.4	46.5	53.1	46.7	53.3	0.04
TUR054-SE	TUR	054-SE	2013	TUR054	548958	7135422	-169.1	18.5	43.1	56.7	43.2	56.8	0.03
TUR055-SA	TUR	055-SA	2012	TUR055	548735	7135388	-174.0	12.8	43.0	56.7	43.1	56.9	0.04
TUR056-SA	TUR	056-SA	2012	TUR056	548815	7135382	-181.1	6.5	47.7	52.1	47.8	52.2	0.86
TUR056-SB	TUR	056-SB	2012	TUR056	548814	7135383	-174.6	13.1	47.3	52.6	47.4	52.6	0.14
TUR057-SA	TUR	057-SA	2012	TUR057	548855	7135411	-181.8	5.8	48.5	51.4	48.5	51.5	0.18
TUR057-SB	TUR	057-SB	2012	TUR057	548854	7135411	-177.8	9.8	46.7	53.0	46.8	53.2	0.08
TUR057-SC	TUR	057-SC	2012	TUR057	548854	7135412	-173.8	13.9	44.2	55.4	44.4	55.6	0.06
TUR057-SE	TUR	057-SE	2012	TUR057	548853	7135412	-171.3	16.5	38.8	61.0	38.9	61.1	0.05
TUR057-SF	TUR	057-SF	2013	TUR057	548855	7135411	-180.2	7.3	47.8	52.2	47.8	52.2	0.03
TUR057-SG	TUR	057-SG	2013	TUR057	548854	7135411	-178.2	9.4	45.1	54.8	45.1	54.9	0.04
TUR057-SH	TUR	057-SH	2013	TUR057	548854	7135412	-175.8	11.9	46.8	53.2	46.8	53.2	0.25
TUR057-SI	TUR	057-SI	2013	TUR057	548854	7135412	-174.7	13.0	46.1	53.9	46.1	53.9	0.03
TUR057-SJ	TUR	057-SJ	2013	TUR057	548854	7135412	-172.8	14.9	42.2	51.7	45.0	55.0	0.03
TUR057-SK	TUR	057-SK	2013	TUR057	548853	7135412	-171.9	15.9	46.1	53.8	46.2	53.8	0.03
TUR058-SA	TUR	058-SA	2012	TUR058	548795	7135400	-174.6	12.4	46.7	53.1	46.8	53.2	0.05
TUR058-SC	TUR	058-SC	2013	TUR058	548795	7135400	-175.6	11.5	41.8	58.1	41.9	58.1	0.02
TUR059-SA	TUR	059-SA	2012	TUR059	548836	7135430	-174.8	12.5	43.9	55.7	44.1	55.9	0.06
TUR059-SB	TUR	059-SB	2013	TUR059	548837	7135429	-184.3	2.9	32.7	67.1	32.7	67.3	0.13
TUR060-SA	TUR	060-SA	2012	TUR060	548896	7135826	-183.8	5.7	45.3	54.3	45.5	54.5	0.1
TUR060-SB	TUR	060-SB	2012	TUR060	548894	7135828	-179.1	11.4	44.8	55.1	44.8	55.2	0.06
TUR060-SD	TUR	060-SD	2012	TUR060	548891	7135830	-174.3	17.3	49.8	50.2	49.8	50.2	0.04
TUR060-SE	TUR	060-SE	2013	TUR060	548892	7135829	-176.0	15.1	40.1	59.8	40.1	59.9	0.04
TUR060-SF	TUR	060-SF	2013	TUR060	548895	7135827	-181.3	8.7	47.8	52.2	47.8	52.2	0.21
TUR061-SA	TUR	061-SA	2012	TUR061	549378	7135748	-175.3	11.7	48.6	51.3	48.6	51.4	0.04
TUR061-SB	TUR	061-SB	2012	TUR061	549377	7135749	-171.3	16.0	51.3	48.6	51.3	48.7	0.18

p: partial digest
t: total digest

Appendix A: Till drill core geochemistry

Sample_ID	Ag_t_ppm	Al2O3_t_pct	As_p_ppm	B_t_ppm	Ba_t_ppm	Be_p_ppm	Be_t_ppm	Bi_p_ppm	Bi_t_ppm	CaO_t_pct
TUR020-SA	0.29	13.4	2.69	256	651	0.66	2.2	0.36	0.5	0.69
TUR021-SA	0.28	12.3	2.38	293	505	0.45	1.9	0.31	0.4	0.62
TUR021-SB	0.3	12.8	2.56	367	401	0.3	1.6	0.16	0.2	0.53
TUR021-SC	0.19	12.3	2.16	218	580	0.62	2	0.33	0.5	0.65
TUR022-SA	0.36	12.6	2.61	264	505	0.56	2.3	0.29	0.4	0.63
TUR022-SB	0.29	11.9	2.44	247	493	0.49	1.8	0.32	0.4	0.6
TUR022-SC	0.39	13.9	2.34	401	421	0.39	1.8	0.14	0.2	0.57
TUR022-SD	0.34	12.4	2.44	294	767	0.87	5.3	0.22	0.3	0.92
TUR022-SE	0.16	12.4	2.23	248	497	0.52	1.8	0.24	0.4	0.58
TUR022-SF	0.18	11.3	2.24	177	947	1.15	4.1	0.53	0.8	0.83
TUR024-SA	0.35	12.1	2.17	266	510	0.51	1.8	0.28	0.4	0.61
TUR025-SA	0.25	12.6	2.33	272	510	0.51	1.8	0.29	0.4	0.62
TUR029-SA	0.35	12.8	2.66	280	499	0.5	1.7	0.26	0.4	0.6
TUR031-SA	0.32	12.8	2.29	266	529	0.5	1.7	0.3	0.4	0.66
TUR031-SB	0.25	13.5	2.28	238	1120	0.9	4	0.38	0.5	0.77
TUR031-SC	0.16	10.2	2.01	165	545	0.51	1.7	0.26	0.4	0.58
TUR031-SD	0.16	11.7	1.92	196	912	0.79	2.9	0.32	0.5	0.7
TUR031-SF	0.16	11.1	2	192	693	0.69	2.1	0.32	0.4	0.7
TUR032-SA	0.24	13.7	2.38	287	544	0.55	2.2	0.32	0.5	0.67
TUR032-SB	0.25	13.9	2.86	384	443	0.31	1.2	0.16	0.2	0.57
TUR032-SC	0.14	8.18	2.12	131	497	0.43	1.6	0.25	0.4	0.59
TUR034-SA	0.24	13.4	3	216	536	0.53	1.7	0.29	0.4	0.67
TUR034-SB	0.24	12	2.47	181	599	0.58	2.2	0.32	0.5	0.69
TUR035-SA	0.25	13.1	2.77	229	637	0.52	2.3	0.41	0.6	0.76
TUR035-SB	0.22	13.1	2.1	231	644	0.75	2.6	0.35	0.5	0.72
TUR036-SA	0.22	12.8	2.37	232	504	0.54	1.8	0.27	0.4	0.62
TUR038-SA	0.22	13.6	2.36	265	507	0.52	1.9	0.28	0.5	0.64
TUR039-SA	0.26	23.6	2.81	526	488	0.91	9.9	0.16	0.2	0.36
TUR039-SB	0.26	13.3	2.69	241	576	0.58	2.1	0.3	0.4	0.66
TUR039-SC	0.16	9.9	2.04	171	481	0.49	1.9	0.23	0.3	0.57
TUR040-SA	0.22	12.7	2.44	294	495	0.39	1.9	0.29	0.4	0.6
TUR041-SA	0.21	12.8	2.38	305	496	0.48	1.8	0.27	0.4	0.61
TUR041-SB	0.25	14.3	3.07	379	430	0.35	1.5	0.15	0.3	0.56

p: partial digest
t: total digest

Appendix A: Till drill core geochemistry

Sample_ID	Ag_t_ppm	Al2O3_t_pct	As_p_ppm	B_t_ppm	Ba_t_ppm	Be_p_ppm	Be_t_ppm	Bi_p_ppm	Bi_t_ppm	CaO_t_pct
TUR042-SA	0.2	13.1	2.43	277	469	0.47	1.9	0.25	0.4	0.58
TUR042-SB	0.2	14.3	3.1	293	558	0.52	2.1	0.3	0.4	0.63
TUR042-SC	0.19	14.1	2.45	358	471	0.31	1.6	0.15	0.3	0.57
TUR042-SD	0.13	7.69	2.1	178	354	0.26	1.1	0.13	0.2	0.52
TUR043-SA	0.2	13.4	2.29	278	438	0.48	1.9	0.22	0.4	0.61
TUR043-SB	0.2	10.8	2.04	190	581	0.41	2.1	0.24	0.4	0.67
TUR044-SA	0.24	13.9	2.21	281	587	0.59	2.3	0.31	0.5	0.64
TUR044-SB	0.56	13.9	2.19	267	730	0.79	2.8	0.38	0.6	0.72
TUR045B-SA	0.27	14.3	2.32	268	898	0.93	3.4	0.31	0.5	0.7
TUR045B-SB	0.28	14.6	2.66	387	476	0.41	1.6	0.16	0.3	0.61
TUR045B-SC	0.16	9.52	1.76	131	1140	0.68	2.6	0.23	0.3	0.74
TUR046-SA	0.22	13.5	2.58	277	490	0.39	1.9	0.22	0.4	0.62
TUR046-SB	0.12	8.62	1.85	128	470	0.39	1.5	0.2	0.3	0.62
TUR046-SC	0.17	9.66	2.96	193	629	0.49	1.5	0.2	0.3	0.58
TUR047-SA	0.24	13.4	2.44	257	598	0.58	2.3	0.32	0.5	0.69
TUR047-SB	0.25	13.5	2.39	332	628	0.44	2.1	0.23	0.4	0.67
TUR048-SA	0.35	14	2.31	239	493	0.53	1.8	0.27	0.4	0.62
TUR048-SB	0.29	14.7	2.59	362	451	0.45	1.6	0.17	0.3	0.56
TUR048-SC	0.22	14	2.44	378	499	0.37	1.5	0.16	0.3	0.6
TUR049-SA	0.23	12.9	2.34	269	600	0.53	2.4	0.3	0.5	0.65
TUR049-SB	0.26	17	2.38	352	918	1.41	5.4	0.34	0.5	0.7
TUR049-SC	0.15	12.7	1.94	146	756	0.67	2.2	0.45	0.5	0.94
TUR050-SA	1.61	13.4	2.38	294	483	0.45	1.8	0.24	0.4	0.63
TUR050-SB	0.33	12.4	1.92	235	902	0.69	2.9	0.33	0.5	0.82
TUR050-SC	0.61	11.5	2.24	173	567	0.59	2.1	0.34	0.5	0.63
TUR051-SA	0.25	12.1	2.3	236	605	0.49	1.9	0.34	0.5	0.69
TUR051-SB	0.23	13.6	2.24	262	667	0.6	2.5	0.38	0.5	0.67
TUR052-SA	2.19	11.9	2.47	254	504	0.59	1.9	0.3	0.4	0.6
TUR052-SB	0.9	11.5	2.16	201	803	0.76	2.1	0.53	0.7	0.74
TUR053-SA	0.26	12.8	2.5	230	638	0.73	2.6	0.41	0.6	0.76
TUR053-SB	0.25	12.5	2.28	231	664	0.75	2.8	0.41	0.6	0.69
TUR053-SC	0.25	14.2	2.32	242	1070	1.3	5.2	0.46	0.6	0.76
TUR054-SA	0.22	13	2.8	265	478	0.49	2.3	0.25	0.4	0.64

p: partial digest
t: total digest

Appendix A: Till drill core geochemistry

Sample_ID	Ag_t_ppm	Al2O3_t_pct	As_p_ppm	B_t_ppm	Ba_t_ppm	Be_p_ppm	Be_t_ppm	Bi_p_ppm	Bi_t_ppm	CaO_t_pct
TUR054-SB	0.19	13.3	2.94	391	397	0.39	1.6	0.13	0.2	0.72
TUR054-SE	0.16	11	2.64	273	403	0.33	1.2	0.13	0.2	0.53
TUR055-SA	0.19	12.8	2.69	256	635	0.64	2.6	0.32	0.5	0.74
TUR056-SA	1.29	12.6	2.83	270	556	0.64	2.2	0.32	0.5	0.65
TUR056-SB	0.33	12.3	2.48	280	554	0.56	2.2	0.28	0.4	0.64
TUR057-SA	0.41	13.2	2.73	227	524	0.67	1.7	0.28	0.4	0.66
TUR057-SB	0.24	13.4	2.3	288	548	0.63	2.1	0.28	0.4	0.65
TUR057-SC	0.21	11.3	2.45	221	566	0.67	2	0.37	0.6	0.69
TUR057-SE	0.18	12	1.92	211	1010	0.88	4.1	0.62	0.9	0.86
TUR057-SF	0.15	13	2.2	230	531	0.55	2.6	0.33	0.4	0.59
TUR057-SG	0.16	11.7	2.76	232	487	0.58	1.9	0.28	0.4	0.55
TUR057-SH	0.34	12.2	2.5	245	544	0.63	2.2	0.3	0.4	0.57
TUR057-SI	0.19	11.4	2.59	218	551	0.59	2	0.28	0.4	0.57
TUR057-SJ	0.16	10.8	2.48	182	536	0.62	1.9	0.41	0.9	0.59
TUR057-SK	0.16	10.7	2.46	196	533	0.56	1.8	0.3	0.4	0.59
TUR058-SA	0.2	12.4	2.63	200	555	0.56	2.2	0.29	0.4	0.63
TUR058-SC	0.16	9.75	1.96	163	595	0.53	1.8	0.28	0.3	0.6
TUR059-SA	0.23	12	2.4	256	595	0.58	2.1	0.36	0.5	0.71
TUR059-SB	0.23	8.96	1.52	68	751	0.38	1.6	0.27	0.4	1.08
TUR060-SA	0.36	11.1	2.31	227	646	0.64	2	0.43	0.7	0.78
TUR060-SB	0.23	13.7	2.54	255	548	0.57	2.2	0.24	0.4	0.67
TUR060-SD	0.25	15.7	2.18	260	788	0.88	3.4	0.4	0.6	0.74
TUR060-SE	0.18	12.4	2.13	211	790	0.73	2.5	0.34	0.5	0.77
TUR060-SF	0.28	12.6	2.35	229	428	0.43	1.6	0.3	0.3	0.58
TUR061-SA	0.2	12.7	2.18	279	492	0.47	2.2	0.27	0.4	0.62
TUR061-SB	0.44	11.8	2.47	290	596	0.7	1.7	0.25	0.4	0.67

p: partial digest
t: total digest

Appendix A: Till drill core geochemistry

Sample_ID	Cd_p_ppm	Cd_t_ppm	Ce_t_ppm	Co_p_ppm	Co_t_ppm	Cr_t_ppm	Cs_p_ppm	Cs_t_ppm	Cu_p_ppm	Cu_t_ppm
TUR020-SA	0.06	0.2	112	3.22	5.48	30	0.73	3.9	6.54	10.1
TUR021-SA	0.06	0.2	98	2.56	4.49	24	0.7	4	5.24	8.2
TUR021-SB	0.06	0.2	91	1.49	3.26	14	0.45	2.9	3.61	6.5
TUR021-SC	0.04	0.2	103	2.73	4.67	25	0.63	3.6	5.1	7.9
TUR022-SA	0.05	0.2	101	2.67	4.46	26	0.69	3.9	5.41	8.5
TUR022-SB	0.05	0.3	95	2.46	4.36	24	0.68	3.8	4.87	7.9
TUR022-SC	0.05	0.2	97	1.46	3.32	15	0.47	3.1	3.54	7
TUR022-SD	0.06	0.3	217	1.95	5	51	0.58	3.8	4.36	7.6
TUR022-SE	0.04	0.2	100	2.12	3.88	22	0.68	3.8	4.14	6.5
TUR022-SF	0.07	0.2	164	4.29	6.89	48	0.7	3.9	10.7	14.1
TUR024-SA	0.05	0.2	98	2.44	4.35	24	0.69	3.9	5.01	8
TUR025-SA	0.06	0.2	99	2.49	4.48	24	0.69	4	4.89	8.1
TUR029-SA	0.06	0.2	99	2.36	4.11	24	0.75	4.3	6.7	9.8
TUR031-SA	0.05	0.3	100	2.53	4.67	46	0.66	4.1	5.19	8.5
TUR031-SB	0.06	0.2	147	3.56	6.26	37	0.75	5.3	5.89	9.2
TUR031-SC	0.03	0.2	94	2.21	3.55	22	0.73	3.4	4.68	6.6
TUR031-SD	0.04	0.2	125	3.2	5.13	31	0.8	4.4	5.26	7.3
TUR031-SF	0.04	0.2	99	2.84	4.79	30	1.1	5.5	5	7.4
TUR032-SA	0.05	0.2	107	2.68	4.91	28	0.71	4.4	5.69	9.7
TUR032-SB	0.05	0.2	99	1.69	3.56	20	0.44	3.2	3.94	8
TUR032-SC	0.03	0.2	79	2.07	3.4	23	0.52	2.4	3.96	5.9
TUR034-SA	0.05	0.2	104	2.63	4.74	27	0.65	4.2	5.27	8.4
TUR034-SB	0.06	0.3	105	3.05	4.95	28	0.66	3.6	5.97	8.9
TUR035-SA	0.07	0.3	113	3.38	5.72	32	0.57	3.8	7.49	9.7
TUR035-SB	0.07	0.2	113	2.98	5.48	37	0.94	5.1	5.53	8.8
TUR036-SA	0.06	0.2	98	2.44	4.58	26	0.7	4.1	4.84	8.5
TUR038-SA	0.06	0.2	105	2.72	5.07	28	0.73	4.4	4.8	8.6
TUR039-SA	0.06	0.2	171	1.45	4.53	22	0.73	10.8	3.62	6.3
TUR039-SB	0.08	0.3	106	3.15	5.4	31	0.7	3.9	6.11	9.9
TUR039-SC	0.03	0.2	87	2.04	3.73	23	0.58	3.1	3.86	6.1
TUR040-SA	0.05	0.2	100	2.6	4.54	27	0.71	4	5.34	8.4
TUR041-SA	0.06	0.2	99	2.51	4.35	26	0.68	4.1	4.78	7.7
TUR041-SB	0.05	0.3	101	1.52	3.36	18	0.62	3.7	3.3	6.6

p: partial digest
t: total digest

Appendix A: Till drill core geochemistry

Sample_ID	Cd_p_ppm	Cd_t_ppm	Ce_t_ppm	Co_p_ppm	Co_t_ppm	Cr_t_ppm	Cs_p_ppm	Cs_t_ppm	Cu_p_ppm	Cu_t_ppm
TUR042-SA	0.05	0.2	100	2.46	4.38	30	0.74	4.5	4.41	7.5
TUR042-SB	0.06	0.2	111	2.73	4.78	29	0.76	4.6	5.01	11
TUR042-SC	0.05	0.2	100	1.64	3.47	16	0.51	3.3	3.48	6.8
TUR042-SD	0.03	0.2	67	1.18	2.2	12	0.36	1.7	2.64	4.3
TUR043-SA	0.05	0.2	98	2.04	4.14	26	0.7	4.3	3.82	7.2
TUR043-SB	0.07	0.2	96	2.5	4.2	29	0.57	3.1	4.81	7.6
TUR044-SA	0.05	0.2	108	2.68	5.16	29	0.68	4.4	5.24	36.7
TUR044-SB	0.05	0.2	127	3.28	5.6	36	0.75	4.8	7.66	11.7
TUR045B-SA	0.05	0.2	155	4.75	8.24	43	0.59	4.5	5.47	9.3
TUR045B-SB	0.05	0.2	102	1.7	3.64	19	0.45	3.5	3.8	7.7
TUR045B-SC	0.03	0.2	141	4.13	6.07	37	0.53	2.9	4.12	5.6
TUR046-SA	0.06	0.2	101	2.22	4.29	24	0.68	4.2	4.2	7.8
TUR046-SB	0.02	0.2	83	1.8	3.61	17	0.54	2.5	3.45	5.2
TUR046-SC	0.02	0.2	101	1.98	3.49	20	0.5	2.6	3.83	5.8
TUR047-SA	0.05	0.2	110	2.82	5.07	29	0.63	4.1	5.47	9.2
TUR047-SB	0.06	0.2	110	2.33	4.32	25	0.64	4	4.67	7.9
TUR048-SA	0.04	0.2	105	2.28	4.28	26	0.72	4.4	5.19	8.6
TUR048-SB	0.05	0.2	101	1.77	3.78	19	0.54	3.7	4	7.4
TUR048-SC	0.04	0.2	100	1.75	3.6	19	0.5	3.4	4.47	8
TUR049-SA	0.05	0.2	110	2.68	4.8	30	0.67	4.1	5.06	8.4
TUR049-SB	0.05	0.3	172	5.68	9.78	79	0.83	6.5	6.96	11.8
TUR049-SC	0.03	0.2	104	4.33	7.08	39	0.77	4.8	6.51	9.3
TUR050-SA	0.05	0.2	101	2.27	4.23	25	0.75	4.5	6.21	10
TUR050-SB	0.06	0.2	135	3.11	5.6	34	0.75	4.7	5.11	8.3
TUR050-SC	0.03	0.1	98	2.56	4.39	25	0.64	3.4	6.06	8.7
TUR051-SA	0.05	0.3	105	3	4.9	29	0.68	4	5.94	8.3
TUR051-SB	0.06	0.2	122	2.96	5.02	34	0.7	4.4	6.46	8.7
TUR052-SA	0.05	0.2	95	2.72	4.31	27	0.67	3.8	11.3	14
TUR052-SB	0.06	0.3	114	3.7	5.67	35	1.02	5.2	13.3	16.8
TUR053-SA	0.06	0.2	107	3.7	5.82	31	0.72	3.9	6.56	9.6
TUR053-SB	0.06	0.3	112	3.72	5.74	32	0.75	3.9	7.29	9.9
TUR053-SC	0.05	0.2	166	4.43	7.24	44	0.96	6	6.76	9.6
TUR054-SA	0.06	0.3	102	2.7	4.5	28	0.84	4.2	5.48	8.2

p: partial digest
t: total digest

Appendix A: Till drill core geochemistry

Sample_ID	Cd_p_ppm	Cd_t_ppm	Ce_t_ppm	Co_p_ppm	Co_t_ppm	Cr_t_ppm	Cs_p_ppm	Cs_t_ppm	Cu_p_ppm	Cu_t_ppm
TUR054-SB	0.05	0.2	93	1.62	3.39	17	0.44	2.9	3.4	6.4
TUR054-SE	0.03	0.2	87	1.3	2.62	14	0.41	2.3	3.08	5.3
TUR055-SA	0.07	0.2	108	3.47	5.64	33	1.19	5.9	7.76	11.3
TUR056-SA	0.06	0.2	102	2.96	4.9	34	0.8	3.9	8.27	11.7
TUR056-SB	0.06	0.3	104	2.92	4.72	27	0.74	3.8	5.27	8.2
TUR057-SA	0.05	0.3	103	2.72	4.86	26	0.75	4	5.94	9.2
TUR057-SB	0.05	0.2	104	2.72	4.82	29	0.76	4.2	5.18	9
TUR057-SC	0.05	0.2	97	3.06	4.89	29	0.72	3.2	5.89	8.3
TUR057-SE	0.04	0.2	182	3.59	6.74	37	1.01	6.2	3.47	6.2
TUR057-SF	0.03	0.2	101	2.3	4.38	26	0.64	4	4.5	7.2
TUR057-SG	0.04	0.2	94	2.44	3.92	25	0.75	3.6	4.73	6.6
TUR057-SH	0.03	0.2	103	2.56	4.29	28	0.68	3.7	5.95	8.1
TUR057-SI	0.04	0.2	100	2.46	4.08	25	0.7	3.5	4.59	6.7
TUR057-SJ	0.04	0.2	94	2.79	4.52	27	0.64	3	5.31	7.4
TUR057-SK	0.04	0.2	91	2.65	4.31	25	0.63	3	5.06	7.2
TUR058-SA	0.05	0.2	108	2.99	4.7	28	0.77	3.7	5.7	8.1
TUR058-SC	0.03	0.2	94	2.36	3.83	26	0.62	3	4.29	6.3
TUR059-SA	0.07	0.2	105	3.26	5.02	29	0.68	3.3	6.6	10.2
TUR059-SB	0.02	0.2	90	3.39	5.32	32	0.62	3	6.14	9.2
TUR060-SA	0.05	0.2	103	3.59	5.13	32	0.67	3.1	7.14	9.8
TUR060-SB	0.05	0.2	106	2.47	3.7	26	0.84	3.5	4.52	7.4
TUR060-SD	0.06	0.2	156	3.63	6.19	36	0.84	5.4	5.77	9.3
TUR060-SE	0.04	0.2	114	3.08	5.16	33	0.95	4.6	5.47	7.9
TUR060-SF	0.04	0.2	90	1.74	3.49	20	0.71	3.9	3.93	6.2
TUR061-SA	0.04	0.2	97	2.38	4.29	26	0.77	4	4.84	10.2
TUR061-SB	0.05	0.2	100	2.67	4.12	24	0.8	3.8	6.09	9.3

p: partial digest
t: total digest

Appendix A: Till drill core geochemistry

Sample_ID	Dy_p_ppm	Dy_t_ppm	Er_p_ppm	Er_t_ppm	Eu_p_ppm	Eu_t_ppm	Fe2O3_t_pct	Ga_p_ppm	Ga_t_ppm	Gd_p_ppm
TUR020-SA	1.5	3.21	0.73	1.75	0.78	1.8	3	1.93	16.1	3.64
TUR021-SA	1.37	3	0.68	1.66	0.68	1.55	2.64	1.62	14.8	3.16
TUR021-SB	0.95	3.28	0.46	1.33	0.47	1.32	2.32	0.93	13.7	2.18
TUR021-SC	1.47	3.07	0.69	1.73	0.72	1.45	2.73	2.06	14.6	3.41
TUR022-SA	1.35	2.9	0.68	1.63	0.66	1.54	2.7	1.66	14.6	3.17
TUR022-SB	1.3	2.78	0.64	1.56	0.65	1.46	2.58	1.55	14.3	2.99
TUR022-SC	0.98	2.67	0.47	1.47	0.48	1.45	2.46	0.95	15.1	2.22
TUR022-SD	1.64	4.57	0.68	2.37	1.33	3.38	3.68	1.22	17.7	5.38
TUR022-SE	1.24	2.83	0.59	1.51	0.64	1.35	2.56	1.6	14.1	2.87
TUR022-SF	1.89	3.73	0.81	1.77	1.32	2.36	3.62	2.72	15.2	5.42
TUR024-SA	1.25	2.74	0.61	1.49	0.64	1.51	2.62	1.53	13.9	2.93
TUR025-SA	1.33	2.88	0.64	1.55	0.66	1.53	2.7	1.61	14.6	3.02
TUR029-SA	1.26	2.68	0.62	1.54	0.64	1.5	2.66	1.54	14.7	2.94
TUR031-SA	1.3	3.03	0.64	1.66	0.65	1.57	2.73	1.59	15.2	3.05
TUR031-SB	1.47	3.25	0.68	1.68	1.21	2.43	3.17	2.12	18.1	4.84
TUR031-SC	1.25	2.66	0.57	1.42	0.67	1.38	2.34	1.62	11.6	3.02
TUR031-SD	1.48	3.14	0.66	1.62	1.03	1.9	2.81	2.2	15	4.12
TUR031-SF	1.32	2.88	0.59	1.52	0.8	1.72	2.69	1.88	14.2	3.31
TUR032-SA	1.39	3.15	0.69	1.68	0.68	1.72	2.9	1.68	16.4	3.15
TUR032-SB	0.99	2.7	0.48	1.51	0.51	1.48	2.52	1.05	15.3	2.28
TUR032-SC	1.17	2.57	0.56	1.36	0.58	1.22	2.03	1.56	10	2.68
TUR034-SA	1.33	3.04	0.66	1.65	0.66	1.63	2.84	1.7	15.8	3.13
TUR034-SB	1.43	3.03	0.68	1.69	0.73	1.69	2.77	1.78	14.1	3.36
TUR035-SA	1.58	3.22	0.79	1.79	0.8	1.76	3.11	2.13	16.1	3.72
TUR035-SB	1.34	3.07	0.65	1.62	0.78	1.83	3.07	1.77	15.9	3.5
TUR036-SA	1.3	2.87	0.63	1.64	0.64	1.53	2.7	1.57	15.4	2.9
TUR038-SA	1.32	2.98	0.66	1.62	0.66	1.61	2.86	1.62	16.2	3.07
TUR039-SA	0.83	2.13	0.38	1.13	0.95	1.91	5.08	1.01	39	3.93
TUR039-SB	1.4	3.02	0.69	1.71	0.71	1.66	2.94	1.82	16	3.24
TUR039-SC	1.2	2.72	0.56	1.48	0.61	1.33	2.27	1.57	12	2.85
TUR040-SA	1.33	2.81	0.66	1.58	0.67	1.53	2.69	1.65	15.4	3.12
TUR041-SA	1.31	2.85	0.64	1.76	0.64	1.52	2.68	1.59	15	2.88
TUR041-SB	0.98	2.72	0.48	1.48	0.5	1.49	2.57	0.97	15.5	2.25

p: partial digest
t: total digest

Appendix A: Till drill core geochemistry

Sample_ID	Dy_p_ppm	Dy_t_ppm	Er_p_ppm	Er_t_ppm	Eu_p_ppm	Eu_t_ppm	Fe2O3_t_pct	Ga_p_ppm	Ga_t_ppm	Gd_p_ppm
TUR042-SA	1.26	2.98	0.62	1.56	0.6	1.55	2.69	1.5	15.5	2.83
TUR042-SB	1.37	2.96	0.66	1.66	0.73	1.7	2.91	1.7	16.6	3.28
TUR042-SC	0.97	2.49	0.48	1.39	0.5	1.42	2.55	1.07	15.2	2.3
TUR042-SD	0.8	2.19	0.37	1.18	0.4	1.03	1.79	0.86	8.4	1.9
TUR043-SA	1.24	2.85	0.62	1.6	0.56	1.48	2.7	1.35	15.9	2.64
TUR043-SB	1.17	2.74	0.56	1.47	0.6	1.57	2.59	1.43	12.4	2.78
TUR044-SA	1.33	3.02	0.62	1.68	0.69	1.68	2.98	1.66	16.3	3.06
TUR044-SB	1.38	3.23	0.65	1.79	0.87	2.09	3.24	1.88	17.1	3.72
TUR045B-SA	1.52	3.31	0.68	1.76	1.19	2.46	3.56	2.3	18.2	4.85
TUR045B-SB	1	2.79	0.49	1.7	0.51	1.53	2.6	1.05	15.6	2.33
TUR045B-SC	1.51	3.28	0.6	1.62	1.2	2.15	2.74	2.15	11.3	4.84
TUR046-SA	1.19	2.9	0.6	1.61	0.58	1.55	2.71	1.4	15.5	2.7
TUR046-SB	1.12	2.41	0.52	1.36	0.55	1.22	2.1	1.35	9.7	2.65
TUR046-SC	1.17	2.68	0.51	1.41	0.72	1.52	2.25	1.51	11	3.14
TUR047-SA	1.38	3.07	0.68	1.72	0.69	1.68	2.88	1.8	15.9	3.23
TUR047-SB	1.14	2.82	0.55	1.52	0.65	1.68	2.77	1.45	15.3	2.86
TUR048-SA	1.29	2.97	0.65	1.67	0.62	1.6	2.89	1.51	16.4	2.91
TUR048-SB	1.02	2.75	0.5	1.43	0.52	1.52	2.58	1.1	16.4	2.42
TUR048-SC	0.99	2.9	0.48	1.47	0.53	1.54	2.58	1.08	15.6	2.37
TUR049-SA	1.21	2.9	0.58	1.6	0.72	1.78	2.88	1.63	15.5	3.08
TUR049-SB	1.76	4.15	0.78	2.1	1.26	2.92	3.7	2.74	24	5.12
TUR049-SC	1.73	3.38	0.81	1.75	0.77	1.56	3.38	2.91	17.5	4.04
TUR050-SA	1.21	2.91	0.59	1.73	0.6	1.54	2.78	1.46	15.2	2.77
TUR050-SB	1.34	3.32	0.63	1.73	0.93	2.27	3.14	1.72	16	3.78
TUR050-SC	1.36	2.81	0.64	1.57	0.69	1.45	2.55	1.9	13.7	3.2
TUR051-SA	1.36	3.01	0.67	1.68	0.71	1.72	2.8	1.85	14.4	3.26
TUR051-SB	1.36	3.02	0.65	1.62	0.83	1.95	3.06	1.77	16.4	3.55
TUR052-SA	1.3	2.79	0.65	1.47	0.67	1.48	2.59	1.74	14.2	3.02
TUR052-SB	1.34	2.92	0.62	1.56	0.92	1.92	3.01	1.98	13.6	3.74
TUR053-SA	1.61	3.3	0.77	1.89	0.81	1.7	2.98	2.4	16.1	3.87
TUR053-SB	1.52	3.11	0.72	1.72	0.87	1.82	2.98	2.34	15.9	3.91
TUR053-SC	1.86	3.89	0.87	2.09	1.37	2.69	3.8	2.78	21.1	5.71
TUR054-SA	1.26	2.85	0.62	1.64	0.64	1.56	2.72	1.7	15.7	3.04

p: partial digest

t: total digest

Appendix A: Till drill core geochemistry

Sample_ID	Dy_p_ppm	Dy_t_ppm	Er_p_ppm	Er_t_ppm	Eu_p_ppm	Eu_t_ppm	Fe2O3_t_pct	Ga_p_ppm	Ga_t_ppm	Gd_p_ppm
TUR054-SB	0.99	2.55	0.48	1.42	0.51	1.35	2.35	1.15	15	2.39
TUR054-SE	0.9	2.58	0.43	1.33	0.45	1.21	2.16	1.04	12	2.24
TUR055-SA	1.33	2.95	0.63	1.68	0.78	1.82	3.02	2.02	15.7	3.41
TUR056-SA	1.36	2.96	0.66	1.68	0.72	1.61	2.81	1.96	15.4	3.25
TUR056-SB	1.34	3.01	0.65	1.73	0.73	1.7	2.68	1.92	15.2	3.3
TUR057-SA	1.4	3.17	0.69	1.82	0.68	1.6	2.86	1.89	16	3.2
TUR057-SB	1.34	3.23	0.65	1.7	0.7	1.65	2.9	1.73	15.7	3.1
TUR057-SC	1.34	2.86	0.63	1.65	0.68	1.57	2.68	1.82	13.5	3.12
TUR057-SE	1.55	3.64	0.7	1.89	1.52	2.84	3.3	1.9	16.8	5.83
TUR057-SF	1.28	2.98	0.62	1.56	0.63	1.41	2.71	1.67	15.4	2.89
TUR057-SG	1.35	2.8	0.64	1.54	0.67	1.35	2.48	1.87	13.6	3.12
TUR057-SH	1.31	3.03	0.62	1.56	0.72	1.46	2.54	1.9	14.9	3.38
TUR057-SI	1.29	2.86	0.6	1.51	0.7	1.44	2.45	1.86	14	3.22
TUR057-SJ	1.39	2.85	0.63	1.56	0.7	1.41	2.46	1.91	13.4	3.22
TUR057-SK	1.31	2.79	0.61	1.62	0.66	1.38	2.42	1.82	12.5	3.06
TUR058-SA	1.35	2.95	0.65	1.65	0.76	1.65	2.73	1.95	15.3	3.42
TUR058-SC	1.23	2.74	0.55	1.47	0.69	1.46	2.38	1.71	11.4	3.12
TUR059-SA	1.46	3.08	0.69	1.72	0.74	1.69	2.8	1.96	14.2	3.42
TUR059-SB	1.44	3.03	0.67	1.61	0.61	1.37	2.67	2.11	11.2	3.32
TUR060-SA	1.48	2.94	0.73	1.62	0.78	1.65	2.77	2.35	13.9	3.61
TUR060-SB	1.25	2.77	0.61	1.5	0.66	1.69	2.81	1.65	15.9	2.92
TUR060-SD	1.63	3.76	0.78	2.11	0.92	2.32	3.71	2.32	21.8	4.15
TUR060-SE	1.39	3.04	0.63	1.57	0.8	1.73	2.96	2.09	14.7	3.47
TUR060-SF	1.17	2.78	0.56	1.5	0.5	1.23	2.51	1.39	13.8	2.5
TUR061-SA	1.26	2.87	0.64	1.62	0.64	1.52	2.7	1.68	15.6	2.91
TUR061-SB	1.28	2.79	0.63	1.55	0.71	1.57	2.61	1.77	13.7	3.15

p: partial digest
t: total digest

Appendix A: Till drill core geochemistry

Sample_ID	Gd_t_ppm	Ge_p_ppm	Hf_p_ppm	Hf_t_ppm	Hg_p_ppm	Ho_p_ppm	Ho_t_ppm	K2O_t_pct	La_t_ppm	Li_t_ppm
TUR020-SA	7.8	0.01	0.21	8.2	0.07	0.23	0.58	3.85	65	56
TUR021-SA	6.9	0.005	0.16	8.7	0.05	0.22	0.53	3.42	57	50
TUR021-SB	6	0.005	0.16	7.6	0.06	0.14	0.42	3.52	53	45
TUR021-SC	5.9	0.01	0.65	8.8	0.005	0.26	0.57	3.55	62	53
TUR022-SA	6.6	0.005	0.19	8.4	0.07	0.22	0.55	3.55	58	52
TUR022-SB	6.6	0.005	0.16	8	0.05	0.2	0.5	3.37	55	49
TUR022-SC	6.3	0.005	0.16	8.3	0.04	0.14	0.48	3.78	56	48
TUR022-SD	12.9	0.02	0.12	11.5	0.06	0.22	0.78	4.39	129	28
TUR022-SE	5.5	0.02	0.61	8.5	0.005	0.21	0.55	3.45	60	50
TUR022-SF	8.6	0.02	0.78	8.8	0.005	0.3	0.67	3.73	102	42
TUR024-SA	6.5	0.005	0.16	8.1	0.07	0.19	0.5	3.43	56	49
TUR025-SA	6.6	0.005	0.17	8.2	0.05	0.2	0.51	3.53	57	52
TUR029-SA	6.4	0.005	0.17	7.9	0.06	0.2	0.5	3.58	57	51
TUR031-SA	7	0.005	0.16	8.4	0.06	0.21	0.55	3.56	58	52
TUR031-SB	9.1	0.01	0.21	8.5	0.04	0.2	0.53	4.43	85	52
TUR031-SC	5.4	0.01	0.34	8.3	0.005	0.21	0.5	2.91	56	42
TUR031-SD	6.9	0.005	0.25	9	0.005	0.23	0.58	3.74	75	48
TUR031-SF	6	0.005	0.5	8.5	0.005	0.21	0.55	3.31	60	47
TUR032-SA	7.4	0.005	0.19	8.9	0.03	0.22	0.57	3.86	61	56
TUR032-SB	6.9	0.005	0.14	8.8	0.04	0.16	0.5	3.9	57	48
TUR032-SC	5	0.02	0.34	9.1	0.005	0.19	0.49	2.48	47	35
TUR034-SA	6.9	0.01	0.16	8.8	0.04	0.21	0.55	3.74	59	54
TUR034-SB	7	0.01	0.23	9	0.05	0.22	0.55	3.48	61	50
TUR035-SA	7.7	0.02	0.18	8.8	0.03	0.24	0.6	3.81	65	55
TUR035-SB	7.3	0.005	0.32	8.8	0.03	0.2	0.53	3.81	65	52
TUR036-SA	6.8	0.005	0.23	8.8	0.03	0.2	0.52	3.58	56	52
TUR038-SA	7	0.005	0.18	8.8	0.04	0.21	0.55	3.8	61	55
TUR039-SA	8.3	0.02	1.11	6.5	0.06	0.1	0.34	8.57	105	28
TUR039-SB	7.4	0.005	0.27	8.1	0.05	0.22	0.55	3.84	61	56
TUR039-SC	5.3	0.01	0.31	9.6	0.005	0.2	0.53	2.85	52	42
TUR040-SA	6.8	0.005	0.18	8.4	0.03	0.21	0.53	3.57	57	51
TUR041-SA	6.8	0.005	0.12	8	0.04	0.2	0.53	3.6	57	53
TUR041-SB	6.7	0.005	0.16	9.1	0.04	0.15	0.49	3.96	58	49

p: partial digest

t: total digest

Appendix A: Till drill core geochemistry

Sample_ID	Gd_t_ppm	Ge_p_ppm	Hf_p_ppm	Hf_t_ppm	Hg_p_ppm	Ho_p_ppm	Ho_t_ppm	K2O_t_pct	La_t_ppm	Li_t_ppm
TUR042-SA	6.9	0.005	0.22	8.1	0.04	0.2	0.53	3.67	57	52
TUR042-SB	7.3	0.005	0.22	8.2	0.04	0.21	0.55	4	65	57
TUR042-SC	6.5	0.005	0.33	7.8	0.03	0.15	0.46	3.99	58	49
TUR042-SD	4.1	0.01	0.45	10	0.005	0.13	0.42	2.23	41	30
TUR043-SA	6.5	0.005	0.18	8.2	0.03	0.2	0.52	3.7	56	55
TUR043-SB	6.4	0.005	0.36	8.9	0.04	0.18	0.48	3.22	56	45
TUR044-SA	7	0.005	0.19	8.4	0.06	0.2	0.56	3.94	62	56
TUR044-SB	8.1	0.005	0.16	9	0.16	0.2	0.58	4.09	75	55
TUR045B-SA	9.7	0.005	0.2	8.1	0.06	0.21	0.58	4.42	92	60
TUR045B-SB	6.8	0.005	0.17	8.8	0.05	0.15	0.56	4.12	60	50
TUR045B-SC	7.2	0.02	0.52	10.7	0.005	0.23	0.59	3.37	85	42
TUR046-SA	7	0.005	0.16	8.2	0.04	0.18	0.55	3.79	59	54
TUR046-SB	4.8	0.01	0.54	9	0.005	0.19	0.48	2.52	50	37
TUR046-SC	5.6	0.005	0.36	9.3	0.005	0.18	0.51	2.92	61	37
TUR047-SA	7.4	0.005	0.19	8.2	0.09	0.21	0.56	3.86	62	55
TUR047-SB	7.1	0.005	0.26	8	0.06	0.17	0.5	3.89	63	51
TUR048-SA	7.2	0.005	0.17	8.2	0.05	0.2	0.53	3.84	61	56
TUR048-SB	6.8	0.005	0.15	7.4	0.06	0.15	0.48	4.06	59	52
TUR048-SC	6.6	0.005	0.15	7.7	0.03	0.16	0.48	3.9	59	49
TUR049-SA	7.4	0.005	0.19	8.4	0.03	0.18	0.52	3.77	65	50
TUR049-SB	11.4	0.005	0.13	8.9	0.04	0.25	0.7	5.08	105	73
TUR049-SC	6.3	0.02	0.26	7.2	0.005	0.3	0.64	3.97	62	48
TUR050-SA	7	0.005	0.16	8.2	0.26	0.18	0.53	3.72	59	53
TUR050-SB	8.9	0.005	0.2	9.1	0.05	0.2	0.58	4.03	79	46
TUR050-SC	5.6	0.01	0.21	8.5	0.005	0.24	0.54	3.29	60	49
TUR051-SA	7.2	0.005	0.19	8.5	0.04	0.21	0.53	3.61	59	49
TUR051-SB	8	0.01	0.2	8.6	0.04	0.2	0.54	4.02	71	52
TUR052-SA	6.4	0.005	0.15	7.7	0.42	0.21	0.49	3.34	54	48
TUR052-SB	7.4	0.005	0.28	8.2	0.16	0.19	0.5	3.58	66	50
TUR053-SA	7.4	0.005	0.18	8.2	0.14	0.24	0.59	3.81	62	53
TUR053-SB	7.7	0.02	0.2	8.8	0.04	0.23	0.59	3.81	65	50
TUR053-SC	10.5	0.02	0.12	9.7	0.03	0.27	0.68	4.9	96	55
TUR054-SA	7	0.005	0.23	9.3	0.02	0.2	0.52	3.64	60	52

p: partial digest
t: total digest

Appendix A: Till drill core geochemistry

Sample_ID	Gd_t_ppm	Ge_p_ppm	Hf_p_ppm	Hf_t_ppm	Hg_p_ppm	Ho_p_ppm	Ho_t_ppm	K2O_t_pct	La_t_ppm	Li_t_ppm
TUR054-SB	6.2	0.005	0.08	8	0.02	0.15	0.49	3.71	54	46
TUR054-SE	5	0.005	0.26	9.2	0.005	0.15	0.47	2.99	52	39
TUR055-SA	7.4	0.01	0.25	9.1	0.03	0.2	0.54	3.81	63	54
TUR056-SA	6.8	0.005	0.14	8.8	0.23	0.21	0.57	3.6	59	52
TUR056-SB	7.2	0.01	0.2	9.6	0.06	0.2	0.56	3.59	59	50
TUR057-SA	7	0.005	0.14	10.1	0.05	0.21	0.56	3.72	58	54
TUR057-SB	7.1	0.005	0.18	8.8	0.02	0.2	0.54	3.8	60	55
TUR057-SC	6.7	0.005	0.3	8.8	0.06	0.2	0.52	3.39	56	49
TUR057-SE	10.5	0.01	0.13	9.9	0.03	0.2	0.62	4.35	112	47
TUR057-SF	5.8	0.02	0.27	8.5	0.005	0.22	0.57	3.58	61	54
TUR057-SG	5.5	0.01	0.25	8.6	0.005	0.23	0.54	3.2	56	49
TUR057-SH	5.8	0.005	0.26	8.7	0.005	0.23	0.55	3.44	62	50
TUR057-SI	5.8	0.01	0.44	9	0.005	0.21	0.54	3.28	61	47
TUR057-SJ	5.7	0.02	0.53	8.1	0.005	0.23	0.55	3.13	56	46
TUR057-SK	5.6	0.02	0.53	8.3	0.005	0.22	0.54	3.12	55	46
TUR058-SA	7	0.01	0.14	9.1	0.03	0.2	0.54	3.62	61	50
TUR058-SC	5.4	0.01	0.25	9.8	0.005	0.2	0.53	2.93	58	40
TUR059-SA	7.2	0.01	0.3	8.4	0.02	0.22	0.57	3.6	59	49
TUR059-SB	5.6	0.02	0.46	7.2	0.005	0.25	0.56	3.1	55	32
TUR060-SA	6.9	0.005	0.21	8.3	0.05	0.23	0.53	3.41	59	46
TUR060-SB	7.2	0.005	0.21	8.5	0.03	0.19	0.64	3.89	61	55
TUR060-SD	9.7	0.02	0.21	9.2	0.02	0.24	0.7	5	92	51
TUR060-SE	6.3	0.02	0.47	8.2	0.005	0.23	0.57	3.66	70	52
TUR060-SF	5.4	0.01	0.26	8.4	0.005	0.2	0.55	3.42	55	52
TUR061-SA	6.8	0.01	0.19	8.6	0.02	0.2	0.53	3.58	56	51
TUR061-SB	6.6	0.005	0.18	8.7	0.06	0.19	0.51	3.36	57	47

p: partial digest
t: total digest

Appendix A: Till drill core geochemistry

Sample_ID	MgO_t_pct	MnO_t_pct	Mo_p_ppm	Mo_t_ppm	Na2O_t_pct	Nb_p_ppm	Nb_t_ppm	Nd_p_ppm	Nd_t_ppm	Ni_p_ppm
TUR020-SA	1.28	0.03	1.12	1.27	0.38	0.03	9.7	23.2	51.4	8.95
TUR021-SA	1.08	0.024	0.33	0.52	0.32	0.005	9.5	20	45.8	7.12
TUR021-SB	0.813	0.018	0.26	0.49	0.21	0.02	9	14.1	40.3	3.59
TUR021-SC	1.19	0.023	0.21	0.54	0.39	0.02	9.4	24.5	43.9	8.3
TUR022-SA	1.12	0.023	0.34	0.62	0.34	0.005	9.3	19.9	45.4	7.85
TUR022-SB	1.05	0.023	0.33	0.56	0.3	0.005	9.1	19.2	43.5	6.71
TUR022-SC	0.887	0.019	0.23	0.48	0.22	0.005	9.4	14.3	43.4	3.58
TUR022-SD	1.16	0.049	0.71	1.05	0.35	0.07	11	36.4	96.6	9.98
TUR022-SE	1.04	0.022	0.22	0.52	0.29	0.02	9	21.3	41.6	6.22
TUR022-SF	1.53	0.045	1.89	2.46	0.58	0.12	10	44.9	68.5	15
TUR024-SA	1.06	0.024	0.26	0.46	0.32	0.005	9.1	19	44.1	6.77
TUR025-SA	1.11	0.024	0.32	0.48	0.34	0.005	9.2	19.5	44.5	6.82
TUR029-SA	1.08	0.023	0.28	0.5	0.31	0.005	9	18.8	43.7	6.47
TUR031-SA	1.12	0.025	0.29	0.54	0.34	0.005	9.7	19.3	46	6.78
TUR031-SB	1.67	0.031	0.42	0.84	0.34	0.01	9.3	34.6	66.5	10.4
TUR031-SC	0.89	0.019	0.27	0.46	0.36	0.04	8.6	22.1	40	6.6
TUR031-SD	1.34	0.026	0.4	0.65	0.36	0.04	9	34.2	53.7	10.4
TUR031-SF	1.17	0.023	0.34	0.66	0.29	0.03	8.4	25	45.6	8.88
TUR032-SA	1.22	0.027	0.29	0.64	0.34	0.005	10	20.1	49.6	7.2
TUR032-SB	0.899	0.019	0.37	0.67	0.25	0.005	9.8	14.8	45.3	4.35
TUR032-SC	0.783	0.018	0.32	0.5	0.38	0.03	8.2	20.1	35	6.16
TUR034-SA	1.16	0.026	0.35	0.64	0.37	0.005	9.7	19.5	46.7	7.17
TUR034-SB	1.14	0.028	0.67	0.97	0.38	0.02	9.4	21.5	48.4	8.22
TUR035-SA	1.39	0.03	0.3	0.6	0.5	0.005	9.9	24.3	50.3	8.83
TUR035-SB	1.28	0.027	0.33	0.64	0.35	0.005	9.3	22.6	52.2	8.66
TUR036-SA	1.1	0.024	0.28	0.54	0.34	0.005	9.5	18.6	45	6.67
TUR038-SA	1.18	0.026	0.32	0.61	0.32	0.005	9.7	19.8	47.2	7.08
TUR039-SA	2.42	0.016	0.3	0.72	0.17	0.005	8.3	31.1	72.7	5.7
TUR039-SB	1.25	0.029	0.83	1.34	0.38	0.02	9.6	21.3	49.1	8.35
TUR039-SC	0.894	0.019	0.24	0.62	0.31	0.03	8.6	20.7	38.9	6.47
TUR040-SA	1.1	0.024	0.24	0.57	0.3	0.005	9.2	19.9	45.1	6.98
TUR041-SA	1.11	0.024	0.28	0.51	0.3	0.005	9.1	19	45.1	6.72
TUR041-SB	0.911	0.017	0.31	0.78	0.21	0.005	9.7	14.6	45.7	3.63

p: partial digest

t: total digest

Appendix A: Till drill core geochemistry

Sample_ID	MgO_t_pct	MnO_t_pct	Mo_p_ppm	Mo_t_ppm	Na2O_t_pct	Nb_p_ppm	Nb_t_ppm	Nd_p_ppm	Nd_t_ppm	Ni_p_ppm
TUR042-SA	1.07	0.022	0.28	0.59	0.31	0.005	9.4	17.8	45.9	6.38
TUR042-SB	1.22	0.027	0.32	0.56	0.31	0.005	9.7	21.6	50.7	7.54
TUR042-SC	0.968	0.018	0.27	0.57	0.24	0.005	9.5	14.9	45.3	4.03
TUR042-SD	0.568	0.013	0.24	0.49	0.23	0.02	7.6	14.1	29	3.24
TUR043-SA	1.07	0.023	0.26	0.51	0.3	0.005	9.6	17	44.7	5.18
TUR043-SB	0.999	0.024	0.73	1.12	0.4	0.005	9.1	18.3	43.8	7
TUR044-SA	1.25	0.024	0.27	0.57	0.31	0.005	9.9	19.9	49.3	7.36
TUR044-SB	1.38	0.03	0.52	0.76	0.34	0.01	9.8	24.6	57.9	9.46
TUR045B-SA	1.83	0.033	0.38	0.76	0.33	0.005	9.9	36	69.6	14.7
TUR045B-SB	0.986	0.021	0.27	0.55	0.26	0.005	10	15	47.4	4.32
TUR045B-SC	1.25	0.023	0.34	0.65	0.35	0.02	9.5	40.2	59.4	15.7
TUR046-SA	1.1	0.023	0.31	0.56	0.33	0.005	9.5	17.8	47	5.55
TUR046-SB	0.771	0.016	0.22	0.42	0.34	0.02	8.3	19.2	35.2	5.26
TUR046-SC	0.817	0.017	0.32	0.59	0.29	0.03	8.7	24.5	43.3	6.6
TUR047-SA	1.25	0.028	0.33	0.62	0.4	0.005	10	21.1	49.6	7.66
TUR047-SB	1.11	0.024	0.25	0.55	0.31	0.005	9.5	18.9	49.7	6.32
TUR048-SA	1.15	0.024	0.26	0.52	0.29	0.005	9.7	18.4	48.2	5.97
TUR048-SB	1.02	0.024	0.27	0.52	0.22	0.005	9.6	15.8	46.3	4.26
TUR048-SC	0.965	0.019	0.28	0.56	0.23	0.005	9.2	15.6	45.5	4.33
TUR049-SA	1.18	0.025	0.38	0.61	0.31	0.005	9.5	20.7	50.8	7.77
TUR049-SB	2	0.029	0.44	0.8	0.34	0.005	10.9	35.4	80.3	26
TUR049-SC	1.62	0.034	0.36	0.49	0.64	0.04	9.6	28.2	46.1	13.1
TUR050-SA	1.1	0.024	0.28	0.58	0.29	0.005	9.5	17.6	46.9	6.06
TUR050-SB	1.34	0.027	0.39	0.84	0.34	0.005	9.3	26.3	61.3	9.6
TUR050-SC	1.11	0.023	0.28	0.51	0.39	0.04	9	23.5	41.9	7.95
TUR051-SA	1.16	0.025	0.3	0.58	0.38	0.005	9.5	21	48.4	8.19
TUR051-SB	1.27	0.026	0.28	0.58	0.3	0.005	9.8	23.8	55.2	8.8
TUR052-SA	1.05	0.022	0.32	0.65	0.28	0.005	8.9	19.6	43.2	7.73
TUR052-SB	1.35	0.029	0.92	1.13	0.3	0.005	8.9	25.8	51.7	9.89
TUR053-SA	1.36	0.03	0.5	0.8	0.46	0.005	9.2	25.2	48.8	10.4
TUR053-SB	1.27	0.028	0.32	0.62	0.38	0.005	9.1	25.4	51.6	10.5
TUR053-SC	1.75	0.032	0.42	0.75	0.43	0.01	10.1	40.7	73	15.9
TUR054-SA	1.06	0.024	0.41	0.65	0.3	0.005	9.4	19.3	45.8	7.82

p: partial digest

t: total digest

Appendix A: Till drill core geochemistry

Sample_ID	MgO_t_pct	MnO_t_pct	Mo_p_ppm	Mo_t_ppm	Na2O_t_pct	Nb_p_ppm	Nb_t_ppm	Nd_p_ppm	Nd_t_ppm	Ni_p_ppm
TUR054-SB	0.889	0.018	0.24	0.47	0.22	0.005	8.8	15.5	42	3.96
TUR054-SE	0.732	0.014	0.36	0.36	0.22	0.02	9.1	16	36.9	3.55
TUR055-SA	1.3	0.028	0.61	0.97	0.31	0.005	9.1	22.9	50.5	9.27
TUR056-SA	1.14	0.024	0.36	0.66	0.33	0.005	9.1	21.5	45.8	8.51
TUR056-SB	1.09	0.024	0.29	0.59	0.32	0.005	9.3	21.6	48.2	8.11
TUR057-SA	1.16	0.025	0.31	0.59	0.32	0.005	9.6	20.7	46.6	7.43
TUR057-SB	1.2	0.026	0.32	0.7	0.31	0.005	9.2	20.6	47.1	7.59
TUR057-SC	1.07	0.027	0.74	1.14	0.38	0.005	8.9	21	44.3	8.42
TUR057-SE	1.54	0.024	0.4	0.7	0.24	0.005	8.8	44.2	79.9	11.8
TUR057-SF	1.16	0.024	0.24	0.53	0.3	0.02	9.2	21	41.9	7.24
TUR057-SG	1.04	0.022	0.32	0.58	0.28	0.03	8.9	22.9	39.4	7.54
TUR057-SH	1.11	0.024	0.28	0.44	0.29	0.03	9	25	43.8	8.51
TUR057-SI	1.03	0.022	0.28	0.59	0.3	0.04	9.2	24	42.9	7.95
TUR057-SJ	1.05	0.024	0.45	0.64	0.35	0.05	8.8	23.7	41	8.5
TUR057-SK	0.999	0.023	0.42	0.64	0.36	0.05	8.6	22.4	40	8.16
TUR058-SA	1.11	0.024	0.54	0.7	0.31	0.005	9.3	23.1	48.5	8.76
TUR058-SC	0.924	0.02	0.26	0.39	0.32	0.03	8.8	23	41.5	7.61
TUR059-SA	1.16	0.028	0.58	1.01	0.42	0.01	9.2	22.3	48.1	9.01
TUR059-SB	1.18	0.03	0.37	0.56	0.96	0.04	10.1	23.3	40.3	9.95
TUR060-SA	1.19	0.026	0.57	1.04	0.48	0.005	9.1	24.1	46.8	9.95
TUR060-SB	1.17	0.025	0.38	0.53	0.32	0.005	9.4	19.8	47.6	6.6
TUR060-SD	1.55	0.031	0.45	0.82	0.47	0.01	10.8	28.4	68.9	10.1
TUR060-SE	1.31	0.028	0.41	0.59	0.4	0.05	8.8	27.2	48.3	9.57
TUR060-SF	1	0.021	0.27	0.49	0.28	0.02	8.9	17.5	38.3	4.89
TUR061-SA	1.06	0.022	0.23	0.52	0.3	0.005	9.3	18.7	45.1	6.41
TUR061-SB	1.04	0.022	0.34	0.53	0.31	0.005	8.9	21.2	45	7.2

p: partial digest
t: total digest

Appendix A: Till drill core geochemistry

Sample_ID	Ni_t_ppm	P2O5_t_pct	Pb_p_ppm	Pb_t_ppm	Pb204_p_ppm	Pb204_t_ppm	Pb206_p_ppm	Pb206_t_ppm	Pb207_p_ppm
TUR020-SA	19.3	0.342	12.4	22.9	0.156	0.296	3.22	5.77	2.45
TUR021-SA	15.6	0.31	11.3	20.9	0.141	0.266	2.89	5.25	2.19
TUR021-SB	10.5	0.337	10.7	20.5	0.135	0.263	2.74	5.07	2.08
TUR021-SC	16.2	0.32	12.6	21.5	0.191	0.297	3.27	4.95	2.61
TUR022-SA	15.6	0.318	12.3	22.4	0.15	0.294	3.16	5.72	2.42
TUR022-SB	15	0.302	10.5	19.8	0.13	0.261	2.67	5.08	2.05
TUR022-SC	11.2	0.354	9.58	20.8	0.114	0.269	2.43	5.13	1.85
TUR022-SD	55.6	0.505	13.4	26.1	0.172	0.341	3.38	6.51	2.66
TUR022-SE	15.5	0.315	11.1	20.7	0.165	0.289	2.83	4.74	2.33
TUR022-SF	28.9	0.336	25.8	36.2	0.419	0.547	6.33	8.13	5.76
TUR024-SA	15.1	0.311	10.6	19.4	0.134	0.242	2.75	4.92	2.09
TUR025-SA	15.4	0.311	10.3	20	0.13	0.258	2.66	5.09	1.99
TUR029-SA	15	0.302	10.6	19.8	0.135	0.251	2.68	4.99	2.06
TUR031-SA	16.5	0.323	10.8	21.4	0.135	0.269	2.8	5.43	2.09
TUR031-SB	22.4	0.33	10.9	21	0.132	0.263	2.83	5.42	2.08
TUR031-SC	13.3	0.303	11.5	19.1	0.17	0.275	3	4.38	2.45
TUR031-SD	19.3	0.316	11.4	20.5	0.169	0.285	2.91	4.77	2.38
TUR031-SF	18.7	0.306	12.5	21	0.193	0.31	3.13	4.8	2.69
TUR032-SA	17	0.344	13.6	24.5	0.171	0.324	3.51	6.24	2.66
TUR032-SB	12.5	0.362	10.1	21.9	0.124	0.276	2.58	5.39	1.96
TUR032-SC	11.6	0.275	11.6	18.5	0.178	0.273	3.01	4.3	2.48
TUR034-SA	16.2	0.333	10.9	21.2	0.137	0.282	2.82	5.37	2.14
TUR034-SB	17	0.334	10.9	21	0.136	0.275	2.84	5.38	2.13
TUR035-SA	19.3	0.349	12	22.2	0.151	0.29	3.13	5.62	2.37
TUR035-SB	23	0.341	12.5	22.7	0.163	0.295	3.16	5.64	2.49
TUR036-SA	15.9	0.316	9.92	21.3	0.119	0.275	2.55	5.46	1.93
TUR038-SA	17.1	0.331	10.1	21.3	0.122	0.285	2.59	5.38	1.95
TUR039-SA	22	0.142	6.09	16.9	0.066	0.198	1.69	4.36	1.05
TUR039-SB	18.6	0.331	10.5	22.2	0.131	0.281	2.73	5.64	2.08
TUR039-SC	13.5	0.291	10.1	19	0.153	0.262	2.55	4.38	2.16
TUR040-SA	15.7	0.316	10.4	20	0.127	0.266	2.65	5.05	2.06
TUR041-SA	15.6	0.312	9.9	20.1	0.122	0.261	2.55	5.03	1.93
TUR041-SB	11.9	0.368	13	24.3	0.164	0.31	3.31	6.08	2.54

p: partial digest
t: total digest

Appendix A: Till drill core geochemistry

Sample_ID	Ni_t_ppm	P2O5_t_pct	Pb_p_ppm	Pb_t_ppm	Pb204_p_ppm	Pb204_t_ppm	Pb206_p_ppm	Pb206_t_ppm	Pb207_p_ppm
TUR042-SA	15.1	0.319	9.59	19.5	0.121	0.251	2.49	4.97	1.86
TUR042-SB	17.6	0.333	12	22.7	0.149	0.29	3.04	5.65	2.38
TUR042-SC	11.2	0.355	9.68	21	0.116	0.262	2.47	5.13	1.87
TUR042-SD	8.3	0.293	9.16	15.8	0.137	0.22	2.28	3.63	1.91
TUR043-SA	13.8	0.323	9.1	19.2	0.11	0.245	2.4	4.87	1.76
TUR043-SB	15.3	0.324	10.5	18.5	0.135	0.249	2.75	4.73	2.09
TUR044-SA	18	0.338	10.2	22	0.127	0.282	2.61	5.49	1.98
TUR044-SB	21	0.355	11.6	22	0.146	0.297	2.94	5.47	2.29
TUR045B-SA	28	0.361	11.2	23.6	0.141	0.323	2.85	5.84	2.18
TUR045B-SB	12.6	0.376	10.4	22.3	0.128	0.269	2.62	5.5	2
TUR045B-SC	23.6	0.389	11	21	0.168	0.303	2.79	4.8	2.34
TUR046-SA	14.8	0.327	9.61	20.6	0.115	0.262	2.47	5.17	1.85
TUR046-SB	11	0.288	10.5	17.7	0.162	0.259	2.67	4.17	2.2
TUR046-SC	13.2	0.334	11.2	23.6	0.167	0.345	2.76	5.34	2.34
TUR047-SA	17.1	0.342	11.5	24.3	0.143	0.316	2.95	6.2	2.28
TUR047-SB	15.5	0.358	11	22	0.14	0.285	2.78	5.44	2.16
TUR048-SA	15.4	0.331	12.2	24.2	0.151	0.296	3.14	6.13	2.46
TUR048-SB	12.2	0.343	10.6	22.4	0.129	0.283	2.7	5.5	2.07
TUR048-SC	12.2	0.348	15	24.1	0.188	0.317	3.83	6.04	2.98
TUR049-SA	17.8	0.324	11.3	21.7	0.142	0.278	2.87	5.44	2.22
TUR049-SB	61.2	0.398	11.3	23.2	0.14	0.292	3.02	6.18	2.22
TUR049-SC	22.6	0.291	9.66	19.5	0.138	0.282	2.6	4.6	2.07
TUR050-SA	15.4	0.328	10.5	20.2	0.13	0.259	2.69	5.1	2.07
TUR050-SB	22.7	0.35	11.1	21.6	0.144	0.287	2.8	5.4	2.21
TUR050-SC	16	0.303	13	22.2	0.196	0.298	3.34	5.12	2.83
TUR051-SA	17.2	0.332	10.2	19.7	0.128	0.247	2.63	5.02	1.99
TUR051-SB	19.3	0.346	14.6	22.3	0.19	0.302	3.72	5.6	2.95
TUR052-SA	15.4	0.304	10.4	18.6	0.124	0.231	2.65	4.74	2.03
TUR052-SB	18.9	0.329	13.2	23.8	0.162	0.305	3.43	6.06	2.6
TUR053-SA	19.2	0.317	13.5	23.6	0.166	0.288	3.49	6.13	2.68
TUR053-SB	19.8	0.329	17.8	30.8	0.228	0.396	4.58	7.75	3.58
TUR053-SC	32.6	0.375	12.9	23.6	0.152	0.297	3.43	6.15	2.43
TUR054-SA	16.4	0.322	10.3	20.8	0.128	0.263	2.6	5.25	2.01

p: partial digest
t: total digest

Appendix A: Till drill core geochemistry

Sample_ID	Ni_t_ppm	P2O5_t_pct	Pb_p_ppm	Pb_t_ppm	Pb204_p_ppm	Pb204_t_ppm	Pb206_p_ppm	Pb206_t_ppm	Pb207_p_ppm
TUR054-SB	11.2	0.342	9.9	21.2	0.12	0.266	2.52	5.23	1.89
TUR054-SE	8.9	0.338	11.2	19.9	0.163	0.274	2.85	4.55	2.38
TUR055-SA	18.4	0.325	11.8	21.8	0.149	0.28	3.08	5.59	2.31
TUR056-SA	16.8	0.32	12.1	22.6	0.151	0.278	3.09	5.8	2.38
TUR056-SB	15.9	0.323	11.8	22.8	0.148	0.291	2.98	5.71	2.29
TUR057-SA	15.8	0.331	10.7	21.5	0.134	0.267	2.75	5.45	2.07
TUR057-SB	16.6	0.328	11.1	23.1	0.137	0.289	2.86	5.82	2.16
TUR057-SC	16.5	0.329	10.4	19.8	0.128	0.259	2.67	5.01	2.01
TUR057-SE	25.2	0.355	6.64	17.5	0.077	0.22	1.76	4.51	1.2
TUR057-SF	15.7	0.307	11.2	21.2	0.165	0.296	2.89	4.89	2.4
TUR057-SG	14.3	0.292	12.7	20.5	0.188	0.285	3.24	4.73	2.66
TUR057-SH	15.9	0.298	14.1	21.8	0.215	0.306	3.59	5.03	3.06
TUR057-SI	15	0.297	12.4	22	0.185	0.306	3.19	4.99	2.64
TUR057-SJ	16	0.291	11.1	19.4	0.162	0.271	2.84	4.56	2.39
TUR057-SK	14.6	0.292	10.6	19.4	0.159	0.281	2.77	4.45	2.3
TUR058-SA	16.2	0.324	11.8	22.9	0.144	0.302	2.99	5.8	2.31
TUR058-SC	14.1	0.3	11	21.3	0.164	0.307	2.79	4.85	2.39
TUR059-SA	17	0.337	10.3	22.2	0.128	0.285	2.69	5.58	2.02
TUR059-SB	17	0.282	11.1	24.5	0.168	0.369	2.9	5.68	2.47
TUR060-SA	16.9	0.328	12.7	22.6	0.158	0.287	3.29	5.79	2.5
TUR060-SB	15.5	0.326	10.3	22.4	0.133	0.283	2.61	5.66	2.04
TUR060-SD	21.9	0.312	10.5	24.3	0.126	0.302	2.75	6.2	2.04
TUR060-SE	18.4	0.32	15.7	25.6	0.247	0.376	3.97	5.77	3.5
TUR060-SF	12.2	0.3	9.74	19.5	0.141	0.269	2.57	4.49	2.07
TUR061-SA	14.4	0.32	11.9	23	0.147	0.292	3.04	5.82	2.34
TUR061-SB	13.5	0.325	12.1	21.1	0.154	0.269	3.04	5.27	2.41

p: partial digest
t: total digest

Appendix A: Till drill core geochemistry

Sample_ID	Pb207_t_ppm	Pb208_p_ppm	Pb208_t_ppm	Pr_p_ppm	Pr_t_ppm	Rb_p_ppm	Rb_t_ppm	Sb_p_ppm	Sc_p_ppm	Sc_t_ppm
TUR020-SA	4.66	6.6	12.1	6.8	14.3	6.89	90.8	0.07	1.4	4.8
TUR021-SA	4.2	6.04	11.2	5.82	12.7	5.6	78.8	0.07	1.2	4.2
TUR021-SB	4.05	5.76	11.1	4.09	11.3	3.93	60.9	0.06	0.8	3.2
TUR021-SC	4.33	6.55	11.9	7.15	12.1	5.7	81.3	0.03	1.5	4.6
TUR022-SA	4.53	6.52	11.8	5.82	12.6	5.69	77.9	0.06	1.2	4.2
TUR022-SB	4.05	5.61	10.4	5.58	12	5.54	76.6	0.06	1.2	4
TUR022-SC	4.16	5.18	11.2	4.21	12.1	4.18	65.7	0.05	0.8	3.6
TUR022-SD	5.36	7.22	13.9	10.4	26.9	4.48	114	0.04	1.2	5.6
TUR022-SE	4.15	5.81	11.5	6.15	11.5	5.42	72.6	0.03	1.2	4.2
TUR022-SF	7.54	13.3	20	12.5	19.3	7.42	104	0.04	2.4	5.9
TUR024-SA	3.88	5.68	10.4	5.57	12.4	5.46	76	0.05	1.1	4
TUR025-SA	4.06	5.54	10.6	5.72	12.4	5.54	78.2	0.06	1.2	4.2
TUR029-SA	3.97	5.72	10.5	5.5	12.2	5.6	75.8	0.05	1.2	4.1
TUR031-SA	4.3	5.77	11.4	5.7	12.8	5.43	81	0.06	1.2	4.3
TUR031-SB	4.2	5.82	11.1	10.1	18.6	6.73	116	0.05	1.5	4.9
TUR031-SC	3.81	5.87	10.6	6.26	11	5.39	66.8	0.05	1.2	3.7
TUR031-SD	4.07	5.9	11.3	9.67	15	6.77	97.6	0.05	1.7	4.7
TUR031-SF	4.32	6.47	11.6	7.18	12.6	7.36	82.9	0.03	1.8	5
TUR032-SA	4.97	7.22	13	5.96	13.8	5.67	85.8	0.06	1.2	4.7
TUR032-SB	4.36	5.45	11.9	4.32	12.7	4.06	67.4	0.06	0.9	3.7
TUR032-SC	3.68	5.92	10.2	5.79	9.8	4.36	63.3	0.04	1.1	3.4
TUR034-SA	4.23	5.8	11.4	5.72	12.9	5.62	81.7	0.06	1.2	4.3
TUR034-SB	4.27	5.82	11.1	6.26	13.3	6.08	82.9	0.06	1.3	4.3
TUR035-SA	4.5	6.36	11.8	7.15	13.9	5.88	94	0.06	1.4	4.7
TUR035-SB	4.67	6.68	12.1	6.66	14.2	6.96	91.4	0.05	1.4	4.9
TUR036-SA	4.26	5.32	11.4	5.39	12.4	5.36	79.8	0.05	1.1	4.2
TUR038-SA	4.28	5.43	11.3	5.79	13.1	5.81	83.5	0.06	1.2	4.6
TUR039-SA	3.07	3.29	9.26	9.07	21.9	4.98	196	0.05	0.7	3.2
TUR039-SB	4.49	5.61	11.8	6.23	13.6	6.79	87.9	0.06	1.4	4.7
TUR039-SC	3.8	5.26	10.5	5.91	10.8	4.8	67	0.04	1.2	3.8
TUR040-SA	4.03	5.61	10.7	5.83	12.6	5.67	78.1	0.06	1.2	4.3
TUR041-SA	4.09	5.3	10.7	5.64	12.7	5.54	79.6	0.06	1.2	4.3
TUR041-SB	4.84	6.94	13	4.29	12.8	4.31	68.3	0.05	0.8	3.5

p: partial digest

t: total digest

Appendix A: Till drill core geochemistry

Sample_ID	Pb207_t_ppm	Pb208_p_ppm	Pb208_t_ppm	Pr_p_ppm	Pr_t_ppm	Rb_p_ppm	Rb_t_ppm	Sb_p_ppm	Sc_p_ppm	Sc_t_ppm
TUR042-SA	3.91	5.12	10.4	5.28	12.9	5.52	80	0.05	1.2	4.1
TUR042-SB	4.56	6.47	12.2	6.36	14.4	6.27	84.4	0.06	1.3	4.3
TUR042-SC	4.15	5.22	11.4	4.4	12.6	4.25	68.1	0.05	0.9	3.4
TUR042-SD	3.12	4.82	8.8	4.05	8	3.05	41.8	0.02	0.7	2.6
TUR043-SA	3.83	4.84	10.3	4.94	12.3	5.14	77.4	0.06	1.1	4.2
TUR043-SB	3.77	5.5	9.76	5.33	12.1	5.24	74.1	0.05	1.1	3.7
TUR044-SA	4.47	5.44	11.7	5.87	13.6	5.47	87.5	0.06	1.2	4.6
TUR044-SB	4.43	6.19	11.8	7.22	16.1	6.32	97.6	0.06	1.6	4.9
TUR045B-SA	4.86	6.01	12.6	10.9	19.6	6.3	111	0.05	1.7	5.4
TUR045B-SB	4.44	5.61	12	4.37	13.4	4.19	69.4	0.05	0.9	3.6
TUR045B-SC	4.24	5.68	11.7	11.6	16.4	5.64	85.6	0.02	1.4	4.2
TUR046-SA	4.1	5.17	11	5.2	13.1	5.24	79	0.06	1.1	4.1
TUR046-SB	3.56	5.45	9.74	5.34	9.7	4.2	57.2	0.03	1	3.3
TUR046-SC	4.73	5.91	13.1	7.05	12.2	4.74	64.6	0.04	1.1	3.6
TUR047-SA	4.93	6.16	12.9	6.24	14	5.72	88.9	0.06	1.3	4.5
TUR047-SB	4.49	5.94	11.8	5.6	14	5.64	79.1	0.06	1.2	4
TUR048-SA	4.86	6.46	12.9	5.32	13.4	5.6	82.7	0.06	1.2	4.2
TUR048-SB	4.46	5.71	12.1	4.63	13	4.67	73.5	0.05	0.9	3.7
TUR048-SC	4.88	8.03	12.9	4.57	12.9	4.79	70	0.05	1	3.6
TUR049-SA	4.47	6.03	11.5	6.11	14.2	5.37	86.4	0.05	1.2	4.3
TUR049-SB	4.59	5.97	12.2	10.4	22.7	6.77	127	0.05	1.7	6.8
TUR049-SC	3.95	4.86	10.6	8.14	12.7	7.37	121	0.05	1.9	5.9
TUR050-SA	4.04	5.64	10.8	5.14	13.1	5.42	78.7	0.06	1.2	4.2
TUR050-SB	4.39	5.93	11.5	7.61	17.1	6.43	104	0.04	1.5	4.8
TUR050-SC	4.52	6.67	12.2	6.86	11.6	5.93	69.2	0.05	1.4	4.2
TUR051-SA	3.99	5.46	10.4	6.12	13.2	5.64	86.6	0.06	1.3	4.2
TUR051-SB	4.54	7.8	11.8	6.91	15.2	5.76	91.9	0.04	1.4	4.5
TUR052-SA	3.74	5.55	9.94	5.68	11.9	5.75	75.3	0.06	1.3	3.9
TUR052-SB	4.9	6.97	12.5	7.53	14.3	6.93	89.6	0.1	1.6	4.5
TUR053-SA	4.73	7.16	12.4	7.48	13.4	6.59	92.9	0.06	1.6	4.7
TUR053-SB	6.23	9.41	16.4	7.49	13.9	6.48	92	0.03	1.5	4.8
TUR053-SC	4.61	6.91	12.5	12	20	7.7	136	0.03	1.9	5.9
TUR054-SA	4.12	5.55	11.2	5.73	12.4	6.07	77.3	0.04	1.3	4.3

p: partial digest
t: total digest

Appendix A: Till drill core geochemistry

Sample_ID	Pb207_t_ppm	Pb208_p_ppm	Pb208_t_ppm	Pr_p_ppm	Pr_t_ppm	Rb_p_ppm	Rb_t_ppm	Sb_p_ppm	Sc_p_ppm	Sc_t_ppm
TUR054-SB	4.22	5.37	11.5	4.64	11.6	4.41	62.5	0.05	0.9	3.4
TUR054-SE	3.91	5.77	11.2	4.7	10.3	3.91	51.8	0.04	0.8	3.1
TUR055-SA	4.32	6.28	11.6	6.69	13.7	7.9	91	0.05	1.6	4.9
TUR056-SA	4.52	6.47	12	6.38	12.6	6.41	81.6	0.06	1.4	4.5
TUR056-SB	4.53	6.34	12.2	6.39	13.2	6.03	80.2	0.04	1.3	4.2
TUR057-SA	4.35	5.73	11.5	6.13	12.8	6.06	80.7	0.06	1.4	4.5
TUR057-SB	4.64	5.98	12.4	6.08	13.1	5.9	82.7	0.04	1.3	4.4
TUR057-SC	3.98	5.54	10.5	6.13	12	6.4	77.9	0.05	1.4	4.2
TUR057-SE	3.45	3.61	9.3	13.3	22.5	5.92	119	0.04	1.8	5.4
TUR057-SF	4.17	5.7	11.9	6.14	11.8	5.49	76.5	0.04	1.3	4.5
TUR057-SG	4.08	6.57	11.4	6.76	11	6.35	71.7	0.06	1.5	4.1
TUR057-SH	4.34	7.26	12.1	7.34	12.4	6.26	78	0.06	1.4	4.2
TUR057-SI	4.45	6.39	12.2	7.09	12.1	6.2	75.4	0.06	1.4	4.1
TUR057-SJ	3.95	5.72	10.6	6.79	11.5	6.37	74.4	0.06	1.5	4.2
TUR057-SK	3.93	5.41	10.7	6.35	11	6.21	73.1	0.06	1.5	4.2
TUR058-SA	4.57	6.4	12.2	6.83	13.3	6.47	78	0.06	1.4	4.2
TUR058-SC	4.3	5.64	11.8	6.68	11.4	5.29	69.7	0.04	1.2	3.9
TUR059-SA	4.49	5.45	11.9	6.49	13.1	6.18	81.3	0.04	1.5	4.3
TUR059-SB	5.1	5.59	13.4	6.58	11.1	5.27	94.6	0.05	1.4	4.4
TUR060-SA	4.64	6.74	11.9	7.02	12.8	6.11	84.2	0.04	1.6	4.3
TUR060-SB	4.47	5.56	12	5.84	13.1	5.88	80.2	0.05	1.3	4.2
TUR060-SD	4.82	5.63	13	8.3	19	7.3	133	0.04	1.6	5.4
TUR060-SE	5.22	8.01	14.2	7.9	13.4	7.65	86.4	0.07	1.8	5
TUR060-SF	3.86	4.96	10.9	4.98	10.6	5.22	67.9	0.05	1.2	4
TUR061-SA	4.58	6.35	12.3	5.57	12.4	5.71	77.9	0.03	1.3	4.2
TUR061-SB	4.25	6.54	11.3	6.23	12.3	6.33	71.4	0.03	1.4	3.9

p: partial digest
t: total digest

Appendix A: Till drill core geochemistry

Sample_ID	Se_p_ppm	Sm_p_ppm	Sm_t_ppm	Sn_p_ppm	Sn_t_ppm	Sr_t_ppm	Ta_p_ppm	Ta_t_ppm	Tb_p_ppm	Tb_t_ppm
TUR020-SA	1.3	3.86	7.7	0.33	1.52	506	0.005	1.17	0.3	0.63
TUR021-SA	1.3	3.35	7	0.34	1.43	478	0.005	1.12	0.26	0.58
TUR021-SB	1.3	2.36	6.2	0.22	1.25	703	0.005	1.16	0.18	0.48
TUR021-SC	0.3	3.58	7.3	0.27	1.31	469	0.005	1	0.28	0.55
TUR022-SA	1.5	3.34	6.8	0.29	1.39	485	0.005	1.13	0.26	0.58
TUR022-SB	1.3	3.2	6.6	0.27	1.37	472	0.005	1.07	0.24	0.55
TUR022-SC	0.9	2.4	6.5	0.21	1.34	741	0.005	1.2	0.18	0.54
TUR022-SD	1.6	5.96	13.8	0.29	1.8	489	0.005	1.09	0.36	0.95
TUR022-SE	0.05	3.03	6.8	0.24	1.16	522	0.005	1.03	0.23	0.5
TUR022-SF	0.5	6.12	10.8	0.35	1.42	510	0.005	1	0.38	0.7
TUR024-SA	1.1	3.21	6.7	0.28	1.57	476	0.005	1.03	0.24	0.54
TUR025-SA	1.1	3.27	6.7	0.31	1.57	483	0.005	1.05	0.25	0.54
TUR029-SA	1.1	3.15	6.6	0.26	1.41	497	0.005	1.04	0.25	0.56
TUR031-SA	1.1	3.26	7	0.29	1.62	488	0.005	1.05	0.25	0.58
TUR031-SB	1.7	5.4	9.7	0.3	1.72	476	0.005	0.93	0.3	0.68
TUR031-SC	0.05	3.21	6.6	0.25	1.12	447	0.005	0.93	0.24	0.48
TUR031-SD	0.05	4.68	8.8	0.28	1.27	439	0.005	0.93	0.3	0.59
TUR031-SF	0.05	3.62	7.5	0.23	1.12	429	0.005	0.9	0.26	0.51
TUR032-SA	1.2	3.39	7.6	0.32	1.68	526	0.005	1.06	0.26	0.62
TUR032-SB	0.9	2.5	6.8	0.24	1.33	764	0.005	1.12	0.19	0.56
TUR032-SC	0.05	2.94	6	0.23	0.96	357	0.005	0.89	0.22	0.52
TUR034-SA	1.2	3.28	7.2	0.29	1.55	514	0.005	1.02	0.26	0.6
TUR034-SB	1.2	3.62	7.4	0.3	1.49	461	0.005	0.93	0.27	0.6
TUR035-SA	1.3	4	7.7	0.31	1.64	471	0.005	1.01	0.3	0.63
TUR035-SB	1.2	3.64	7.7	0.28	1.47	493	0.005	0.93	0.26	0.6
TUR036-SA	1.2	3.14	7.1	0.26	1.48	484	0.005	1.02	0.24	0.56
TUR038-SA	1.2	3.32	7.2	0.27	1.48	515	0.005	1.04	0.25	0.6
TUR039-SA	1.5	4.3	8.4	0.29	2.19	253	0.005	1.09	0.21	0.46
TUR039-SB	1.1	3.55	7.4	0.3	1.47	501	0.005	1.04	0.26	0.62
TUR039-SC	0.05	2.96	6.6	0.22	1.13	407	0.005	0.92	0.23	0.49
TUR040-SA	1	3.32	6.9	0.26	1.39	484	0.005	0.99	0.25	0.57
TUR041-SA	1.2	3.22	6.8	0.25	1.44	490	0.005	1	0.25	0.56
TUR041-SB	0.9	2.49	6.9	0.21	1.47	751	0.005	1.11	0.18	0.54

p: partial digest
t: total digest

Appendix A: Till drill core geochemistry

Sample_ID	Se_p_ppm	Sm_p_ppm	Sm_t_ppm	Sn_p_ppm	Sn_t_ppm	Sr_t_ppm	Ta_p_ppm	Ta_t_ppm	Tb_p_ppm	Tb_t_ppm
TUR042-SA	1.1	3.02	7	0.25	1.47	500	0.005	1.03	0.24	0.67
TUR042-SB	1	3.56	7.5	0.28	1.68	570	0.005	1.02	0.27	0.59
TUR042-SC	1.1	2.51	6.7	0.2	1.31	745	0.005	1.06	0.19	0.53
TUR042-SD	0.05	2.04	5	0.16	0.81	486	0.005	0.88	0.15	0.41
TUR043-SA	1	2.87	6.8	0.25	1.56	502	0.005	0.96	0.23	0.62
TUR043-SB	0.8	3.06	6.7	0.24	1.38	425	0.005	0.87	0.22	0.52
TUR044-SA	0.9	3.31	7.3	0.26	1.64	514	0.005	0.98	0.25	0.6
TUR044-SB	1	3.94	8.6	0.3	1.53	507	0.005	0.91	0.27	0.66
TUR045B-SA	1.3	5.49	10.2	0.3	1.58	532	0.005	0.93	0.32	0.7
TUR045B-SB	0.9	2.48	7.2	0.2	1.43	786	0.005	1.11	0.19	0.55
TUR045B-SC	0.3	5.33	9.5	0.22	1.02	483	0.005	0.95	0.32	0.6
TUR046-SA	0.8	2.98	7.1	0.24	1.41	557	0.005	1	0.22	0.56
TUR046-SB	0.05	2.74	5.8	0.21	1	400	0.005	0.92	0.2	0.45
TUR046-SC	0.05	3.42	7.1	0.22	0.92	551	0.005	0.97	0.23	0.5
TUR047-SA	1.1	3.48	7.6	0.28	1.47	529	0.005	0.96	0.26	0.62
TUR047-SB	1.1	3.12	7.6	0.25	1.44	638	0.005	0.94	0.22	0.58
TUR048-SA	1	3.05	7.3	0.26	1.45	531	0.005	0.96	0.24	0.61
TUR048-SB	0.8	2.63	7	0.22	1.37	739	0.005	1.03	0.19	0.51
TUR048-SC	1	2.58	6.8	0.2	1.42	733	0.005	1.01	0.19	0.54
TUR049-SA	1.2	3.43	7.8	0.25	1.53	511	0.005	0.9	0.24	0.59
TUR049-SB	1.6	5.73	11.7	0.42	2.33	536	0.005	1	0.36	0.87
TUR049-SC	0.05	4.22	7.8	0.37	1.49	318	0.005	0.94	0.31	0.58
TUR050-SA	1.2	3	7.1	0.27	1.47	538	0.005	0.96	0.23	0.57
TUR050-SB	1.3	4.29	9.3	0.26	1.5	468	0.005	0.84	0.28	0.69
TUR050-SC	0.05	3.38	7	0.31	1.17	472	0.005	1.32	0.25	0.5
TUR051-SA	1.2	3.5	7.3	0.28	1.44	472	0.005	0.93	0.26	0.6
TUR051-SB	1	3.83	8.4	0.26	1.46	528	0.005	0.92	0.27	0.62
TUR052-SA	1.3	3.29	6.5	0.26	1.3	458	0.005	0.85	0.25	0.53
TUR052-SB	1.3	4.18	7.8	0.32	1.44	407	0.005	0.79	0.26	0.58
TUR053-SA	0.9	4.15	7.4	1.26	2.44	437	0.005	0.98	0.3	0.65
TUR053-SB	1	4.21	7.7	0.34	1.57	467	0.005	0.94	0.29	0.61
TUR053-SC	1.3	6.39	10.8	0.48	1.84	466	0.005	1.06	0.4	0.83
TUR054-SA	1	3.29	6.7	0.3	1.41	526	0.005	1.02	0.24	0.57

p: partial digest

t: total digest

Appendix A: Till drill core geochemistry

Sample_ID	Se_p_ppm	Sm_p_ppm	Sm_t_ppm	Sn_p_ppm	Sn_t_ppm	Sr_t_ppm	Ta_p_ppm	Ta_t_ppm	Tb_p_ppm	Tb_t_ppm
TUR054-SB	0.8	2.62	6.3	0.23	1.24	694	0.005	1.02	0.19	0.52
TUR054-SE	0.05	2.32	6	0.2	0.98	666	0.005	1.11	0.17	0.46
TUR055-SA	1.2	3.7	7.6	0.47	1.37	457	0.005	0.93	0.26	0.59
TUR056-SA	1	3.54	6.7	0.31	1.39	488	0.005	0.95	0.26	0.61
TUR056-SB	1	3.56	7.1	0.27	1.39	505	0.005	0.94	0.26	0.6
TUR057-SA	1.1	3.48	7.1	0.3	1.49	494	0.005	0.96	0.26	0.61
TUR057-SB	0.8	3.44	7.1	0.28	1.4	505	0.005	0.95	0.25	0.62
TUR057-SC	0.9	3.49	6.9	0.29	1.28	455	0.005	0.86	0.26	0.55
TUR057-SE	1.5	6.87	11.3	0.3	1.36	353	0.005	0.75	0.34	0.76
TUR057-SF	0.05	3.07	6.8	0.27	1.22	489	0.005	1.03	0.23	0.52
TUR057-SG	0.05	3.34	6.5	0.33	1.22	452	0.005	1	0.25	0.51
TUR057-SH	0.05	3.58	7.2	0.3	1.22	484	0.005	1.01	0.25	0.56
TUR057-SI	0.05	3.44	7.1	0.3	1.02	477	0.005	1	0.24	0.52
TUR057-SJ	0.05	3.45	6.9	0.32	1.19	426	0.005	0.92	0.26	0.52
TUR057-SK	0.05	3.21	6.6	0.3	1.09	425	0.005	0.94	0.24	0.54
TUR058-SA	0.8	3.69	7.1	0.31	1.3	502	0.005	0.92	0.26	0.59
TUR058-SC	0.05	3.3	6.9	0.25	1.01	436	0.005	0.98	0.23	0.47
TUR059-SA	0.9	3.72	7.4	0.37	1.47	480	0.005	0.84	0.28	0.6
TUR059-SB	0.05	3.44	6.9	0.28	1.37	284	0.005	0.93	0.26	0.54
TUR060-SA	1	3.93	7.1	0.38	1.57	446	0.005	0.85	0.29	0.58
TUR060-SB	0.9	3.23	7.2	0.28	1.4	568	0.005	0.94	0.24	0.58
TUR060-SD	1.2	4.6	10.1	0.33	1.97	435	0.005	0.93	0.32	0.76
TUR060-SE	0.05	3.79	7.9	0.34	1.21	497	0.005	0.91	0.26	0.55
TUR060-SF	0.05	2.56	6.4	0.27	1.16	513	0.005	1.02	0.21	0.5
TUR061-SA	0.9	3.2	6.8	0.25	1.4	533	0.005	0.92	0.24	0.59
TUR061-SB	0.9	3.43	6.7	0.28	1.36	545	0.005	0.87	0.24	0.59

p: partial digest
t: total digest

Appendix A: Till drill core geochemistry

Sample_ID	Te_p_ppm	Th_p_ppm	Th_t_ppm	TiO2_t_pct	U_p_ppm	U_t_ppm	V_p_ppm	V_t_ppm	W_p_ppm	W_t_ppm	Y_p_ppm
TUR020-SA	0.01	18.6	35.9	0.42	4.55	6.59	11.8	39.4	0.3	3.4	6.82
TUR021-SA	0.005	19.7	34.2	0.393	3.89	5.63	9.1	33.3	0.3	3.1	6.29
TUR021-SB	0.005	17.2	36.8	0.348	2.6	4.48	7.4	29.2	0.3	2.7	4.27
TUR021-SC	0.01	18.6	31.2	0.435	3.74	8.19	9.3	35.7	0.05	1.6	7.1
TUR022-SA	0.02	18.7	33.9	0.395	3.59	5.51	9.9	34.3	0.4	3.2	6.27
TUR022-SB	0.005	18.1	32.1	0.384	3.55	5.25	9.3	32.5	0.2	2.6	5.97
TUR022-SC	0.005	18.1	38.9	0.361	2.68	4.61	7	31.9	0.3	3.5	4.43
TUR022-SD	0.005	23.6	47.5	0.512	14.3	18.1	10.9	38.4	0.5	3.1	6.64
TUR022-SE	0.005	18.3	32.9	0.414	3.1	5.32	8.2	33.9	0.05	1.7	5.92
TUR022-SF	0.02	24.7	39.4	0.488	9.09	12.9	18.4	52.5	0.05	1.6	8.43
TUR024-SA	0.005	17.6	31.6	0.391	3.47	5.2	8.5	33.5	0.4	4.1	5.81
TUR025-SA	0.005	18	32.8	0.4	3.98	6.02	9.1	33.8	0.2	2.6	6.05
TUR029-SA	0.005	18.3	33.2	0.387	3.4	4.98	8.6	33.1	0.4	3.9	5.93
TUR031-SA	0.005	18.1	33.8	0.397	3.97	5.99	8.8	34.3	0.5	3.8	6.07
TUR031-SB	0.005	26.5	43.2	0.424	5.53	8.46	11.4	42.1	0.3	2.4	5.97
TUR031-SC	0.005	16.3	27.7	0.405	3.74	4.91	8.7	30.2	0.05	1.6	5.77
TUR031-SD	0.01	21.4	33.8	0.436	4.35	7.21	11.7	38.3	0.05	1.6	6.68
TUR031-SF	0.01	16	28.3	0.428	3.46	5.48	10.9	37.9	0.1	2	5.97
TUR032-SA	0.005	19.2	37.2	0.42	3.86	6.09	9.1	36.6	0.2	2.6	6.44
TUR032-SB	0.005	18.4	41.1	0.383	2.91	4.8	7.6	31.8	0.3	2.8	4.6
TUR032-SC	0.01	13.7	22.9	0.376	2.62	4.58	8.3	26.5	0.1	1.7	5.52
TUR034-SA	0.01	19.2	35.3	0.417	3.84	5.99	9.6	35.6	0.2	2.9	6.21
TUR034-SB	0.005	16.8	29.6	0.409	4.13	6.32	10.5	36.4	0.3	2.8	6.46
TUR035-SA	0.01	19	32.4	0.443	4.02	6.04	10.8	39.2	0.2	2.6	7.47
TUR035-SB	0.005	18	32.6	0.427	3.68	5.49	10.2	38.9	0.2	2.3	6.2
TUR036-SA	0.01	17.8	34.2	0.397	3.66	5.84	8.5	33.9	0.2	2.4	5.99
TUR038-SA	0.005	18.4	36.3	0.412	4.11	6.52	9	35.8	0.3	3.3	6.23
TUR039-SA	0.01	29.1	60.4	0.252	6.86	12.4	8.2	47.7	0.6	6.3	3.2
TUR039-SB	0.01	17.9	33.2	0.431	4.52	6.65	11	38.5	0.2	2.7	6.5
TUR039-SC	0.01	16.1	28.2	0.384	2.93	5.06	8	28.7	0.05	1.8	5.77
TUR040-SA	0.01	18.9	34.2	0.392	3.42	5.44	9.1	33.5	0.2	2.3	6.26
TUR041-SA	0.005	18.3	33.4	0.387	3.54	5.64	9.4	33	0.2	2.6	5.96
TUR041-SB	0.005	18	40.4	0.368	2.98	5.78	7.4	32.4	0.3	2.4	4.47

p: partial digest
t: total digest

Appendix A: Till drill core geochemistry

Sample_ID	Te_p_ppm	Th_p_ppm	Th_t_ppm	TiO2_t_pct	U_p_ppm	U_t_ppm	V_p_ppm	V_t_ppm	W_p_ppm	W_t_ppm	Y_p_ppm
TUR042-SA	0.005	17.8	34	0.387	3.85	6.62	8.5	33.8	0.2	2.4	5.9
TUR042-SB	0.005	20.7	38.3	0.405	3.74	5.84	9.7	37	0.2	2.6	6.29
TUR042-SC	0.005	18.4	40	0.368	2.73	4.6	7.2	31.9	0.2	2	4.48
TUR042-SD	0.005	13.9	24.7	0.326	2.09	3.52	5.2	22.8	0.05	1.2	3.69
TUR043-SA	0.005	17.2	34.4	0.399	3.01	5.04	7.8	32.9	0.2	2.9	5.79
TUR043-SB	0.005	13.9	26.2	0.41	3.25	5.56	8.5	33.4	0.2	2.4	5.5
TUR044-SA	0.01	18.4	35.6	0.424	3.02	5.22	8.9	37.1	0.6	3.1	6.04
TUR044-SB	0.01	19.8	36.6	0.436	4.29	6.66	11.5	41.1	1.6	10.2	6.14
TUR045B-SA	0.005	23	41.4	0.451	4.53	7.18	12.4	45	0.3	2.4	6.42
TUR045B-SB	0.005	19.1	42.7	0.387	2.86	5.13	7.5	33.4	0.5	4.1	4.58
TUR045B-SC	0.005	19.7	31.9	0.488	3.33	6.28	10.5	35.8	0.05	1.4	6.26
TUR046-SA	0.01	17.8	36.5	0.406	3.16	5.5	8.5	34	0.2	2.5	5.61
TUR046-SB	0.005	14.2	24.9	0.412	2.35	4.21	6.7	26.7	0.05	1.6	5.36
TUR046-SC	0.01	18.5	31	0.394	2.53	4.39	9.1	29.6	0.1	1.9	5.18
TUR047-SA	0.01	18.8	35.6	0.422	3.7	6.8	10	36.6	1.8	3.1	6.63
TUR047-SB	0.005	18.2	35.6	0.399	3.06	5.11	9.1	35.5	0.4	2.3	5.26
TUR048-SA	0.005	18.7	35.4	0.407	2.72	4.62	9.2	35.2	0.3	3.4	6
TUR048-SB	0.005	19.4	42.3	0.368	2.92	4.71	7.8	33.5	0.2	2.7	4.78
TUR048-SC	0.005	17.9	38.1	0.361	2.56	4.28	7.9	32.8	0.2	2.1	4.65
TUR049-SA	0.01	18.6	34.6	0.415	3.7	5.86	9.9	35.6	0.2	2.1	5.54
TUR049-SB	0.02	25.5	45.9	0.501	23.3	32.3	15.8	55.7	0.2	2.6	7.64
TUR049-SC	0.02	16.9	24.5	0.491	3.54	5.4	14.4	45.4	0.1	1.9	8.43
TUR050-SA	0.01	17.6	34.6	0.409	3.18	5.34	8.9	34.1	1.1	8.4	5.72
TUR050-SB	0.005	19.1	34.3	0.438	3.87	6.22	10.4	39.2	0.2	2.3	6.08
TUR050-SC	0.01	19.9	30.7	0.426	3.51	5.57	9.8	33	0.4	5.8	6.75
TUR051-SA	0.01	17.9	31.6	0.427	3.87	5.75	10.1	35	0.2	2.4	6.36
TUR051-SB	0.005	20.6	36.1	0.434	4.54	6.26	9.8	38.1	0.1	2.2	6.29
TUR052-SA	0.005	18.8	31.2	0.379	3.52	5.01	9.6	32.1	3.8	22.1	6.22
TUR052-SB	0.02	16.6	27.9	0.441	3.75	5.75	12.6	39.6	2	10	5.87
TUR053-SA	0.01	19.5	32.4	0.418	5.35	8.68	12.2	37.6	2.7	13.9	7.37
TUR053-SB	0.01	21.2	35	0.426	4.05	6.32	11.2	37.2	0.3	3	6.82
TUR053-SC	0.02	30.5	47.5	0.468	10.8	15.2	14	42.2	0.3	3.1	7.92
TUR054-SA	0.005	20.1	36.5	0.412	3.6	5.85	9	33.8	0.2	3.1	6.02

p: partial digest
t: total digest

Appendix A: Till drill core geochemistry

Sample_ID	Te_p_ppm	Th_p_ppm	Th_t_ppm	TiO2_t_pct	U_p_ppm	U_t_ppm	V_p_ppm	V_t_ppm	W_p_ppm	W_t_ppm	Y_p_ppm
TUR054-SB	0.005	19.8	41.4	0.344	2.78	4.59	7.7	29.9	0.1	2	4.55
TUR054-SE	0.005	19.3	35.4	0.368	2.35	3.79	6.7	27.8	0.05	1.6	4.46
TUR055-SA	0.01	17.9	33	0.43	4.03	6.31	11.9	40	0.2	3.4	5.95
TUR056-SA	0.01	20	35.4	0.41	3.81	6.14	10.3	34.5	1.1	10.9	6.44
TUR056-SB	0.01	21.1	36.2	0.401	3.8	6.01	9.8	33.6	0.2	3.8	6.08
TUR057-SA	0.005	19.7	36.7	0.419	3.48	6.55	9.9	35.2	0.4	5.9	6.72
TUR057-SB	0.01	19.4	36.3	0.415	3.56	6.1	9	36	0.2	3	6.23
TUR057-SC	0.005	16.3	29.2	0.412	3.48	5.64	10.6	34.5	1.1	6.2	6.12
TUR057-SE	0.01	26.5	44	0.463	4.58	8.18	11.4	40.5	0.3	2.8	6.09
TUR057-SF	0.005	20.1	34	0.422	3.37	5.78	8.5	36.3	0.05	1.8	6.2
TUR057-SG	0.01	21.4	31.9	0.395	3.5	5.52	10.6	33.1	0.05	1.7	6.61
TUR057-SH	0.01	22.1	34	0.402	3.69	5.66	10.5	34.1	0.4	4.4	6.62
TUR057-SI	0.01	21.2	32.8	0.407	3.44	5.66	10.4	31.7	0.05	1.6	6.09
TUR057-SJ	0.01	18.2	28	0.401	3.69	5.6	11.7	34.3	0.1	1.8	6.71
TUR057-SK	0.01	17.4	27.1	0.406	3.54	5.42	10.7	33.7	0.05	1.6	6.44
TUR058-SA	0.01	21.5	37	0.402	3.56	5.85	11.2	33.9	0.2	2.8	6.25
TUR058-SC	0.01	18.9	28.8	0.425	2.92	4.62	9	30.2	0.05	1.6	5.74
TUR059-SA	0.005	17.3	30.6	0.428	4.02	6.05	10.3	35.7	0.2	3.4	6.78
TUR059-SB	0.01	11.6	17	0.514	1.7	3.69	11.9	36.2	0.2	1.8	7.18
TUR060-SA	0.01	19.3	29.5	0.422	3.4	5.25	11.2	34.2	0.5	5.3	7.06
TUR060-SB	0.01	18.8	37.5	0.418	2.68	4.97	9.9	35.6	0.3	3.2	5.79
TUR060-SD	0.02	21.1	41	0.472	4.85	8.45	11.9	44.6	0.2	2.6	7.45
TUR060-SE	0.01	19.5	30.3	0.465	3.64	5.83	13.1	41.6	0.05	1.7	6.58
TUR060-SF	0.02	18	32.3	0.416	2.72	4.65	8.4	32.4	0.2	3.1	5.77
TUR061-SA	0.005	18.8	35.5	0.402	2.32	4.28	8.6	32.8	0.2	2.9	5.9
TUR061-SB	0.005	20.6	33	0.4	2.67	4.55	9.8	32.4	0.4	4.8	6

p: partial digest
t: total digest

Appendix A: Till drill core geochemistry

Sample_ID	Y_t_ppm	Yb_p_ppm	Yb_t_ppm	Zn_p_ppm	Zn_t_ppm	Zr_p_ppm	Zr_t_ppm	Sample_Top	Sample_Bottom	Avg_Depth
TUR020-SA	15.7	0.56	1.72	20.8	34	15.8	283	12.69	12.97	12.83
TUR021-SA	14.3	0.54	1.58	16.8	29	15	302	5.56	5.86	5.71
TUR021-SB	11.9	0.38	1.34	10.5	23	12.7	275	11.61	11.94	11.78
TUR021-SC	15.9	0.55	1.57	17.3	29	30.2	303	4.35	4.6	4.48
TUR022-SA	14.3	0.54	1.63	17.3	30	15	299	5.4	5.7	5.55
TUR022-SB	13.7	0.51	1.46	16.3	29	13.3	286	8.95	9.25	9.1
TUR022-SC	12.8	0.39	1.43	9.8	23	12.7	297	12.1	12.3	12.2
TUR022-SD	22.2	0.43	1.94	15.7	32	11.5	413	15.55	15.76	15.66
TUR022-SE	14.8	0.45	1.49	13.6	25	27.5	287	10.53	10.74	10.64
TUR022-SF	21.8	0.53	1.67	28.3	46	33.4	301	13.54	13.71	13.63
TUR024-SA	13.6	0.49	1.42	15.4	28	14.7	292	6.3	6.61	6.46
TUR025-SA	14	0.52	1.52	16.3	29	14.5	302	7.3	7.6	7.45
TUR029-SA	13.8	0.51	1.44	16.1	27	16.1	286	10.1	10.34	10.22
TUR031-SA	14.8	0.54	1.58	17.1	30	14.4	301	5.77	5.97	5.87
TUR031-SB	15.2	0.46	1.43	22.5	36	17.1	314	17	17.22	17.11
TUR031-SC	13.8	0.43	1.37	15.2	26	19.6	285	11.2	11.47	11.34
TUR031-SD	15.7	0.46	1.51	19.1	29	19	302	14.2	14.44	14.32
TUR031-SF	15.1	0.43	1.64	18.4	29	23.6	273	20	20.26	20.13
TUR032-SA	15.4	0.55	1.72	19.2	35	16.5	315	7.48	7.81	7.65
TUR032-SB	13.4	0.42	1.46	11.4	24	12.2	300	12.38	12.67	12.53
TUR032-SC	13.1	0.42	1.68	13.8	22	19.4	309	4.51	4.71	4.61
TUR034-SA	14.9	0.53	1.58	17.4	31	15.2	320	3.02	3.3	3.16
TUR034-SB	14.9	0.53	1.64	19.5	32	18.6	331	12.5	12.7	12.6
TUR035-SA	16.2	0.63	1.65	21.1	36	18.1	327	6.14	6.4	6.27
TUR035-SB	14.8	0.49	1.48	19.6	34	23.5	316	12.18	12.41	12.3
TUR036-SA	14.7	0.51	1.61	16.5	31	18.2	311	4.75	5	4.88
TUR038-SA	16.2	0.54	1.63	16.6	32	17.1	314	6.77	7.04	6.91
TUR039-SA	10	0.21	1.02	10.5	30	38.7	198	15.7	16	15.85
TUR039-SB	15	0.54	1.59	19.8	33	20	283	14.82	15.1	14.96
TUR039-SC	14.1	0.43	1.64	13.6	24	20.6	313	7.4	7.62	7.51
TUR040-SA	13.9	0.53	1.54	16.7	30	16.8	312	5.47	5.74	5.61
TUR041-SA	14	0.51	1.56	16.2	29	14.1	284	8.97	9.2	9.09
TUR041-SB	13.3	0.38	1.48	13.5	27	13.8	315	14.65	14.9	14.78

p: partial digest
t: total digest

Appendix A: Till drill core geochemistry

Sample_ID	Y_t_ppm	Yb_p_ppm	Yb_t_ppm	Zn_p_ppm	Zn_t_ppm	Zr_p_ppm	Zr_t_ppm	Sample_Top	Sample_Bottom	Avg_Depth
TUR042-SA	14.2	0.5	1.52	16.2	30	19.6	289	7.7	7.9	7.8
TUR042-SB	14.8	0.52	1.57	18.9	35	18.5	293	14.4	14.6	14.5
TUR042-SC	12.6	0.37	1.35	11.7	24	17.8	284	25.16	25.5	25.33
TUR042-SD	11.4	0.29	1.23	8.3	16	18.9	352	20.75	21.01	20.88
TUR043-SA	15.6	0.51	1.48	14.3	28	15.7	305	7.6	7.89	7.75
TUR043-SB	15.1	0.45	1.4	16.4	28	21.3	347	22.1	22.4	22.25
TUR044-SA	15.4	0.5	1.61	17	48	17.3	308	12.18	12.46	12.32
TUR044-SB	15.9	0.5	1.56	19.7	34	15	333	17.58	17.92	17.75
TUR045B-SA	15.8	0.48	1.8	25.4	41	16.9	300	17.99	18.31	18.15
TUR045B-SB	14.9	0.4	1.5	11.7	25	13.8	318	26.13	26.45	26.29
TUR045B-SC	15.8	0.38	1.49	18.6	28	23	381	23.37	23.58	23.48
TUR046-SA	14.2	0.47	1.57	14.4	29	15.9	291	7.22	7.51	7.37
TUR046-SB	12.7	0.41	1.34	12	21	22.1	318	3.84	4.09	3.97
TUR046-SC	16.8	0.36	1.35	13.5	23	20.2	309	12.56	12.8	12.68
TUR047-SA	15.6	0.55	1.63	17.8	33	16.7	295	4.45	4.74	4.6
TUR047-SB	13.9	0.44	1.43	16.1	30	18.2	291	10.4	10.7	10.55
TUR048-SA	15	0.54	1.48	19.7	36	14.9	309	9	9.28	9.14
TUR048-SB	13.1	0.4	1.39	14.9	29	14.1	262	15.05	15.31	15.18
TUR048-SC	12.7	0.39	1.38	17	32	13.4	278	18	18.31	18.16
TUR049-SA	15.3	0.44	1.45	17.5	31	15.5	315	8.76	9	8.88
TUR049-SB	19.8	0.54	1.74	30.6	50	14	320	13.87	14.16	14.02
TUR049-SC	16.6	0.62	1.63	26.2	42	18.8	241	4.59	4.83	4.71
TUR050-SA	14.4	0.48	1.52	15.4	29	15.3	297	11.72	12	11.86
TUR050-SB	16	0.45	1.56	20.1	34	17	330	15.52	15.82	15.67
TUR050-SC	14.5	0.52	1.54	17.5	39	19.1	284	7.64	7.84	7.74
TUR051-SA	14.6	0.51	1.5	18.2	30	15.8	324	8.67	9	8.84
TUR051-SB	15.1	0.5	1.57	19	31	15.8	323	12.9	13.2	13.05
TUR052-SA	13.5	0.53	1.42	17.5	28	14.4	286	7.27	7.55	7.41
TUR052-SB	15.2	0.44	1.36	25.7	37	17.6	306	14.08	14.4	14.24
TUR053-SA	15.7	0.61	1.73	22.6	36	17.2	282	8.45	8.86	8.66
TUR053-SB	15.6	0.57	1.57	25.8	37	18.2	308	11.8	12	11.9
TUR053-SC	18.6	0.61	1.8	23.6	37	14.1	334	13.96	14.12	14.04
TUR054-SA	14.5	0.51	1.57	16.7	29	19.1	320	11.14	11.46	11.3

p: partial digest

t: total digest

Appendix A: Till drill core geochemistry

Sample_ID	Y_t_ppm	Yb_p_ppm	Yb_t_ppm	Zn_p_ppm	Zn_t_ppm	Zr_p_ppm	Zr_t_ppm	Sample_Top	Sample_Bottom	Avg_Depth
TUR054-SB	12.4	0.38	1.43	10.7	23	11.8	270	17.2	17.5	17.35
TUR054-SE	12.1	0.34	1.39	9.9	19	17.9	307	18.38	18.58	18.48
TUR055-SA	15	0.49	1.66	37.4	50	19.8	316	12.64	12.93	12.79
TUR056-SA	14.4	0.53	1.54	19.5	31	16.7	305	6.4	6.66	6.53
TUR056-SB	14.7	0.51	1.62	19.5	31	17.7	324	12.94	13.3	13.12
TUR057-SA	15.6	0.55	1.77	17.7	31	16.3	357	5.6	6	5.8
TUR057-SB	14.9	0.52	1.66	17.6	31	17.5	312	9.6	10	9.8
TUR057-SC	14.4	0.5	1.53	19	31	21.6	317	13.71	14.1	13.91
TUR057-SE	16.4	0.42	1.58	17.4	28	14.5	348	16.26	16.66	16.46
TUR057-SF	15.1	0.49	1.55	15	28	22.1	296	7.22	7.47	7.35
TUR057-SG	14.5	0.51	1.49	16.4	26	22.1	284	9.3	9.6	9.45
TUR057-SH	15.1	0.48	1.51	17.2	28	23.1	286	11.75	12	11.88
TUR057-SI	14.6	0.46	1.51	16.8	26	28	299	12.86	13.1	12.98
TUR057-SJ	14.7	0.49	1.48	17	27	29.8	268	14.72	15	14.86
TUR057-SK	14.2	0.48	1.5	17.1	27	29.8	273	15.77	15.97	15.87
TUR058-SA	14.4	0.51	1.56	18.8	31	14.9	310	12.3	12.58	12.44
TUR058-SC	13.5	0.42	1.52	15.8	26	18.8	324	11.33	11.59	11.46
TUR059-SA	14.9	0.54	1.64	21.4	32	23.3	293	12.4	12.6	12.5
TUR059-SB	15.4	0.5	1.55	25.2	36	21	253	2.85	3	2.93
TUR060-SA	15.7	0.57	1.51	23.1	32	18.5	286	5.56	5.82	5.69
TUR060-SB	15	0.47	1.59	15.9	29	17.5	305	11.22	11.52	11.37
TUR060-SD	18.9	0.58	1.92	22.4	39	19	316	17.14	17.4	17.27
TUR060-SE	15.7	0.47	1.48	21.3	34	29.5	286	15	15.3	15.15
TUR060-SF	14.2	0.46	1.49	12.4	23	21.6	284	8.6	8.83	8.72
TUR061-SA	14.4	0.5	1.57	18.6	32	18.1	287	11.6	11.87	11.74
TUR061-SB	13.4	0.49	1.53	18.8	30	17.6	302	15.9	16.16	16.03

p: partial digest
t: total digest

Appendix A: Till drill core geochemistry

Sample_ID	Azimuth	Dip	Northing	Easting	Elevation	Quat_Sed_Thickness
TUR020-SA	120	-85	7135474.8	548869.79	188	13.3
TUR021-SA	120	-85	7135508.94	548891	188	12.6
TUR021-SB	120	-85	7135508.94	548891	188	12.6
TUR021-SC	120	-85	7135508.94	548891	188	12.6
TUR022-SA	120	-85	7135515.33	548907.67	188	15.91
TUR022-SB	120	-85	7135515.33	548907.67	188	15.91
TUR022-SC	120	-85	7135515.33	548907.67	188	15.91
TUR022-SD	120	-85	7135515.33	548907.67	188	15.91
TUR022-SE	120	-85	7135515.33	548907.67	188	15.91
TUR022-SF	120	-85	7135515.33	548907.67	188	15.91
TUR024-SA	120	-85	7135465	548837.19	188	12.9
TUR025-SA	120	-85	7135464.98	548852.68	188	13.3
TUR029-SA	205	-85	7135826.33	548656.43	187.98	16.9
TUR031-SA	205	-85	7135874.52	548666.13	188.44	20.8
TUR031-SB	205	-85	7135874.52	548666.13	188.44	20.8
TUR031-SC	205	-85	7135874.52	548666.13	188.44	20.8
TUR031-SD	205	-85	7135874.52	548666.13	188.44	20.8
TUR031-SF	205	-85	7135874.52	548666.13	188.44	20.8
TUR032-SA	305	-76	7135489.05	548912.65	186	13.2
TUR032-SB	305	-76	7135489.05	548912.65	186	13.2
TUR032-SC	305	-76	7135489.05	548912.65	186	13.2
TUR034-SA	305	-75	7135446.82	548884.71	188	16.7
TUR034-SB	305	-75	7135446.82	548884.71	188	16.7
TUR035-SA	205	-85	7135710.89	549040.86	189.22	12.5
TUR035-SB	205	-85	7135710.89	549040.86	189.22	12.5
TUR036-SA	308	-75	7135459.39	548863.04	186.85	16.8
TUR038-SA	310	-75	7135398.7	548935.16	187.09	16.3
TUR039-SA	305	-76	7135428.81	548931.28	189	16.16
TUR039-SB	305	-76	7135428.81	548931.28	189	16.16
TUR039-SC	305	-76	7135428.81	548931.28	189	16.16
TUR040-SA	316	-76	7135458.67	548951.38	191.54	15.7
TUR041-SA	355	-76	7135454.66	548939.58	192.4	15
TUR041-SB	355	-76	7135454.66	548939.58	192.4	15

p: partial digest
t: total digest

Appendix A: Till drill core geochemistry

Sample_ID	Azimuth	Dip	Northing	Easting	Elevation	Quat_Sed_Thickness
TUR042-SA	303	-50	7135397.8	548987.54	188	25.8
TUR042-SB	303	-50	7135397.8	548987.54	188	25.8
TUR042-SC	303	-50	7135397.8	548987.54	188	25.8
TUR042-SD	303	-50	7135397.8	548987.54	188	25.8
TUR043-SA	308	-48	7135362.48	548928.91	187.57	23
TUR043-SB	308	-48	7135362.48	548928.91	187.57	23
TUR044-SA	310	-48	7135317.85	548766.83	186.95	18.1
TUR044-SB	310	-48	7135317.85	548766.83	186.95	18.1
TUR045B-SA	310	-48	7135455.05	549105.11	188.8	33.7
TUR045B-SB	310	-48	7135455.05	549105.11	188.8	33.7
TUR045B-SC	310	-48	7135455.05	549105.11	188.8	33.7
TUR046-SA	310	-80	7135558.83	549472.29	184.87	13.6
TUR046-SB	310	-80	7135558.83	549472.29	184.87	13.6
TUR046-SC	310	-80	7135558.83	549472.29	184.87	13.6
TUR047-SA	130	-85	7135552.81	549316.22	185.38	11.84
TUR047-SB	130	-85	7135552.81	549316.22	185.38	11.84
TUR048-SA	310	-80	7135477.16	549014.95	187.74	18.3
TUR048-SB	310	-80	7135477.16	549014.95	187.74	18.3
TUR048-SC	310	-80	7135477.16	549014.95	187.74	18.3
TUR049-SA	310	-80	7135355.39	548699.48	186.96	14.3
TUR049-SB	310	-80	7135355.39	548699.48	186.96	14.3
TUR049-SC	310	-80	7135355.39	548699.48	186.96	14.3
TUR050-SA	310	-80	7135529.75	549040.03	187.27	16.51
TUR050-SB	310	-80	7135529.75	549040.03	187.27	16.51
TUR050-SC	310	-80	7135529.75	549040.03	187.27	16.51
TUR051-SA	310	-80	7135322.98	548737.84	186.65	14.3
TUR051-SB	310	-80	7135322.98	548737.84	186.65	14.3
TUR052-SA	310	-80	7135354.35	548776.38	187.38	16.63
TUR052-SB	310	-80	7135354.35	548776.38	187.38	16.63
TUR053-SA	310	-80	7135384.84	548657.82	186.18	14.12
TUR053-SB	310	-80	7135384.84	548657.82	186.18	14.12
TUR053-SC	310	-80	7135384.84	548657.82	186.18	14.12
TUR054-SA	310	-80	7135420.39	548960.04	187.33	19.9

p: partial digest
t: total digest

Appendix A: Till drill core geochemistry

Sample_ID	Azimuth	Dip	Northing	Easting	Elevation	Quat_Sed_Thickness
TUR054-SB	310	-80	7135420.39	548960.04	187.33	19.9
TUR054-SE	310	-80	7135420.39	548960.04	187.33	19.9
TUR055-SA	310	-80	7135387.02	548737.07	186.55	14.17
TUR056-SA	310	-80	7135381.43	548815.65	187.57	15.36
TUR056-SB	310	-80	7135381.43	548815.65	187.57	15.36
TUR057-SA	310	-80	7135410.32	548855.58	187.48	16.86
TUR057-SB	310	-80	7135410.32	548855.58	187.48	16.86
TUR057-SC	310	-80	7135410.32	548855.58	187.48	16.86
TUR057-SE	310	-80	7135410.32	548855.58	187.48	16.86
TUR057-SF	310	-80	7135410.32	548855.58	187.48	16.86
TUR057-SG	310	-80	7135410.32	548855.58	187.48	16.86
TUR057-SH	310	-80	7135410.32	548855.58	187.48	16.86
TUR057-SI	310	-80	7135410.32	548855.58	187.48	16.86
TUR057-SJ	310	-80	7135410.32	548855.58	187.48	16.86
TUR057-SK	310	-80	7135410.32	548855.58	187.48	16.86
TUR058-SA	310	-80	7135399.04	548796.49	186.85	14.7
TUR058-SC	310	-80	7135399.04	548796.49	186.85	14.7
TUR059-SA	310	-80	7135428.57	548837.27	187.16	15.46
TUR059-SB	310	-80	7135428.57	548837.27	187.16	15.46
TUR060-SA	310	-55	7135823.62	548898.78	188.44	18.2
TUR060-SB	310	-55	7135823.62	548898.78	188.44	18.2
TUR060-SD	310	-55	7135823.62	548898.78	188.44	18.2
TUR060-SE	310	-55	7135823.62	548898.78	188.44	18.2
TUR060-SF	310	-55	7135823.62	548898.78	188.44	18.2
TUR061-SA	310	-70	7135745.27	549381.57	186.38	17
TUR061-SB	310	-70	7135745.27	549381.57	186.38	17

p: partial digest
t: total digest

Appendix B: Surficial Geochemistry

Sample_ID	Year	Northing	Easting	Elevation	Ag_p_ppm	Ag_t_ppm	Al2O3_t_pct	As_p_ppm	B_t_ppm	Ba_t_ppm	Be_p_ppm
12-MR-S007A	2012	7135524	548883	184	0.005	0.28	6.01	0.85	16	789	0.2
12-MR-S008A	2012	7135902	548749	182	0.01	0.29	6.09	0.83	14	807	0.24
12-MR-S009A	2012	7135750	548860	188	0.005	0.28	5.44	0.5	13	749	0.14
12-MR-S010A	2012	7135606	548867	185	0.02	0.31	6.12	1.24	22	707	0.28
12-MR-S011A	2012	7135443	549007	185	0.01	0.32	7.25	3.62	31	693	0.31
12-MR-S012A	2012	7135764	548487	181	0.01	0.33	5.93	1.04	15	729	0.24
12-MR-S013A	2012	7135658	548655	182	0.02	0.36	8.38	5.97	40	728	0.45
12-MR-S014A	2012	7135614	548766	182	0.02	0.3	7.22	1.34	24	817	0.42
12-MR-S015A	2012	7135530	548872	184	0.01	0.31	6.1	1.63	20	735	0.21
12-MR-S016A	2012	7135390	548367	183	0.02	0.34	5.89	0.76	16	745	0.26
12-MR-S017A	2012	7135384	548576	188	0.02	0.33	6.32	1	22	770	0.4
12-MR-S018A	2012	7135414	548677	186	0.02	0.32	6.17	0.88	16	773	0.33
12-MR-S019A	2012	7135411	548671	185	0.02	0.31	6.19	0.79	15	767	0.27
12-MR-S020A	2012	7135380	548790	187	0.005	0.32	5.77	1.06	15	734	0.18
12-MR-S021A	2012	7135052	548496	184	0.02	0.33	6.72	1.29	24	773	0.54
12-MR-S022A	2012	7135230	548741	185	0.01	0.34	6.19	0.72	12	762	0.26
12-MR-S023A	2012	7135355	548888	183	0.02	0.3	7.78	1.17	31	829	0.53
12-MR-S024A	2012	7134797	548970	183	0.01	0.27	5.69	0.87	14	674	0.22
12-MR-S025A	2012	7134998	548987	186	0.01	0.27	6.09	0.56	15	756	0.24
12-MR-S026A	2012	7135087	548984	184	0.03	0.33	7.59	2.31	34	708	0.58
12-MR-S027A	2012	7135321	548988	185	0.01	0.29	6.64	0.88	19	837	0.32
12-MR-S028A	2012	7135383	549000	188	0.01	0.33	6.56	1.37	18	782	0.31
12-MR-S029A	2012	7135077	549560	185	0.01	0.32	6.4	0.66	16	751	0.28
12-MR-S030A	2012	7135219	549369	185	0.01	0.3	6.03	1.07	18	679	0.29
12-MR-S031A	2012	7135221	549364	188	0.02	0.3	7.57	1.7	35	765	0.47
12-MR-S032A	2012	7135269	549281	188	0.02	0.36	6.24	0.85	17	750	0.31
12-MR-S033A	2012	7135329	549178	188	0.02	0.28	6.11	1.32	15	735	0.27
12-MR-S034A	2012	7135416	549058	187	0.02	0.36	6.7	1.73	24	756	0.35
12-MR-S035A	2012	7135466	549658	187	0.02	0.31	4.94	0.41	14	629	0.11
12-MR-S036A	2012	7135477	549455	187	0.01	0.29	5.84	0.85	17	708	0.26
12-MR-S038A	2012	7135481	549348	186	0.01	0.29	5.64	0.74	17	687	0.21
12-MR-S039A	2012	7135497	549225	184	0.02	0.24	5.62	1.26	19	699	0.29
12-MR-S040A	2012	7137120	547387	188	0.03	0.22	6.6	1.17	33	739	0.54

p: partial digest
t: total digest

Appendix B: Surficial Geochemistry

Sample_ID	Year	Northing	Easting	Elevation	Ag_p_ppm	Ag_t_ppm	Al2O3_t_pct	As_p_ppm	B_t_ppm	Ba_t_ppm	Be_p_ppm
12-MR-S041A	2012	7136918	547384	186	0.01	0.2	5.62	1.08	19	704	0.23
12-MR-S042A	2012	7136556	547540	189	0.01	0.23	5.54	1.34	15	691	0.24
12-MR-S043A	2012	7136353	547559	187	0.01	0.2	4.94	0.83	17	642	0.18
12-MR-S044A	2012	7136142	547541	187	0.01	0.21	5.44	1.01	15	691	0.19
12-MR-S045A	2012	7135955	547619	186	0.01	0.21	5.53	1.25	15	680	0.22
12-MR-S045A_D	2012	7135955	547619	186	0.01	0.24	5.61	1.26	17	693	0.22
12-MR-S046A	2012	7135761	547667	185	0.02	0.25	7.51	2.3	66	768	0.67
12-MR-S047A	2012	7135563	547685	193	0.03	0.21	7.24	1.55	24	826	0.51
12-MR-S048A	2012	7135305	547735	190	0.02	0.23	7.08	1.62	29	782	0.48
12-MR-S049A	2012	7135102	547769	192	0.005	0.21	5.47	0.55	18	705	0.16
12-MR-S050A	2012	7134925	547794	191	0.005	0.2	5.61	0.39	17	684	0.15
12-MR-S051A	2012	7134720	547782	192	0.01	0.22	6.62	1.32	28	712	0.26
12-MR-S052A	2012	7134882	548416	185	0.01	0.24	6.02	0.67	23	670	0.19
12-MR-S053A	2012	7135092	548280	186	0.01	0.23	5.62	0.43	17	705	0.18
12-MR-S053A_D	2012	7135092	548280	186	0.01	0.25	5.59	0.46	18	700	0.17
12-MR-S060A	2012	7142011	545868	183	0.02	0.32	6.21	0.51	12	1280	0.3
12-MR-S060A_D	2012	7142011	545868	183	0.02	0.31	6.42	0.54	13	1320	0.33
12-MR-S061A	2012	7140213	545707	194	0.04	0.31	7.14	0.9	24	1320	0.53
12-MR-S063A	2012	7138789	545218	195	0.02	0.31	6.72	0.9	18	1070	0.32
12-MR-S069A	2012	7138776	548073	181	0.005	0.31	5.09	0.66	13	682	0.13
12-MR-S070A	2012	7137678	548391	182	0.01	0.29	5.61	0.8	18	699	0.22
12-MR-S071A	2012	7137172	548486	183	0.05	0.41	5.66	0.97	17	698	0.22
12-MR-S072A	2012	7136335	548724	180	0.02	0.37	5.84	0.71	17	756	0.24
12-MR-S076A	2012	7134937	546614	183	0.005	0.34	5.62	0.46	16	670	0.17
12-MR-S077A	2012	7134275	547039	184	0.02	0.27	5.61	0.95	20	651	0.24
12-MR-S078A	2012	7133355	548117	190	0.03	0.32	8.16	1.52	54	744	0.58
12-MR-S079A	2012	7133010	548491	192	0.01	0.28	6.57	1.04	15	749	0.3
12-MR-S080A	2012	7133013	548491	191	0.01	0.3	5.95	0.85	14	722	0.23
12-MR-S086A	2012	7135930	549535	183	0.02	0.3	6.7	1.02	21	820	0.41
12-MR-S087A	2012	7136239	549360	181	0.02	0.3	7.77	0.52	14	1180	0.32
12-TH-S103A	2012	7140534	543595	176	0.02	0.32	6.81	0.86	11	1420	0.29
12-TH-S104A	2012	7138669	543867	187	0.02	0.33	6.87	0.7	16	1340	0.4
12-TH-S105A	2012	7138217	543286	191	0.02	0.32	7.02	1.1	17	1090	0.41

p: partial digest
t: total digest

Appendix B: Surficial Geochemistry

Sample_ID	Year	Northing	Easting	Elevation	Ag_p_ppm	Ag_t_ppm	Al2O3_t_pct	As_p_ppm	B_t_ppm	Ba_t_ppm	Be_p_ppm
12-TH-S106A	2012	7137514	542995	199	0.02	0.28	6.28	1.16	18	916	0.37
12-TH-S107A	2012	7137508	543001	201	0.01	0.32	5.85	0.51	12	875	0.18
12-TH-S110A	2012	7136699	543104	208	0.01	0.3	6.55	1.21	16	1050	0.34
12-TH-S111A	2012	7135952	543141	200	0.005	0.29	5.68	0.55	14	874	0.17
12-TH-S112A	2012	7135090	543525	194	0.005	0.26	5.98	0.69	13	758	0.22
12-TH-S113A	2012	7134409	543870	189	0.01	0.24	5.83	0.64	16	757	0.22
12-TH-S114A	2012	7134403	543878	190	0.02	0.24	5.97	0.78	15	751	0.22
12-TH-S116A	2012	7136862	542012	199	0.01	0.29	6.67	0.77	12	1350	0.26
12-TH-S117A	2012	7138154	541837	191	0.02	0.3	6.53	1.92	21	800	0.27
12-TH-S190A	2012	7134180	550145	171	0.01	0.23	5.68	1.72	16	651	0.23
12-TH-S191A	2012	7134829	550794	166	0.02	0.27	7.81	2.05	31	708	0.45
12-TH-S192A	2012	7135633	550767	173	0.01	0.21	5.33	1.25	22	616	0.17
12-TH-S193A	2012	7136603	550606	178	0.01	0.28	5.62	1.62	20	699	0.23
12-TH-S194A	2012	7137500	550554	180	0.02	0.27	5.85	1.49	20	783	0.35
12-TH-S195A	2012	7137500	550554	180	0.02	0.23	6	1.9	21	779	0.4
13-AB-244A	2013	7136377	545393	183	0.02	0.17	5.84	1.02	14	761	0.22
13-AB-245A	2013	7136388	545871	183	0.05	0.24	5.84	1.09	20	802	0.26
13-AB-246A	2013	7136733	545644	183	0.02	0.18	6.31	0.99	18	792	0.27
13-AB-246A_D	2013	7136733	545644	183	0.02	0.17	6.38	1	17	803	0.25
13-AB-247A	2013	7137015	545330	184	0.02	0.19	5.49	0.91	13	743	0.14
13-AB-248A	2013	7137015	545330	184	0.01	0.18	5.1	0.9	11	682	0.14
13-AB-249A	2013	7136023	544674	187	0.02	0.22	6.58	1.02	18	819	0.25
13-AB-250A	2013	7138248	546057	188	0.005	0.19	5.81	1.02	14	994	0.19
13-AB-252A	2013	7137877	546770	185	0.02	0.21	5.88	0.91	28	892	0.2
13-AB-253A	2013	7139335	547274	190	0.005	0.14	5.46	0.65	12	827	0.19
13-AB-254A	2013	7139335	547274	190	0.005	0.14	5.53	0.7	25	830	0.18
13-AB-S199A	2013	7134642	549563	178	0.01	0.18	5.92	1.86	18	702	0.2
13-AB-S200A	2013	7135190	548005	185	0.005	0.16	5.93	1.15	17	753	0.21
13-AB-S201A	2013	7135473	547928	185	0.005	0.16	6.81	1.2	14	754	0.21
13-AB-S202A	2013	7135439	547372	183	0.01	0.16	6.26	1.18	28	758	0.18
13-AB-S203A	2013	7135696	548024	185	0.01	0.16	7.5	1.69	38	753	0.4
13-AB-S204A	2013	7136015	547979	185	0.01	0.21	7.54	1.84	34	740	0.29
13-AB-S205A	2013	7136324	547899	185	0.02	0.2	7.31	1.47	27	735	0.35

p: partial digest
t: total digest

Appendix B: Surficial Geochemistry

Sample_ID	Year	Northing	Easting	Elevation	Ag_p_ppm	Ag_t_ppm	Al2O3_t_pct	As_p_ppm	B_t_ppm	Ba_t_ppm	Be_p_ppm
13-AB-S206A	2013	7135911	548298	184	0.01	0.18	6.07	1.55	18	756	0.2
13-AB-S207A	2013	7135837	548626	184	0.01	0.19	5.93	1.56	17	746	0.19
13-AB-S209A	2013	7135683	548771	184	0.02	0.16	7.15	3.51	31	727	0.38
13-AB-S210A	2013	7135598	549050	184	0.01	0.18	5.55	1.28	14	704	0.18
13-AB-S210A_D	2013	7135598	549050	184	0.01	0.25	5.62	1.24	12	709	0.17
13-AB-S211A	2013	7135816	549393	182	0.005	0.16	5.5	1.33	14	699	0.15
13-AB-S212A	2013	7136064	549359	182	0.01	0.16	6.35	1.72	19	734	0.26
13-AB-S213A	2013	7136193	548955	185	0.005	0.16	5.55	0.87	13	723	0.13
13-AB-S214A	2013	7136133	548724	184	0.01	0.19	8.36	2.63	31	885	0.34
13-AB-S215A	2013	7136009	548551	180	0.01	0.15	6.02	1.43	17	748	0.26
13-AB-S216A	2013	7135893	549075	182	0.005	0.18	5.2	1.19	15	692	0.16
13-AB-S217A	2013	7135857	548890	179	0.005	0.16	5.25	0.82	23	723	0.14
13-AB-S218A	2013	7135896	548760	180	0.01	0.18	6.08	1.02	27	818	0.2
13-AB-S228A	2013	7136662	548414	181	0.02	0.16	6.62	1.29	32	817	0.43
13-AB-S229A	2013	7136679	548986	185	0.01	0.16	5.75	0.9	23	693	0.2
13-AB-S230A	2013	7136639	549466	182	0.01	0.15	6.09	0.98	23	702	0.24
13-AB-S231A	2013	7136412	549827	176	0.01	0.14	5.23	0.95	22	676	0.29
13-AB-S232A	2013	7137183	549430	184	0.005	0.15	4.68	0.69	26	633	0.1
13-AB-S234A	2013	7137169	548982	185	0.01	0.15	5.29	1.26	21	695	0.19
13-AB-S235A	2013	7137674	548956	184	0.01	0.16	6.74	5.71	34	706	0.22
13-AB-S236A	2013	7137692	549482	183	0.02	0.17	5.63	1.54	23	777	0.24
13-AB-S237A	2013	7137187	549973	183	0.02	0.18	6.58	1.38	41	741	0.38
13-AB-S239A	2013	7138749	549792	181	0.02	0.15	7.14	3.04	28	890	0.45
13-AB-S240A	2013	7139639	548918	176	0.01	0.15	5.8	1.11	24	914	0.24

p: partial digest
t: total digest

Appendix B: Surficial Geochemistry

Sample_ID	Be_t_ppm	Bi_p_ppm	Bi_t_ppm	CaO_t_pct	Cd_p_ppm	Cd_t_ppm	Ce_t_ppm	Co_p_ppm	Co_t_ppm	Cr_t_ppm
12-MR-S007A	1.7	0.56	0.6	0.99	0.02	0.3	70	1.76	3.7	20
12-MR-S008A	1.2	0.43	0.5	0.9	0.02	0.2	65	1.89	3.74	21
12-MR-S009A	1	0.3	0.4	1.05	0.01	0.3	74	1.12	3.03	21
12-MR-S010A	1.3	0.34	0.5	0.96	0.02	0.3	74	2.15	4.12	27
12-MR-S011A	1.2	0.24	0.3	1	0.04	0.2	87	4.38	7.02	47
12-MR-S012A	1.2	0.31	0.5	0.98	0.02	0.2	80	2.34	4.44	28
12-MR-S013A	1.4	0.32	0.4	0.98	0.03	0.3	89	4.64	7.66	53
12-MR-S014A	1.5	0.48	0.7	1.05	0.02	0.3	86	3.08	5.32	30
12-MR-S015A	1.1	0.49	0.7	0.93	0.02	0.2	72	2.38	4.32	29
12-MR-S016A	1.2	0.33	0.5	0.99	0.02	0.2	74	1.86	3.59	23
12-MR-S017A	1.1	0.42	0.6	0.99	0.02	0.3	80	2.7	4.09	26
12-MR-S018A	1.2	0.41	0.6	0.97	0.02	0.2	76	2.75	4.29	25
12-MR-S019A	1.1	0.32	0.6	0.89	0.01	0.2	80	1.86	3.95	27
12-MR-S020A	1	0.24	0.4	0.98	0.01	0.2	78	1.83	3.64	24
12-MR-S021A	1.2	0.52	0.6	0.98	0.02	0.3	81	3.38	4.47	27
12-MR-S022A	1	0.3	0.5	0.97	0.02	0.3	86	2.08	3.82	25
12-MR-S023A	1.5	0.54	0.8	1	0.03	0.2	83	3.24	5.85	33
12-MR-S024A	0.9	0.26	0.4	0.72	0.02	0.1	61	2.1	3.33	20
12-MR-S025A	1.2	0.32	0.5	0.82	0.01	0.2	66	2.16	3.31	21
12-MR-S026A	1.4	0.51	0.7	0.88	0.04	0.2	92	4.92	7.12	47
12-MR-S027A	1.3	0.41	0.6	1.04	0.02	0.2	76	2.24	4.24	24
12-MR-S028A	1.2	0.42	0.6	1.01	0.02	0.2	79	2.8	4.92	28
12-MR-S029A	1.2	0.34	0.6	0.98	0.02	0.3	87	1.97	4.04	24
12-MR-S030A	1	0.34	0.5	0.94	0.02	0.3	73	2.58	4.46	27
12-MR-S031A	1.3	0.47	0.6	0.91	0.03	0.2	78	3.81	6.38	35
12-MR-S032A	1	0.35	0.5	1.01	0.02	0.3	91	2.48	4.67	28
12-MR-S033A	0.9	0.33	0.5	0.86	0.02	0.2	73	2.31	4.08	24
12-MR-S034A	1	0.35	0.5	0.97	0.02	0.2	79	3.15	5.07	30
12-MR-S035A	0.9	0.16	0.3	0.92	0.01	0.3	66	0.89	2.32	15
12-MR-S036A	1	0.34	0.5	0.87	0.02	0.3	73	2.2	3.84	22
12-MR-S038A	1	0.23	0.4	0.88	0.01	0.3	67	1.59	3.34	23
12-MR-S039A	1	0.36	0.4	0.83	0.02	0.2	71	2.9	4.05	23
12-MR-S040A	1.7	0.31	0.5	0.76	0.04	0.2	98	2.99	4.94	36

p: partial digest
t: total digest

Appendix B: Surficial Geochemistry

Sample_ID	Be_t_ppm	Bi_p_ppm	Bi_t_ppm	CaO_t_pct	Cd_p_ppm	Cd_t_ppm	Ce_t_ppm	Co_p_ppm	Co_t_ppm	Cr_t_ppm
12-MR-S041A	1.4	0.25	0.3	0.74	0.02	0.2	69	2.48	3.81	21
12-MR-S042A	1.1	0.26	0.4	0.94	0.02	0.3	79	1.88	3.39	20
12-MR-S043A	1.1	0.19	0.3	0.82	0.01	0.2	66	1.32	2.6	18
12-MR-S044A	0.9	0.26	0.4	0.8	0.02	0.2	70	1.78	3.04	19
12-MR-S045A	1.2	0.25	0.4	0.85	0.02	0.2	73	2	3.36	21
12-MR-S045A_D	1.1	0.28	0.4	0.86	0.01	0.2	74	2.11	3.46	21
12-MR-S046A	1.6	0.58	0.7	0.93	0.02	0.3	79	4.31	5.58	33
12-MR-S047A	1.4	0.44	0.7	0.83	0.02	0.2	106	3.6	5.58	34
12-MR-S048A	1.6	0.94	1.2	0.92	0.02	0.3	81	3.51	5.29	29
12-MR-S049A	1.4	0.24	0.3	0.85	0.01	0.2	71	1.34	3.01	20
12-MR-S050A	1.2	0.28	0.4	0.82	0.01	0.2	70	1.26	3.1	22
12-MR-S051A	1.6	0.3	0.5	0.91	0.02	0.3	81	2.13	4.44	27
12-MR-S052A	1.4	0.21	0.4	0.78	0.02	0.2	81	1.58	4.24	31
12-MR-S053A	1.3	0.22	0.4	0.88	0.02	0.3	80	1.45	3.5	22
12-MR-S053A_D	1.3	0.21	0.4	0.87	0.01	0.3	82	1.47	3.5	24
12-MR-S060A	1.7	0.25	0.4	1.32	0.02	0.3	110	2.18	4.15	27
12-MR-S060A_D	1.7	0.26	0.4	1.33	0.02	0.3	117	2.3	4.22	29
12-MR-S061A	1.6	0.32	0.5	1.37	0.03	0.3	120	3	5.4	31
12-MR-S063A	1.4	0.27	0.4	1.14	0.03	0.2	110	2.8	5.15	32
12-MR-S069A	0.9	0.16	0.3	0.92	0.01	0.3	74	0.97	2.54	16
12-MR-S070A	0.9	0.22	0.3	0.92	0.02	0.3	69	1.72	3.31	22
12-MR-S071A	1.4	0.27	0.3	0.95	0.02	0.3	74	1.9	3.77	22
12-MR-S072A	1.5	0.3	0.4	1.08	0.02	0.3	80	1.73	3.7	22
12-MR-S076A	1.2	0.23	0.3	0.9	0.02	0.3	65	1.45	3.06	19
12-MR-S077A	1.4	0.24	0.3	0.86	0.02	0.2	63	1.87	3.41	20
12-MR-S078A	1.9	0.49	0.6	0.93	0.03	0.2	87	3.04	4.98	27
12-MR-S079A	1.5	0.37	0.6	1.02	0.02	0.2	79	2.72	5.16	26
12-MR-S080A	1.3	0.29	0.4	1.11	0.02	0.3	77	2	3.98	22
12-MR-S086A	1.5	0.5	0.6	1.04	0.02	0.2	79	2.6	4.84	29
12-MR-S087A	2	0.38	0.5	1.19	0.02	0.2	95	2.27	4.74	25
12-TH-S103A	1.9	0.27	0.4	1.67	0.03	0.3	134	2.85	6.04	38
12-TH-S104A	2	0.33	0.5	1.5	0.03	0.3	127	4.31	7.26	37
12-TH-S105A	1.9	0.41	0.5	1.19	0.02	0.3	109	2.78	4.87	27

p: partial digest
t: total digest

Appendix B: Surficial Geochemistry

Sample_ID	Be_t_ppm	Bi_p_ppm	Bi_t_ppm	CaO_t_pct	Cd_p_ppm	Cd_t_ppm	Ce_t_ppm	Co_p_ppm	Co_t_ppm	Cr_t_ppm
12-TH-S106A	1.5	0.34	0.4	0.97	0.02	0.2	112	2.71	4.49	25
12-TH-S107A	1.7	0.2	0.3	1.15	0.02	0.4	101	1.2	3.06	19
12-TH-S110A	1.6	0.27	0.4	1.2	0.02	0.3	110	2.35	4.77	27
12-TH-S111A	1.4	0.22	0.4	1.19	0.02	0.3	87	1.16	3.09	23
12-TH-S112A	1.4	0.22	0.3	0.88	0.02	0.2	67	1.79	3.28	20
12-TH-S113A	1.3	0.2	0.3	0.98	0.02	0.3	79	1.53	3.05	19
12-TH-S114A	1.4	0.19	0.3	0.95	0.02	0.3	80	1.69	3.28	21
12-TH-S116A	1.7	0.47	0.6	1.42	0.02	0.3	105	1.96	4.5	24
12-TH-S117A	1.5	0.28	0.4	0.95	0.02	0.2	81	2.95	5.18	28
12-TH-S190A	1.3	0.23	0.3	0.82	0.02	0.2	70	2.2	3.78	25
12-TH-S191A	1.3	0.38	0.5	0.8	0.03	0.2	81	3.87	5.42	32
12-TH-S192A	0.9	0.16	0.3	0.77	0.01	0.2	67	1.77	3.65	24
12-TH-S193A	1.2	0.22	0.3	0.88	0.01	0.3	91	2.02	3.49	23
12-TH-S194A	1.8	0.22	0.3	0.99	0.02	0.3	100	2.18	3.96	32
12-TH-S195A	1.6	0.24	0.3	0.91	0.02	0.3	95	2.54	4.04	29
13-AB-244A	1.5	0.31	0.4	0.9	0.03	0.2	85	1.58	3.22	20
13-AB-245A	1.9	0.5	0.6	0.81	0.03	0.2	77	1.76	3.3	18
13-AB-246A	1.5	0.31	0.4	0.88	0.02	0.2	83	1.99	3.62	25
13-AB-246A_D	1.5	0.34	0.4	0.9	0.02	0.2	83	2	3.61	25
13-AB-247A	1.4	0.23	0.3	0.97	0.02	0.2	82	1.03	2.56	19
13-AB-248A	1.2	0.22	0.3	0.9	0.02	0.2	76	1.02	2.37	18
13-AB-249A	1.6	0.34	0.4	0.87	0.02	0.2	85	2.11	3.7	25
13-AB-250A	1.6	0.19	0.3	1.17	0.02	0.3	105	1.64	3.61	31
13-AB-252A	1.5	0.33	0.5	1.07	0.03	0.2	108	1.78	3.49	24
13-AB-253A	1.4	0.17	0.2	0.89	0.01	0.2	76	1.37	2.72	19
13-AB-254A	1.2	0.16	0.2	0.89	0.02	0.2	83	1.34	2.72	19
13-AB-S199A	1.2	0.31	0.4	0.95	0.02	0.2	79	2.04	3.78	26
13-AB-S200A	1.2	0.31	0.4	0.84	0.02	0.2	76	2.04	3.5	23
13-AB-S201A	1.4	0.25	0.4	0.89	0.02	0.1	79	2.4	4.42	27
13-AB-S202A	1.2	0.25	0.4	0.85	0.01	0.1	73	1.75	3.19	21
13-AB-S203A	1.9	0.37	0.5	0.87	0.02	0.2	80	2.45	4.24	28
13-AB-S204A	1.5	0.42	0.5	0.92	0.02	0.2	84	2.65	4.54	28
13-AB-S205A	1.4	0.36	0.5	0.91	0.02	0.2	88	2.93	4.78	29

p: partial digest
t: total digest

Appendix B: Surficial Geochemistry

Sample_ID	Be_t_ppm	Bi_p_ppm	Bi_t_ppm	CaO_t_pct	Cd_p_ppm	Cd_t_ppm	Ce_t_ppm	Co_p_ppm	Co_t_ppm	Cr_t_ppm
13-AB-S206A	1.1	0.36	0.6	1	0.02	0.2	85	2.04	3.92	26
13-AB-S207A	1.4	0.41	0.6	1.01	0.02	0.2	81	1.84	3.7	25
13-AB-S209A	1.5	0.33	0.5	0.88	0.03	0.2	73	3.64	5.26	39
13-AB-S210A	1.4	0.26	0.4	0.92	0.02	0.2	74	1.62	3.14	22
13-AB-S210A_D	1.3	0.25	0.4	0.94	0.02	0.2	76	1.56	3.21	21
13-AB-S211A	1.1	0.2	0.3	1.01	0.02	0.2	77	1.16	2.79	20
13-AB-S212A	1.4	0.39	0.5	0.9	0.02	0.2	74	2.3	4.03	27
13-AB-S213A	1.2	0.19	0.3	0.96	0.02	0.2	69	1.08	2.7	20
13-AB-S214A	1.7	0.39	0.6	1.03	0.02	0.2	96	3.05	5.5	32
13-AB-S215A	1.6	0.32	0.4	0.89	0.02	0.1	71	2.05	3.63	29
13-AB-S216A	1.5	0.24	0.3	1.09	0.02	0.2	91	1.34	3.08	24
13-AB-S217A	1	0.28	0.3	0.97	0.01	0.2	74	1.11	2.58	21
13-AB-S218A	1.4	0.31	0.4	1.1	0.02	0.2	93	1.69	3.46	22
13-AB-S228A	1.6	0.34	0.4	0.96	0.02	0.2	107	2.59	4.47	30
13-AB-S229A	1.3	0.18	0.2	0.81	0.02	0.1	76	1.8	3.43	23
13-AB-S230A	1.2	0.2	0.2	0.82	0.02	0.2	78	2.02	3.5	23
13-AB-S231A	1.2	0.19	0.2	0.78	0.02	0.2	72	1.99	3.14	25
13-AB-S232A	1.2	0.12	0.2	0.84	0.01	0.3	64	0.77	2.01	21
13-AB-S234A	1.1	0.23	0.3	0.78	0.02	0.2	80	1.51	2.8	23
13-AB-S235A	1.3	0.18	0.2	1	0.03	0.2	92	3.88	6.23	47
13-AB-S236A	1.5	0.26	0.3	0.91	0.02	0.2	84	1.93	3.54	26
13-AB-S237A	1.5	0.34	0.4	0.79	0.03	0.2	90	3.01	4.57	33
13-AB-S239A	1.6	0.32	0.4	0.89	0.03	0.1	91	3.86	5.2	35
13-AB-S240A	1.6	0.18	0.2	1.09	0.02	0.3	100	1.71	3.63	27

p: partial digest
t: total digest

Appendix B: Surficial Geochemistry

Sample_ID	Cs_p_ppm	Cs_t_ppm	Cu_p_ppm	Cu_t_ppm	Dy_p_ppm	Dy_t_ppm	Er_p_ppm	Er_t_ppm	Eu_p_ppm	Eu_t_ppm
12-MR-S007A	0.2	1.4	3.68	6.7	1.2	2.75	0.51	1.5	0.49	1.6
12-MR-S008A	0.23	1.4	4.34	7.4	1.14	2.61	0.51	1.35	0.52	1.52
12-MR-S009A	0.14	1.1	3.2	6.1	1.07	2.91	0.46	1.57	0.48	1.69
12-MR-S010A	0.33	1.5	6.64	10.9	1.3	3.25	0.62	1.76	0.56	1.68
12-MR-S011A	0.51	2	10.7	14.5	1.49	3.2	0.68	1.76	0.61	1.71
12-MR-S012A	0.25	1.4	4.74	8.6	1.26	2.96	0.56	1.7	0.54	1.66
12-MR-S013A	0.82	2.8	20.7	25.4	1.68	3.76	0.79	2.06	0.68	1.97
12-MR-S014A	0.54	2.1	9.56	13.6	1.58	3.13	0.7	1.7	0.68	1.8
12-MR-S015A	0.25	1.4	4.78	8.3	1.24	2.81	0.54	1.55	0.53	1.6
12-MR-S016A	0.28	1.5	6.22	9.4	1.35	2.96	0.61	1.62	0.56	1.62
12-MR-S017A	0.44	1.6	8.3	10.2	1.56	3.09	0.72	1.62	0.68	1.7
12-MR-S018A	0.38	1.6	6.3	9	1.42	3.01	0.62	1.61	0.63	1.74
12-MR-S019A	0.26	1.5	5.05	10	1.22	2.88	0.55	1.5	0.56	1.68
12-MR-S020A	0.18	1.3	3.18	6.3	1.12	2.95	0.49	1.6	0.52	1.69
12-MR-S021A	0.71	1.9	11.1	11.8	1.77	3.22	0.81	1.78	0.74	1.76
12-MR-S022A	0.27	1.5	4.94	8.4	1.39	3.1	0.62	1.66	0.61	1.68
12-MR-S023A	0.62	2.6	11.1	18.4	1.61	3.41	0.71	1.78	0.67	1.83
12-MR-S024A	0.27	1.4	2.73	5.2	1.05	2.16	0.45	1.15	0.45	1.24
12-MR-S025A	0.3	1.4	6.5	7.1	1.22	2.43	0.55	1.31	0.53	1.4
12-MR-S026A	0.78	2.6	13.2	18.1	1.87	3.29	0.85	1.7	0.82	1.77
12-MR-S027A	0.33	1.7	6.35	10.4	1.44	2.94	0.66	1.59	0.64	1.69
12-MR-S028A	0.38	1.7	8.33	12.4	1.42	3.04	0.64	1.6	0.62	1.64
12-MR-S029A	0.28	1.6	4.51	8.9	1.43	3.08	0.62	1.67	0.6	1.74
12-MR-S030A	0.36	1.5	6.42	9.6	1.43	3.03	0.66	1.67	0.61	1.61
12-MR-S031A	0.66	2.5	12	17.4	1.6	3.36	0.72	1.69	0.66	1.64
12-MR-S032A	0.34	1.6	6.55	11	1.37	3.12	0.62	1.67	0.62	1.77
12-MR-S033A	0.3	1.5	5.93	9.3	1.19	2.52	0.52	1.33	0.54	1.4
12-MR-S034A	0.44	1.8	8.43	11.6	1.48	2.95	0.64	1.58	0.63	1.7
12-MR-S035A	0.11	1	1.44	3.9	1.02	2.68	0.44	1.5	0.4	1.31
12-MR-S036A	0.27	1.4	4.76	7.6	1.29	2.61	0.57	1.47	0.56	1.47
12-MR-S038A	0.24	1.3	3.45	6.6	1.13	2.79	0.5	1.59	0.48	1.46
12-MR-S039A	0.34	1.3	5.79	7.4	1.27	2.48	0.59	1.36	0.61	1.4
12-MR-S040A	0.64	2.5	10.2	15.3	1.55	2.94	0.68	1.52	0.82	1.7

p: partial digest
t: total digest

Appendix B: Surficial Geochemistry

Sample_ID	Cs_p_ppm	Cs_t_ppm	Cu_p_ppm	Cu_t_ppm	Dy_p_ppm	Dy_t_ppm	Er_p_ppm	Er_t_ppm	Eu_p_ppm	Eu_t_ppm
12-MR-S041A	0.27	1.4	3.49	5.6	1.18	2.32	0.53	1.23	0.58	1.34
12-MR-S042A	0.22	1.2	4.33	7.4	1.4	2.89	0.67	1.55	0.65	1.56
12-MR-S043A	0.18	1.1	2.44	4.6	1.04	2.47	0.49	1.32	0.48	1.29
12-MR-S044A	0.2	1.2	2.71	4.8	1.1	2.36	0.5	1.3	0.52	1.32
12-MR-S045A	0.27	1.3	3.55	5.9	1.2	2.49	0.54	1.36	0.53	1.38
12-MR-S045A_D	0.28	1.4	3.77	5.8	1.21	2.61	0.55	1.4	0.54	1.39
12-MR-S046A	0.97	2.6	19.4	19.9	1.84	3.07	0.9	1.67	0.82	1.65
12-MR-S047A	0.53	2.1	12.2	16.9	1.97	3.47	0.9	1.69	1.02	1.95
12-MR-S048A	0.59	2	10.8	13.2	1.61	2.95	0.76	1.57	0.73	1.62
12-MR-S049A	0.19	1.2	3.8	4.8	1.05	2.52	0.44	1.32	0.45	1.34
12-MR-S050A	0.19	1.3	2.1	5	0.96	2.46	0.42	1.35	0.4	1.34
12-MR-S051A	0.38	1.9	7.04	12.5	1.41	2.92	0.62	1.6	0.57	1.58
12-MR-S052A	0.27	1.7	3.45	8.2	1.05	2.51	0.45	1.38	0.44	1.39
12-MR-S053A	0.22	1.3	2.62	5.5	1.08	2.74	0.48	1.48	0.47	1.5
12-MR-S053A_D	0.21	1.3	2.52	5.6	1.04	2.81	0.45	1.51	0.45	1.52
12-MR-S060A	0.25	1.3	5.19	7.6	1.39	3.31	0.59	1.59	0.8	2.47
12-MR-S060A_D	0.26	1.4	5.3	8.3	1.52	3.4	0.65	1.63	0.89	2.6
12-MR-S061A	0.45	1.8	10.4	14	1.65	3.48	0.73	1.7	0.93	2.61
12-MR-S063A	0.34	1.6	7	10.8	1.42	3.08	0.61	1.58	0.77	2.11
12-MR-S069A	0.12	1.1	1.32	3.7	1.02	2.81	0.44	1.6	0.45	1.54
12-MR-S070A	0.25	1.4	3.17	5.8	1.25	2.66	0.54	1.41	0.53	1.46
12-MR-S071A	0.28	1.3	4.47	7.4	1.36	2.94	0.61	1.64	0.55	1.61
12-MR-S072A	0.3	1.4	4.8	7.6	1.4	3.16	0.62	1.65	0.61	1.72
12-MR-S076A	0.2	1.3	2.07	4.9	1	2.64	0.45	1.44	0.41	1.32
12-MR-S077A	0.3	1.4	4.59	7.6	1.34	2.55	0.61	1.43	0.53	1.33
12-MR-S078A	0.57	2.4	10.3	15.1	1.64	3.07	0.74	1.72	0.74	1.84
12-MR-S079A	0.38	1.7	5.9	10.4	1.37	3.04	0.63	1.57	0.57	1.67
12-MR-S080A	0.25	1.3	5.98	9	1.63	3.25	0.73	1.74	0.66	1.7
12-MR-S086A	0.45	1.8	11.5	17.1	1.64	3.17	0.75	1.68	0.7	1.79
12-MR-S087A	0.33	1.9	4.41	7.8	1.33	3.04	0.57	1.6	0.67	2.13
12-TH-S103A	0.24	1.4	6.9	11	1.52	4.06	0.64	1.99	0.86	3
12-TH-S104A	0.52	1.8	13.4	17.9	1.52	3.75	0.65	1.89	0.88	2.8
12-TH-S105A	0.4	1.7	6.47	9.5	1.68	3.26	0.72	1.74	0.86	2.24

p: partial digest
t: total digest

Appendix B: Surficial Geochemistry

Sample_ID	Cs_p_ppm	Cs_t_ppm	Cu_p_ppm	Cu_t_ppm	Dy_p_ppm	Dy_t_ppm	Er_p_ppm	Er_t_ppm	Eu_p_ppm	Eu_t_ppm
12-TH-S106A	0.29	1.4	5.36	8.5	1.6	3.09	0.68	1.65	0.87	2.02
12-TH-S107A	0.14	1.2	2.47	5.5	1.35	3.5	0.58	1.87	0.69	2.1
12-TH-S110A	0.21	1.4	4.13	7.6	1.36	3.33	0.62	1.75	0.75	2.14
12-TH-S111A	0.15	1.2	2.37	5.4	1.27	3.29	0.55	1.73	0.61	1.84
12-TH-S112A	0.26	1.5	2.96	5.4	1.13	2.41	0.48	1.34	0.49	1.4
12-TH-S113A	0.24	1.3	3.39	5.6	1.31	2.86	0.58	1.57	0.57	1.57
12-TH-S114A	0.24	1.4	3.86	6.8	1.24	2.74	0.55	1.55	0.55	1.58
12-TH-S116A	0.18	1.4	3.87	7.7	1.36	3.29	0.58	1.68	0.73	2.48
12-TH-S117A	0.37	1.6	5.36	8.6	1.28	2.85	0.58	1.49	0.63	1.66
12-TH-S190A	0.28	1.3	4.65	7.1	1.21	2.57	0.54	1.42	0.54	1.33
12-TH-S191A	0.71	2.3	10.8	12.7	1.55	2.74	0.78	1.48	0.71	1.45
12-TH-S192A	0.24	1.3	3.05	6.6	1	2.31	0.46	1.28	0.45	1.26
12-TH-S193A	0.23	1.2	3.55	6	1.34	2.93	0.62	1.54	0.68	1.62
12-TH-S194A	0.3	1.3	4.19	6.7	1.47	3.05	0.65	1.64	0.84	1.88
12-TH-S195A	0.38	1.4	5.88	7.9	1.45	2.82	0.64	1.48	0.87	1.78
13-AB-244A	0.22	1.4	4.1	6.4	1.3	3.08	0.58	1.64	0.64	1.52
13-AB-245A	0.19	1.4	2.75	4.5	1.16	2.7	0.49	1.31	0.62	1.43
13-AB-246A	0.31	1.6	5.45	7.6	1.26	2.9	0.56	1.51	0.62	1.48
13-AB-246A_D	0.32	1.6	5.54	7.8	1.29	2.9	0.57	1.51	0.62	1.48
13-AB-247A	0.15	1.2	2.62	4.1	1.15	2.92	0.5	1.57	0.55	1.42
13-AB-248A	0.16	1	2.63	5	1.13	2.75	0.5	1.42	0.54	1.34
13-AB-249A	0.31	1.6	3.98	5.9	1.31	2.79	0.58	1.46	0.64	1.49
13-AB-250A	0.15	1.2	3.04	4.8	1.21	3.15	0.52	1.62	0.69	1.87
13-AB-252A	0.17	1.2	4.88	6.3	1.29	2.94	0.57	1.56	0.66	1.67
13-AB-253A	0.16	1.1	2.6	4	1.05	2.53	0.46	1.32	0.55	1.39
13-AB-254A	0.16	1.1	2.85	4	1.05	2.45	0.46	1.26	0.55	1.36
13-AB-S199A	0.23	1.2	5.15	7.4	1.24	2.96	0.57	1.52	0.57	1.38
13-AB-S200A	0.27	1.4	2.91	4.3	1	2.49	0.46	1.33	0.5	1.23
13-AB-S201A	0.3	1.8	2.69	4.9	1.06	2.56	0.47	1.32	0.45	1.22
13-AB-S202A	0.2	1.4	2.47	4	1.03	2.34	0.45	1.23	0.48	1.2
13-AB-S203A	0.51	2.2	8.59	10	1.48	3.02	0.68	1.61	0.68	1.44
13-AB-S204A	0.46	2.2	6.3	9.3	1.42	3.19	0.65	1.68	0.62	1.41
13-AB-S205A	0.49	2.2	7.35	8.9	1.46	3.02	0.66	1.63	0.65	1.43

p: partial digest

t: total digest

Appendix B: Surficial Geochemistry

Sample_ID	Cs_p_ppm	Cs_t_ppm	Cu_p_ppm	Cu_t_ppm	Dy_p_ppm	Dy_t_ppm	Er_p_ppm	Er_t_ppm	Eu_p_ppm	Eu_t_ppm
13-AB-S206A	0.22	1.3	4.86	6.7	1.17	2.89	0.53	1.49	0.57	1.46
13-AB-S207A	0.21	1.3	4.55	6.2	1.21	2.89	0.53	1.52	0.56	1.47
13-AB-S209A	0.66	2.1	15.1	15.2	1.46	2.87	0.69	1.5	0.64	1.37
13-AB-S210A	0.21	1.2	3.81	5.5	1.14	2.73	0.52	1.45	0.52	1.3
13-AB-S210A_D	0.2	1.2	3.78	5.6	1.12	2.71	0.5	1.44	0.51	1.35
13-AB-S211A	0.16	1.1	2.62	3.9	1.18	2.79	0.54	1.49	0.54	1.38
13-AB-S212A	0.36	1.6	6.02	8	1.35	2.78	0.6	1.42	0.62	1.33
13-AB-S213A	0.13	1.1	2.39	3.8	0.99	2.54	0.45	1.39	0.46	1.28
13-AB-S214A	0.48	2.4	8.23	12.1	1.46	3.1	0.65	1.6	0.68	1.56
13-AB-S215A	0.3	1.4	6.92	8.6	1.29	2.79	0.59	1.41	0.6	1.38
13-AB-S216A	0.18	1.1	3.68	5.1	1.3	3.4	0.6	1.71	0.62	1.62
13-AB-S217A	0.18	1.1	3.25	4.7	1.1	2.84	0.49	1.45	0.52	1.4
13-AB-S218A	0.21	1.3	4.34	6	1.34	3.1	0.59	1.55	0.66	1.57
13-AB-S228A	0.41	1.8	15.6	20.6	2.08	3.8	0.94	1.9	1.02	1.91
13-AB-S229A	0.24	1.3	4.17	6.3	1.09	2.58	0.48	1.4	0.5	1.26
13-AB-S230A	0.3	1.5	4.26	5.7	1.26	2.75	0.59	1.5	0.59	1.33
13-AB-S231A	0.23	1.2	5.55	6.7	1.24	2.64	0.53	1.36	0.62	1.28
13-AB-S232A	0.1	0.9	2.4	4.4	0.95	2.76	0.42	1.44	0.41	1.14
13-AB-S234A	0.18	1.2	3.66	5.3	1.15	2.6	0.5	1.51	0.58	1.33
13-AB-S235A	0.3	1.5	11.4	14.9	1.4	3.15	0.64	1.74	0.65	1.48
13-AB-S236A	0.24	1.3	4.68	7	1.14	2.8	0.5	1.4	0.59	1.47
13-AB-S237A	0.38	1.8	5.59	7.2	1.32	2.75	0.57	1.49	0.69	1.48
13-AB-S239A	0.59	1.9	12.6	12.9	1.52	2.86	0.67	1.42	0.78	1.56
13-AB-S240A	0.22	1.2	6.48	8.8	1.34	3.1	0.59	1.61	0.74	1.77

p: partial digest
t: total digest

Appendix B: Surficial Geochemistry

Sample_ID	Fe2O3_t_pe	Ga_p_ppm	Ga_t_ppm	Gd_p_ppm	Gd_t_ppm	Ge_p_ppm	Hf_p_ppm	Hf_t_ppm	Hg_p_ppm	Ho_p_ppm
12-MR-S007A	1.92	0.99	6.1	2.7	6.3	0.02	0.34	7.3	0.005	0.19
12-MR-S008A	1.78	1.14	6.5	2.7	6.2	0.02	0.21	6.5	0.005	0.18
12-MR-S009A	1.85	0.75	5.5	2.47	6.8	0.02	0.18	9.8	0.005	0.17
12-MR-S010A	2.26	1.24	6.5	2.94	7.2	0.02	0.22	10	0.005	0.21
12-MR-S011A	2.92	1.71	7.8	3.36	7.4	0.02	0.29	8	0.005	0.23
12-MR-S012A	2.13	1.08	6.3	2.87	7.2	0.01	0.19	9.5	0.005	0.2
12-MR-S013A	3.42	2.07	9.4	3.55	8.6	0.01	0.46	9.4	0.005	0.28
12-MR-S014A	2.48	1.77	8.1	3.63	7.6	0.01	0.33	9.1	0.005	0.26
12-MR-S015A	2.11	1.1	6.2	2.8	6.8	0.02	0.16	7.9	0.005	0.19
12-MR-S016A	1.97	1.05	6.1	3.08	6.7	0.01	0.22	9.1	0.005	0.22
12-MR-S017A	2.15	1.54	6.6	3.62	7.2	0.005	0.32	9.1	0.005	0.25
12-MR-S018A	2.05	1.42	6.6	3.32	7.2	0.005	0.22	8.6	0.005	0.22
12-MR-S019A	2.03	1.19	6.5	2.93	7.2	0.02	0.13	7.7	0.005	0.19
12-MR-S020A	2.07	0.89	5.7	2.7	7.2	0.005	0.1	9.3	0.005	0.18
12-MR-S021A	2.38	1.95	7.2	3.88	7.6	0.01	0.44	9.8	0.005	0.28
12-MR-S022A	1.98	1.2	6.4	3.25	7.4	0.005	0.17	8.8	0.005	0.23
12-MR-S023A	2.64	1.92	9.1	3.55	7.8	0.005	0.43	8.6	0.005	0.25
12-MR-S024A	1.66	1.12	5.9	2.43	5	0.01	0.13	5.8	0.005	0.16
12-MR-S025A	1.63	1.22	6.2	2.81	5.8	0.005	0.18	6.6	0.005	0.19
12-MR-S026A	2.97	2.6	9	4.12	7.8	0.005	0.49	7.5	0.005	0.3
12-MR-S027A	2.02	1.27	7.4	3.28	6.7	0.005	0.32	7.4	0.005	0.24
12-MR-S028A	2.29	1.35	7.3	3.24	7	0.005	0.28	8.3	0.005	0.23
12-MR-S029A	2.17	1.1	6.9	3.33	7.5	0.01	0.16	8.6	0.005	0.23
12-MR-S030A	2.3	1.39	6.8	3.26	6.8	0.02	0.21	10	0.005	0.24
12-MR-S031A	2.61	2.05	9	3.43	7.4	0.005	0.28	7.7	0.005	0.26
12-MR-S032A	2.26	1.27	7	3.21	7.6	0.005	0.1	9.9	0.005	0.22
12-MR-S033A	1.97	1.18	6.5	2.78	6	0.005	0.1	6.3	0.005	0.2
12-MR-S034A	2.33	1.49	7.3	3.37	7.3	0.005	0.29	8.1	0.005	0.23
12-MR-S035A	1.72	0.49	5	2.27	5.7	0.005	0.08	10.7	0.005	0.16
12-MR-S036A	1.93	1.13	6.1	2.95	6.3	0.005	0.15	8.2	0.005	0.21
12-MR-S038A	1.89	0.91	6.1	2.56	6.4	0.005	0.09	9.2	0.005	0.18
12-MR-S039A	1.82	1.87	6.3	3.23	5.7	0.08	0.2	7.6	0.005	0.21
12-MR-S040A	2.07	2.61	8.2	3.97	7.4	0.08	0.1	6	0.02	0.25

p: partial digest

t: total digest

Appendix B: Surficial Geochemistry

Sample_ID	Fe2O3_t_pe	Ga_p_ppm	Ga_t_ppm	Gd_p_ppm	Gd_t_ppm	Ge_p_ppm	Hf_p_ppm	Hf_t_ppm	Hg_p_ppm	Ho_p_ppm
12-MR-S041A	1.68	1.55	6.1	3.07	5.6	0.06	0.14	6	0.005	0.19
12-MR-S042A	1.88	1.52	6.2	3.68	6.6	0.07	0.19	8.2	0.005	0.24
12-MR-S043A	1.53	1.22	5.5	2.65	5.4	0.05	0.12	8.4	0.005	0.17
12-MR-S044A	1.68	1.33	5.8	2.87	5.4	0.06	0.12	7.5	0.005	0.18
12-MR-S045A	1.83	1.52	6	3.09	5.8	0.06	0.13	8.1	0.005	0.19
12-MR-S045A_D	1.86	1.56	6.2	3.09	6	0.07	0.14	8.1	0.005	0.2
12-MR-S046A	2.62	3.26	9.2	4.31	7	0.08	0.49	9.1	0.005	0.31
12-MR-S047A	2.3	2.77	8.6	5.23	8.6	0.1	0.12	6	0.01	0.34
12-MR-S048A	2.29	2.58	8.3	3.93	6.8	0.07	0.31	7.3	0.005	0.27
12-MR-S049A	1.69	0.87	5.9	2.47	5.7	0.02	0.12	7.7	0.005	0.17
12-MR-S050A	1.72	0.87	6	2.32	5.7	0.02	0.05	7.7	0.005	0.15
12-MR-S051A	2.21	1.28	7.8	3.11	7	0.02	0.19	7.5	0.005	0.23
12-MR-S052A	1.89	1.09	7	2.36	6.2	0.02	0.08	6.9	0.005	0.17
12-MR-S053A	1.81	0.98	6.3	2.53	6.3	0.02	0.07	8.9	0.005	0.17
12-MR-S053A_D	1.85	0.94	6.1	2.49	6.4	0.01	0.07	8.8	0.005	0.17
12-MR-S060A	2.21	1.25	6.7	3.6	9	0.005	0.25	10.5	0.005	0.22
12-MR-S060A_D	2.32	1.35	7.1	3.93	9.4	0.01	0.29	10.2	0.005	0.23
12-MR-S061A	2.53	1.59	8.2	4.42	9.7	0.005	0.31	9.8	0.005	0.26
12-MR-S063A	2.35	1.41	7.4	3.55	8.2	0.005	0.15	8.8	0.005	0.22
12-MR-S069A	1.84	0.64	5.3	2.44	6.5	0.005	0.08	11.4	0.005	0.16
12-MR-S070A	1.9	0.93	6.2	2.79	6.2	0.005	0.18	9.2	0.005	0.2
12-MR-S071A	2.02	0.95	6.6	2.91	6.6	0.005	0.2	9.9	0.005	0.22
12-MR-S072A	1.99	1.05	7.1	3.2	7.1	0.005	0.17	10.2	0.005	0.23
12-MR-S076A	1.79	0.87	6.3	2.32	5.7	0.005	0.07	9.6	0.005	0.16
12-MR-S077A	1.81	1.03	6.6	2.93	5.6	0.005	0.23	8.6	0.005	0.22
12-MR-S078A	2.53	1.99	10	3.74	7.4	0.005	0.45	8.4	0.005	0.26
12-MR-S079A	2.34	1.34	7.9	3.16	6.9	0.01	0.23	8.5	0.005	0.22
12-MR-S080A	2.17	1	6.9	3.63	7.2	0.005	0.17	9.8	0.005	0.26
12-MR-S086A	2.33	1.44	8.1	3.55	7.3	0.005	0.21	8.3	0.005	0.26
12-MR-S087A	2.29	1.33	9.7	3.31	7.7	0.005	0.12	8	0.005	0.21
12-TH-S103A	2.94	1.09	8.2	3.98	10.7	0.005	0.13	11.7	0.005	0.24
12-TH-S104A	2.9	1.82	8.7	4.16	10.1	0.005	0.11	11.1	0.005	0.23
12-TH-S105A	2.49	1.54	8.8	4.23	8.8	0.005	0.27	10	0.005	0.25

p: partial digest
t: total digest

Appendix B: Surficial Geochemistry

Sample_ID	Fe2O3_t_pe	Ga_p_ppm	Ga_t_ppm	Gd_p_ppm	Gd_t_ppm	Ge_p_ppm	Hf_p_ppm	Hf_t_ppm	Hg_p_ppm	Ho_p_ppm
12-TH-S106A	2.21	1.33	7.4	4.28	8.2	0.005	0.13	8.5	0.005	0.24
12-TH-S107A	2.01	0.8	6.9	3.42	8.1	0.005	0.14	13.3	0.005	0.21
12-TH-S110A	2.6	1.16	7.5	3.59	8.4	0.005	0.19	10.4	0.005	0.21
12-TH-S111A	2.05	0.75	6.6	3.06	7.4	0.005	0.13	10.8	0.005	0.2
12-TH-S112A	1.87	1.04	6.8	2.7	5.7	0.005	0.1	7.6	0.005	0.18
12-TH-S113A	1.69	0.96	6.9	3.07	6.6	0.005	0.1	9.5	0.005	0.21
12-TH-S114A	1.54	1.09	6.8	3.07	6.6	0.005	0.11	9.3	0.005	0.21
12-TH-S116A	2.46	1.05	7.5	3.52	8.8	0.005	0.14	9	0.005	0.2
12-TH-S117A	2.51	1.46	7.9	3.09	6.9	0.005	0.08	8	0.005	0.21
12-TH-S190A	1.94	1.57	6.4	2.97	5.9	0.06	0.1	8	0.005	0.19
12-TH-S191A	2.57	2.78	9.2	3.94	6.5	0.07	0.34	6.7	0.005	0.27
12-TH-S192A	1.74	1.34	5.9	2.46	5.4	0.05	0.11	7.7	0.005	0.16
12-TH-S193A	2.06	1.57	6	3.78	7	0.08	0.14	8.5	0.005	0.22
12-TH-S194A	2.17	1.9	6.6	4.26	7.6	0.09	0.17	10.3	0.005	0.23
12-TH-S195A	2	2.02	6.5	4.23	7.3	0.09	0.15	7.8	0.005	0.23
13-AB-244A	1.85	1.15	6.8	3.37	5.8	0.02	0.18	10	0.005	0.22
13-AB-245A	1.77	1.14	6.7	3.16	5.4	0.03	0.22	7.5	0.005	0.18
13-AB-246A	1.86	1.3	7.1	3.18	5.4	0.02	0.23	8.2	0.005	0.21
13-AB-246A_D	1.9	1.36	7.2	3.22	5.8	0.03	0.24	8.8	0.005	0.22
13-AB-247A	1.7	0.87	5.9	2.89	5.5	0.03	0.17	10	0.005	0.18
13-AB-248A	1.61	0.86	5.3	2.87	5.1	0.03	0.19	9.6	0.005	0.19
13-AB-249A	2.1	1.48	7.5	3.32	5.6	0.03	0.2	8	0.005	0.22
13-AB-250A	2.32	1.02	6.2	3.24	6.6	0.03	0.19	11	0.02	0.2
13-AB-252A	2.09	1.14	6.2	3.27	6.3	0.03	0.21	9.2	0.02	0.2
13-AB-253A	1.72	0.92	6	2.74	5	0.02	0.16	8.5	0.01	0.17
13-AB-254A	1.74	0.96	6	2.75	4.9	0.02	0.13	7.9	0.01	0.17
13-AB-S199A	2.14	1.11	6.3	3.08	5.6	0.02	0.18	8.7	0.005	0.21
13-AB-S200A	1.92	1.28	6.7	2.58	4.7	0.02	0.12	8.2	0.005	0.17
13-AB-S201A	2.18	1.3	7.4	2.46	4.8	0.02	0.12	7.2	0.005	0.18
13-AB-S202A	1.82	1.1	6.7	2.6	4.6	0.02	0.18	5.8	0.005	0.17
13-AB-S203A	2.35	1.78	9.1	3.46	5.8	0.02	0.44	7.9	0.005	0.25
13-AB-S204A	2.53	1.61	8.9	3.36	6	0.02	0.31	8.3	0.005	0.25
13-AB-S205A	2.35	1.89	8.7	3.56	5.8	0.02	0.22	7.4	0.005	0.25

p: partial digest

t: total digest

Appendix B: Surficial Geochemistry

Sample_ID	Fe2O3_t_pe	Ga_p_ppm	Ga_t_ppm	Gd_p_ppm	Gd_t_ppm	Ge_p_ppm	Hf_p_ppm	Hf_t_ppm	Hg_p_ppm	Ho_p_ppm
13-AB-S206A	2.14	1.04	6.5	2.93	5.7	0.02	0.27	7.9	0.005	0.2
13-AB-S207A	2.12	1.03	6.4	3.05	5.7	0.02	0.18	8.4	0.005	0.2
13-AB-S209A	2.62	1.92	8.2	3.44	5.2	0.02	0.41	7.5	0.005	0.25
13-AB-S210A	1.75	1.04	5.9	2.81	5.1	0.02	0.26	8.3	0.005	0.2
13-AB-S210A_D	1.77	1	6.2	2.73	5.2	0.03	0.25	8.6	0.005	0.19
13-AB-S211A	1.96	0.83	5.8	2.88	5.2	0.03	0.25	9.5	0.005	0.2
13-AB-S212A	2.18	1.4	7.3	3.23	5.5	0.03	0.22	7.5	0.005	0.23
13-AB-S213A	1.65	0.74	6	2.33	4.7	0.01	0.18	8.9	0.005	0.16
13-AB-S214A	2.61	1.75	9.7	3.56	6.3	0.03	0.43	7	0.005	0.24
13-AB-S215A	1.93	1.28	6.9	3.17	5.2	0.02	0.37	7	0.005	0.22
13-AB-S216A	2.1	0.92	5.8	3.29	6.6	0.02	0.24	11.8	0.005	0.22
13-AB-S217A	1.63	0.85	5.7	2.78	5.2	0.03	0.2	9.5	0.005	0.18
13-AB-S218A	2.05	1.08	6.5	3.39	6.2	0.03	0.27	8.5	0.005	0.22
13-AB-S228A	2.12	1.64	7.5	5.16	7.8	0.03	0.17	8	0.01	0.35
13-AB-S229A	1.69	1.15	6.5	2.65	5	0.02	0.23	7.4	0.005	0.18
13-AB-S230A	1.77	1.27	7	3.08	5.2	0.02	0.19	8	0.005	0.21
13-AB-S231A	1.25	1.24	5.8	3.08	4.9	0.02	0.15	8.2	0.005	0.2
13-AB-S232A	1.5	0.58	5.1	2.29	4.6	0.02	0.13	12	0.005	0.16
13-AB-S234A	1.57	0.97	5.8	2.92	5.2	0.02	0.24	8.4	0.005	0.19
13-AB-S235A	2.96	1.44	7.4	3.46	6	0.03	0.2	8.2	0.005	0.24
13-AB-S236A	1.98	1.07	6.2	2.93	5.6	0.02	0.2	8.8	0.005	0.19
13-AB-S237A	2.16	1.9	8	3.43	5.6	0.02	0.29	8.1	0.005	0.22
13-AB-S239A	2.37	2.08	8.3	3.9	5.8	0.03	0.42	7.4	0.005	0.25
13-AB-S240A	1.96	1.15	6.2	3.56	6.6	0.04	0.31	11	0.005	0.21

p: partial digest
t: total digest

Appendix B: Surficial Geochemistry

Sample_ID	Ho_t_ppm	K2O_t_pct	La_t_ppm	Li_t_ppm	MgO_t_pct	MnO_t_pct	Mo_p_ppm	Mo_t_ppm	Na2O_t_pct	Nb_p_ppm
12-MR-S007A	0.5	2.4	46	16	0.5	0.02	0.17	0.39	1.2	0.1
12-MR-S008A	0.45	2.42	43	17	0.522	0.019	0.11	0.32	1.18	0.11
12-MR-S009A	0.53	2.17	46	14	0.449	0.016	0.11	0.38	1.14	0.12
12-MR-S010A	0.57	2.3	49	19	0.586	0.021	0.18	0.43	1.09	0.09
12-MR-S011A	0.59	2.31	55	23	0.893	0.034	0.26	0.57	1.07	0.06
12-MR-S012A	0.55	2.27	49	18	0.578	0.023	0.15	0.44	1.11	0.14
12-MR-S013A	0.67	2.5	60	29	1.06	0.034	0.23	0.6	0.99	0.06
12-MR-S014A	0.56	2.64	54	22	0.758	0.025	0.17	0.47	1.18	0.11
12-MR-S015A	0.52	2.28	48	18	0.601	0.022	0.14	0.43	1.12	0.09
12-MR-S016A	0.53	2.3	47	17	0.505	0.019	0.12	0.54	1.11	0.11
12-MR-S017A	0.56	2.43	51	19	0.597	0.024	0.18	0.42	1.13	0.12
12-MR-S018A	0.54	2.37	49	18	0.619	0.023	0.18	0.38	1.12	0.14
12-MR-S019A	0.49	2.34	54	19	0.629	0.019	0.13	0.42	1.1	0.11
12-MR-S020A	0.53	2.19	51	16	0.524	0.019	0.1	0.44	1.11	0.1
12-MR-S021A	0.57	2.53	53	21	0.682	0.023	0.16	0.41	1.12	0.1
12-MR-S022A	0.56	2.35	54	19	0.592	0.018	0.14	0.44	1.12	0.12
12-MR-S023A	0.6	2.73	53	26	0.906	0.03	0.21	0.55	1.11	0.1
12-MR-S024A	0.39	2.24	39	17	0.475	0.017	0.14	0.34	1.01	0.11
12-MR-S025A	0.45	2.39	42	18	0.533	0.016	0.14	0.39	1.12	0.1
12-MR-S026A	0.57	2.48	58	28	0.986	0.024	1	1.41	1.02	0.14
12-MR-S027A	0.52	2.57	49	19	0.62	0.02	0.17	0.39	1.23	0.12
12-MR-S028A	0.55	2.45	49	19	0.652	0.022	0.17	0.53	1.16	0.12
12-MR-S029A	0.56	2.47	54	19	0.583	0.02	0.14	0.43	1.18	0.14
12-MR-S030A	0.56	2.22	47	18	0.595	0.021	0.16	0.49	1.05	0.09
12-MR-S031A	0.57	2.62	52	25	0.895	0.03	0.22	0.45	1.09	0.08
12-MR-S032A	0.57	2.33	56	19	0.644	0.021	0.21	0.5	1.11	0.13
12-MR-S033A	0.46	2.3	45	19	0.579	0.021	0.13	0.33	1.12	0.09
12-MR-S034A	0.54	2.46	50	21	0.7	0.023	0.14	0.39	1.13	0.07
12-MR-S035A	0.48	1.99	40	13	0.328	0.015	0.06	0.34	1.01	0.1
12-MR-S036A	0.47	2.24	45	18	0.527	0.022	0.12	0.37	1.07	0.12
12-MR-S038A	0.49	2.16	43	17	0.501	0.017	0.11	0.39	1.05	0.1
12-MR-S039A	0.44	2.14	42	18	0.554	0.018	0.23	0.42	1.02	0.14
12-MR-S040A	0.52	2.2	58	22	0.71	0.015	0.19	0.46	0.85	0.53

p: partial digest
t: total digest

Appendix B: Surficial Geochemistry

Sample_ID	Ho_t_ppm	K2O_t_pct	La_t_ppm	Li_t_ppm	MgO_t_pct	MnO_t_pct	Mo_p_ppm	Mo_t_ppm	Na2O_t_pct	Nb_p_ppm
12-MR-S041A	0.4	2.22	40	17	0.499	0.018	0.13	0.34	1.01	0.14
12-MR-S042A	0.52	2.17	49	16	0.461	0.018	0.13	0.35	1.04	0.19
12-MR-S043A	0.43	1.95	38	15	0.393	0.014	0.1	0.38	0.94	0.15
12-MR-S044A	0.43	2.15	39	16	0.416	0.016	0.11	0.36	1.03	0.17
12-MR-S045A	0.44	2.15	43	17	0.467	0.017	0.12	0.35	1.03	0.18
12-MR-S045A_D	0.46	2.22	44	17	0.473	0.017	0.12	0.38	1.07	0.18
12-MR-S046A	0.54	2.66	50	25	0.859	0.027	0.22	0.41	1.03	0.09
12-MR-S047A	0.59	2.61	68	25	0.817	0.026	0.21	0.45	1.1	0.3
12-MR-S048A	0.49	2.6	52	23	0.755	0.025	0.14	0.38	1.12	0.15
12-MR-S049A	0.44	2.2	42	15	0.429	0.016	0.14	0.4	1.07	0.1
12-MR-S050A	0.42	2.19	42	17	0.477	0.014	0.1	0.34	1.06	0.08
12-MR-S051A	0.53	2.41	50	21	0.635	0.022	0.1	0.42	1.07	0.09
12-MR-S052A	0.46	2.2	48	20	0.644	0.016	0.13	0.44	1	0.08
12-MR-S053A	0.49	2.16	47	17	0.497	0.017	0.12	0.39	1.06	0.09
12-MR-S053A_D	0.48	2.12	47	17	0.499	0.017	0.1	0.39	1.03	0.08
12-MR-S060A	0.54	2.64	66	16	0.664	0.021	0.15	0.38	1.29	0.23
12-MR-S060A_D	0.58	2.74	69	17	0.677	0.022	0.15	0.4	1.33	0.31
12-MR-S061A	0.59	2.91	77	20	0.789	0.028	0.21	0.48	1.33	0.27
12-MR-S063A	0.54	2.54	68	20	0.74	0.023	0.19	0.5	1.24	0.2
12-MR-S069A	0.52	2.05	45	14	0.374	0.015	0.08	0.35	1	0.11
12-MR-S070A	0.48	2.17	44	17	0.479	0.017	0.12	0.36	1.02	0.1
12-MR-S071A	0.54	2.16	45	16	0.464	0.02	0.16	0.47	1.03	0.12
12-MR-S072A	0.57	2.24	49	16	0.535	0.019	0.13	0.46	1.1	0.17
12-MR-S076A	0.48	2.16	41	16	0.45	0.015	0.09	0.37	1.08	0.16
12-MR-S077A	0.47	2.14	40	16	0.464	0.016	0.15	0.44	1.01	0.12
12-MR-S078A	0.56	2.78	57	28	0.845	0.024	0.24	0.52	0.94	0.07
12-MR-S079A	0.53	2.43	50	20	0.681	0.029	0.18	0.5	1.18	0.11
12-MR-S080A	0.58	2.27	49	16	0.546	0.021	0.14	0.45	1.18	0.13
12-MR-S086A	0.58	2.51	53	21	0.732	0.023	0.18	0.46	1.15	0.2
12-MR-S087A	0.53	3.1	60	20	0.716	0.025	0.14	0.5	1.64	0.21
12-TH-S103A	0.71	2.82	80	18	0.785	0.029	0.2	0.58	1.35	0.19
12-TH-S104A	0.63	2.81	80	23	0.994	0.03	0.19	0.62	1.32	0.18
12-TH-S105A	0.59	2.78	74	20	0.684	0.025	0.19	0.52	1.3	0.19

p: partial digest

t: total digest

Appendix B: Surficial Geochemistry

Sample_ID	Ho_t_ppm	K2O_t_pct	La_t_ppm	Li_t_ppm	MgO_t_pct	MnO_t_pct	Mo_p_ppm	Mo_t_ppm	Na2O_t_pct	Nb_p_ppm
12-TH-S106A	0.54	2.35	71	19	0.595	0.02	0.17	0.46	1.11	0.18
12-TH-S107A	0.62	2.32	64	15	0.453	0.017	0.08	0.47	1.16	0.14
12-TH-S110A	0.58	2.56	72	19	0.672	0.026	0.26	0.57	1.22	0.13
12-TH-S111A	0.57	2.35	55	16	0.459	0.017	0.15	0.5	1.09	0.13
12-TH-S112A	0.44	2.3	43	17	0.478	0.017	0.12	0.38	1.12	0.11
12-TH-S113A	0.51	2.23	48	16	0.466	0.016	0.14	0.37	1.12	0.12
12-TH-S114A	0.52	2.26	50	17	0.512	0.016	0.14	0.39	1.12	0.1
12-TH-S116A	0.57	2.89	64	17	0.65	0.024	0.11	0.43	1.25	0.14
12-TH-S117A	0.51	2.3	54	20	0.692	0.025	0.16	0.48	1.06	0.14
12-TH-S190A	0.47	2.11	42	17	0.519	0.019	0.15	0.4	1.04	0.19
12-TH-S191A	0.48	2.67	51	26	0.816	0.025	0.17	0.39	0.99	0.07
12-TH-S192A	0.41	1.92	39	16	0.523	0.015	0.08	0.3	0.93	0.14
12-TH-S193A	0.52	2.17	56	17	0.493	0.019	0.1	0.39	1.01	0.13
12-TH-S194A	0.55	2.2	61	18	0.6	0.018	0.13	0.46	1.07	0.16
12-TH-S195A	0.49	2.22	58	18	0.629	0.018	0.14	0.4	1.1	0.16
13-AB-244A	0.57	2.35	51	17	0.531	0.016	0.12	0.3	1.1	0.14
13-AB-245A	0.48	2.4	49	17	0.509	0.018	0.12	0.25	1.08	0.17
13-AB-246A	0.54	2.5	52	20	0.626	0.017	0.16	0.21	1.12	0.14
13-AB-246A_D	0.57	2.51	54	20	0.64	0.017	0.14	0.27	1.12	0.14
13-AB-247A	0.55	2.22	48	16	0.448	0.015	0.1	0.25	1.08	0.13
13-AB-248A	0.53	2.06	45	14	0.418	0.014	0.1	0.25	1	0.12
13-AB-249A	0.54	2.47	54	20	0.641	0.018	0.14	0.28	1.12	0.14
13-AB-250A	0.58	2.4	61	16	0.56	0.02	0.22	0.52	1.22	0.2
13-AB-252A	0.58	2.38	62	17	0.548	0.018	0.18	0.46	1.17	0.15
13-AB-253A	0.47	2.27	45	16	0.459	0.015	0.1	0.31	1.08	0.12
13-AB-254A	0.47	2.3	46	16	0.461	0.015	0.1	0.31	1.09	0.11
13-AB-S199A	0.56	2.26	51	18	0.584	0.02	0.11	0.43	1.13	0.11
13-AB-S200A	0.48	2.39	44	19	0.567	0.019	0.2	0.44	1.12	0.15
13-AB-S201A	0.5	2.57	47	21	0.68	0.026	0.18	0.42	1.18	0.2
13-AB-S202A	0.46	2.55	46	19	0.552	0.018	0.11	0.33	1.2	0.13
13-AB-S203A	0.57	2.76	52	24	0.767	0.02	0.19	0.35	1.08	0.1
13-AB-S204A	0.62	2.75	54	26	0.814	0.023	0.15	0.39	1.06	0.1
13-AB-S205A	0.58	2.67	54	24	0.8	0.021	0.18	0.41	1.05	0.22

p: partial digest
t: total digest

Appendix B: Surficial Geochemistry

Sample_ID	Ho_t_ppm	K2O_t_pct	La_t_ppm	Li_t_ppm	MgO_t_pct	MnO_t_pct	Mo_p_ppm	Mo_t_ppm	Na2O_t_pct	Nb_p_ppm
13-AB-S206A	0.56	2.34	52	18	0.603	0.018	0.15	0.48	1.14	0.16
13-AB-S207A	0.56	2.31	50	17	0.592	0.02	0.13	0.38	1.16	0.14
13-AB-S209A	0.55	2.41	48	24	0.853	0.025	0.26	0.43	1.04	0.12
13-AB-S210A	0.51	2.18	44	16	0.504	0.015	0.2	0.45	1.07	0.17
13-AB-S210A_D	0.53	2.23	45	16	0.509	0.015	0.2	0.42	1.1	0.19
13-AB-S211A	0.56	2.18	47	15	0.458	0.017	0.1	0.37	1.07	0.18
13-AB-S212A	0.53	2.4	48	20	0.702	0.021	0.2	0.35	1.1	0.15
13-AB-S213A	0.5	2.21	41	15	0.444	0.014	0.08	0.36	1.13	0.1
13-AB-S214A	0.59	3.13	60	26	0.93	0.028	0.15	0.43	1.26	0.09
13-AB-S215A	0.53	2.33	46	17	0.609	0.019	0.24	0.46	1.09	0.13
13-AB-S216A	0.64	2	55	15	0.51	0.017	0.13	0.38	1.03	0.16
13-AB-S217A	0.54	2.09	45	15	0.466	0.015	0.13	0.41	1.06	0.16
13-AB-S218A	0.57	2.43	56	16	0.564	0.018	0.18	0.38	1.23	0.23
13-AB-S228A	0.7	2.39	72	21	0.741	0.021	0.14	0.21	1.06	0.32
13-AB-S229A	0.49	2.24	45	18	0.551	0.014	0.17	0.28	1.03	0.12
13-AB-S230A	0.54	2.36	47	19	0.58	0.015	0.14	0.28	1.05	0.13
13-AB-S231A	0.48	1.98	43	17	0.585	0.013	0.12	0.16	0.9	0.16
13-AB-S232A	0.51	1.92	37	13	0.326	0.012	0.09	0.22	0.96	0.11
13-AB-S234A	0.51	2.1	48	16	0.454	0.013	0.18	0.2	0.96	0.14
13-AB-S235A	0.64	2.23	58	21	0.871	0.031	0.2	0.33	1.09	0.11
13-AB-S236A	0.52	2.24	50	17	0.559	0.016	0.12	0.23	1.08	0.13
13-AB-S237A	0.52	2.4	55	24	0.821	0.018	0.33	0.38	1	0.1
13-AB-S239A	0.53	2.66	57	23	0.822	0.026	0.22	0.26	1.12	0.12
13-AB-S240A	0.57	2.37	61	16	0.581	0.017	0.12	0.31	1.15	0.21

p: partial digest
t: total digest

Appendix B: Surficial Geochemistry

Sample_ID	Nb_t_ppm	Nd_p_ppm	Nd_t_ppm	Ni_p_ppm	Ni_t_ppm	P2O5_t_pct	Pb_p_ppm	Pb_t_ppm	Pb204_p_pp	Pb204_t_pp
12-MR-S007A	9.8	19.6	37.8	4.29	10.5	0.268	6.46	18.3	0.087	0.261
12-MR-S008A	9.3	19.2	36.4	5.42	12.2	0.248	7.04	19.1	0.098	0.256
12-MR-S009A	10.1	17.7	39	3.38	9.7	0.294	5.88	17.9	0.082	0.247
12-MR-S010A	10.9	20.7	40.5	6.46	13.6	0.288	6.75	18.9	0.093	0.255
12-MR-S011A	11.5	22.2	43.5	13.2	25.1	0.289	7.12	18.7	0.098	0.256
12-MR-S012A	11	20.6	41.9	6.8	14.8	0.284	7.35	20.3	0.102	0.27
12-MR-S013A	12.2	23.6	48.7	16.3	29.9	0.295	8.58	21.6	0.118	0.305
12-MR-S014A	11.4	25.6	44.7	9.08	17.4	0.296	10.3	22.4	0.141	0.303
12-MR-S015A	10.1	19.6	38.7	6.88	15	0.274	6.9	19.5	0.095	0.265
12-MR-S016A	10.7	21	38.7	5.65	12	0.286	6.76	18.6	0.092	0.252
12-MR-S017A	11	25.4	42.4	8.46	14	0.291	9.63	21.2	0.136	0.291
12-MR-S018A	10.1	23.8	41.3	7.76	13.8	0.278	9.24	20.9	0.129	0.288
12-MR-S019A	10.1	21.3	43.2	6	14.3	0.262	7.04	20.2	0.101	0.284
12-MR-S020A	10.5	19.9	41	5.06	12.2	0.288	5.72	17.9	0.078	0.251
12-MR-S021A	11.3	27.1	43.2	9.92	14.3	0.29	10.9	20.8	0.15	0.284
12-MR-S022A	11.6	23.3	43.5	6.3	12.6	0.287	7.64	20.2	0.105	0.272
12-MR-S023A	10	25.1	44.3	9.46	18.5	0.266	10.8	24.6	0.148	0.334
12-MR-S024A	8.6	17.7	30.5	6.02	11.3	0.227	6.08	16.5	0.084	0.224
12-MR-S025A	9	20.5	33.9	6.55	11.7	0.237	8.14	19.1	0.114	0.264
12-MR-S026A	10.6	29.4	46	16.4	26.6	0.253	13.2	24.7	0.188	0.334
12-MR-S027A	10.5	23.2	40.5	6.66	13.6	0.289	8.56	21.2	0.117	0.289
12-MR-S028A	11.1	22.9	40.9	7.78	15.7	0.297	8.71	20.9	0.12	0.291
12-MR-S029A	11.8	22.8	44	5.77	16.6	0.296	7.38	20.6	0.101	0.284
12-MR-S030A	11	22	39.2	7.58	14.6	0.277	7.81	19.1	0.108	0.261
12-MR-S031A	10.8	23.7	42.3	11.6	21.7	0.27	9.91	22.3	0.137	0.308
12-MR-S032A	11.8	23	44.5	7.58	15.3	0.306	9.72	22.8	0.135	0.308
12-MR-S033A	9.2	20	36.3	6.39	12.9	0.248	7.61	18.8	0.105	0.259
12-MR-S034A	11	23.4	41.6	8.93	16.5	0.286	8.94	21	0.121	0.286
12-MR-S035A	10.5	16.1	32.7	2.1	6.7	0.291	3.56	14.3	0.048	0.198
12-MR-S036A	9.8	21.2	37.1	5.91	11.3	0.266	7.07	18	0.099	0.248
12-MR-S038A	10.3	17.7	35.8	5.38	12	0.268	5.34	16.8	0.071	0.231
12-MR-S039A	9.8	22.7	35.3	7.8	12.4	0.262	8.35	17	0.12	0.234
12-MR-S040A	8.6	28.2	46.7	10.4	18.6	0.263	9.32	19.5	0.142	0.271

p: partial digest
t: total digest

Appendix B: Surficial Geochemistry

Sample_ID	Nb_t_ppm	Nd_p_ppm	Nd_t_ppm	Ni_p_ppm	Ni_t_ppm	P2O5_t_pct	Pb_p_ppm	Pb_t_ppm	Pb204_p_pp	Pb204_t_pp
12-MR-S041A	8.5	21.4	34.6	6.92	11.7	0.237	6.75	16	0.094	0.216
12-MR-S042A	11.1	25	41.8	5.04	10	0.305	6.4	16.8	0.091	0.234
12-MR-S043A	9.4	18.7	33.2	4.33	9.1	0.266	4.06	13.2	0.057	0.167
12-MR-S044A	9.5	20.2	33.6	5.09	9.6	0.258	5.42	15.1	0.076	0.204
12-MR-S045A	10.2	21.2	36	5.51	10.2	0.272	5.72	15.3	0.082	0.199
12-MR-S045A_D	10.5	21.6	36.8	5.69	10.6	0.273	6.13	15.5	0.082	0.211
12-MR-S046A	10.7	27.9	41.9	14.1	19	0.286	11.3	19.9	0.159	0.275
12-MR-S047A	9.2	36.5	55.2	12	19.9	0.25	10	20.7	0.144	0.281
12-MR-S048A	10.4	27.2	43.5	10.4	16.8	0.27	9.56	20	0.135	0.263
12-MR-S049A	9.6	17.4	35	3.92	9.7	0.278	6	15.4	0.081	0.212
12-MR-S050A	9.9	15.2	35.1	3.84	10.3	0.253	5	15.2	0.07	0.207
12-MR-S051A	11	21	42.2	6.44	14.7	0.284	6.58	17.3	0.09	0.227
12-MR-S052A	10.2	16.3	40.2	5.34	15.9	0.244	6.18	17.6	0.09	0.237
12-MR-S053A	10.6	18.1	38.8	4.24	11.2	0.265	6.27	17	0.086	0.23
12-MR-S053A_D	10.6	17.4	40.1	4.1	11	0.267	6.04	17.1	0.086	0.231
12-MR-S060A	10.2	30	54.2	6.38	12.9	0.328	21.6	36.1	0.327	0.517
12-MR-S060A_D	10.7	31.3	55.5	6.55	14	0.334	22.2	38.6	0.338	0.555
12-MR-S061A	11	34.9	60.9	8.58	16.7	0.317	27.2	41.8	0.41	0.604
12-MR-S063A	11	29.1	51.3	8.05	16.7	0.31	22.1	37.7	0.335	0.54
12-MR-S069A	11.5	17.3	37.3	2.54	7.3	0.302	5	17.2	0.069	0.23
12-MR-S070A	10.6	20	36	5.32	11.2	0.288	5.9	16.2	0.082	0.225
12-MR-S071A	10.8	20.1	37.1	4.66	11	0.301	7.35	18	0.105	0.252
12-MR-S072A	11.1	23.2	40.9	5.2	11.8	0.32	7.54	18.1	0.103	0.245
12-MR-S076A	10.1	16.4	32.7	3.78	9.1	0.275	5.51	16.1	0.074	0.22
12-MR-S077A	9.1	20	32.4	5.58	11	0.261	6.43	15.6	0.091	0.207
12-MR-S078A	10.8	27.3	45.1	8.75	16.6	0.298	12.8	23.6	0.179	0.312
12-MR-S079A	10.6	21.7	40.5	6.66	14.9	0.287	10	21.8	0.138	0.298
12-MR-S080A	11.2	24.3	41.4	4.82	11	0.315	8.07	19.1	0.113	0.255
12-MR-S086A	10.1	24.6	43.1	7.96	16.8	0.291	9.19	19.9	0.131	0.268
12-MR-S087A	10.5	25.6	47.4	6.11	14.7	0.288	11.8	25.8	0.167	0.361
12-TH-S103A	12.7	31	66.7	7.02	17.2	0.412	21.5	36.8	0.323	0.517
12-TH-S104A	12.1	33.2	63.3	13.8	24.6	0.385	27.6	41.4	0.413	0.602
12-TH-S105A	12.2	34.9	55.1	7.52	14.9	0.329	19.2	32.3	0.284	0.449

p: partial digest
t: total digest

Appendix B: Surficial Geochemistry

Sample_ID	Nb_t_ppm	Nd_p_ppm	Nd_t_ppm	Ni_p_ppm	Ni_t_ppm	P2O5_t_pct	Pb_p_ppm	Pb_t_ppm	Pb204_p_pp	Pb204_t_pp
12-TH-S106A	11.5	34.4	52.5	7.22	14	0.291	15.1	26.8	0.226	0.369
12-TH-S107A	13.6	26.7	50.5	3.22	9.2	0.355	9.69	23.4	0.142	0.323
12-TH-S110A	12.6	28.8	52.5	6.32	14.3	0.346	17.1	31.2	0.257	0.441
12-TH-S111A	12	22.4	44.6	4.32	11.4	0.389	8.45	21.1	0.121	0.302
12-TH-S112A	9.8	19.5	33.9	5.11	10.4	0.258	6.36	16.8	0.089	0.229
12-TH-S113A	10.8	22	38.6	4.66	9.8	0.306	7.51	17.6	0.105	0.239
12-TH-S114A	11.1	21.8	39.6	5.36	11.2	0.294	7.07	17.7	0.1	0.237
12-TH-S116A	11.2	26.6	54.7	5.24	13	0.397	21.5	37.6	0.329	0.531
12-TH-S117A	11.8	24.1	42.6	8.04	16.8	0.264	10.6	21.5	0.152	0.316
12-TH-S190A	9.8	20.6	35.9	6.97	13.1	0.252	5.47	15.1	0.074	0.205
12-TH-S191A	10.4	26.8	40.9	11.4	17.4	0.272	8.33	17.2	0.118	0.234
12-TH-S192A	9	17.2	32.8	5.49	12.2	0.244	4.55	14	0.062	0.179
12-TH-S193A	11.8	26.1	46.2	5.96	11.2	0.295	5.29	15.4	0.072	0.207
12-TH-S194A	12.4	30.4	49.4	7.9	14.3	0.334	9.67	20.8	0.141	0.288
12-TH-S195A	10.7	31.8	47	8.86	14.6	0.287	10.1	20.5	0.147	0.282
13-AB-244A	11	24.3	41.9	5.28	11.2	0.299	11.1	23.1	0.182	0.342
13-AB-245A	9.4	23.3	38.8	5.36	10.3	0.255	19.8	32.2	0.337	0.507
13-AB-246A	10	23	39.6	6.7	12.2	0.288	9.9	21.1	0.159	0.321
13-AB-246A_D	10	23.1	40.2	6.9	13	0.294	10.2	21.9	0.164	0.331
13-AB-247A	11.4	21	38.7	3.53	8.6	0.326	6.88	18.1	0.111	0.277
13-AB-248A	10.4	21.1	35.6	3.5	7.6	0.303	7.12	17.5	0.114	0.251
13-AB-249A	10.5	25.2	40.6	6.74	13	0.287	13.4	26.1	0.222	0.396
13-AB-250A	11	25.8	48	5.24	12.1	0.35	17.6	29.1	0.297	0.46
13-AB-252A	10.6	26.5	47	5.59	11.1	0.324	22.3	33.4	0.386	0.532
13-AB-253A	9.2	20.4	34.6	4.41	8.9	0.282	12.2	22.4	0.213	0.359
13-AB-254A	9.1	21.2	36	4.2	9	0.298	11.7	22.1	0.2	0.343
13-AB-S199A	10.2	22.3	38.4	6.11	12	0.292	8.1	18.4	0.124	0.282
13-AB-S200A	9.6	19.2	33.1	5.62	10.6	0.259	7.61	17.5	0.118	0.268
13-AB-S201A	10.1	18.6	34.4	5.87	12.2	0.272	6.3	17.4	0.098	0.272
13-AB-S202A	9.4	19.4	34.5	5.29	10.6	0.264	5.53	16.2	0.086	0.251
13-AB-S203A	10.2	25.1	41.2	7.96	13.9	0.28	7.78	19	0.12	0.292
13-AB-S204A	11.1	23.3	41.1	7.45	14.1	0.317	7.16	17.9	0.11	0.263
13-AB-S205A	10.4	24.8	41.2	8.57	15.1	0.294	7.76	17.7	0.122	0.256

p: partial digest
t: total digest

Appendix B: Surficial Geochemistry

Sample_ID	Nb_t_ppm	Nd_p_ppm	Nd_t_ppm	Ni_p_ppm	Ni_t_ppm	P2O5_t_pct	Pb_p_ppm	Pb_t_ppm	Pb204_p_pp	Pb204_t_pp
13-AB-S206A	10.6	21.5	40	5.9	12.6	0.305	8.1	19	0.125	0.292
13-AB-S207A	10.4	22	39.4	5.81	11.8	0.296	7.52	17.7	0.114	0.275
13-AB-S209A	9.2	22.8	36.7	12.2	18.7	0.257	9.53	18.2	0.15	0.282
13-AB-S210A	9.6	20	35.1	4.94	9.6	0.283	6.76	16.2	0.103	0.248
13-AB-S210A_D	9.9	19.6	36.4	4.74	10	0.282	6.64	16.5	0.097	0.242
13-AB-S211A	10.5	20.8	36.4	3.45	8.1	0.317	5.24	15.3	0.08	0.227
13-AB-S212A	9.3	22.7	38	8.1	13.7	0.268	7.54	17.8	0.117	0.261
13-AB-S213A	9.4	16.8	32.4	3.16	8.2	0.289	4.66	14.9	0.07	0.234
13-AB-S214A	10.8	25.5	45.8	8.19	16.3	0.302	9.25	21	0.143	0.322
13-AB-S215A	8.9	21.9	36.8	7.14	13.8	0.268	7.6	17.4	0.114	0.252
13-AB-S216A	11.5	23.5	45	4.56	10.7	0.335	6.36	16.3	0.097	0.236
13-AB-S217A	10.2	19.6	36	3.73	9.4	0.283	5.92	15.7	0.089	0.236
13-AB-S218A	10.9	25	44.3	4.68	10.6	0.308	8.36	19.7	0.128	0.29
13-AB-S228A	9.2	36.7	55	8.96	15.9	0.279	9.34	20.2	0.145	0.293
13-AB-S229A	9.4	18.9	35.5	6.21	12.1	0.267	6.75	17	0.104	0.248
13-AB-S230A	9.8	21.7	35.9	6.68	12.2	0.273	6.24	15.9	0.095	0.239
13-AB-S231A	9.1	21.7	34.2	7.56	12.2	0.259	4.81	13.7	0.071	0.204
13-AB-S232A	9.4	16	30.1	4.01	8.5	0.273	4.38	14.8	0.067	0.21
13-AB-S234A	9.6	21	37.1	5.09	9.7	0.26	6.38	15.9	0.1	0.233
13-AB-S235A	11.2	23.9	43.5	12.2	22.6	0.308	8.53	19.2	0.134	0.277
13-AB-S236A	10.2	21.3	39	5.93	11.7	0.291	13.4	24.2	0.219	0.376
13-AB-S237A	10.1	26	41.3	10.5	16.5	0.269	10.7	20.6	0.172	0.305
13-AB-S239A	9.4	28.6	42.4	12.2	17.7	0.272	16.3	25.3	0.264	0.363
13-AB-S240A	10.5	28.2	47.4	6.71	13.3	0.317	14.6	27.1	0.24	0.409

p: partial digest
t: total digest

Appendix B: Surficial Geochemistry

Sample_ID	Pb206_p_pp	Pb206_t_pp	Pb207_p_pp	Pb207_t_pp	Pb208_p_pp	Pb208_t_pp	Pr_p_ppm	Pr_t_ppm	Rb_p_ppm
12-MR-S007A	1.66	4.52	1.33	3.89	3.38	9.65	5.73	11	1.4
12-MR-S008A	1.76	4.66	1.46	4.11	3.72	10	5.72	10.6	1.7
12-MR-S009A	1.48	4.49	1.19	3.86	3.13	9.35	5.36	11.2	1.04
12-MR-S010A	1.7	4.75	1.37	4.08	3.59	9.84	6.02	11.7	2.4
12-MR-S011A	1.81	4.69	1.44	4.01	3.77	9.78	6.75	12.6	3.37
12-MR-S012A	1.86	5.07	1.51	4.35	3.88	10.7	6.05	11.9	1.85
12-MR-S013A	2.15	5.36	1.76	4.63	4.55	11.3	7.06	14	5.58
12-MR-S014A	2.59	5.6	2.12	4.73	5.42	11.8	7.63	12.7	4.18
12-MR-S015A	1.73	4.82	1.42	4.18	3.66	10.2	5.71	11.2	1.77
12-MR-S016A	1.7	4.64	1.38	3.96	3.58	9.79	6.31	11.3	2.13
12-MR-S017A	2.39	5.24	1.99	4.55	5.11	11.1	7.59	12.2	3.4
12-MR-S018A	2.27	5.23	1.88	4.41	4.96	10.9	7.16	11.8	2.86
12-MR-S019A	1.75	4.92	1.48	4.32	3.71	10.6	6.47	12.4	1.99
12-MR-S020A	1.42	4.43	1.18	3.83	3.04	9.43	6.07	11.9	1.29
12-MR-S021A	2.71	5.13	2.24	4.47	5.83	10.9	8.07	12.6	5.65
12-MR-S022A	1.93	5.11	1.58	4.29	4.02	10.6	7.09	12.5	2.08
12-MR-S023A	2.72	6.1	2.21	5.22	5.71	12.9	7.45	12.6	4.85
12-MR-S024A	1.54	4.09	1.24	3.49	3.21	8.68	5.38	9	1.94
12-MR-S025A	2.04	4.77	1.67	4	4.31	10.1	6.08	9.8	2.34
12-MR-S026A	3.29	6.18	2.75	5.22	6.99	13	8.84	13.4	5.98
12-MR-S027A	2.11	5.22	1.78	4.53	4.55	11.2	6.87	11.6	2.56
12-MR-S028A	2.16	5.21	1.8	4.43	4.64	11	6.67	11.7	2.78
12-MR-S029A	1.88	5.06	1.51	4.4	3.89	10.9	6.9	12.9	2.05
12-MR-S030A	1.94	4.8	1.6	4.09	4.16	9.92	6.66	11.4	2.77
12-MR-S031A	2.46	5.54	2.03	4.73	5.28	11.8	7.19	12.2	4.87
12-MR-S032A	2.44	5.75	2	4.79	5.15	11.9	7	13	2.56
12-MR-S033A	1.89	4.62	1.54	4.01	4.07	9.94	5.89	10.4	2.11
12-MR-S034A	2.29	5.15	1.81	4.53	4.72	11	7.01	12.2	3.24
12-MR-S035A	0.904	3.57	0.716	3.04	1.89	7.49	4.76	9.3	0.72
12-MR-S036A	1.77	4.53	1.45	3.85	3.75	9.39	6.36	10.6	1.95
12-MR-S038A	1.36	4.2	1.08	3.58	2.83	8.85	5.22	10.3	1.84
12-MR-S039A	2.07	4.18	1.7	3.59	4.46	8.95	6.78	9.7	2.49
12-MR-S040A	2.27	4.78	1.99	4.16	4.91	10.3	8.48	12.7	5.14

p: partial digest
t: total digest

Appendix B: Surficial Geochemistry

Sample_ID	Pb206_p_pp	Pb206_t_pp	Pb207_p_pp	Pb207_t_pp	Pb208_p_pp	Pb208_t_pp	Pr_p_ppm	Pr_t_ppm	Rb_p_ppm
12-MR-S041A	1.71	3.93	1.41	3.39	3.53	8.47	6.31	9.5	2.02
12-MR-S042A	1.62	4.16	1.3	3.58	3.39	8.8	7.35	11.3	1.67
12-MR-S043A	1.03	3.35	0.824	2.76	2.15	6.92	5.52	9	1.39
12-MR-S044A	1.36	3.75	1.11	3.24	2.87	7.92	5.99	9.2	1.54
12-MR-S045A	1.44	3.82	1.17	3.24	3.03	8.03	6.29	9.8	2.02
12-MR-S045A_D	1.56	3.86	1.26	3.31	3.22	8.16	6.54	9.9	2.08
12-MR-S046A	2.83	4.98	2.31	4.2	6.02	10.4	8.59	11.3	7.91
12-MR-S047A	2.46	5.08	2.1	4.41	5.33	10.9	10.8	15.1	4.49
12-MR-S048A	2.38	4.91	1.93	4.23	5.11	10.6	8.26	11.7	4.83
12-MR-S049A	1.51	3.83	1.23	3.27	3.18	8.14	5.21	9.5	1.43
12-MR-S050A	1.25	3.77	1.03	3.26	2.65	8.01	4.58	9.6	1.49
12-MR-S051A	1.69	4.31	1.34	3.65	3.46	9.11	6.29	11.5	2.72
12-MR-S052A	1.56	4.37	1.27	3.75	3.26	9.3	4.88	11.2	2
12-MR-S053A	1.59	4.2	1.3	3.62	3.3	8.9	5.44	10.6	1.69
12-MR-S053A_D	1.51	4.27	1.24	3.62	3.2	8.97	5.21	11	1.62
12-MR-S060A	4.93	8.52	4.73	7.99	11.6	19	9.06	15.5	2.91
12-MR-S060A_D	5.13	9.09	4.81	8.44	11.9	20.6	9.69	16.8	2.97
12-MR-S061A	6.29	9.91	5.91	9.13	14.6	22.1	10.8	17.8	3.88
12-MR-S063A	5.13	8.98	4.79	8.28	11.9	19.9	9.02	15.2	3.2
12-MR-S069A	1.25	4.3	1.03	3.66	2.65	9.02	5.02	10.8	0.85
12-MR-S070A	1.49	4.04	1.18	3.45	3.14	8.51	5.93	10.4	1.78
12-MR-S071A	1.82	4.48	1.52	3.84	3.9	9.45	5.98	11	2.09
12-MR-S072A	1.87	4.52	1.58	3.86	3.99	9.48	6.83	11.9	2.12
12-MR-S076A	1.39	4.04	1.13	3.38	2.91	8.46	4.78	9.5	1.59
12-MR-S077A	1.64	3.95	1.31	3.3	3.38	8.2	5.95	9.3	2.08
12-MR-S078A	3.13	5.82	2.68	4.91	6.85	12.5	8.17	13.3	4.46
12-MR-S079A	2.52	5.44	2.05	4.66	5.29	11.4	6.47	11.9	2.62
12-MR-S080A	2.07	4.79	1.69	4.01	4.2	10	7.14	12	1.72
12-MR-S086A	2.31	4.96	1.88	4.16	4.88	10.5	7.34	12.5	3.44
12-MR-S087A	2.95	6.37	2.47	5.53	6.23	13.6	7.69	13.9	2.76
12-TH-S103A	4.99	8.77	4.67	8.01	11.5	19.5	9.88	19.1	2.37
12-TH-S104A	6.29	9.81	6.08	9.05	14.8	22	10.2	18.5	6.84
12-TH-S105A	4.47	7.57	4.18	7.1	10.3	17.2	10.8	16.5	3.31

p: partial digest
t: total digest

Appendix B: Surficial Geochemistry

Sample_ID	Pb206_p_pp	Pb206_t_pp	Pb207_p_pp	Pb207_t_pp	Pb208_p_pp	Pb208_t_pp	Pr_p_ppm	Pr_t_ppm	Rb_p_ppm
12-TH-S106A	3.53	6.36	3.26	5.77	8.08	14.2	10.6	15.8	2.23
12-TH-S107A	2.31	5.65	2.05	5.12	5.19	12.3	8.26	15	1
12-TH-S110A	3.97	7.37	3.67	6.85	9.19	16.6	8.97	15.6	1.9
12-TH-S111A	2.01	5.18	1.77	4.54	4.54	11.1	6.89	13	1.38
12-TH-S112A	1.56	4.15	1.31	3.55	3.4	8.82	5.89	10	1.96
12-TH-S113A	1.85	4.38	1.55	3.77	4	9.2	6.75	11.4	1.72
12-TH-S114A	1.78	4.37	1.44	3.77	3.75	9.34	6.58	11.6	1.76
12-TH-S116A	4.9	8.82	4.72	8.18	11.5	20	8.26	15.9	2
12-TH-S117A	2.52	5.18	2.27	4.57	5.64	11.4	7.3	12.7	3.28
12-TH-S190A	1.38	3.75	1.11	3.19	2.91	7.97	6.12	9.7	2.14
12-TH-S191A	2.1	4.36	1.69	3.59	4.42	9.07	8	11.2	5.48
12-TH-S192A	1.15	3.5	0.916	2.94	2.42	7.4	4.94	9	1.68
12-TH-S193A	1.33	3.87	1.07	3.25	2.82	8.13	7.76	12.7	1.7
12-TH-S194A	2.31	5.07	2	4.46	5.22	11	9.24	13.5	2.19
12-TH-S195A	2.42	5.03	2.14	4.36	5.35	10.8	9.59	12.8	2.58
13-AB-244A	2.68	5.11	2.59	5.01	5.64	12.7	6.97	11.2	1.78
13-AB-245A	4.74	6.97	4.78	7.05	9.93	17.6	6.88	10.6	1.57
13-AB-246A	2.44	4.72	2.3	4.6	5	11.4	6.55	10.8	2.46
13-AB-246A_D	2.52	4.91	2.36	4.72	5.15	11.9	6.69	10.7	2.54
13-AB-247A	1.75	4.09	1.57	3.87	3.45	9.82	6.05	10.4	1.25
13-AB-248A	1.75	3.98	1.62	3.75	3.63	9.53	5.92	9.5	1.22
13-AB-249A	3.28	5.79	3.08	5.69	6.82	14.2	7.3	11	2.66
13-AB-250A	4.11	6.43	4.03	6.3	9.2	15.9	7.42	12.8	1.7
13-AB-252A	5.18	7.31	5.15	7.26	11.6	18.3	7.79	12.8	1.72
13-AB-253A	2.89	4.94	2.79	4.84	6.34	12.3	5.81	9.5	1.62
13-AB-254A	2.79	4.93	2.68	4.81	6.01	12	5.87	9.8	1.59
13-AB-S199A	2.07	4.22	1.76	3.87	4.14	10.1	6.43	10.4	1.83
13-AB-S200A	1.96	3.99	1.69	3.71	3.84	9.49	5.63	9.2	2.37
13-AB-S201A	1.62	4.05	1.4	3.67	3.18	9.44	5.13	9.2	2.4
13-AB-S202A	1.43	3.76	1.23	3.45	2.78	8.78	5.56	9.4	1.64
13-AB-S203A	2.02	4.4	1.72	3.97	3.93	10.3	7.08	11.1	4.15
13-AB-S204A	1.86	4.2	1.59	3.71	3.6	9.77	6.69	11.1	3.49
13-AB-S205A	2.04	4.1	1.74	3.68	3.85	9.63	6.96	11	4.22

p: partial digest

t: total digest

Appendix B: Surficial Geochemistry

Sample_ID	Pb206_p_pp	Pb206_t_pp	Pb207_p_pp	Pb207_t_pp	Pb208_p_pp	Pb208_t_pp	Pr_p_ppm	Pr_t_ppm	Rb_p_ppm
13-AB-S206A	2.04	4.31	1.81	4.05	4.13	10.3	6.02	10.7	1.69
13-AB-S207A	1.93	4.02	1.68	3.81	3.8	9.63	6.28	10.7	1.73
13-AB-S209A	2.42	4.17	2.16	3.84	4.81	9.93	6.45	9.9	5.59
13-AB-S210A	1.78	3.73	1.48	3.42	3.4	8.76	5.76	9.4	1.7
13-AB-S210A_D	1.74	3.79	1.44	3.46	3.36	9	5.64	9.7	1.6
13-AB-S211A	1.39	3.59	1.14	3.24	2.63	8.25	5.9	9.8	1.33
13-AB-S212A	1.96	4.14	1.69	3.77	3.76	9.64	6.52	10.1	2.86
13-AB-S213A	1.24	3.39	1.02	3.18	2.34	8.13	4.88	8.7	1.04
13-AB-S214A	2.34	4.8	2.06	4.44	4.7	11.4	7.26	12.3	3.81
13-AB-S215A	1.98	4.09	1.68	3.7	3.83	9.32	6.21	9.8	2.42
13-AB-S216A	1.69	3.76	1.37	3.38	3.2	8.9	6.75	12.1	1.46
13-AB-S217A	1.53	3.61	1.29	3.33	3.01	8.49	5.57	9.6	1.41
13-AB-S218A	2.16	4.48	1.86	4.17	4.21	10.7	7.34	12	1.7
13-AB-S228A	2.35	4.52	2.15	4.32	4.7	11.1	10.3	14.7	3.73
13-AB-S229A	1.7	3.84	1.52	3.65	3.42	9.29	5.46	9.7	1.96
13-AB-S230A	1.62	3.64	1.37	3.37	3.15	8.65	6.16	9.7	2.5
13-AB-S231A	1.25	3.12	1.03	2.89	2.46	7.51	6.01	9.1	2.14
13-AB-S232A	1.14	3.35	0.978	3.18	2.19	8.03	4.49	8	0.79
13-AB-S234A	1.63	3.55	1.4	3.4	3.25	8.72	6.03	10.1	1.65
13-AB-S235A	2.16	4.34	1.93	4.1	4.31	10.5	6.91	11.7	2.04
13-AB-S236A	3.24	5.33	3.14	5.16	6.82	13.3	6.09	10.3	2.03
13-AB-S237A	2.63	4.62	2.45	4.44	5.46	11.2	7.3	11.3	3.14
13-AB-S239A	3.98	5.56	3.76	5.49	8.33	13.9	8.21	11.4	5.18
13-AB-S240A	3.51	5.96	3.35	5.93	7.51	14.8	8.37	12.8	2.65

p: partial digest
t: total digest

Appendix B: Surficial Geochemistry

Sample_ID	Rb_t_ppm	Sb_p_ppm	Sc_p_ppm	Sc_t_ppm	Se_p_ppm	Sm_p_ppm	Sm_t_ppm	Sn_p_ppm	Sn_t_ppm	Sr_t_ppm
12-MR-S007A	71.6	0.02	0.6	3.1	0.05	3.02	6.5	0.16	1.07	278
12-MR-S008A	74.6	0.02	0.7	3.2	0.05	2.99	6.3	0.13	0.99	276
12-MR-S009A	64.5	0.02	0.5	3.1	0.05	2.71	6.8	0.11	1.12	277
12-MR-S010A	67.8	0.02	0.9	3.6	0.05	3.23	7	0.15	1.16	278
12-MR-S011A	69.7	0.05	1.6	4.8	0.05	3.54	7.4	0.19	1.27	295
12-MR-S012A	67.3	0.02	0.8	3.4	0.05	3.22	7.2	0.14	1.12	285
12-MR-S013A	79.3	0.04	2.4	5.7	0.05	3.78	8.2	0.21	1.44	315
12-MR-S014A	80.9	0.03	1.4	4.1	0.05	4	7.4	0.23	1.37	297
12-MR-S015A	66.8	0.02	0.8	3.3	0.05	3.1	6.5	0.13	1.2	278
12-MR-S016A	69	0.02	0.8	3.2	0.05	3.24	6.5	0.14	1.16	261
12-MR-S017A	73.2	0.02	1.2	3.4	0.05	3.97	7.3	0.22	1.17	275
12-MR-S018A	72.1	0.02	1	3.2	0.05	3.72	6.9	0.18	1.24	271
12-MR-S019A	70.7	0.01	0.8	3.3	0.05	3.35	7.1	0.13	1.33	273
12-MR-S020A	63.7	0.02	0.6	3.2	0.05	3.04	7.1	0.12	1.2	286
12-MR-S021A	74.9	0.02	1.8	3.6	0.05	4.23	7.4	0.22	1.28	278
12-MR-S022A	70	0.02	0.9	3.3	0.05	3.63	7.3	0.15	1.25	274
12-MR-S023A	86.4	0.02	1.6	4.2	0.05	3.89	7.6	0.23	1.35	280
12-MR-S024A	65.8	0.02	0.7	2.5	0.05	2.75	5.1	0.14	1.01	234
12-MR-S025A	70.7	0.02	0.8	2.7	0.05	3.14	5.7	0.17	1.06	253
12-MR-S026A	78.3	0.04	2.2	4.7	0.05	4.67	7.5	0.32	1.46	265
12-MR-S027A	78.8	0.02	1	3.4	0.05	3.62	6.8	0.16	1.18	287
12-MR-S028A	75.1	0.03	1.2	3.8	0.05	3.54	7	0.16	1.25	282
12-MR-S029A	73.6	0.02	0.8	3.4	0.05	3.67	7.3	0.17	1.26	277
12-MR-S030A	68.4	0.02	1	3.5	0.05	3.55	6.7	0.14	1.28	251
12-MR-S031A	84.5	0.02	1.6	4.3	0.05	3.79	7.3	0.18	1.33	274
12-MR-S032A	71.5	0.02	0.9	3.7	0.05	3.65	7.5	0.15	1.4	277
12-MR-S033A	67.4	0.02	0.8	3.1	0.05	3.1	6	0.13	1.14	262
12-MR-S034A	74.7	0.03	1.2	3.6	0.05	3.69	6.9	0.18	1.34	288
12-MR-S035A	57.2	0.01	0.4	2.6	0.05	2.47	5.7	0.1	1.22	232
12-MR-S036A	65.9	0.02	0.8	3	0.05	3.3	6.3	0.16	1.11	258
12-MR-S038A	63.8	0.02	0.7	3.1	0.05	2.78	6.1	0.12	1.08	253
12-MR-S039A	63.6	0.02	1.1	3.2	1	3.65	5.7	0.19	1.11	251
12-MR-S040A	70.5	0.03	1.7	4.2	1.6	4.33	7.1	0.25	1.03	241

p: partial digest
t: total digest

Appendix B: Surficial Geochemistry

Sample_ID	Rb_t_ppm	Sb_p_ppm	Sc_p_ppm	Sc_t_ppm	Se_p_ppm	Sm_p_ppm	Sm_t_ppm	Sn_p_ppm	Sn_t_ppm	Sr_t_ppm
12-MR-S041A	65	0.02	0.9	2.8	1	3.39	5.5	0.15	0.86	243
12-MR-S042A	63.7	0.02	0.9	3.3	1	4	6.4	0.21	1.19	256
12-MR-S043A	58.1	0.02	0.6	2.8	0.7	2.96	5.2	0.15	0.9	222
12-MR-S044A	63	0.02	0.7	2.8	0.8	3.14	5.4	0.19	0.96	237
12-MR-S045A	63.6	0.02	0.8	3.1	1	3.42	5.7	0.16	1.29	242
12-MR-S045A_D	64.4	0.02	0.8	3.1	0.8	3.35	5.8	0.18	1	251
12-MR-S046A	81.4	0.04	2.6	4.4	1.4	4.66	6.7	0.35	1.25	255
12-MR-S047A	80.9	0.02	1.7	4	1.6	5.88	8.6	0.22	1.16	262
12-MR-S048A	78.7	0.03	1.6	3.9	1.4	4.31	6.7	0.26	1.16	272
12-MR-S049A	63.8	0.01	0.5	2.8	0.05	2.71	5.5	0.1	0.93	246
12-MR-S050A	63	0.005	0.5	2.9	0.05	2.47	5.6	0.09	0.92	239
12-MR-S051A	72.6	0.02	1	3.9	0.05	3.45	6.8	0.12	1.14	248
12-MR-S052A	66.8	0.02	0.7	3.6	0.05	2.68	6.2	0.11	1.06	250
12-MR-S053A	64.5	0.01	0.6	3.2	0.05	2.79	6.2	0.09	1.05	254
12-MR-S053A_D	62.8	0.01	0.5	3.2	0.05	2.78	6.3	0.09	1.02	252
12-MR-S060A	80.7	0.02	0.8	3.4	0.05	4.2	9	0.18	1.35	416
12-MR-S060A_D	82.2	0.01	0.9	3.5	0.05	4.62	9.5	0.2	1.37	431
12-MR-S061A	89	0.02	1.1	3.8	0.05	4.89	9.8	0.23	1.44	426
12-MR-S063A	78.1	0.02	0.9	3.8	0.05	4.01	8.3	0.17	1.39	372
12-MR-S069A	61.1	0.01	0.4	2.7	0.05	2.66	6.4	0.12	1.19	254
12-MR-S070A	64.8	0.02	0.8	3	0.05	3.12	6	0.14	1.08	264
12-MR-S071A	68.1	0.02	0.8	3.5	0.05	3.23	6.4	0.14	1.23	256
12-MR-S072A	72.5	0.01	0.8	3.6	0.05	3.57	7.1	0.14	1.3	275
12-MR-S076A	67	0.02	0.5	3	0.05	2.56	5.6	0.13	1.32	237
12-MR-S077A	67.2	0.02	0.8	3.1	0.05	3.21	5.6	0.14	1.05	231
12-MR-S078A	82.9	0.03	1.4	4.1	0.05	4.16	7.4	0.24	1.32	328
12-MR-S079A	77	0.02	0.9	3.9	0.05	3.43	7	0.16	1.19	300
12-MR-S080A	71.2	0.02	0.8	3.9	0.05	3.92	7.2	0.14	1.2	288
12-MR-S086A	79.6	0.02	1.2	4	0.05	3.98	7.4	0.17	1.15	295
12-MR-S087A	106	0.01	0.7	3.7	0.05	3.74	8	0.18	1.35	372
12-TH-S103A	87.8	0.02	0.8	4.8	0.05	4.45	11.1	0.15	1.6	499
12-TH-S104A	92.2	0.01	1	4.6	0.05	4.75	10.6	0.19	1.45	445
12-TH-S105A	88.4	0.02	1.1	4	0.05	4.87	8.9	0.2	1.37	379

p: partial digest
t: total digest

Appendix B: Surficial Geochemistry

Sample_ID	Rb_t_ppm	Sb_p_ppm	Sc_p_ppm	Sc_t_ppm	Se_p_ppm	Sm_p_ppm	Sm_t_ppm	Sn_p_ppm	Sn_t_ppm	Sr_t_ppm
12-TH-S106A	75.6	0.02	1	3.7	0.05	4.95	8.3	0.18	1.25	340
12-TH-S107A	73.8	0.02	0.6	3.7	0.05	3.98	8.5	0.15	1.38	345
12-TH-S110A	78.2	0.02	0.8	4	0.05	4.3	8.5	0.19	1.34	369
12-TH-S111A	72.1	0.01	0.5	3.5	0.05	3.42	7.7	0.12	1.41	313
12-TH-S112A	72	0.01	0.7	3	0.05	2.98	5.7	0.13	1.1	260
12-TH-S113A	71	0.02	0.7	3.2	0.05	3.37	6.5	0.13	1.22	260
12-TH-S114A	71.3	0.03	0.7	3.4	0.05	3.36	6.8	0.15	1.15	267
12-TH-S116A	89.5	0.02	0.6	3.9	0.05	3.95	9.1	0.14	1.26	428
12-TH-S117A	76	0.02	1.1	4.1	0.05	3.65	6.8	0.17	1.28	297
12-TH-S190A	62.7	0.02	0.9	3.3	1	3.3	5.8	0.16	0.96	233
12-TH-S191A	78.9	0.03	1.8	4.1	1.3	4.17	6.5	0.25	1.14	271
12-TH-S192A	57.2	0.02	0.8	3.2	0.8	2.66	5.2	0.14	0.94	240
12-TH-S193A	62.3	0.03	0.9	3.3	1.2	4.05	7	0.17	1.02	269
12-TH-S194A	66.7	0.02	0.9	3.8	1.2	4.63	7.7	0.18	1.18	297
12-TH-S195A	67.5	0.03	1.1	3.6	1.2	4.73	7.2	0.16	1.02	287
13-AB-244A	77.8	0.02	0.7	3.8	0.05	3.55	7.1	0.15	1.08	265
13-AB-245A	80.3	0.01	0.7	3.1	0.05	3.35	6.6	0.15	1.02	270
13-AB-246A	80.2	0.02	0.9	3.7	0.05	3.36	6.7	0.17	1	271
13-AB-246A_D	79.8	0.02	0.9	3.8	0.05	3.42	6.7	0.17	1.08	274
13-AB-247A	70.8	0.02	0.5	3.4	0.05	3.08	6.6	0.13	1.07	273
13-AB-248A	64.6	0.02	0.6	3.2	0.05	3.02	6.3	0.14	1.03	256
13-AB-249A	84.1	0.02	1	3.8	0.05	3.59	6.7	0.19	1.22	270
13-AB-250A	76.2	0.06	0.6	3.8	0.05	3.46	8.1	0.18	1.24	344
13-AB-252A	76.2	0.04	0.7	3.5	0.05	3.55	7.9	0.13	1.1	318
13-AB-253A	74.4	0.03	0.5	3	0.05	2.9	6	0.11	0.87	281
13-AB-254A	74.1	0.03	0.5	3	0.05	2.94	6.2	0.13	0.97	283
13-AB-S199A	70.2	0.02	0.8	3.7	0.05	3.28	6.5	0.16	1.23	262
13-AB-S200A	76	0.02	0.7	3.3	0.05	2.84	5.9	0.18	1.06	256
13-AB-S201A	81.3	0.03	0.8	3.7	0.05	2.73	6	0.2	1.03	255
13-AB-S202A	78.1	0.02	0.7	3.2	0.05	2.85	5.8	0.15	0.95	265
13-AB-S203A	89.4	0.04	1.4	4.2	0.05	3.71	7	0.27	1.19	279
13-AB-S204A	87.1	0.03	1.2	4.3	0.05	3.48	7	0.2	1.1	269
13-AB-S205A	86.6	0.03	1.3	4.3	0.05	3.66	7	0.25	1.11	265

p: partial digest
t: total digest

Appendix B: Surficial Geochemistry

Sample_ID	Rb_t_ppm	Sb_p_ppm	Sc_p_ppm	Sc_t_ppm	Se_p_ppm	Sm_p_ppm	Sm_t_ppm	Sn_p_ppm	Sn_t_ppm	Sr_t_ppm
13-AB-S206A	74.2	0.03	0.8	3.7	0.05	3.19	7	0.17	1.03	296
13-AB-S207A	73.1	0.02	0.7	3.7	0.05	3.12	6.7	0.13	1	286
13-AB-S209A	79.8	0.04	1.9	4.5	0.05	3.46	6.5	0.23	1.08	265
13-AB-S210A	69.5	0.04	0.7	3.3	0.05	2.98	6.2	0.18	1.5	258
13-AB-S210A_D	71.5	0.02	0.7	3.4	0.05	2.87	6.4	0.17	1.01	265
13-AB-S211A	66.9	0.02	0.6	3.3	0.05	3.06	6.4	0.14	1.04	269
13-AB-S212A	78.3	0.02	1	3.7	0.05	3.32	6.7	0.17	0.97	275
13-AB-S213A	69.9	0.02	0.5	3.2	0.05	2.52	5.7	0.13	0.92	262
13-AB-S214A	100	0.03	1.2	4.4	0.05	3.79	7.7	0.24	1.27	325
13-AB-S215A	76.3	0.02	0.9	3.6	0.05	3.35	6.3	0.17	1.06	262
13-AB-S216A	64.8	0.02	0.7	3.8	0.05	3.39	7.9	0.16	1.25	275
13-AB-S217A	67.4	0.02	0.6	3.4	0.05	2.95	6.3	0.16	0.96	261
13-AB-S218A	78.5	0.02	0.7	3.8	0.05	3.6	7.6	0.18	1.14	296
13-AB-S228A	80.7	0.02	1.7	4.6	0.2	5.32	9.2	0.21	1.05	275
13-AB-S229A	73.1	0.02	0.8	3.6	0.05	2.85	6.2	0.24	1.06	251
13-AB-S230A	75.7	0.03	1	3.7	0.05	3.22	6.3	0.2	0.97	244
13-AB-S231A	63	0.03	1.1	3.6	0.05	3.24	6	0.18	0.94	235
13-AB-S232A	60.1	0.01	0.4	2.9	0.05	2.4	5.4	0.2	1.1	215
13-AB-S234A	68.6	0.03	0.8	3.3	0.05	3.11	6.4	0.2	0.97	240
13-AB-S235A	69	0.06	1.4	5.1	0.05	3.6	7.2	0.17	1.21	317
13-AB-S236A	71.6	0.02	0.8	3.7	0.05	3.07	6.6	0.16	1.04	293
13-AB-S237A	80.5	0.03	1.3	4.1	0.05	3.72	6.9	0.22	1.11	280
13-AB-S239A	87.3	0.04	1.8	4.3	0.05	3.95	7	0.23	1.06	300
13-AB-S240A	79.3	0.02	0.8	3.8	0.05	4	7.8	0.15	1.05	317

p: partial digest
t: total digest

Appendix B: Surficial Geochemistry

Sample_ID	Ta_p_ppm	Ta_t_ppm	Tb_p_ppm	Tb_t_ppm	Te_p_ppm	Th_p_ppm	Th_t_ppm	TiO2_t_pct	U_p_ppm	U_t_ppm
12-MR-S007A	0.005	0.83	0.2	0.56	0.01	6.14	11.1	0.443	1.14	2.14
12-MR-S008A	0.005	0.78	0.2	0.52	0.01	6.04	11.4	0.405	0.92	2.3
12-MR-S009A	0.005	0.83	0.19	0.59	0.005	5.06	11.1	0.482	0.76	2.6
12-MR-S010A	0.005	0.92	0.23	0.64	0.02	7.14	14.4	0.513	0.88	2.74
12-MR-S011A	0.005	0.94	0.26	0.63	0.01	7.54	15.5	0.601	0.83	2.79
12-MR-S012A	0.005	0.96	0.22	0.61	0.005	6.48	13.8	0.497	0.85	2.84
12-MR-S013A	0.005	1.02	0.29	0.74	0.02	9.02	18.8	0.608	1.05	3.27
12-MR-S014A	0.005	0.98	0.28	0.64	0.02	9.55	17	0.52	1.11	2.88
12-MR-S015A	0.005	0.88	0.21	0.57	0.01	6.35	14.9	0.484	0.92	2.94
12-MR-S016A	0.005	0.87	0.23	0.58	0.005	6.87	13.6	0.485	0.8	2.71
12-MR-S017A	0.005	0.95	0.27	0.72	0.01	9.22	15.3	0.499	0.93	2.76
12-MR-S018A	0.005	0.84	0.26	0.61	0.01	8.4	14.7	0.464	0.88	2.89
12-MR-S019A	0.005	0.83	0.22	0.57	0.005	6.66	15.7	0.464	0.79	2.94
12-MR-S020A	0.005	0.91	0.2	0.59	0.005	5.78	13.1	0.507	0.75	2.68
12-MR-S021A	0.005	0.95	0.31	0.62	0.02	11.5	17.7	0.518	1.07	2.99
12-MR-S022A	0.005	0.94	0.26	0.63	0.005	7.74	15.7	0.53	1.06	3.29
12-MR-S023A	0.005	0.86	0.27	0.69	0.02	10.9	21.5	0.454	0.89	2.91
12-MR-S024A	0.005	0.71	0.18	0.43	0.005	5.9	11.6	0.382	0.78	2.31
12-MR-S025A	0.005	0.77	0.21	0.48	0.005	7.8	14	0.406	0.84	2.38
12-MR-S026A	0.005	0.99	0.33	0.63	0.01	12.8	21.2	0.495	2.29	4.78
12-MR-S027A	0.005	0.84	0.25	0.59	0.02	8.64	15.8	0.466	0.84	2.63
12-MR-S028A	0.005	0.91	0.24	0.61	0.02	8.01	15.4	0.505	0.81	2.92
12-MR-S029A	0.005	0.94	0.24	0.64	0.01	7.07	15.3	0.52	1.06	3.42
12-MR-S030A	0.005	0.88	0.25	0.6	0.01	7.22	14.1	0.499	0.93	3.05
12-MR-S031A	0.005	0.89	0.27	0.66	0.02	9.25	18.1	0.482	1.14	3.19
12-MR-S032A	0.005	0.97	0.25	0.64	0.01	7.48	16.3	0.54	1.12	3.52
12-MR-S033A	0.005	0.72	0.21	0.5	0.01	6.04	12.4	0.44	0.96	2.64
12-MR-S034A	0.005	0.91	0.25	0.6	0.01	8.74	16.3	0.508	1.41	2.78
12-MR-S035A	0.005	0.82	0.17	0.51	0.005	4.51	10.3	0.478	0.59	2.86
12-MR-S036A	0.005	0.79	0.23	0.53	0.005	6.45	13	0.453	0.82	2.74
12-MR-S038A	0.005	0.83	0.2	0.54	0.005	5.35	12.5	0.476	0.77	2.85
12-MR-S039A	0.005	1	0.24	0.5	0.02	7.77	10.7	0.451	0.89	2.18
12-MR-S040A	0.005	0.86	0.3	0.59	0.02	8.11	15.6	0.412	2.25	4.09

p: partial digest
t: total digest

Appendix B: Surficial Geochemistry

Sample_ID	Ta_p_ppm	Ta_t_ppm	Tb_p_ppm	Tb_t_ppm	Te_p_ppm	Th_p_ppm	Th_t_ppm	TiO2_t_pct	U_p_ppm	U_t_ppm
12-MR-S041A	0.005	0.84	0.22	0.47	0.005	6.54	10.6	0.396	1	2.01
12-MR-S042A	0.005	1.07	0.28	0.58	0.005	6.76	11.1	0.493	0.89	2.46
12-MR-S043A	0.005	0.88	0.2	0.47	0.005	5.14	10.8	0.429	0.69	2.64
12-MR-S044A	0.005	0.96	0.21	0.48	0.005	5.47	9.15	0.426	0.72	2.39
12-MR-S045A	0.005	1.02	0.23	0.49	0.005	6.23	9.96	0.461	0.86	2.32
12-MR-S045A_D	0.005	1.03	0.23	0.5	0.01	6.33	10.8	0.478	0.88	2.34
12-MR-S046A	0.005	1.09	0.35	0.61	0.02	12.9	16.2	0.485	0.97	2.58
12-MR-S047A	0.005	0.89	0.39	0.69	0.01	11.2	18.4	0.415	1.98	3.65
12-MR-S048A	0.005	1.06	0.3	0.59	0.02	10.6	15.3	0.469	1.11	2.69
12-MR-S049A	0.005	0.92	0.18	0.48	0.005	5.19	9.94	0.437	0.72	2.08
12-MR-S050A	0.005	0.96	0.16	0.48	0.005	4.12	9.86	0.454	0.84	2.22
12-MR-S051A	0.005	1.1	0.23	0.59	0.005	6.83	13.1	0.492	0.93	2.49
12-MR-S052A	0.005	1.02	0.18	0.54	0.005	5.2	12.5	0.468	0.89	2.77
12-MR-S053A	0.005	1.01	0.18	0.56	0.005	5.27	11.4	0.479	0.77	2.56
12-MR-S053A_D	0.005	0.97	0.17	0.54	0.005	5.22	11.5	0.479	0.76	2.6
12-MR-S060A	0.005	0.79	0.25	0.71	0.005	9.73	16.9	0.506	1.12	3.33
12-MR-S060A_D	0.005	0.81	0.27	0.74	0.005	9.9	17.1	0.531	1.16	3.38
12-MR-S061A	0.005	0.83	0.29	0.74	0.01	12.8	21.5	0.537	1.05	3.17
12-MR-S063A	0.005	0.85	0.24	0.64	0.005	9.84	18.9	0.548	1.12	3.4
12-MR-S069A	0.005	0.93	0.18	0.55	0.005	5	12.7	0.51	0.66	2.97
12-MR-S070A	0.005	0.82	0.22	0.54	0.005	6.49	13.6	0.477	0.85	2.81
12-MR-S071A	0.005	0.9	0.24	0.6	0.005	6.34	11.5	0.495	0.77	2.39
12-MR-S072A	0.005	1.1	0.24	0.62	0.01	7.44	12.8	0.501	0.94	2.57
12-MR-S076A	0.005	0.87	0.18	0.54	0.005	4.86	9.84	0.47	0.68	2.46
12-MR-S077A	0.005	0.76	0.22	0.51	0.005	6.86	11	0.422	0.83	2.2
12-MR-S078A	0.005	1.01	0.29	0.65	0.02	13	20.4	0.479	1.24	2.81
12-MR-S079A	0.005	0.89	0.25	0.61	0.01	8.06	14.1	0.503	0.97	2.57
12-MR-S080A	0.005	0.93	0.29	0.65	0.01	7.42	12.1	0.526	1.13	2.72
12-MR-S086A	0.005	0.85	0.28	0.65	0.02	9.54	15.5	0.484	1.18	2.7
12-MR-S087A	0.005	0.86	0.24	0.65	0.02	8.78	14.6	0.467	1.09	2.69
12-TH-S103A	0.005	0.98	0.27	0.85	0.005	8.84	15.4	0.651	1.24	3.16
12-TH-S104A	0.005	0.95	0.27	0.8	0.01	8.77	15.2	0.656	1.26	3.24
12-TH-S105A	0.005	0.93	0.29	0.7	0.01	11.6	17.2	0.571	1.14	3.02

p: partial digest
t: total digest

Appendix B: Surficial Geochemistry

Sample_ID	Ta_p_ppm	Ta_t_ppm	Tb_p_ppm	Tb_t_ppm	Te_p_ppm	Th_p_ppm	Th_t_ppm	TiO2_t_pct	U_p_ppm	U_t_ppm
12-TH-S106A	0.005	0.88	0.28	0.65	0.005	9.22	14.9	0.532	1.44	3.05
12-TH-S107A	0.005	1.16	0.24	0.69	0.005	6.99	13.3	0.625	0.93	3.2
12-TH-S110A	0.005	0.99	0.26	0.65	0.01	9.41	15.4	0.626	1.13	3.18
12-TH-S111A	0.005	0.93	0.22	0.64	0.005	6.18	12	0.569	0.88	3.16
12-TH-S112A	0.005	0.79	0.2	0.49	0.005	5.88	10.8	0.454	0.86	2.31
12-TH-S113A	0.005	0.84	0.22	0.57	0.005	6.36	10.9	0.491	1.07	2.56
12-TH-S114A	0.005	0.88	0.22	0.56	0.005	6.5	11.6	0.514	1.28	2.88
12-TH-S116A	0.005	0.88	0.24	0.72	0.005	7.3	13.3	0.563	0.79	2.56
12-TH-S117A	0.005	0.92	0.24	0.6	0.01	7.41	13.2	0.554	0.8	2.26
12-TH-S190A	0.005	1	0.22	0.52	0.005	6.06	10.6	0.465	0.98	2.36
12-TH-S191A	0.005	1.09	0.3	0.53	0.02	10.2	14.6	0.484	1	2.25
12-TH-S192A	0.005	0.9	0.19	0.48	0.005	5.06	9.8	0.449	0.62	1.94
12-TH-S193A	0.005	1.16	0.26	0.56	0.005	7.06	12.7	0.543	0.86	2.52
12-TH-S194A	0.005	1.18	0.28	0.66	0.005	8.01	13.3	0.581	1.16	3.05
12-TH-S195A	0.005	1.02	0.29	0.58	0.005	8.28	12.8	0.503	1.36	2.88
13-AB-244A	0.005	0.91	0.24	0.54	0.01	8.04	12.6	0.536	0.99	2.59
13-AB-245A	0.005	0.8	0.22	0.48	0.01	8.52	12.1	0.455	0.87	2.1
13-AB-246A	0.005	0.87	0.24	0.51	0.005	8.56	13	0.524	1.03	2.3
13-AB-246A_D	0.005	0.85	0.23	0.54	0.005	8.49	13.3	0.53	1.06	2.49
13-AB-247A	0.005	1.01	0.21	0.53	0.005	6.62	10.8	0.572	0.82	2.63
13-AB-248A	0.005	0.86	0.21	0.48	0.005	6.54	10.3	0.535	0.77	2.26
13-AB-249A	0.005	0.92	0.24	0.53	0.005	9.44	13.9	0.516	1.17	2.78
13-AB-250A	0.005	0.96	0.23	0.58	0.005	7.47	12.7	0.599	0.86	2.82
13-AB-252A	0.005	0.93	0.24	0.55	0.005	8.11	13.6	0.56	0.98	2.74
13-AB-253A	0.005	0.78	0.2	0.45	0.005	6.22	10.2	0.471	0.72	2.28
13-AB-254A	0.005	0.75	0.2	0.46	0.005	6.18	10.4	0.479	0.82	2.26
13-AB-S199A	0.005	0.89	0.23	0.52	0.02	7.05	11.2	0.562	0.82	2.88
13-AB-S200A	0.005	0.84	0.2	0.44	0.02	7.56	12	0.491	0.86	2.52
13-AB-S201A	0.005	0.81	0.19	0.46	0.005	6.51	11.6	0.533	0.71	2.8
13-AB-S202A	0.005	0.83	0.19	0.42	0.02	6.92	10.8	0.485	0.74	3.38
13-AB-S203A	0.005	0.93	0.27	0.54	0.02	11	15.8	0.506	0.95	2.76
13-AB-S204A	0.005	0.96	0.27	0.56	0.02	8.84	14.9	0.571	0.89	2.9
13-AB-S205A	0.005	0.94	0.27	0.55	0.02	8.69	14	0.556	2.04	3.72

p: partial digest
t: total digest

Appendix B: Surficial Geochemistry

Sample_ID	Ta_p_ppm	Ta_t_ppm	Tb_p_ppm	Tb_t_ppm	Te_p_ppm	Th_p_ppm	Th_t_ppm	TiO2_t_pct	U_p_ppm	U_t_ppm
13-AB-S206A	0.005	0.92	0.23	0.53	0.02	7.87	12	0.57	0.9	2.46
13-AB-S207A	0.005	0.89	0.22	0.54	0.02	7.44	11.2	0.544	0.78	2.38
13-AB-S209A	0.005	0.8	0.26	0.5	0.02	9.61	14.8	0.52	1.14	2.76
13-AB-S210A	0.005	0.8	0.21	0.48	0.01	7.5	11	0.491	1.03	2.6
13-AB-S210A_D	0.005	0.84	0.21	0.49	0.005	7.38	11.4	0.504	1	2.55
13-AB-S211A	0.005	0.89	0.22	0.5	0.01	6.72	10.2	0.544	0.89	3.36
13-AB-S212A	0.005	0.87	0.25	0.52	0.01	8.3	12.5	0.507	1.05	2.49
13-AB-S213A	0.005	0.8	0.18	0.47	0.005	5.62	9.49	0.492	0.71	2.23
13-AB-S214A	0.005	1	0.27	0.57	0.02	11.1	16.9	0.553	0.9	2.6
13-AB-S215A	0.005	0.78	0.24	0.49	0.02	9.1	12.6	0.454	1	2.84
13-AB-S216A	0.005	0.96	0.25	0.59	0.01	7.47	13.7	0.598	1.02	3.04
13-AB-S217A	0.005	0.87	0.21	0.48	0.005	6.72	9.98	0.527	0.74	2.05
13-AB-S218A	0.005	0.95	0.26	0.56	0.01	8.45	12.8	0.555	0.94	2.41
13-AB-S228A	0.005	0.84	0.39	0.7	0.02	11	17.1	0.476	1.75	3.25
13-AB-S229A	0.005	0.83	0.2	0.47	0.005	7.28	11.9	0.486	0.96	2.27
13-AB-S230A	0.005	0.81	0.23	0.49	0.005	7.82	11.9	0.5	1.07	2.17
13-AB-S231A	0.005	0.75	0.24	0.47	0.005	6.66	10	0.493	1.88	2.87
13-AB-S232A	0.005	0.8	0.17	0.45	0.005	4.77	8.65	0.476	0.72	2.13
13-AB-S234A	0.005	0.77	0.22	0.49	0.005	7.68	11.2	0.482	0.87	2.07
13-AB-S235A	0.005	1.02	0.26	0.58	0.02	8.06	12.6	0.693	1	2.32
13-AB-S236A	0.005	0.87	0.22	0.51	0.01	7.82	12.1	0.545	0.78	2.02
13-AB-S237A	0.005	0.9	0.25	0.5	0.005	11.2	15.8	0.525	1.69	3.2
13-AB-S239A	0.005	0.81	0.28	0.52	0.02	13.6	16.6	0.508	1.08	2.16
13-AB-S240A	0.005	0.86	0.25	0.56	0.005	9.66	13.4	0.558	1.06	2.58

p: partial digest
t: total digest

Appendix B: Surficial Geochemistry

Sample_ID	V_p_ppm	V_t_ppm	W_p_ppm	W_t_ppm	Y_p_ppm	Y_t_ppm	Yb_p_ppm	Yb_t_ppm	Zn_p_ppm	Zn_t_ppm	Zr_p_ppm
12-MR-S007A	5.8	26.8	0.2	2	5.2	12.8	0.36	1.4	9.9	19	13.9
12-MR-S008A	6.5	25.3	0.2	1.9	5.1	12	0.34	1.38	11.7	19	6.68
12-MR-S009A	4.8	28.2	0.2	2.1	4.69	13.5	0.31	1.52	7.8	16	5.91
12-MR-S010A	7.9	32	0.3	2.6	6.03	14.9	0.44	1.71	13.6	21	7.21
12-MR-S011A	14.1	44.6	0.3	2.9	6.49	15.2	0.48	1.69	18.6	26	8.41
12-MR-S012A	7.5	30.7	0.3	4.4	5.57	14.2	0.39	1.63	11.5	19	6.5
12-MR-S013A	15	50.2	0.2	3.1	7.72	17.3	0.57	1.94	21.8	31	13
12-MR-S014A	10.7	35.4	0.3	2.5	6.98	15.1	0.49	1.61	18.3	26	10.6
12-MR-S015A	7.9	31.1	0.4	3.2	5.34	13	0.37	1.44	13.8	20	5.18
12-MR-S016A	6.4	28.2	0.3	2.3	6.18	14.2	0.42	1.53	11.8	18	6.97
12-MR-S017A	9.4	30.3	0.3	2.5	6.98	14.1	0.48	1.62	15.5	20	9.81
12-MR-S018A	9.3	29.7	0.3	2.1	6.16	13.8	0.42	1.51	14.9	21	7.84
12-MR-S019A	7.1	29.7	0.2	2.5	5.52	13.2	0.37	1.4	11.6	21	4.34
12-MR-S020A	6.5	30.5	0.2	2.5	4.87	13.4	0.33	1.54	9	16	3.1
12-MR-S021A	11.3	32.7	0.5	2.6	7.9	15	0.57	1.67	20.9	23	13
12-MR-S022A	7.6	29.9	0.2	2.4	6.07	14.6	0.41	1.55	13	22	5.44
12-MR-S023A	11.2	37	0.3	2.3	7.04	15.4	0.51	1.66	19.6	30	14.1
12-MR-S024A	7.1	22.6	0.2	1.7	4.57	10.4	0.3	1.1	12	17	4.32
12-MR-S025A	7.3	24.5	0.2	1.8	5.37	11.4	0.37	1.23	15.2	18	5.28
12-MR-S026A	18.7	42.4	0.2	2.4	8.26	15.2	0.59	1.56	29.4	35	15.1
12-MR-S027A	8.4	30	0.2	2.4	6.43	14.1	0.46	1.47	13.4	22	9.84
12-MR-S028A	9.4	33.3	0.2	2.2	6.33	14.6	0.45	1.54	15	23	8.47
12-MR-S029A	7.5	30.6	0.2	2.4	6.16	15	0.44	1.61	12.5	21	5.48
12-MR-S030A	8.9	32.4	0.2	4.8	6.53	15.3	0.47	1.64	15.2	23	6.42
12-MR-S031A	11.6	36.4	0.1	2.1	7.21	15.1	0.51	1.56	22.2	31	8.75
12-MR-S032A	8.4	34	0.2	2.2	6.1	15.3	0.41	1.61	14	23	4.37
12-MR-S033A	7.8	28.7	0.2	1.9	5.43	12.1	0.38	1.26	12.9	20	3.44
12-MR-S034A	10.3	33.4	0.2	2.2	6.43	13.8	0.45	1.49	17.1	23	8.81
12-MR-S035A	3.5	24.8	0.2	2.5	4.42	13.5	0.3	1.47	5.9	12	2.61
12-MR-S036A	7.4	27.7	0.2	1.8	5.73	12.6	0.4	1.38	12.7	20	4.5
12-MR-S038A	6.4	27.4	0.2	2.1	5.11	13.4	0.36	1.5	10.7	18	2.85
12-MR-S039A	12.7	27.7	0.2	2	5.89	11.9	0.41	1.3	15.9	23	7.84
12-MR-S040A	15.5	32.6	0.2	1.9	7.09	13.8	0.45	1.4	17.7	28	5.16

p: partial digest
t: total digest

Appendix B: Surficial Geochemistry

Sample_ID	V_p_ppm	V_t_ppm	W_p_ppm	W_t_ppm	Y_p_ppm	Y_t_ppm	Yb_p_ppm	Yb_t_ppm	Zn_p_ppm	Zn_t_ppm	Zr_p_ppm
12-MR-S041A	10.3	24.3	0.2	1.9	5.14	11	0.34	1.2	13.8	20	6.15
12-MR-S042A	10.5	26.7	0.3	2.2	6.52	14	0.44	1.49	11	19	8.51
12-MR-S043A	8.1	23	0.3	2.1	4.76	11.8	0.32	1.26	9.5	17	5.2
12-MR-S044A	9.6	24	0.2	2.3	5	11.7	0.33	1.23	10.5	17	5.16
12-MR-S045A	11	26.5	0.3	2.2	5.32	12	0.35	1.33	11.1	19	6.05
12-MR-S045A_D	11.1	26.8	0.3	2.3	5.41	12.3	0.36	1.34	12.2	20	6.26
12-MR-S046A	19	35.8	0.3	2.4	8.64	15	0.63	1.62	29.3	32	21.9
12-MR-S047A	15	32.1	0.3	2.1	9.2	16	0.61	1.53	20.6	30	7.17
12-MR-S048A	15.9	32.5	0.3	2	7.48	13.9	0.52	1.4	21	30	13.6
12-MR-S049A	4.8	24.7	0.2	2.1	4.52	12	0.3	1.24	9.7	18	4.86
12-MR-S050A	4.7	25.7	0.2	2.1	4.21	11.5	0.28	1.29	8.4	18	2.58
12-MR-S051A	7.1	30.9	0.2	2.4	6.48	14.4	0.45	1.55	13.1	25	7.52
12-MR-S052A	7	31.4	0.1	2.1	4.43	12.2	0.3	1.31	11.4	25	3.09
12-MR-S053A	5.5	27.9	0.2	2.1	4.65	13.1	0.31	1.46	9	19	3.21
12-MR-S053A_D	5.2	27.7	0.2	2.1	4.54	12.8	0.3	1.44	9	19	3.14
12-MR-S060A	8.8	33.6	0.2	1.5	6.06	14.6	0.39	1.46	13.9	24	8.36
12-MR-S060A_D	8.8	35.5	0.3	1.9	6.36	15.3	0.41	1.49	14.9	25	8.45
12-MR-S061A	9.5	36.4	0.2	1.8	7.26	16.1	0.48	1.49	21.2	32	11.4
12-MR-S063A	9.9	35.8	0.4	2.6	6.04	14.4	0.4	1.48	18.3	28	5.47
12-MR-S069A	3.8	25.4	0.2	2.2	4.3	13.4	0.28	1.5	7	15	2.68
12-MR-S070A	6.6	27.3	0.3	2.2	5.47	13.2	0.37	1.38	11.6	20	5.42
12-MR-S071A	6.3	28.4	0.2	2.2	5.96	15	0.42	1.61	11.3	18	6.31
12-MR-S072A	6.5	29.9	0.5	2.9	6.2	15.3	0.43	1.52	11.4	21	5.47
12-MR-S076A	6.1	26.6	0.2	2.1	4.36	12.8	0.3	1.42	9.4	17	2.51
12-MR-S077A	6.6	25.6	0.4	2.4	5.72	13.5	0.42	1.4	11.7	19	6.53
12-MR-S078A	10.9	33.6	0.2	2.4	7.22	15.3	0.54	1.71	20.4	29	15.4
12-MR-S079A	9.1	33.9	0.4	2.5	6.15	15	0.44	1.55	14.1	25	7.18
12-MR-S080A	7.3	31.9	0.3	2.7	7.46	16.5	0.5	1.69	11	20	5.7
12-MR-S086A	9.4	33.6	0.4	2.4	7.64	16.3	0.55	1.67	16.2	26	7.86
12-MR-S087A	8.7	33.3	0.3	2	5.81	15	0.38	1.41	13	26	5.2
12-TH-S103A	9.1	44.5	0.2	2.2	6.52	20	0.4	1.74	14.4	30	5.56
12-TH-S104A	11.5	42.9	0.2	2.3	6.34	17.6	0.4	1.63	22.6	35	5.18
12-TH-S105A	9.9	34.9	0.2	2.1	7.15	16.7	0.45	1.59	19.8	30	8.87

p: partial digest
t: total digest

Appendix B: Surficial Geochemistry

Sample_ID	V_p_ppm	V_t_ppm	W_p_ppm	W_t_ppm	Y_p_ppm	Y_t_ppm	Yb_p_ppm	Yb_t_ppm	Zn_p_ppm	Zn_t_ppm	Zr_p_ppm
12-TH-S106A	9.9	32	0.3	2.2	6.9	15.1	0.44	1.47	15.8	24	4.74
12-TH-S107A	5.5	30.6	0.2	2.8	5.8	17.1	0.36	1.74	9.7	18	4.34
12-TH-S110A	8.6	36.6	0.2	2.2	5.82	15.9	0.37	1.57	15.4	25	7.1
12-TH-S111A	4.5	28.4	0.2	2.3	5.54	16.1	0.36	1.66	8.8	19	4.5
12-TH-S112A	6.5	25.9	0.2	1.8	4.78	12.2	0.32	1.3	11.2	18	3.22
12-TH-S113A	6.7	27	0.4	2.3	5.7	14.6	0.38	1.48	10.7	19	3.61
12-TH-S114A	7.4	26.9	0.2	2.1	5.44	14.3	0.38	1.47	11.6	19	3.61
12-TH-S116A	7.3	35.3	0.2	2	5.55	15.7	0.35	1.47	13.1	26	4.87
12-TH-S117A	11.1	35.1	0.2	2.3	5.59	14.2	0.39	1.51	17	26	3.62
12-TH-S190A	11.6	29.1	0.2	2.2	5.31	12.5	0.37	1.35	13.4	20	4.73
12-TH-S191A	16.3	35	0.2	2.2	7.29	13.4	0.53	1.4	24.2	31	13.3
12-TH-S192A	10.9	27.9	0.2	2	4.4	11.4	0.3	1.24	11	19	4.93
12-TH-S193A	11.1	29.7	0.2	2.3	5.85	13.9	0.39	1.5	11.1	18	6.72
12-TH-S194A	11.4	32.7	0.2	2.4	6.26	15.3	0.38	1.59	13.1	21	7.31
12-TH-S195A	12.8	30.3	0.2	2.2	6.28	13.4	0.39	1.38	15	22	7.15
13-AB-244A	7.3	28.5	0.2	1.5	6.25	15.3	0.39	1.52	15	26	9.54
13-AB-245A	7	24.7	0.2	1.3	5.38	12.6	0.34	1.2	18.3	30	9.31
13-AB-246A	8.1	29	0.2	1.5	6.21	14.1	0.41	1.4	18.7	30	10.2
13-AB-246A_D	8.2	29.2	0.2	1.5	6.24	14.2	0.4	1.42	19	31	10.5
13-AB-247A	5.6	27.5	0.2	1.6	5.55	14.5	0.34	1.52	9.6	19	7.53
13-AB-248A	5.6	25.4	0.2	1.5	5.57	13.4	0.34	1.41	10.7	20	7.5
13-AB-249A	9.2	29.7	0.2	1.5	6.15	13.9	0.4	1.39	21.2	33	10.2
13-AB-250A	8.3	35	0.2	1.4	5.71	15.8	0.36	1.49	12.2	24	7.4
13-AB-252A	7.3	32	0.1	1.6	5.84	14.8	0.38	1.48	13.8	26	8.51
13-AB-253A	5.7	25.4	0.1	1.2	4.82	12.6	0.3	1.27	12.8	22	6.08
13-AB-254A	5.4	25.2	0.1	1.2	4.74	12.3	0.3	1.2	11.2	21	5.59
13-AB-S199A	8.6	32.6	0.1	1.5	6.03	14.9	0.38	1.44	13.3	23	8.06
13-AB-S200A	8.6	29.4	0.2	1.4	4.94	12.8	0.31	1.29	16.1	25	6.7
13-AB-S201A	8.8	31.4	0.2	1.6	5.05	12.8	0.33	1.28	14.5	26	6.88
13-AB-S202A	7.3	26.4	0.1	1.3	4.79	11.7	0.32	1.18	14.6	24	7.56
13-AB-S203A	11.9	33	0.2	1.8	7.46	14.8	0.51	1.51	18	28	19
13-AB-S204A	10.3	34.5	0.2	1.8	7.11	16.4	0.49	1.59	18.1	30	13.8
13-AB-S205A	10.9	33.5	0.2	1.6	7.18	15.6	0.49	1.49	22.1	32	12.2

p: partial digest
t: total digest

Appendix B: Surficial Geochemistry

Sample_ID	V_p_ppm	V_t_ppm	W_p_ppm	W_t_ppm	Y_p_ppm	Y_t_ppm	Yb_p_ppm	Yb_t_ppm	Zn_p_ppm	Zn_t_ppm	Zr_p_ppm
13-AB-S206A	8.7	33.2	0.2	2.9	5.97	14.6	0.39	1.45	12.6	23	11
13-AB-S207A	7.5	32.4	0.1	1.5	5.83	14.6	0.38	1.42	13.4	24	8.48
13-AB-S209A	14.2	38.3	0.2	1.3	7.68	14.9	0.53	1.42	23.5	31	16.3
13-AB-S210A	7.9	28.2	0.2	2.1	5.73	13.7	0.38	1.38	12.6	22	10.9
13-AB-S210A_D	7.4	28.5	0.2	1.8	5.55	13.8	0.38	1.35	11.7	24	10.8
13-AB-S211A	6.2	28.9	0.1	1.3	5.89	14.4	0.39	1.41	8.4	17	10.1
13-AB-S212A	10	33	0.2	1.4	6.65	14.2	0.44	1.38	17.9	27	9.9
13-AB-S213A	5.4	26.5	0.1	1.2	4.88	13.3	0.33	1.33	9.1	18	7.42
13-AB-S214A	10.1	37.6	0.05	1.5	7.16	15.4	0.48	1.5	18.8	33	17
13-AB-S215A	8.6	29.1	0.1	1.2	6.27	13.5	0.45	1.31	15	25	14.6
13-AB-S216A	7	33.7	0.2	3.7	6.35	16.2	0.42	1.62	10.3	21	9.89
13-AB-S217A	6	27.5	0.2	1.5	5.36	14	0.35	1.42	9.6	20	8.14
13-AB-S218A	7.7	31.5	0.2	1.6	6.6	14.9	0.43	1.44	11	23	11.3
13-AB-S228A	9.7	31.5	0.2	1.5	10.6	18.6	0.69	1.67	18.5	30	9.85
13-AB-S229A	7.9	27.2	0.2	1.5	5.2	12.7	0.35	1.32	15.6	26	9.09
13-AB-S230A	8.6	28.2	0.1	1.3	6.24	14	0.41	1.44	21.4	30	9.26
13-AB-S231A	9.4	25	0.2	1.2	5.85	13	0.38	1.33	13.8	21	7.38
13-AB-S232A	3.8	23.2	0.2	1.5	4.57	13.5	0.3	1.46	8.6	16	5.49
13-AB-S234A	7.1	25	0.1	1.2	5.67	13.4	0.36	1.35	11.3	21	10.5
13-AB-S235A	14.5	47.3	0.1	1.7	6.68	15.6	0.44	1.63	17.8	29	8.89
13-AB-S236A	8.1	30.8	0.2	1.3	5.51	13.4	0.36	1.35	13.2	23	8.78
13-AB-S237A	12.3	33.3	0.1	1.3	6.21	13.8	0.41	1.43	28.4	39	12.7
13-AB-S239A	13.6	35.7	0.1	1.3	7.28	13.8	0.5	1.4	28.5	36	17.9
13-AB-S240A	7.4	31.9	0.1	1.2	6.52	15.4	0.4	1.49	12.6	24	12.8

p: partial digest
t: total digest

Appendix B: Surficial Geochemistry

Sample_ID	Zr_t_ppm
12-MR-S007A	217
12-MR-S008A	206
12-MR-S009A	331
12-MR-S010A	324
12-MR-S011A	272
12-MR-S012A	309
12-MR-S013A	297
12-MR-S014A	312
12-MR-S015A	269
12-MR-S016A	304
12-MR-S017A	289
12-MR-S018A	276
12-MR-S019A	255
12-MR-S020A	299
12-MR-S021A	327
12-MR-S022A	304
12-MR-S023A	279
12-MR-S024A	197
12-MR-S025A	220
12-MR-S026A	249
12-MR-S027A	250
12-MR-S028A	282
12-MR-S029A	302
12-MR-S030A	351
12-MR-S031A	253
12-MR-S032A	342
12-MR-S033A	222
12-MR-S034A	266
12-MR-S035A	387
12-MR-S036A	294
12-MR-S038A	312
12-MR-S039A	255
12-MR-S040A	194

p: partial digest
t: total digest

Appendix B: Surficial Geochemistry

Sample_ID	Zr_t_ppm
12-MR-S041A	201
12-MR-S042A	281
12-MR-S043A	283
12-MR-S044A	254
12-MR-S045A	267
12-MR-S045A_D	272
12-MR-S046A	303
12-MR-S047A	206
12-MR-S048A	252
12-MR-S049A	259
12-MR-S050A	255
12-MR-S051A	250
12-MR-S052A	225
12-MR-S053A	301
12-MR-S053A_D	298
12-MR-S060A	366
12-MR-S060A_D	361
12-MR-S061A	354
12-MR-S063A	321
12-MR-S069A	383
12-MR-S070A	323
12-MR-S071A	339
12-MR-S072A	345
12-MR-S076A	321
12-MR-S077A	294
12-MR-S078A	281
12-MR-S079A	299
12-MR-S080A	332
12-MR-S086A	288
12-MR-S087A	283
12-TH-S103A	424
12-TH-S104A	387
12-TH-S105A	360

p: partial digest
t: total digest

Appendix B: Surficial Geochemistry

Sample_ID	Zr_t_ppm
12-TH-S106A	303
12-TH-S107A	491
12-TH-S110A	376
12-TH-S111A	377
12-TH-S112A	263
12-TH-S113A	346
12-TH-S114A	346
12-TH-S116A	316
12-TH-S117A	274
12-TH-S190A	266
12-TH-S191A	231
12-TH-S192A	261
12-TH-S193A	284
12-TH-S194A	356
12-TH-S195A	272
13-AB-244A	329
13-AB-245A	244
13-AB-246A	282
13-AB-246A_D	303
13-AB-247A	342
13-AB-248A	329
13-AB-249A	273
13-AB-250A	383
13-AB-252A	317
13-AB-253A	297
13-AB-254A	275
13-AB-S199A	301
13-AB-S200A	280
13-AB-S201A	256
13-AB-S202A	196
13-AB-S203A	257
13-AB-S204A	287
13-AB-S205A	254

p: partial digest
t: total digest

Appendix B: Surficial Geochemistry

Sample_ID	Zr_t_ppm
13-AB-S206A	279
13-AB-S207A	292
13-AB-S209A	267
13-AB-S210A	289
13-AB-S210A_D	295
13-AB-S211A	329
13-AB-S212A	263
13-AB-S213A	318
13-AB-S214A	243
13-AB-S215A	238
13-AB-S216A	405
13-AB-S217A	330
13-AB-S218A	284
13-AB-S228A	273
13-AB-S229A	246
13-AB-S230A	276
13-AB-S231A	278
13-AB-S232A	416
13-AB-S234A	289
13-AB-S235A	284
13-AB-S236A	300
13-AB-S237A	273
13-AB-S239A	254
13-AB-S240A	380

p: partial digest
t: total digest

Appendix C: Whole Rock PCA Results

Rock Type	Alt_type	Major Oxides										Transition Metals, Total Digest							
		PC-1	PC-2	PC-3	PC-4	PC-5	PC-6	PC-7	PC-8	PC-1	PC-2	PC-3	PC-4	PC-5	PC-6	PC-7	PC-8		
1 Archean Gneiss	Altered	-2.37	2.14	-1.80	-0.77	0.41	-1.05	0.01	-0.03	-2.37	2.14	-1.80	-0.77	0.41	-1.05	0.01	-0.03		
2 Archean Gneiss	Altered	-0.32	-2.58	1.14	-0.16	0.17	0.27	1.43	0.27	-0.32	-2.58	1.14	-0.16	0.17	0.27	1.43	0.27		
3 Archean Gneiss	Altered	1.31	-0.61	0.00	-1.33	0.52	0.29	1.71	-0.70	1.31	-0.61	0.00	-1.33	0.52	0.29	1.71	-0.70		
4 Archean Gneiss	Altered	-2.35	-0.71	-1.24	-0.92	0.13	0.29	0.31	-0.03	-2.35	-0.71	-1.24	-0.92	0.13	0.29	0.31	-0.03		
5 Archean Gneiss	Altered	2.37	-5.68	-1.55	-0.16	0.39	-0.11	1.34	0.61	2.37	-5.68	-1.55	-0.16	0.39	-0.11	1.34	0.61		
6 Hornblende Syenite	Altered	2.00	-3.03	1.25	-0.29	-0.48	0.11	-0.07	0.87	2.00	-3.03	1.25	-0.29	-0.48	0.11	-0.07	0.87		
7 Hornblende Syenite	Altered	-5.16	-1.08	0.37	-0.52	-0.12	0.02	-0.18	0.54	-5.16	-1.08	0.37	-0.52	-0.12	0.02	-0.18	0.54		
8 Hornblende Syenite	Altered	-1.19	-1.03	-1.54	-0.50	-0.82	-0.27	-0.57	1.14	-1.19	-1.03	-1.54	-0.50	-0.82	-0.27	-0.57	1.14		
9 Hornblende Syenite	Altered	-2.13	1.38	-1.00	-0.15	-0.73	0.26	-0.16	-0.07	-2.13	1.38	-1.00	-0.15	-0.73	0.26	-0.16	-0.07		
10 Hornblende Syenite	Altered	-4.89	-3.23	4.77	-0.04	0.99	-0.70	-0.49	1.32	-4.89	-3.23	4.77	-0.04	0.99	-0.70	-0.49	1.32		
11 Hornblende Syenite	Altered	-6.72	-1.28	3.06	0.47	1.16	-0.35	-1.08	0.73	-6.72	-1.28	3.06	0.47	1.16	-0.35	-1.08	0.73		
12 Hornblende Syenite	Altered	-0.12	-3.59	1.73	0.39	0.78	-0.17	0.41	0.11	-0.12	-3.59	1.73	0.39	0.78	-0.17	0.41	0.11		
13 Pegmatite	Altered	-1.22	-1.87	-1.60	0.51	-1.46	1.27	-0.37	-0.76	-1.22	-1.87	-1.60	0.51	-1.46	1.27	-0.37	-0.76		
14 Pegmatite	Altered	-1.22	-2.30	-3.14	0.36	-0.83	0.78	1.06	-1.27	-1.22	-2.30	-3.14	0.36	-0.83	0.78	1.06	-1.27		
15 Pegmatite	Altered	0.31	-3.86	-4.32	0.49	-1.03	0.64	0.03	-0.03	0.31	-3.86	-4.32	0.49	-1.03	0.64	0.03	-0.03		
16 Pegmatite	Altered	2.00	-4.41	-4.54	-0.32	-1.01	1.00	0.80	-0.17	2.00	-4.41	-4.54	-0.32	-1.01	1.00	0.80	-0.17		
17 Quartz Syenite	Altered	-5.76	-1.24	1.72	1.03	-0.69	-0.78	-0.26	1.38	-5.76	-1.24	1.72	1.03	-0.69	-0.78	-0.26	1.38		
18 Quartz Syenite	Altered	-0.73	-3.49	-0.79	-0.15	0.34	-0.46	0.34	-0.02	-0.73	-3.49	-0.79	-0.15	0.34	-0.46	0.34	-0.02		
19 Quartz Syenite	Altered	-0.24	1.09	-0.90	2.60	0.09	0.37	-0.29	0.60	-0.24	1.09	-0.90	2.60	0.09	0.37	-0.29	0.60		
20 Quartz Syenite	Altered	1.54	-1.56	-0.76	-0.26	-1.09	0.17	0.51	0.45	1.54	-1.56	-0.76	-0.26	-1.09	0.17	0.51	0.45		
21 Quartz Syenite	Altered	1.37	-1.15	-1.85	-0.54	-0.48	-0.63	0.88	0.96	1.37	-1.15	-1.85	-0.54	-0.48	-0.63	0.88	0.96		
22 Thelon Formation	Altered	0.66	1.05	0.90	-0.13	-0.44	0.54	0.34	-0.29	0.66	1.05	0.90	-0.13	-0.44	0.54	0.34	-0.29		
23 Thelon Formation	Altered	-0.25	0.05	0.73	-0.60	-0.42	0.39	0.62	-0.09	-0.25	0.05	0.73	-0.60	-0.42	0.39	0.62	-0.09		
24 Thelon Formation	Altered	0.81	0.02	1.80	0.27	-1.29	-0.38	0.10	-0.04	0.81	0.02	1.80	0.27	-1.29	-0.38	0.10	-0.04		
25 Thelon Formation	Altered	0.08	0.09	0.00	-0.08	-1.42	1.09	-0.51	-0.25	0.08	0.09	0.00	-0.08	-1.42	1.09	-0.51	-0.25		
26 Thelon Formation	Altered	-0.47	1.44	-0.43	-0.46	-1.15	0.76	0.38	-0.04	-0.47	1.44	-0.43	-0.46	-1.15	0.76	0.38	-0.04		
27 Thelon Formation	Altered	0.30	1.00	-1.21	-0.23	-0.76	0.87	0.04	-0.06	0.30	1.00	-1.21	-0.23	-0.76	0.87	0.04	-0.06		
28 Woodburn Lake Group	Altered	-0.75	-1.50	2.05	0.45	0.89	-0.23	0.90	0.19	-0.75	-1.50	2.05	0.45	0.89	-0.23	0.90	0.19		
29 Woodburn Lake Group	Altered	-0.23	0.31	0.82	0.99	0.88	0.03	-0.60	0.07	-0.23	0.31	0.82	0.99	0.88	0.03	-0.60	0.07		
30 Woodburn Lake Group	Altered	-5.17	-2.29	2.06	-1.23	1.41	-1.23	-1.03	0.36	-5.17	-2.29	2.06	-1.23	1.41	-1.23	-1.03	0.36		
31 Woodburn Lake Group	Altered	-3.22	-1.09	-1.17	-0.82	-1.72	-0.29	-0.20	0.87	-3.22	-1.09	-1.17	-0.82	-1.72	-0.29	-0.20	0.87		
32 Woodburn Lake Group	Altered	-1.85	-1.67	1.87	0.54	0.55	-2.51	-0.84	1.34	-1.85	-1.67	1.87	0.54	0.55	-2.51	-0.84	1.34		

Appendix C: Whole Rock PCA Results

	Rock Type	Alt_type	Major Oxides									Transition Metals, Total Digest							
			PC-1	PC-2	PC-3	PC-4	PC-5	PC-6	PC-7	PC-8	PC-1	PC-2	PC-3	PC-4	PC-5	PC-6	PC-7	PC-8	
33	Woodburn Lake Group	Altered	-1.79	1.41	0.83	-0.18	1.88	-1.47	0.15	0.21	-1.79	1.41	0.83	-0.18	1.88	-1.47	0.15	0.21	
34	Woodburn Lake Group	Altered	-6.38	-2.49	4.29	0.69	2.45	-1.43	-2.80	1.89	-6.38	-2.49	4.29	0.69	2.45	-1.43	-2.80	1.89	
35	Woodburn Lake Group	Altered	1.54	5.09	-0.82	2.71	0.49	1.26	0.96	0.57	1.54	5.09	-0.82	2.71	0.49	1.26	0.96	0.57	
36	Woodburn Lake Group	Altered	-2.59	-0.16	2.19	-0.75	3.22	-0.31	0.04	0.04	-2.59	-0.16	2.19	-0.75	3.22	-0.31	0.04	0.04	
37	Woodburn Lake Group	Altered	0.17	-3.32	-2.85	-0.29	0.61	0.50	0.05	0.34	0.17	-3.32	-2.85	-0.29	0.61	0.50	0.05	0.34	
38	Archean Gneiss	Fresh	1.49	-0.82	0.41	-0.50	-1.05	-1.98	-0.39	-0.14	1.49	-0.82	0.41	-0.50	-1.05	-1.98	-0.39	-0.14	
39	Archean Gneiss	Fresh	-0.15	2.13	-0.62	-1.26	0.54	-0.07	-0.41	0.03	-0.15	2.13	-0.62	-1.26	0.54	-0.07	-0.41	0.03	
40	Archean Gneiss	Fresh	1.66	0.94	-1.87	0.52	1.35	0.82	0.01	0.08	1.66	0.94	-1.87	0.52	1.35	0.82	0.01	0.08	
41	Archean Gneiss	Fresh	-1.99	0.95	-0.68	-1.60	1.61	0.02	-0.95	-0.34	-1.99	0.95	-0.68	-1.60	1.61	0.02	-0.95	-0.34	
42	Archean Gneiss	Fresh	-3.87	1.61	-0.93	-2.27	0.92	-0.12	-1.04	-0.23	-3.87	1.61	-0.93	-2.27	0.92	-0.12	-1.04	-0.23	
43	Archean Gneiss	Fresh	2.74	-2.75	-1.29	0.44	0.47	0.90	-0.38	-0.80	2.74	-2.75	-1.29	0.44	0.47	0.90	-0.38	-0.80	
44	Hornblende Syenite	Fresh	-1.69	0.01	0.53	0.60	0.08	0.26	-0.29	0.30	-1.69	0.01	0.53	0.60	0.08	0.26	-0.29	0.30	
45	Hornblende Syenite	Fresh	-1.30	-1.16	1.03	0.66	0.52	0.37	-0.07	-0.03	-1.30	-1.16	1.03	0.66	0.52	0.37	-0.07	-0.03	
46	Hornblende Syenite	Fresh	-0.39	0.65	-0.19	0.55	-0.44	0.46	-0.28	0.14	-0.39	0.65	-0.19	0.55	-0.44	0.46	-0.28	0.14	
47	Hornblende Syenite	Fresh	-2.07	0.44	0.18	0.40	-0.21	0.41	-0.81	0.27	-2.07	0.44	0.18	0.40	-0.21	0.41	-0.81	0.27	
48	Hornblende Syenite	Fresh	0.77	0.84	-0.39	0.01	-0.01	-0.38	-0.28	-0.07	0.77	0.84	-0.39	0.01	-0.01	-0.38	-0.28	-0.07	
49	Hornblende Syenite	Fresh	-0.95	0.50	0.21	0.02	0.06	-0.03	-0.56	-0.20	-0.95	0.50	0.21	0.02	0.06	-0.03	-0.56	-0.20	
50	Pegmatite	Fresh	0.12	-6.79	0.17	2.11	0.89	1.03	1.67	-0.64	0.12	-6.79	0.17	2.11	0.89	1.03	1.67	-0.64	
51	Pegmatite	Fresh	0.82	-6.27	1.44	2.13	1.24	1.28	1.13	-0.56	0.82	-6.27	1.44	2.13	1.24	1.28	1.13	-0.56	
52	Pegmatite	Fresh	2.96	-6.04	0.79	1.60	0.22	2.22	-0.13	-0.36	2.96	-6.04	0.79	1.60	0.22	2.22	-0.13	-0.36	
53	Pegmatite	Fresh	1.71	-7.18	1.23	2.58	0.60	1.73	0.56	-0.52	1.71	-7.18	1.23	2.58	0.60	1.73	0.56	-0.52	
54	Pegmatite	Fresh	2.92	-4.28	-1.57	2.74	0.87	1.36	0.33	-0.51	2.92	-4.28	-1.57	2.74	0.87	1.36	0.33	-0.51	
55	Pegmatite	Fresh	2.39	-6.13	1.01	1.07	-1.95	1.22	0.65	0.40	2.39	-6.13	1.01	1.07	-1.95	1.22	0.65	0.40	
56	Quartz Syenite	Fresh	2.69	-2.15	0.25	-0.83	-0.84	-0.09	-0.19	-0.05	2.69	-2.15	0.25	-0.83	-0.84	-0.09	-0.19	-0.05	
57	Quartz Syenite	Fresh	2.70	-1.95	-0.34	-0.61	-0.25	-0.08	-0.56	-0.13	2.70	-1.95	-0.34	-0.61	-0.25	-0.08	-0.56	-0.13	
58	Quartz Syenite	Fresh	2.22	-0.64	-0.37	0.69	-0.04	0.37	0.03	-0.24	2.22	-0.64	-0.37	0.69	-0.04	0.37	0.03	-0.24	
59	Quartz Syenite	Fresh	3.48	-1.68	-0.38	-0.51	-0.41	0.09	-0.18	-0.08	3.48	-1.68	-0.38	-0.51	-0.41	0.09	-0.18	-0.08	
60	Quartz Syenite	Fresh	2.50	-1.67	-0.71	-1.02	0.15	0.42	-0.55	-0.02	2.50	-1.67	-0.71	-1.02	0.15	0.42	-0.55	-0.02	
61	Quartz Syenite	Fresh	3.50	-0.53	-0.63	-0.01	-0.68	0.19	-0.45	-0.03	3.50	-0.53	-0.63	-0.01	-0.68	0.19	-0.45	-0.03	
62	Quartz Syenite	Fresh	3.52	-1.03	-1.55	0.13	-0.92	0.22	-0.24	-0.11	3.52	-1.03	-1.55	0.13	-0.92	0.22	-0.24	-0.11	
63	Thelon Formation	Fresh	0.39	-0.51	1.77	1.06	-1.45	0.53	0.28	-0.10	0.39	-0.51	1.77	1.06	-1.45	0.53	0.28	-0.10	
64	Thelon Formation	Fresh	0.18	-0.80	0.58	0.65	-0.91	0.82	0.46	-0.03	0.18	-0.80	0.58	0.65	-0.91	0.82	0.46	-0.03	

Appendix C: Whole Rock PCA Results

	Rock Type	Alt_type	Major Oxides								Transition Metals, Total Digest									
				PC-1	PC-2	PC-3	PC-4	PC-5	PC-6	PC-7	PC-8		PC-1	PC-2	PC-3	PC-4	PC-5	PC-6	PC-7	PC-8
65	Thelon Formation	Fresh		1.71	0.18	-0.75	0.58	-1.75	0.19	0.37	-0.42		1.71	0.18	-0.75	0.58	-1.75	0.19	0.37	-0.42
66	Thelon Formation	Fresh		1.03	-0.77	2.35	0.47	-0.53	0.12	0.66	-0.36		1.03	-0.77	2.35	0.47	-0.53	0.12	0.66	-0.36
67	Woodburn Lake Group	Fresh		0.44	2.37	-0.67	0.64	0.38	-0.13	0.45	-0.14		0.44	2.37	-0.67	0.64	0.38	-0.13	0.45	-0.14
68	Woodburn Lake Group	Fresh		1.08	2.20	-1.04	0.63	0.56	0.48	0.35	-0.13		1.08	2.20	-1.04	0.63	0.56	0.48	0.35	-0.13
69	Woodburn Lake Group	Fresh		0.43	1.77	-0.54	0.27	0.91	-0.05	-0.18	0.11		0.43	1.77	-0.54	0.27	0.91	-0.05	-0.18	0.11
70	Woodburn Lake Group	Fresh		2.03	2.31	-0.32	1.32	-0.60	-0.64	0.43	0.06		2.03	2.31	-0.32	1.32	-0.60	-0.64	0.43	0.06
71	Woodburn Lake Group	Fresh		2.87	2.26	-0.41	0.46	-0.84	-0.30	0.87	-0.40		2.87	2.26	-0.41	0.46	-0.84	-0.30	0.87	-0.40
72	Woodburn Lake Group	Fresh		2.46	1.66	0.79	1.25	-1.17	-0.99	0.42	0.01		2.46	1.66	0.79	1.25	-1.17	-0.99	0.42	0.01
73	Woodburn Lake Group	Fresh		2.64	2.24	-1.89	0.52	-0.53	-0.93	-0.65	0.01		2.64	2.24	-1.89	0.52	-0.53	-0.93	-0.65	0.01
74	Woodburn Lake Group	Fresh		-0.89	2.84	-0.53	0.23	0.53	-0.16	0.23	-0.08		-0.89	2.84	-0.53	0.23	0.53	-0.16	0.23	-0.08
		Loadings	K2O_t_pct	-0.91	0.91	-0.28	-0.15	-0.07	-0.10	0.08	0.03	Sc_t_ppm	-0.52	-0.59	-0.23	0.39	0.39	-0.13	0.07	-0.15
			Al2O3_t_pct	-0.18	0.16	0.51	0.36	-0.16	-0.11	0.06	-0.09	V_t_ppm	0.24	-0.08	0.50	-0.27	0.51	0.03	0.08	0.23
			MgO_t_pct	0.06	-0.32	0.11	-0.12	0.47	-0.18	0.10	0.01	Cr_t_ppm	-0.52	0.40	0.73	-0.03	-0.13	0.05	-0.13	-0.22
			Fe2O3_t_pct	0.63	0.08	0.10	-0.16	-0.06	0.41	0.14	0.02	Co_t_ppm	0.17	0.45	-0.39	0.08	0.13	-0.13	-0.52	0.07
			Na2O_t_pct	0.78	0.54	-0.24	0.38	0.19	0.06	-0.12	0.01	Ni_t_ppm	-0.86	0.20	-0.34	-0.29	-0.24	-0.13	0.20	0.19
			P2O5_t_pct	-0.65	-0.43	-0.24	-0.09	0.03	0.15	-0.08	-0.18	Cu_t_ppm	0.32	0.56	-0.13	0.50	-0.03	0.30	0.29	0.05
			MnO_t_pct	0.85	0.09	0.15	-0.42	-0.17	-0.20	-0.12	-0.02	Zn_t_ppm	0.55	0.07	-0.37	-0.51	0.05	0.01	0.15	-0.27
			CaO_t_pct	0.25	-0.75	-0.38	0.20	-0.24	-0.14	0.08	0.07	Y_t_ppm	0.04	-0.71	-0.04	-0.06	-0.30	0.43	-0.20	0.06
			TiO2_t_pct	-0.83	-0.27	0.27	0.02	0.01	0.13	-0.14	0.15	Mo_t_ppm	0.60	-0.29	0.27	0.19	-0.38	-0.43	0.07	0.05

Appendix C: Whole Rock PCA Results

	Rock Type	Alt_type	Transition Metals, Partial Digest							Alteration Elements, Total Digest									
			PC-1	PC-2	PC-3	PC-4	PC-5	PC-6	PC-7	PC-1	PC-2	PC-3	PC-4	PC-5	PC-6	PC-7	PC-8		
1	Archean Gneiss	Altered	2.38	-2.64	1.87	-1.46	-0.21	0.22	-0.71			-0.05	3.30	1.72	0.27	0.24	-0.09	-0.20	0.17
2	Archean Gneiss	Altered	-5.21	-0.79	-0.73	1.22	-0.81	0.31	0.03			1.39	1.03	0.14	1.57	0.13	-0.15	0.01	-0.22
3	Archean Gneiss	Altered	-2.88	-0.43	1.63	0.83	-1.09	0.67	0.28			0.38	1.50	1.36	0.75	2.57	0.43	-0.17	-0.02
4	Archean Gneiss	Altered	-3.46	-1.31	-0.07	0.28	-0.79	0.12	0.07			2.34	2.65	1.93	0.60	-0.43	0.59	0.05	0.08
5	Archean Gneiss	Altered	-5.38	-0.55	-0.76	0.41	-0.66	0.10	-0.12			4.02	-1.82	2.00	2.73	0.54	-0.99	-0.43	-0.37
6	Hornblende Syenite	Altered	-2.79	0.15	0.38	2.03	-0.13	-0.29	0.07			3.53	-0.78	-0.53	0.73	-0.41	-0.46	0.53	-0.58
7	Hornblende Syenite	Altered	1.71	-2.54	-1.39	-0.69	0.82	0.18	0.01			-1.47	2.18	0.33	0.48	-2.40	0.00	-0.03	0.13
8	Hornblende Syenite	Altered	0.94	-1.81	0.24	0.88	0.93	-0.24	0.07			1.35	1.52	1.40	0.52	-1.08	-0.96	0.13	-0.24
9	Hornblende Syenite	Altered	2.82	-0.35	0.21	-1.05	0.59	0.61	-0.09			-0.55	1.30	0.65	-1.12	-1.07	0.21	-0.27	0.16
10	Hornblende Syenite	Altered	-1.03	-2.53	-0.72	2.48	-0.69	-0.68	0.30			-1.17	2.66	-2.85	2.81	-2.55	-0.27	0.77	-0.32
11	Hornblende Syenite	Altered	1.46	-3.16	-1.54	-0.04	-0.55	-0.37	0.22			-1.41	3.01	-2.12	2.01	-3.45	0.60	0.44	0.10
12	Hornblende Syenite	Altered	-2.92	-0.86	-0.96	1.40	-0.75	0.11	0.12			2.71	-0.56	-0.78	2.34	-0.46	0.06	0.63	0.00
13	Pegmatite	Altered	-2.99	-0.23	0.21	-1.38	0.60	0.39	0.30			4.57	1.83	0.82	0.04	-0.28	0.70	0.09	0.51
14	Pegmatite	Altered	-5.38	0.73	-2.24	-1.45	1.02	1.29	-0.06			5.68	1.60	2.40	0.31	0.29	0.73	-0.77	0.58
15	Pegmatite	Altered	-4.38	-0.12	-1.84	-2.81	2.07	-0.28	-0.54			6.94	0.21	3.08	1.23	-0.44	-0.24	-0.42	0.21
16	Pegmatite	Altered	-4.18	0.12	-2.28	-1.95	1.51	-0.10	-0.36			7.55	-1.44	3.97	0.51	-0.01	-0.02	-0.45	0.01
17	Quartz Syenite	Altered	0.65	-1.40	-2.27	0.92	0.57	0.13	0.15			0.65	3.78	-1.29	1.61	-3.34	-1.04	0.53	-0.01
18	Quartz Syenite	Altered	0.12	-0.36	1.19	0.38	0.27	0.19	-0.09			3.20	-1.53	0.96	1.02	-1.18	-0.10	-0.16	0.06
19	Quartz Syenite	Altered	3.68	3.32	-2.26	-0.28	1.04	-0.35	-0.06			4.94	0.15	0.02	1.19	-2.39	0.32	0.91	0.06
20	Quartz Syenite	Altered	-1.87	0.19	0.66	2.19	-0.23	0.23	0.41			4.62	-0.54	0.94	-0.61	-0.64	-0.33	0.09	-0.41
21	Quartz Syenite	Altered	-1.64	-1.31	0.46	1.76	-0.18	0.06	-0.13			5.59	-0.38	2.46	0.25	-0.83	-0.83	0.58	-0.44
22	Thelon Formation	Altered	0.90	1.50	-0.45	0.68	-0.21	0.05	0.13			1.68	1.27	-0.48	-0.80	0.32	0.69	0.18	-0.15
23	Thelon Formation	Altered	0.77	1.24	0.27	0.49	0.69	0.05	0.21			0.74	1.86	-0.03	-0.35	0.39	0.33	-0.13	-0.19
24	Thelon Formation	Altered	0.12	1.13	-1.07	0.49	0.37	-0.65	0.03			2.42	1.41	-1.78	-0.71	0.29	-0.38	0.26	-0.18
25	Thelon Formation	Altered	0.67	1.26	-0.57	-0.19	0.99	-0.39	0.36			2.12	1.68	-0.31	-1.11	-0.01	0.58	0.04	-0.02
26	Thelon Formation	Altered	1.89	1.34	-0.43	-0.56	1.29	0.21	0.10			1.39	2.73	0.74	-1.04	0.22	0.35	0.12	-0.07
27	Thelon Formation	Altered	0.75	1.57	-0.93	-1.10	0.79	0.12	0.07			2.75	2.06	1.20	-0.49	0.25	0.57	0.24	-0.05
28	Woodburn Lake Group	Altered	-0.71	0.69	-0.15	1.92	-0.92	-0.22	-0.01			-0.78	1.44	-1.23	2.09	0.32	-0.11	-0.25	-0.17
29	Woodburn Lake Group	Altered	2.17	-0.44	-0.90	-0.22	-0.54	-1.21	0.08			-0.83	1.43	-1.39	1.51	0.21	0.35	-0.41	-0.09
30	Woodburn Lake Group	Altered	-2.77	-2.20	-0.97	1.13	1.07	0.08	-0.29			-2.09	3.62	-1.09	2.28	-0.84	0.09	-0.24	0.02
31	Woodburn Lake Group	Altered	0.11	-1.88	-1.05	0.58	1.23	-0.22	-0.11			0.65	3.25	1.14	-0.28	-1.23	-1.11	-0.27	-0.09
32	Woodburn Lake Group	Altered	-1.02	-1.21	-1.09	2.96	0.46	-1.26	-0.64			-1.48	1.96	-2.23	2.57	-0.64	-2.00	-0.30	-0.35

Appendix C: Whole Rock PCA Results

	Rock Type	Alt_type	Transition Metals, Partial Digest							Alteration Elements, Total Digest							
			PC-1	PC-2	PC-3	PC-4	PC-5	PC-6	PC-7	PC-1	PC-2	PC-3	PC-4	PC-5	PC-6	PC-7	PC-8
33	Woodburn Lake Group	Altered	4.28	-0.10	1.03	-0.09	0.67	0.17	-0.46	-1.97	2.46	-0.20	2.12	0.52	-0.12	0.15	0.03
34	Woodburn Lake Group	Altered	1.77	-3.26	-0.89	0.43	-0.19	-1.71	-0.09	-1.53	4.07	-3.33	5.02	-3.17	-0.14	1.29	-0.16
35	Woodburn Lake Group	Altered	6.98	4.45	-3.12	-0.41	0.61	0.89	0.43	1.25	2.27	0.69	1.66	0.13	0.47	1.41	0.07
36	Woodburn Lake Group	Altered	-0.97	-1.90	0.28	0.43	-0.76	0.53	-0.19	-1.80	2.27	-0.18	3.30	0.17	1.35	0.73	0.04
37	Woodburn Lake Group	Altered	-1.69	-1.61	-0.93	-0.89	0.80	0.53	0.10	6.00	-0.60	3.22	2.10	-0.85	0.38	0.69	0.07
38	Archean Gneiss	Fresh	0.55	-0.71	2.48	1.22	0.13	-0.46	-0.53	-0.60	-1.74	-1.14	-0.87	0.76	-1.66	-0.12	0.07
39	Archean Gneiss	Fresh	3.82	-0.96	2.11	-0.44	-0.79	0.03	0.06	-3.79	-0.95	0.95	-0.94	-0.02	0.26	0.11	0.02
40	Archean Gneiss	Fresh	4.01	1.85	0.37	-0.77	-0.82	0.51	0.06	-3.81	-2.95	1.38	1.02	0.19	0.30	-0.19	0.12
41	Archean Gneiss	Fresh	4.63	-0.78	1.90	-1.23	-0.17	0.27	0.08	-6.59	-1.18	0.96	0.05	-0.07	0.74	-0.36	0.31
42	Archean Gneiss	Fresh	4.46	-2.53	1.96	-0.84	-0.51	0.04	0.00	-5.94	0.48	1.63	-0.65	-0.66	0.66	0.12	0.45
43	Archean Gneiss	Fresh	-2.20	0.60	0.86	-1.71	-0.81	0.17	0.01	1.26	-2.98	0.56	1.32	1.14	0.54	0.00	0.36
44	Hornblende Syenite	Fresh	0.85	-1.65	-1.15	-0.36	-0.70	-0.32	-0.12	-2.69	-0.30	-0.71	0.40	-1.32	-0.07	-0.11	0.10
45	Hornblende Syenite	Fresh	-0.47	-1.15	-0.66	0.06	-1.28	-0.15	0.07	-1.19	-0.72	-0.92	0.93	-1.11	0.36	-0.02	0.14
46	Hornblende Syenite	Fresh	1.91	-0.24	-2.12	-0.23	-0.70	-0.19	0.10	-2.87	-1.40	-0.30	-0.42	-0.93	-0.22	0.02	0.18
47	Hornblende Syenite	Fresh	1.70	-1.90	-1.04	-0.68	-0.95	-0.45	0.01	-3.31	0.11	-0.61	0.06	-1.30	-0.04	-0.05	0.20
48	Hornblende Syenite	Fresh	1.89	0.16	1.29	0.23	0.08	-0.22	-0.11	-1.06	-0.75	0.00	-0.11	0.28	-0.27	0.12	0.11
49	Hornblende Syenite	Fresh	1.25	-1.81	0.21	-1.03	-1.03	-0.20	-0.10	-1.96	-0.19	-0.50	-0.14	-0.39	0.16	-0.03	0.21
50	Pegmatite	Fresh	-5.22	0.28	0.17	-1.63	0.16	0.30	-0.03	3.41	-3.22	0.35	4.33	-0.47	0.10	0.68	0.76
51	Pegmatite	Fresh	-4.40	0.86	-0.57	-1.19	0.52	0.39	0.17	3.75	-2.78	-0.76	4.30	-0.33	0.65	0.83	0.51
52	Pegmatite	Fresh	-5.14	0.58	-0.83	-1.76	0.52	-0.29	0.08	6.15	-3.18	-0.32	3.25	-0.08	1.00	1.70	0.38
53	Pegmatite	Fresh	-6.64	1.06	-1.54	-1.15	0.55	-0.12	-0.01	6.10	-3.75	-0.93	4.11	-0.83	0.72	1.31	0.56
54	Pegmatite	Fresh	-2.75	1.81	-1.13	-1.22	-1.00	0.20	0.22	3.72	-4.44	0.41	3.21	-0.23	0.43	0.25	0.49
55	Pegmatite	Fresh	-5.49	-0.55	-0.33	0.87	1.51	-0.53	0.11	7.28	-2.25	-0.15	1.81	-0.72	-0.79	2.06	0.19
56	Quartz Syenite	Fresh	-2.02	-0.77	2.18	0.26	0.15	-0.52	-0.14	2.42	-2.91	-0.06	-0.97	0.07	-0.29	0.37	-0.19
57	Quartz Syenite	Fresh	-0.77	0.24	2.05	-0.05	0.32	-0.39	0.01	2.23	-3.26	0.26	-0.39	0.09	-0.05	0.47	-0.06
58	Quartz Syenite	Fresh	1.00	1.27	0.68	-0.66	0.90	0.03	0.03	1.68	-2.10	-0.18	-0.01	0.00	0.23	-0.07	-0.04
59	Quartz Syenite	Fresh	-1.19	0.26	1.84	-0.21	0.43	-0.35	-0.11	2.23	-3.69	0.38	-0.62	0.24	-0.15	0.48	-0.14
60	Quartz Syenite	Fresh	-0.39	-0.27	1.67	-1.01	0.02	-0.20	0.04	1.06	-2.91	0.83	-0.37	0.17	0.33	0.12	-0.20
61	Quartz Syenite	Fresh	-0.36	0.94	1.23	-0.19	0.49	-0.19	-0.02	2.26	-2.52	0.05	-0.80	0.40	-0.14	0.24	-0.18
62	Quartz Syenite	Fresh	-0.96	0.70	1.63	-0.19	0.71	-0.26	-0.07	6.20	-2.45	1.10	-0.71	-0.11	0.06	0.81	-0.07
63	Thelon Formation	Fresh	-0.45	1.07	-1.77	0.40	0.51	-0.29	-0.12	2.33	0.87	-1.98	-0.64	-0.46	-0.01	0.05	-0.11
64	Thelon Formation	Fresh	-1.77	0.97	-1.79	0.07	0.29	0.13	-0.15	1.91	0.84	-0.71	-0.28	-0.41	0.23	-0.35	-0.18

Appendix C: Whole Rock PCA Results

Rock Type	Alt_type	Transition Metals, Partial Digest								Alteration Elements, Total Digest								
		PC-1	PC-2	PC-3	PC-4	PC-5	PC-6	PC-7	PC-1	PC-2	PC-3	PC-4	PC-5	PC-6	PC-7	PC-8		
65 Thelon Formation	Fresh	0.64	1.01	-0.14	1.09	0.51	-0.12	-0.34		3.42	0.07	-0.29	-1.71	0.20	-0.18	-0.60	-0.11	
66 Thelon Formation	Fresh	-0.21	1.59	0.77	2.03	0.07	0.07	0.13		1.45	-0.52	-2.13	-0.82	-0.17	0.29	-0.39	-0.28	
67 Woodburn Lake Group	Fresh	2.73	1.01	0.02	0.40	-0.86	0.36	-0.23		-3.05	-0.26	0.28	0.30	0.57	-0.24	-0.01	0.24	
68 Woodburn Lake Group	Fresh	2.87	1.16	-0.12	-0.50	-0.87	0.39	0.01		-2.85	-1.05	0.63	0.19	0.42	0.18	-0.08	0.15	
69 Woodburn Lake Group	Fresh	2.98	0.75	0.15	-0.13	-0.60	0.04	0.00		-1.99	0.25	0.30	0.79	0.43	0.16	-0.01	0.01	
70 Woodburn Lake Group	Fresh	2.09	1.90	-0.27	1.02	-0.42	0.11	-0.17		-0.29	-0.43	-0.63	-0.25	0.58	-0.91	0.08	0.03	
71 Woodburn Lake Group	Fresh	2.26	2.21	1.00	0.34	0.15	0.84	-0.31		-1.58	-0.25	-0.28	-0.83	1.98	-0.78	-0.30	0.04	
72 Woodburn Lake Group	Fresh	2.49	1.08	-0.76	0.63	-0.62	0.08	0.02		-0.21	-1.26	-1.58	-0.71	0.55	-1.33	0.39	0.06	
73 Woodburn Lake Group	Fresh	3.56	0.08	1.68	-1.09	0.13	-0.16	-0.09		1.05	-0.07	0.33	-0.47	1.14	-0.77	-0.11	-0.01	
74 Woodburn Lake Group	Fresh	2.02	-0.35	-0.75	-0.74	-0.95	0.34	-0.43		-2.46	1.97	0.24	0.13	0.44	0.19	-0.47	0.04	
	Loadings	Sc_p_ppm	-0.71	-0.22	-0.41	-0.20	-0.37	0.05	-0.17	Ni_t_ppm	-0.45	0.62	0.56	-0.20	-0.30	-0.30	0.00	0.01
		V_p_ppm	0.26	-0.07	0.34	0.39	-0.50	-0.04	0.14	Sc_t_ppm	-0.10	-0.20	0.01	0.65	-0.10	0.01	-0.17	0.15
		Co_p_ppm	0.69	0.14	0.07	-0.35	0.02	-0.40	-0.09	Cr_t_ppm	-0.50	0.44	-0.65	-0.34	0.02	0.21	0.07	0.09
		Ni_p_ppm	0.70	-0.76	-0.19	0.20	0.24	0.14	-0.04	Mo_t_ppm	0.34	-0.25	-0.47	-0.07	0.22	-0.50	-0.01	-0.02
		Cu_p_ppm	0.48	0.71	-0.49	-0.05	0.01	0.22	0.08	Zn_t_ppm	-0.06	-0.34	0.50	-0.33	0.59	0.13	-0.05	0.04
		Zn_p_ppm	-0.15	0.07	0.72	-0.38	0.10	0.26	-0.04	Sr_t_ppm	0.04	-0.76	-0.04	-0.37	-0.50	0.13	-0.11	-0.06
		Y_p_ppm	-0.73	-0.22	-0.15	-0.20	0.22	-0.14	0.25	U_t_ppm	0.83	-0.01	0.16	0.11	-0.14	0.09	0.33	0.04
		Mo_p_ppm	-0.54	0.35	0.11	0.59	0.27	-0.10	-0.13	B_t_ppm	0.68	0.67	-0.05	0.11	0.08	0.17	-0.21	-0.11
										V_t_ppm	-0.78	-0.17	-0.02	0.44	0.11	0.06	0.15	-0.15

Appendix C: Whole Rock PCA Results

	Rock Type	Alt_type	Alteration Elements, Partial Digest				
			PC-1	PC-2	PC-3	PC-4	PC-5
1	Archean Gneiss	Altered	-2.80	1.67	1.03	1.27	-0.36
2	Archean Gneiss	Altered	2.25	-1.66	-1.44	0.73	-0.23
3	Archean Gneiss	Altered	-0.02	-1.71	0.20	0.41	0.47
4	Archean Gneiss	Altered	1.73	-0.71	-0.84	1.13	0.14
5	Archean Gneiss	Altered	1.85	-2.02	-1.23	1.15	-0.55
6	Hornblende Syenite	Altered	2.04	-1.65	-0.57	-1.07	0.05
7	Hornblende Syenite	Altered	-0.68	3.18	-0.24	0.73	-0.34
8	Hornblende Syenite	Altered	-0.21	1.66	0.21	-0.98	-0.10
9	Hornblende Syenite	Altered	-1.77	1.60	1.24	0.49	-0.20
10	Hornblende Syenite	Altered	-0.38	0.30	-2.41	-0.96	0.18
11	Hornblende Syenite	Altered	-0.85	2.55	-1.84	0.97	0.28
12	Hornblende Syenite	Altered	2.28	-0.55	-1.55	0.34	0.17
13	Pegmatite	Altered	2.29	-0.09	1.23	1.36	0.07
14	Pegmatite	Altered	4.54	-0.18	0.62	2.22	-0.85
15	Pegmatite	Altered	5.30	0.57	1.09	2.17	-1.27
16	Pegmatite	Altered	4.87	0.28	0.31	1.89	-1.05
17	Quartz Syenite	Altered	1.51	2.30	-1.18	-0.11	-0.08
18	Quartz Syenite	Altered	0.35	0.10	0.91	-0.32	0.09
19	Quartz Syenite	Altered	3.81	0.86	0.36	-0.45	0.27
20	Quartz Syenite	Altered	0.91	-1.24	-0.21	-1.24	0.39
21	Quartz Syenite	Altered	2.55	0.22	-0.46	-0.50	0.28
22	Thelon Formation	Altered	0.53	-0.76	-0.16	-0.38	0.21
23	Thelon Formation	Altered	1.13	-0.17	0.95	-0.84	0.22
24	Thelon Formation	Altered	2.17	-0.45	-0.46	-0.46	0.01
25	Thelon Formation	Altered	1.63	0.11	0.69	-0.50	0.18
26	Thelon Formation	Altered	1.11	0.91	1.42	-0.32	-0.05
27	Thelon Formation	Altered	1.90	0.30	0.91	0.58	-0.01
28	Woodburn Lake Group	Altered	-0.01	-1.82	-1.28	-0.79	0.04
29	Woodburn Lake Group	Altered	-1.32	0.09	-1.39	0.18	0.10
30	Woodburn Lake Group	Altered	1.29	0.95	-0.59	-0.36	-1.01
31	Woodburn Lake Group	Altered	-0.08	1.76	-0.34	-0.57	-0.74
32	Woodburn Lake Group	Altered	0.72	-0.53	-2.18	-2.09	-1.08

Appendix C: Whole Rock PCA Results

	Rock Type	Alt_type	Alteration Elements, Partial Digest				
			PC-1	PC-2	PC-3	PC-4	PC-5
33	Woodburn Lake Group	Altered	-0.52	1.76	1.41	-0.56	0.04
34	Woodburn Lake Group	Altered	0.63	2.19	-2.00	-0.02	0.30
35	Woodburn Lake Group	Altered	0.65	1.68	0.50	-0.28	0.58
36	Woodburn Lake Group	Altered	0.99	0.77	-0.48	0.96	0.24
37	Woodburn Lake Group	Altered	3.50	2.14	0.49	1.39	0.13
38	Archean Gneiss	Fresh	-0.41	-0.65	0.83	-1.29	-0.14
39	Archean Gneiss	Fresh	-3.53	0.65	0.82	0.16	0.63
40	Archean Gneiss	Fresh	-3.64	-0.66	0.58	0.44	0.16
41	Archean Gneiss	Fresh	-3.58	1.46	1.57	0.39	0.50
42	Archean Gneiss	Fresh	-3.70	2.25	0.82	0.51	0.60
43	Archean Gneiss	Fresh	-0.82	-2.13	0.58	1.86	-0.14
44	Hornblende Syenite	Fresh	-2.19	0.60	-1.53	1.00	-0.39
45	Hornblende Syenite	Fresh	-2.07	-0.63	-1.63	1.01	-0.12
46	Hornblende Syenite	Fresh	-1.83	0.51	-1.72	0.81	-0.19
47	Hornblende Syenite	Fresh	-3.16	0.80	-1.62	1.20	-0.20
48	Hornblende Syenite	Fresh	-1.29	-0.23	0.77	-0.61	0.06
49	Hornblende Syenite	Fresh	-2.83	0.44	-0.69	1.44	-0.03
50	Pegmatite	Fresh	3.60	-1.51	0.90	2.05	-0.20
51	Pegmatite	Fresh	3.72	-1.12	0.81	1.49	-0.17
52	Pegmatite	Fresh	4.95	-1.24	0.46	1.94	-0.15
53	Pegmatite	Fresh	6.09	-1.85	-0.01	1.82	-0.43
54	Pegmatite	Fresh	1.17	-2.37	-0.55	1.96	0.00
55	Pegmatite	Fresh	6.04	-0.44	0.35	-0.50	-0.19
56	Quartz Syenite	Fresh	0.52	-1.26	0.89	-0.34	-0.03
57	Quartz Syenite	Fresh	0.39	-1.17	1.36	-0.43	0.15
58	Quartz Syenite	Fresh	-0.24	-0.35	1.58	-0.29	-0.19
59	Quartz Syenite	Fresh	0.65	-1.23	1.35	-0.26	-0.06
60	Quartz Syenite	Fresh	-0.99	-0.78	1.19	0.53	0.03
61	Quartz Syenite	Fresh	0.11	-1.19	1.25	-0.37	-0.12
62	Quartz Syenite	Fresh	2.35	-0.76	1.67	-0.33	0.21
63	Thelon Formation	Fresh	1.95	-0.33	-0.65	-0.16	-0.45
64	Thelon Formation	Fresh	1.68	-0.77	-0.62	0.48	-0.66

Appendix C: Whole Rock PCA Results

	Rock Type	Alt_type	Alteration Elements, Partial Digest					
				PC-1	PC-2	PC-3	PC-4	PC-5
65	Thelon Formation	Fresh		0.76	-0.52	0.13	-1.03	-0.42
66	Thelon Formation	Fresh		0.83	-1.58	0.32	-1.69	0.21
67	Woodburn Lake Group	Fresh		-2.80	-0.72	-0.32	-0.03	-0.18
68	Woodburn Lake Group	Fresh		-2.87	-0.53	-0.05	0.59	0.05
69	Woodburn Lake Group	Fresh		-2.33	-0.24	-0.03	0.08	0.13
70	Woodburn Lake Group	Fresh		-1.56	-1.29	-0.32	-0.80	-0.24
71	Woodburn Lake Group	Fresh		-2.29	-1.18	1.40	-0.71	-0.46
72	Woodburn Lake Group	Fresh		-2.13	-0.52	-0.76	-0.29	-0.08
73	Woodburn Lake Group	Fresh		-3.10	0.30	1.46	0.01	0.05
74	Woodburn Lake Group	Fresh		-3.26	0.03	-0.83	1.27	-0.61
		Loadings	Ni_p_ppm	-0.37	0.91	-0.09	-0.16	-0.09
			Sc_p_ppm	0.00	-0.22	-0.47	0.50	-0.18
			Mo_p_ppm	0.45	-0.40	0.01	-0.51	-0.18
			Zn_p_ppm	-0.33	-0.16	0.84	0.20	-0.02
			U_p_ppm	0.98	0.22	0.02	0.12	0.23
			V_p_ppm	-0.73	-0.34	-0.31	-0.16	0.25

Appendix D: Till drill core PCA Results

Sample_ID	Lithofacies	Major Oxides								Transition Metals, Total Digest							
		PC-1	PC-2	PC-3	PC-4	PC-5	PC-6	PC-7	PC-8	PC-1	PC-2	PC-3	PC-4	PC-5	PC-6	PC-7	PC-8
TUR020-SA	Dmm3	2.74	3.83	0.63	-0.53	-0.43	-0.10	0.06	-0.14	3.16	-0.42	-2.90	1.84	0.50	-0.16	0.41	-0.04
TUR021-SA	Dmm3	-0.02	0.06	0.19	-0.13	-0.25	-0.11	0.03	0.03	-0.76	-0.87	0.51	-0.25	0.95	0.52	-0.19	0.02
TUR021-SB	Dmm2	-12.02	-8.68	4.75	0.37	0.83	1.09	-1.02	-0.08	-5.28	-4.63	-2.83	-1.24	1.77	2.11	0.20	0.13
TUR021-SC	Dmm3	0.95	-0.61	-2.49	0.79	-0.07	0.18	0.14	-0.23	-2.80	0.55	0.17	-0.22	0.91	0.80	-0.39	0.07
TUR022-SA	Dmm3	-0.58	-0.18	-0.12	0.84	0.05	-0.03	-0.09	-0.11	-0.29	-1.08	-0.23	-0.07	0.16	-0.08	0.17	0.02
TUR022-SB	Dmm3	-0.35	-0.24	0.26	-0.10	0.11	-0.13	0.00	0.07	-0.09	-1.31	0.23	-0.03	0.40	0.47	0.01	0.03
TUR022-SC	Dmm2	-12.22	-7.66	4.85	0.88	0.94	1.03	-0.79	-0.12	-7.28	-3.27	-3.10	-1.83	2.15	1.53	0.22	0.30
TUR022-SD	Dmm1	9.57	-5.81	8.85	-6.03	-1.81	0.52	-0.63	0.08	8.37	19.41	1.61	-0.64	1.52	-1.25	3.53	-2.57
TUR022-SE	Dmm3	-3.85	-2.35	-0.55	-0.56	0.46	0.26	-0.21	-0.04	-4.42	2.67	-0.94	-1.18	0.98	1.02	0.29	0.02
TUR022-SF	Dmm1	19.18	9.24	-1.56	-2.96	-1.78	-1.37	0.25	0.33	5.94	1.35	-4.42	1.98	-0.94	-1.60	1.54	-0.87
TUR024-SA	Dmm3	-0.10	-0.19	0.38	-0.31	-0.26	0.08	-0.12	0.03	-0.56	-0.81	0.61	-1.17	0.62	0.42	-0.34	0.15
TUR025-SA	Dmm3	-0.23	0.76	-0.39	0.20	-0.13	-0.06	-0.13	0.09	-0.94	-0.97	0.78	-0.70	0.86	0.61	-0.29	0.20
TUR029-SA	Dmm3	-1.89	1.06	0.01	0.49	0.33	-0.11	-0.17	0.29	-1.47	-1.29	-0.49	-1.09	1.42	-1.19	0.03	-0.11
TUR031-SA	Dmm3	0.52	0.17	0.70	0.28	-0.54	-0.04	0.15	0.01	2.16	3.15	2.32	-0.10	-3.77	-3.35	-0.34	-0.11
TUR031-SB	Dmm1	5.36	9.52	-0.49	1.22	1.96	-0.28	1.67	-0.32	6.30	1.98	0.39	0.14	-0.49	0.39	-0.45	0.37
TUR031-SC	Dmm3	0.55	-7.96	-1.79	-0.04	-1.23	0.49	-0.48	-0.19	-3.84	-0.30	0.26	-0.88	-0.24	0.35	0.60	-0.23
TUR031-SD	Dmm1	4.83	2.71	-2.07	0.41	0.73	0.13	1.07	-0.26	0.81	4.25	-0.02	-0.33	-0.14	0.62	-0.50	0.18
TUR031-SF	Dmm1	4.16	-2.30	-1.20	0.15	0.77	-0.83	1.25	-0.04	-1.02	4.10	-0.08	-0.12	0.25	0.14	0.07	0.51
TUR032-SA	Dmm3	-0.64	1.45	0.76	-0.14	0.05	0.06	0.04	-0.14	-0.21	-2.37	0.76	0.24	0.42	-0.03	0.39	0.09
TUR032-SB	Dmm2	-12.02	-8.22	3.71	0.91	0.83	1.35	-1.14	-0.06	-4.02	-1.64	-3.46	-0.43	0.83	-0.47	0.44	-0.14
TUR032-SC	Dmm3	6.16	-10.31	-2.06	-0.24	-2.81	1.06	0.28	-0.20	-3.36	1.27	-0.37	0.71	-1.27	-0.65	-0.12	-0.39
TUR034-SA	Dmm3	0.15	0.65	0.18	0.22	-0.61	0.12	-0.07	0.09	0.11	-0.84	-0.12	0.00	-0.03	0.32	-0.06	0.02
TUR034-SB	Dmm3	4.33	0.23	0.85	-0.76	-1.34	0.17	0.21	-0.18	2.15	-0.99	-1.95	1.16	-0.17	0.08	0.30	-0.11
TUR035-SA	Dmm3	6.65	3.59	-1.30	0.62	-1.21	-0.13	0.31	-0.38	2.72	-0.90	1.52	-0.31	0.00	0.47	-0.52	-0.01
TUR035-SB	Dmm3	3.03	1.24	0.42	0.45	0.45	-0.79	0.26	-0.05	4.92	3.79	1.91	-0.58	-0.16	-0.38	0.20	0.21
TUR036-SA	Dmm3	-0.91	0.50	0.04	0.28	-0.20	0.09	-0.22	0.07	-0.14	-1.41	0.87	-0.22	0.27	0.27	0.00	-0.10
TUR038-SA	Dmm3	-1.50	1.65	0.63	-0.18	0.36	-0.14	-0.12	0.04	-0.30	-0.34	0.72	0.50	0.32	0.50	-0.36	-0.12
TUR039-SA	Dmm1	-12.71	47.76	-6.51	13.91	17.81	-7.64	-3.06	4.78	9.25	1.68	-3.75	-6.80	0.31	4.10	1.08	1.09
TUR039-SB	Dmm3	1.73	3.74	-0.45	-0.75	-0.29	0.08	-0.08	0.05	3.70	-0.18	-3.14	2.18	0.03	-0.59	0.35	0.06
TUR039-SC	Dmm3	0.77	-6.68	-1.09	-0.21	-0.70	0.29	-0.04	-0.24	-2.94	1.94	-0.84	1.20	-0.35	0.17	0.21	-0.35
TUR040-SA	Dmm3	-1.85	0.69	0.62	-0.20	0.46	-0.09	-0.22	-0.03	0.12	-0.65	0.70	0.16	0.13	-0.26	0.00	0.19
TUR041-SA	Dmm3	-1.62	1.23	0.66	0.12	0.41	-0.07	-0.03	0.05	-1.09	0.23	1.09	-0.18	0.23	0.08	0.06	0.20
TUR041-SB	Dmm2	-14.63	-9.37	4.63	1.96	2.29	0.71	-1.22	-0.28	-4.75	-3.59	-3.71	-0.41	-0.16	1.36	1.46	-0.05
TUR042-SA	Dmm3	-4.18	-0.34	0.48	0.72	0.70	0.09	-0.70	0.00	-0.09	0.13	0.68	-0.03	-1.64	-0.46	0.13	0.08
TUR042-SB	Dmm3	-2.76	3.65	1.14	-0.16	0.71	-0.04	-0.20	0.06	1.74	-3.02	0.90	-1.29	0.37	-0.77	0.49	-0.19
TUR042-SC	Dmm2	-12.31	-6.45	3.44	2.14	1.79	1.03	-0.89	-0.29	-4.98	-3.77	-3.42	-1.29	1.11	1.70	0.18	0.20
TUR042-SD	Dmm2	-2.27	-21.54	2.89	-0.02	-1.73	0.97	-0.56	-0.51	-9.95	-0.23	-4.74	-0.69	0.56	1.20	1.04	-0.64
TUR043-SA	Dmm3	-3.98	-0.88	0.80	0.31	0.38	0.11	-0.32	0.17	-4.22	-0.12	0.47	0.01	-0.81	0.02	-0.14	-0.11
TUR043-SB	Dmm3	4.65	-4.52	-0.02	-0.32	-1.82	0.48	-0.09	-0.04	1.35	0.71	-3.47	1.35	-1.96	-0.80	0.75	-0.77
TUR044-SA	Dmm3	-2.78	1.01	-0.09	0.75	1.58	-0.53	-0.23	-0.13	4.28	-14.90	1.00	-1.30	4.02	-5.50	1.40	-1.18
TUR044-SB	Dmm3	2.38	3.74	1.00	-0.19	0.97	-0.79	0.15	-0.13	3.70	0.78	-0.35	-0.51	0.31	-1.55	-0.13	-0.08

Appendix D: Till drill core PCA Results

Sample_ID	Lithofacies	Major Oxides									Transition Metals, Total Digest							
		PC-1	PC-2	PC-3	PC-4	PC-5	PC-6	PC-7	PC-8	PC-1	PC-2	PC-3	PC-4	PC-5	PC-6	PC-7	PC-8	
TUR045B-SA	Dmm3	3.47	10.68	-0.71	-0.19	3.33	-1.45	0.46	-1.02	10.82	3.25	2.92	0.52	-0.15	1.69	-1.55	0.60	
TUR045B-SB	Dmm2	-11.09	-6.06	4.14	0.97	0.67	1.55	-0.67	-0.24	-5.30	-2.38	-2.86	-1.60	0.78	0.72	0.16	-0.45	
TUR045B-SC	Dmm3	6.36	-9.22	-1.20	-0.68	0.98	0.64	0.84	-1.69	7.68	8.82	1.79	0.45	-1.40	1.99	-1.56	-0.36	
TUR046-SA	Dmm3	-3.70	-0.63	0.17	0.72	0.17	0.46	-0.31	0.10	-1.60	-1.18	-0.20	-0.47	0.23	0.53	0.08	0.10	
TUR046-SB	Dmm3	3.29	-15.08	-2.54	0.32	-1.99	0.53	0.37	-0.03	-4.13	-0.13	-0.57	0.30	0.58	2.13	-1.09	-0.03	
TUR046-SC	Dmm3	-2.24	-13.91	0.85	0.01	-0.39	0.96	-0.57	-0.68	-6.34	1.83	-2.10	0.20	0.01	1.18	0.31	-1.13	
TUR047-SA	Dmm3	1.56	2.45	0.01	0.12	-0.74	0.48	0.15	-0.19	0.70	-1.18	0.60	0.06	0.04	0.10	-0.22	-0.05	
TUR047-SB	Dmm2	-3.16	-2.58	2.53	0.71	0.15	0.57	-0.09	-0.24	-0.40	-1.18	-0.13	-1.35	-0.11	0.59	0.25	0.14	
TUR048-SA	Dmm3	-3.90	0.51	0.97	0.31	1.14	-0.51	-0.41	0.12	-1.65	-3.92	1.62	-0.96	-0.56	0.51	1.08	-0.07	
TUR048-SB	Dmm2	-10.70	-0.12	4.44	-0.70	1.19	1.06	-0.48	0.01	-3.93	-4.86	-1.09	-1.33	0.31	1.48	0.50	0.34	
TUR048-SC	Dmm2	-10.25	-5.90	4.23	1.93	1.47	0.55	-0.51	-0.07	-3.19	-6.87	-0.81	-1.26	0.08	1.13	1.43	0.20	
TUR049-SA	Dmm3	-0.05	0.86	0.30	0.11	0.88	-0.42	0.00	0.15	1.35	0.90	0.57	-0.32	-0.34	-0.11	0.01	-0.23	
TUR049-SB	Dmm1	-3.84	8.79	-2.29	1.41	4.48	-0.81	0.24	-1.31	17.42	12.61	5.59	-1.88	-0.04	-0.39	0.09	-0.40	
TUR049-SC	Dmm4	16.67	9.30	-5.45	1.87	-1.79	-1.08	1.93	1.15	3.18	0.72	4.41	-0.61	-0.23	1.37	-1.22	1.06	
TUR050-SA	Dmm3	-3.02	-0.84	1.02	-0.06	0.58	-0.19	-0.16	0.19	-1.26	-1.83	-0.73	-0.66	1.04	-1.08	0.33	-0.19	
TUR050-SB	Dmm1	6.07	-0.38	0.98	1.29	0.93	-0.62	1.06	0.07	4.48	3.41	0.26	0.38	-0.07	0.59	0.23	-0.12	
TUR050-SC	Dmm3	2.11	-0.91	-2.84	0.05	-0.87	0.41	0.32	-0.13	-0.05	-5.08	2.98	-0.14	-0.04	1.00	1.40	-0.13	
TUR051-SA	Dmm3	2.86	-1.25	-0.51	0.32	-0.46	0.17	0.17	-0.07	1.98	0.62	0.62	-0.27	-0.15	0.09	-0.43	-0.07	
TUR051-SB	Dmm3	-0.98	1.00	0.67	0.05	1.63	-0.56	-0.04	-0.04	2.31	2.48	0.85	-1.14	-0.61	-0.65	-0.19	0.02	
TUR052-SA	Dmm3	-0.98	-1.08	0.61	0.23	0.58	-0.44	0.03	-0.05	2.36	-3.44	-1.61	-0.23	1.55	-3.47	0.11	-0.67	
TUR052-SB	Dmm3	7.20	1.89	-0.01	-1.07	1.14	-1.17	1.21	-0.27	6.23	-4.69	-2.51	0.87	0.49	-3.15	0.24	-0.51	
TUR053-SA	Dmm3	7.62	5.81	-1.18	0.92	-1.18	-0.10	0.87	0.14	3.91	-1.13	0.51	1.27	0.20	0.55	-0.32	-0.01	
TUR053-SB	Dmm3	4.18	2.91	-0.39	-0.06	0.10	-0.21	0.13	0.02	3.66	-1.05	2.19	0.51	0.37	0.29	-0.25	0.02	
TUR053-SC	Dmm1	5.51	8.23	-0.76	1.38	2.76	-0.86	-0.27	-0.32	7.72	7.58	2.85	0.73	1.17	0.34	-0.55	-0.34	
TUR054-SA	Dmm3	-1.97	-1.65	0.79	-0.21	0.05	-0.02	-0.04	0.38	0.19	0.83	-0.13	0.35	-0.04	-0.47	0.14	-0.06	
TUR054-SB	Dmm2	-7.57	-10.08	5.76	3.21	-0.11	1.06	1.11	0.21	-4.98	-2.32	-1.92	-1.19	0.81	1.24	0.00	0.16	
TUR054-SE	Dmm2	-11.10	-16.94	2.62	1.09	0.63	0.82	-1.02	-0.57	-10.80	-1.93	-2.80	-2.45	0.61	1.14	0.28	0.14	
TUR055-SA	Dmm3	4.16	2.33	0.37	-0.02	0.77	-0.92	0.97	0.24	4.03	-6.96	1.43	1.43	-1.11	0.26	1.56	0.37	
TUR056-SA	Dmm3	0.51	-0.22	-0.07	0.42	0.32	-0.41	-0.03	0.10	2.39	-0.93	0.29	0.57	-0.11	-2.88	-0.19	-0.13	
TUR056-SB	Dmm3	-0.20	-1.05	0.66	0.07	-0.01	0.23	0.04	0.02	0.58	-1.02	0.78	0.40	-0.13	0.32	-0.15	-0.08	
TUR057-SA	Dmm3	-0.61	-0.15	0.41	0.08	0.36	-0.32	0.00	0.09	-1.15	-1.71	0.18	0.33	0.75	0.14	-0.40	-0.04	
TUR057-SB	Dmm3	-0.67	1.74	0.54	-0.14	0.70	-0.41	0.02	0.09	0.73	-0.46	-0.46	0.26	-0.15	-0.43	-0.04	0.01	
TUR057-SC	Dmm3	5.07	-1.79	0.74	-0.93	-1.61	0.44	0.22	-0.01	3.01	-0.30	-2.34	2.29	-0.79	-0.20	0.35	-0.12	
TUR057-SE	Dmm1	5.10	-1.59	0.63	2.23	4.43	-1.45	2.02	-0.19	4.90	10.04	1.12	0.88	0.31	1.90	-2.00	0.53	
TUR057-SF	Dmm3	-2.51	1.74	-1.43	-0.58	0.86	-0.25	0.00	0.05	-3.30	1.54	-0.06	-0.89	0.04	0.56	-0.14	0.33	
TUR057-SG	Dmm3	-2.20	-0.23	-1.18	-0.92	0.53	-0.21	-0.07	-0.12	-3.59	1.67	-0.77	-0.30	-0.60	0.14	0.24	0.06	
TUR057-SH	Dmm3	-1.93	1.95	-1.01	-1.01	0.51	0.21	0.17	-0.07	-1.77	1.09	1.16	-1.34	-0.17	-0.55	-0.19	-0.18	
TUR057-SI	Dmm3	-1.42	-1.46	-1.44	-0.80	0.18	0.40	0.06	-0.04	-2.25	2.04	-0.31	0.39	-0.14	0.23	0.08	-0.14	
TUR057-SJ	Dmm3	2.89	0.22	-1.77	-1.11	-0.87	0.32	0.18	-0.10	-0.41	1.90	-0.76	0.10	-0.15	0.12	-0.34	-0.02	
TUR057-SK	Dmm3	2.33	-1.62	-1.90	-0.95	-1.16	0.58	0.04	0.04	-1.90	0.64	-0.97	0.32	-0.12	0.29	-0.17	0.22	
TUR058-SA	Dmm3	-0.57	-0.60	0.66	0.01	0.44	0.00	-0.09	-0.03	1.34	-0.50	0.04	0.76	-0.46	0.08	0.12	-0.04	

Appendix D: Till drill core PCA Results

Sample_ID	Lithofacies	Major Oxides									Transition Metals, Total Digest								
		PC-1	PC-2	PC-3	PC-4	PC-5	PC-6	PC-7	PC-8	PC-1	PC-2	PC-3	PC-4	PC-5	PC-6	PC-7	PC-8		
TUR058-SC	Dmm3	2.33	-7.81	-1.94	-0.92	-0.51	0.22	0.04	-0.06		-2.45	1.75	2.11	-0.82	-0.91	-0.05	0.00	0.07	
TUR059-SA	Dmm3	4.91	-0.14	-0.07	-0.48	-1.52	0.54	0.22	-0.05		2.91	-1.66	-2.13	1.51	0.08	-0.84	0.22	-0.28	
TUR059-SB	Dmm4	25.46	-2.72	-7.03	1.49	-6.63	1.19	2.76	1.33		2.27	-2.24	2.21	0.11	-1.00	0.10	-0.36	-0.02	
TUR060-SA	Dmm3	9.12	-1.46	-1.09	1.13	-2.00	0.27	0.83	-0.18		3.18	-0.84	-1.52	2.44	-0.78	-1.22	0.02	-0.56	
TUR060-SB	Dmm3	-1.65	0.71	0.29	0.49	0.26	0.14	0.30	0.30		-4.34	0.78	-0.26	-1.94	-0.60	-0.28	1.30	-0.07	
TUR060-SD	Dmm1	4.06	10.70	-2.90	2.00	1.55	-0.99	-0.39	1.56		1.42	1.06	0.47	0.23	-0.51	0.90	-0.15	0.00	
TUR060-SE	Dmm3	6.59	1.51	-2.23	0.06	-0.57	-0.47	1.14	0.27		-0.63	1.47	1.05	-1.09	-0.99	0.50	-0.06	0.66	
TUR060-SF	Dmm3	-4.65	-2.79	-1.10	-0.27	0.37	0.14	-0.04	0.39		-7.71	0.84	-1.79	-1.00	0.37	0.63	0.04	0.26	
TUR061-SA	Dmm3	-2.51	-2.30	0.42	0.56	0.55	-0.17	-0.24	0.14		-1.36	-4.02	0.94	-0.12	0.30	-1.13	0.37	-0.15	
TUR061-SB	Dmm3	0.46	-4.59	0.80	0.60	-0.28	-0.07	0.36	-0.10		-1.09	-4.08	0.08	-0.45	0.15	-0.65	0.25	0.01	
		K2O_t_pct	-0.27	0.20	0.17	0.17	0.26	0.32	-0.03	0.14	Sc_t_ppm	-0.88	0.31	0.23	0.30	0.27	-0.08	0.03	0.21
		Al2O3_t_pct	-1.50	0.27	0.02	0.11	-0.21	-0.15	0.03	0.04	V_t_ppm	-0.32	-0.02	-0.41	-0.67	-0.13	0.16	-0.04	0.14
		MgO_t_pct	0.15	0.62	-0.27	0.11	0.23	-0.05	0.14	-0.18	Cr_t_ppm	0.25	0.41	0.26	-0.02	-0.52	-0.38	-0.04	0.01
		Fe2O3_t_pct	0.42	-0.04	0.13	0.05	0.21	-0.34	-0.19	0.07	Co_t_ppm	0.58	-0.12	0.14	0.21	0.07	0.25	-0.35	0.05
		Na2O_t_pct	0.61	0.11	-0.35	0.25	-0.31	0.12	-0.17	-0.03	Ni_t_ppm	0.68	0.72	0.17	-0.23	0.32	0.13	0.16	-0.08
		P2O5_t_pct	-0.34	-0.69	0.38	-0.08	0.02	0.09	-0.08	-0.20	Cu_t_ppm	0.17	-0.63	-0.11	-0.15	0.35	-0.46	-0.04	-0.07
		MnO_t_pct	0.48	0.62	0.29	-0.49	-0.16	0.04	0.02	0.03	Zn_t_ppm	0.10	-0.77	0.45	0.02	-0.17	0.23	0.22	0.02
		CaO_t_pct	0.67	-0.49	0.22	0.24	-0.12	-0.06	0.24	0.07	Y_t_ppm	-0.90	0.08	-0.01	0.05	-0.07	0.13	-0.07	-0.29
		TiO2_t_pct	-0.21	-0.60	-0.60	-0.34	0.08	0.02	0.04	0.07	Mo_t_ppm	0.32	0.02	-0.71	0.50	-0.10	0.04	0.14	0.01

Appendix D: Till drill core PCA Results

Sample_ID	Lithofacies	Transition Metals, Partial Digest							Alteration Elements, Total Digest							
		PC-1	PC-2	PC-3	PC-4	PC-5	PC-6	PC-7	PC-1	PC-2	PC-3	PC-4	PC-5	PC-6	PC-7	PC-8
TUR020-SA	Dmm3	-2.57	-2.78	-5.53	-0.02	-2.66	0.99	-0.40	-4.58	-0.68	-1.35	-1.11	0.55	0.38	-0.06	-0.31
TUR021-SA	Dmm3	0.32	-1.01	0.23	0.26	-0.33	0.48	-0.09	2.70	-0.63	0.25	-1.04	0.40	-0.17	-0.23	-0.03
TUR021-SB	Dmm2	-7.18	-1.79	-0.58	0.24	0.34	-0.39	-0.13	10.80	-3.77	-3.24	-3.33	0.73	-0.86	0.96	-1.51
TUR021-SC	Dmm3	2.59	2.76	3.00	0.13	0.58	0.02	0.18	1.32	3.95	0.30	-2.08	-0.66	-0.23	0.10	0.08
TUR022-SA	Dmm3	0.56	-1.23	-0.77	0.60	0.10	0.43	-0.16	1.03	-0.84	-0.04	-0.22	0.08	0.11	-0.12	-0.14
TUR022-SB	Dmm3	-0.63	-0.60	-0.32	-0.11	-0.09	0.16	-0.02	1.73	-0.69	0.07	-0.29	0.31	0.31	-0.04	-0.09
TUR022-SC	Dmm2	-7.11	-0.79	0.36	0.64	0.35	-0.11	-0.08	11.69	-3.08	-4.13	-2.98	0.64	-1.52	0.66	-1.30
TUR022-SD	Dmm1	-4.92	2.32	-5.37	-0.13	-0.74	1.01	-1.75	-21.23	3.76	7.11	-6.72	4.64	-4.24	1.25	1.97
TUR022-SE	Dmm3	-0.92	2.42	1.73	0.07	0.45	0.08	0.07	3.20	0.97	-1.94	-0.68	0.87	-1.13	0.04	0.05
TUR022-SF	Dmm1	-3.43	-0.42	-7.15	1.38	-3.40	-0.55	-0.66	-14.38	4.23	0.90	-1.15	-0.03	1.06	0.52	-0.35
TUR024-SA	Dmm3	1.14	-1.08	0.71	0.79	0.12	0.43	0.03	3.29	-0.08	0.28	0.19	0.51	-0.27	-0.18	-0.08
TUR025-SA	Dmm3	-0.10	-0.51	-0.02	-0.04	-0.14	0.29	0.00	3.21	0.48	0.50	-0.94	0.14	-0.15	-0.10	-0.05
TUR029-SA	Dmm3	-0.16	-2.23	2.20	2.01	-0.86	-0.41	-0.18	3.06	-0.92	-0.61	-0.10	0.41	-0.64	-0.19	-0.01
TUR031-SA	Dmm3	1.14	-1.26	1.00	-0.01	-0.21	0.16	0.00	-4.95	-2.53	3.16	2.26	-2.43	-1.51	0.06	0.37
TUR031-SB	Dmm1	5.19	-1.18	-2.63	-0.33	-0.22	-0.27	0.21	-5.51	2.26	2.12	-0.09	0.43	-0.11	0.02	0.06
TUR031-SC	Dmm3	-0.46	0.60	0.73	0.12	0.05	-0.17	-0.16	2.25	1.57	-0.41	0.78	-0.12	0.59	0.29	0.11
TUR031-SD	Dmm1	1.70	3.08	-2.01	-0.10	-0.02	-0.21	0.18	-3.28	3.86	0.29	0.24	0.25	-0.76	-0.15	0.38
TUR031-SF	Dmm1	1.28	3.96	-0.79	-0.65	-0.21	-1.32	0.29	-1.74	2.68	-1.47	1.58	0.50	-0.26	-0.67	0.77
TUR032-SA	Dmm3	2.28	-2.65	1.48	-0.14	-0.11	0.25	-0.15	1.86	-1.10	0.48	-0.48	-0.04	0.82	-0.14	0.03
TUR032-SB	Dmm2	-6.11	-1.13	-1.69	0.32	-0.83	0.06	-0.21	5.57	-4.99	-3.37	-2.50	-0.02	-1.90	0.97	-1.08
TUR032-SC	Dmm3	-1.85	1.06	-0.78	-0.41	-0.18	0.38	-0.19	-1.70	1.78	-0.64	1.03	-1.40	0.14	0.12	0.27
TUR034-SA	Dmm3	0.12	-1.52	-0.45	0.09	-0.15	0.36	-0.07	0.37	0.62	-0.09	0.19	-0.03	0.40	0.25	-0.07
TUR034-SB	Dmm3	-0.41	-2.49	-3.28	0.00	-1.71	0.82	-0.17	-3.84	1.27	-0.62	0.01	0.07	0.98	0.21	-0.24
TUR035-SA	Dmm3	2.85	-2.71	1.71	1.46	0.06	0.30	0.14	-0.49	1.04	1.50	1.65	0.64	0.91	-0.30	0.28
TUR035-SB	Dmm3	3.05	-0.44	-0.44	-0.13	-0.04	-0.16	0.08	-3.83	-0.05	1.31	2.36	1.58	-0.20	-0.24	0.89
TUR036-SA	Dmm3	1.25	-1.57	0.74	-0.11	0.03	0.54	-0.09	1.40	0.24	0.78	-0.06	0.08	0.55	0.08	0.06
TUR038-SA	Dmm3	1.09	-0.55	-0.09	-0.17	-0.14	0.74	0.22	0.76	0.04	0.50	-0.83	-0.13	0.10	0.02	0.11
TUR039-SA	Dmm1	-3.08	-2.11	-5.93	1.88	0.95	-0.83	-0.92	-3.64	7.04	6.00	-4.26	4.19	-1.94	-1.54	-2.79
TUR039-SB	Dmm3	-1.41	-2.02	-4.18	-0.12	-2.22	0.70	-0.12	-5.72	-0.78	-1.40	-1.08	0.04	0.24	0.06	-0.35
TUR039-SC	Dmm3	-0.61	3.02	1.07	-0.39	0.20	0.13	-0.12	-1.54	0.77	-1.23	-0.49	-0.52	-0.06	0.09	0.25
TUR040-SA	Dmm3	1.36	-0.98	1.62	0.61	0.47	0.17	0.12	1.31	-1.69	0.38	-0.40	-0.12	-0.12	-0.26	0.06
TUR041-SA	Dmm3	-0.03	-0.38	0.15	-0.05	0.46	0.07	0.13	2.22	-1.32	0.49	-0.90	-0.10	-0.44	-0.22	0.12
TUR041-SB	Dmm2	-5.29	-3.63	-0.67	-2.50	0.17	-0.29	-0.51	6.05	-4.31	-2.47	-3.92	-0.16	-0.61	1.23	-1.77
TUR042-SA	Dmm3	0.85	-0.03	0.75	-0.84	-0.04	0.25	0.19	-0.52	-1.04	1.58	-0.75	-1.28	-0.46	0.23	-0.29
TUR042-SB	Dmm3	1.70	-0.77	0.07	-0.85	0.09	0.07	0.00	1.93	-1.61	1.58	0.47	0.62	0.48	0.24	-0.18
TUR042-SC	Dmm2	-4.59	-0.72	-0.17	-0.79	-0.09	-0.28	-0.04	9.41	-3.58	-3.66	-2.43	0.53	-1.07	0.97	-1.54
TUR042-SD	Dmm2	-5.72	0.73	-0.13	-0.39	-0.87	0.30	-0.33	6.07	-1.00	-4.95	-2.22	0.07	-1.14	1.00	-1.08
TUR043-SA	Dmm3	-1.84	0.48	1.48	-1.37	0.05	0.29	0.04	3.17	-1.57	-0.50	0.20	-0.89	-0.34	-0.20	-0.04
TUR043-SB	Dmm3	-0.97	-2.15	-4.13	-0.50	-2.56	1.18	-0.36	-6.90	-0.77	-0.58	0.24	-0.33	0.11	0.25	-0.65
TUR044-SA	Dmm3	2.38	-1.01	0.78	0.43	0.05	0.31	0.11	3.79	-2.99	3.07	1.44	0.85	3.71	-0.26	0.08
TUR044-SB	Dmm3	0.90	-0.98	-2.10	1.92	-1.54	-0.67	0.10	-3.34	0.37	0.91	0.88	0.52	-0.51	-0.20	0.18

Appendix D: Till drill core PCA Results

Sample_ID	Lithofacies	Transition Metals, Partial Digest								Alteration Elements, Total Digest							
		PC-1	PC-2	PC-3	PC-4	PC-5	PC-6	PC-7	PC-1	PC-2	PC-3	PC-4	PC-5	PC-6	PC-7	PC-8	
TUR045B-SA	Dmm3	10.35	0.69	-3.59	-0.77	0.59	0.38	0.68		-5.29	0.54	2.78	1.74	1.94	0.05	-0.15	0.70
TUR045B-SB	Dmm2	-4.50	-0.99	-0.34	0.04	0.01	-0.21	-0.08		7.86	-3.66	-2.52	-2.24	0.40	-1.68	1.06	-1.31
TUR045B-SC	Dmm3	10.13	3.62	-4.74	0.19	0.87	1.96	0.52		-9.01	3.39	1.66	2.55	1.80	-1.06	0.90	1.00
TUR046-SA	Dmm3	-2.14	-0.29	-0.17	-0.54	-0.07	0.29	0.14		3.31	-1.14	-0.54	-0.63	0.07	-0.19	0.25	-0.31
TUR046-SB	Dmm3	-1.05	1.98	1.72	-0.53	-0.10	0.64	-0.11		3.56	2.99	-2.35	0.54	-0.09	0.44	0.31	0.07
TUR046-SC	Dmm3	-2.56	1.66	-2.19	-0.18	0.46	-0.09	-0.35		2.11	-0.71	-2.85	-0.27	0.57	-0.62	0.73	-0.17
TUR047-SA	Dmm3	0.52	-0.67	0.07	0.28	0.03	0.38	0.09		0.43	0.20	0.98	-0.56	-0.27	0.23	0.21	-0.07
TUR047-SB	Dmm2	0.50	-0.44	0.32	-0.27	0.52	-0.77	0.12		4.13	-2.84	-0.28	-0.03	0.70	-0.56	0.42	-0.55
TUR048-SA	Dmm3	0.46	-2.89	2.17	-1.48	0.37	-0.80	-0.33		4.29	-1.77	0.65	1.91	0.46	1.95	-0.01	-0.05
TUR048-SB	Dmm2	-2.81	-3.65	0.53	-1.58	0.25	-0.52	-0.33		9.48	-4.04	-1.88	-1.23	0.22	0.01	0.77	-1.19
TUR048-SC	Dmm2	-1.89	-4.18	1.29	-2.06	-0.27	-1.47	-0.52		9.46	-5.79	-1.30	-0.90	0.52	0.99	0.73	-1.27
TUR049-SA	Dmm3	1.18	-1.34	-2.22	0.05	-0.12	0.03	-0.06		-0.87	-0.90	1.01	0.25	0.44	-0.37	0.07	0.06
TUR049-SB	Dmm1	13.26	-0.25	-5.82	1.01	1.55	1.25	-0.14		-18.15	7.41	11.79	-4.80	2.13	-3.03	1.03	1.26
TUR049-SC	Dmm4	4.81	0.96	-0.87	-0.44	1.14	0.09	0.33		-1.03	6.06	1.76	5.97	0.80	2.69	-1.89	1.52
TUR050-SA	Dmm3	-1.57	-1.68	1.63	1.72	-0.53	-0.66	-0.09		2.53	-1.61	-0.52	-0.54	0.23	-0.37	0.03	-0.17
TUR050-SB	Dmm1	3.81	0.84	-1.79	-0.76	-0.36	-0.12	0.09		-5.17	0.45	0.84	0.76	1.63	0.00	-0.21	0.45
TUR050-SC	Dmm3	0.34	0.40	1.73	1.04	-0.08	-0.28	-0.22		2.63	0.50	2.16	0.96	0.35	3.39	0.30	0.31
TUR051-SA	Dmm3	2.21	-1.24	0.11	0.98	0.18	0.18	0.20		-0.94	0.18	0.93	0.62	0.39	-0.19	-0.02	0.11
TUR051-SB	Dmm3	3.62	-0.78	1.05	1.25	-0.19	-0.31	0.05		-1.77	0.12	1.34	1.06	0.38	-1.00	0.10	0.21
TUR052-SA	Dmm3	0.28	-4.67	2.63	5.27	-1.76	-0.88	-0.32		-1.30	-1.88	0.22	0.15	0.16	-0.26	-0.06	-0.10
TUR052-SB	Dmm3	1.26	-7.32	-3.15	3.43	-3.60	-1.40	-0.37		-6.35	-0.07	0.55	1.95	0.23	1.55	-0.48	-0.21
TUR053-SA	Dmm3	2.32	-0.87	-1.90	0.09	-0.54	0.40	0.13		-3.69	2.10	2.21	-1.73	-0.27	0.92	0.00	-0.02
TUR053-SB	Dmm3	6.95	-3.27	0.55	0.11	0.06	-0.27	0.05		-1.28	0.42	1.95	0.70	0.56	1.21	-0.21	0.53
TUR053-SC	Dmm1	5.85	2.33	-2.65	1.11	0.45	0.45	0.23		-10.23	5.64	5.08	-3.67	0.88	-1.37	0.40	1.19
TUR054-SA	Dmm3	1.01	-0.14	-0.88	0.64	-1.30	0.40	-0.02		-0.56	-1.25	-0.06	-0.68	-0.12	-0.57	0.20	0.05
TUR054-SB	Dmm2	-6.26	0.25	-0.32	-0.14	0.68	-0.34	0.12		9.02	-4.17	-2.53	-2.62	0.15	-1.60	0.77	-1.18
TUR054-SE	Dmm2	-8.92	-0.07	-1.34	-0.83	-0.84	0.27	-0.61		12.15	-1.95	-4.53	-1.22	-0.39	-1.64	0.87	-1.16
TUR055-SA	Dmm3	6.65	-7.45	-1.31	-3.26	-1.59	-1.81	-0.66		-1.13	-1.98	2.34	0.77	-0.21	3.88	-0.47	-0.26
TUR056-SA	Dmm3	1.57	-2.78	0.85	2.47	-1.07	-0.50	-0.17		-2.51	-1.62	1.18	0.06	-1.07	-0.47	-0.06	0.23
TUR056-SB	Dmm3	3.57	-1.21	0.05	-0.42	0.33	-0.05	0.12		0.81	-1.33	0.96	-0.86	-0.17	0.10	0.10	-0.10
TUR057-SA	Dmm3	-0.06	-0.14	1.26	0.65	-0.25	-0.13	0.06		1.52	1.30	0.01	-0.75	-0.48	0.44	0.06	0.05
TUR057-SB	Dmm3	2.04	-0.22	0.44	-0.10	-0.49	0.29	0.07		-0.47	-1.10	0.22	-0.52	-0.21	-0.29	-0.09	-0.20
TUR057-SC	Dmm3	-0.62	-1.32	-4.04	0.03	-2.12	0.45	-0.07		-5.25	-1.58	-0.92	-0.41	-0.10	0.57	0.02	-0.32
TUR057-SE	Dmm1	4.27	7.19	-4.65	-1.74	0.52	0.41	0.87		-7.94	5.62	0.96	-0.09	1.13	-1.97	-0.97	1.16
TUR057-SF	Dmm3	0.67	2.53	1.60	0.11	0.14	0.09	-0.05		2.32	1.80	-1.00	0.42	-0.15	-0.48	-0.22	0.12
TUR057-SG	Dmm3	-2.27	2.98	-0.03	-0.38	0.37	-0.46	-0.06		0.77	0.63	-0.91	-0.23	-0.53	-0.63	-0.18	-0.09
TUR057-SH	Dmm3	0.01	0.87	0.75	1.32	0.41	-0.40	-0.28		1.60	0.58	0.89	0.71	-0.15	-0.71	-0.05	0.24
TUR057-SI	Dmm3	-0.08	2.22	-0.39	-0.39	0.84	-0.56	-0.09		-0.20	0.31	-0.70	-0.75	-0.28	-0.59	0.18	0.16
TUR057-SJ	Dmm3	-2.55	1.89	-2.29	0.41	-0.10	0.00	-0.01		-1.86	2.15	-0.72	0.80	0.02	-0.21	-0.14	0.20
TUR057-SK	Dmm3	-1.50	2.10	-1.52	-0.13	-0.42	-0.19	-0.06		-0.07	1.58	-1.29	0.33	-0.40	0.07	-0.29	0.03
TUR058-SA	Dmm3	-0.30	-0.59	-3.20	0.22	-0.83	0.17	-0.07		-1.50	-0.08	0.16	0.18	-0.19	0.61	0.39	0.04

Appendix D: Till drill core PCA Results

Sample_ID	Lithofacies	Transition Metals, Partial Digest								Alteration Elements, Total Digest								
		PC-1	PC-2	PC-3	PC-4	PC-5	PC-6	PC-7	PC-1	PC-2	PC-3	PC-4	PC-5	PC-6	PC-7	PC-8		
TUR058-SC	Dmm3	1.51	1.21	-0.23	-0.28	0.61	0.09	-0.14	1.37	1.28	0.34	2.15	-0.42	0.17	0.07	0.66		
TUR059-SA	Dmm3	1.90	-1.66	-1.47	-0.01	-1.97	0.38	-0.09	-3.66	-1.54	-0.34	-0.81	0.03	0.34	0.01	-0.38		
TUR059-SB	Dmm4	4.15	-2.99	-0.72	-1.01	0.62	0.17	-0.25	-3.56	6.02	0.34	8.20	0.59	4.37	-1.03	1.33		
TUR060-SA	Dmm3	2.76	-1.79	-1.53	0.20	-1.66	0.23	0.00	-5.51	-2.42	-0.26	0.50	-0.27	0.63	-0.16	-0.02		
TUR060-SB	Dmm3	-2.11	0.76	-1.53	-0.60	-0.15	-0.18	0.15	3.17	-0.81	-0.84	1.07	0.35	-0.35	0.16	-0.10		
TUR060-SD	Dmm1	2.62	-0.01	-1.54	-0.75	-0.15	0.51	0.21	-3.21	2.89	1.70	-0.01	0.12	0.61	-0.69	0.11		
TUR060-SE	Dmm3	0.14	2.12	-1.95	-0.97	0.40	-1.21	0.06	0.61	2.13	-0.12	2.64	-0.02	0.39	-0.41	0.34		
TUR060-SF	Dmm3	-6.29	2.77	1.35	-0.42	0.05	-0.51	-0.17	5.73	0.79	-3.42	-0.09	-0.45	-0.95	-0.08	-0.24		
TUR061-SA	Dmm3	2.27	-0.62	2.62	-1.37	0.19	-0.75	-0.03	4.08	-3.45	-0.16	1.21	-0.11	0.91	-0.16	0.08		
TUR061-SB	Dmm3	0.69	-1.23	0.62	0.23	-0.67	-0.77	0.00	4.40	-3.19	-0.29	0.38	-0.19	0.46	0.08	-0.38		
		Sc_p_ppm	-0.09	0.80	0.29	-0.14	-0.15	-0.28	0.08	Ni_t_ppm	-0.50	0.16	0.20	0.00	0.57	-0.08	0.02	0.12
		V_p_ppm	-0.76	-0.06	-0.39	0.04	0.40	-0.16	0.01	Sc_t_ppm	0.46	0.19	-0.46	-0.11	-0.20	0.04	-0.13	0.20
		Co_p_ppm	0.57	-0.17	-0.12	0.04	0.04	0.17	0.26	Cr_t_ppm	-0.75	-0.23	0.35	0.46	-0.35	-0.16	0.00	0.05
		Ni_p_ppm	0.92	0.47	-0.32	0.24	0.08	0.09	-0.15	Mo_t_ppm	-1.11	-0.24	-0.57	-0.18	0.01	0.13	-0.02	-0.10
		Cu_p_ppm	-0.10	-0.52	0.35	0.56	-0.15	-0.15	-0.03	Zn_t_ppm	0.37	-0.19	0.38	0.11	0.01	0.49	0.00	-0.01
		Zn_p_ppm	0.60	-0.56	0.21	-0.51	0.05	-0.13	-0.08	Sr_t_ppm	0.65	-0.33	-0.27	0.05	0.01	-0.10	0.32	0.00
		Y_p_ppm	-0.58	0.17	0.59	-0.08	0.09	0.35	-0.05	U_t_ppm	-0.14	0.66	0.36	-0.51	-0.22	-0.05	0.09	-0.05
		Mo_p_ppm	-0.56	-0.12	-0.61	-0.16	-0.36	0.10	-0.04	B_t_ppm	0.55	-0.64	0.21	-0.28	0.07	-0.22	-0.19	-0.07
										V_t_ppm	0.47	0.61	-0.21	0.45	0.10	-0.07	-0.09	-0.14

Appendix D: Till drill core PCA Results

Sample_ID	Lithofacies	Alteration Elements, Partial Digest				
		PC-1	PC-2	PC-3	PC-4	PC-5
TUR020-SA	Dmm3	3.74	-7.89	-1.89	-1.63	0.40
TUR021-SA	Dmm3	-1.21	-1.03	-0.93	-0.13	0.16
TUR021-SB	Dmm2	3.50	1.78	-3.08	-1.25	1.28
TUR021-SC	Dmm3	-2.31	2.30	0.93	1.53	-0.61
TUR022-SA	Dmm3	-0.38	-0.63	0.47	-0.35	0.58
TUR022-SB	Dmm3	0.21	-0.20	-0.72	-0.35	0.22
TUR022-SC	Dmm2	2.87	1.85	-3.32	-0.54	1.25
TUR022-SD	Dmm1	-5.53	-10.08	-9.07	2.40	3.35
TUR022-SE	Dmm3	0.15	1.80	-0.14	0.98	-0.04
TUR022-SF	Dmm1	4.06	-9.49	-3.70	0.18	0.84
TUR024-SA	Dmm3	-1.67	0.12	-0.20	0.06	0.32
TUR025-SA	Dmm3	-1.00	-0.64	-1.42	-0.01	0.26
TUR029-SA	Dmm3	-0.76	0.39	-0.54	-0.11	-0.27
TUR031-SA	Dmm3	-2.23	-0.20	-1.24	-0.14	-0.11
TUR031-SB	Dmm1	-3.36	-2.36	-0.65	0.16	0.25
TUR031-SC	Dmm3	-0.97	0.32	-1.12	0.48	0.17
TUR031-SD	Dmm1	0.75	-0.97	0.71	1.25	0.15
TUR031-SF	Dmm1	2.27	1.09	1.24	1.16	-0.84
TUR032-SA	Dmm3	-3.12	0.06	-0.34	-0.76	-0.30
TUR032-SB	Dmm2	3.66	-1.50	-3.08	-0.86	0.86
TUR032-SC	Dmm3	2.44	-0.49	0.58	-0.25	0.07
TUR034-SA	Dmm3	-0.68	-0.78	-0.75	-0.52	0.34
TUR034-SB	Dmm3	1.43	-5.07	-1.14	-1.19	0.18
TUR035-SA	Dmm3	-2.34	1.01	0.95	-0.36	-0.03
TUR035-SB	Dmm3	-1.09	-0.11	1.08	-0.11	-0.27
TUR036-SA	Dmm3	-2.32	-0.35	-0.69	-0.38	0.09
TUR038-SA	Dmm3	-1.69	-1.06	-1.36	0.08	0.20
TUR039-SA	Dmm1	-4.28	-3.91	-6.68	0.95	4.24
TUR039-SB	Dmm3	2.52	-6.16	-2.05	-1.09	0.14
TUR039-SC	Dmm3	0.48	0.78	0.38	0.97	-0.24
TUR040-SA	Dmm3	-1.62	1.72	0.36	-0.04	0.08
TUR041-SA	Dmm3	-0.34	1.10	-0.42	-0.16	0.35
TUR041-SB	Dmm2	0.81	0.48	-3.80	-2.67	0.48
TUR042-SA	Dmm3	-1.73	0.03	-1.54	0.05	-0.23
TUR042-SB	Dmm3	-1.34	0.09	0.00	-0.48	-0.23
TUR042-SC	Dmm2	2.20	0.83	-2.68	-0.91	0.34
TUR042-SD	Dmm2	2.91	-1.32	-2.82	-0.26	0.20
TUR043-SA	Dmm3	0.34	1.08	-1.35	-0.40	-0.42
TUR043-SB	Dmm3	2.63	-7.28	-1.05	-1.43	-0.23
TUR044-SA	Dmm3	-0.89	0.62	1.46	-0.27	-0.25
TUR044-SB	Dmm3	1.57	-2.55	-0.17	0.24	0.02

Appendix D: Till drill core PCA Results

Sample_ID	Lithofacies	Alteration Elements, Partial Digest				
		PC-1	PC-2	PC-3	PC-4	PC-5
TUR045B-SA	Dmm3	-3.56	-1.80	3.60	0.65	-0.09
TUR045B-SB	Dmm2	2.00	0.75	-2.46	-0.70	0.73
TUR045B-SC	Dmm3	-2.13	-3.62	5.98	1.83	0.65
TUR046-SA	Dmm3	1.32	0.26	-1.36	-0.52	0.18
TUR046-SB	Dmm3	0.76	0.49	0.44	0.36	-0.52
TUR046-SC	Dmm3	3.54	0.20	1.42	-0.16	0.76
TUR047-SA	Dmm3	-0.28	0.06	0.07	-0.19	0.18
TUR047-SB	Dmm2	0.13	2.29	0.32	-0.37	-0.05
TUR048-SA	Dmm3	-0.54	3.12	1.09	-2.03	-0.95
TUR048-SB	Dmm2	-0.09	1.62	-2.21	-2.24	0.09
TUR048-SC	Dmm2	0.38	2.25	-1.10	-2.81	-0.97
TUR049-SA	Dmm3	-0.16	-1.43	0.02	-0.52	0.53
TUR049-SB	Dmm1	-15.89	-7.62	-3.74	3.51	3.38
TUR049-SC	Dmm4	0.33	2.10	4.74	-0.13	-0.22
TUR050-SA	Dmm3	0.78	1.32	-0.56	-0.25	-0.05
TUR050-SB	Dmm1	-0.75	-1.64	1.15	0.24	-0.42
TUR050-SC	Dmm3	-0.40	1.10	0.81	0.48	-0.21
TUR051-SA	Dmm3	-1.43	0.36	0.43	0.05	0.31
TUR051-SB	Dmm3	-3.42	-0.09	-0.17	0.76	-0.08
TUR052-SA	Dmm3	-0.38	-0.15	0.46	-0.02	-0.06
TUR052-SB	Dmm3	3.13	-5.12	0.82	-2.26	-0.67
TUR053-SA	Dmm3	-1.28	-2.54	-0.69	0.01	0.27
TUR053-SB	Dmm3	-4.07	0.35	2.36	-0.84	-0.68
TUR053-SC	Dmm1	-6.64	-3.64	-2.44	2.96	1.57
TUR054-SA	Dmm3	0.32	-2.90	-0.20	0.21	-0.31
TUR054-SB	Dmm2	3.22	2.40	-2.82	-0.42	1.12
TUR054-SE	Dmm2	5.25	-1.49	-3.20	-1.24	0.65
TUR055-SA	Dmm3	-3.25	-2.02	1.12	-4.02	-2.30
TUR056-SA	Dmm3	-0.70	-0.61	0.57	-0.19	-0.19
TUR056-SB	Dmm3	-2.42	0.46	0.64	-0.32	-0.16
TUR057-SA	Dmm3	0.41	0.96	0.26	0.05	-0.30
TUR057-SB	Dmm3	-1.10	-0.81	0.17	0.05	-0.49
TUR057-SC	Dmm3	3.76	-5.21	-0.03	-1.06	-0.22
TUR057-SE	Dmm1	0.85	-2.19	0.95	2.61	0.28
TUR057-SF	Dmm3	-0.81	0.79	0.31	1.20	-0.30
TUR057-SG	Dmm3	2.36	1.51	0.11	0.68	0.10
TUR057-SH	Dmm3	-0.15	1.32	1.00	0.73	0.42
TUR057-SI	Dmm3	0.76	1.79	0.96	0.56	0.29
TUR057-SJ	Dmm3	3.66	-0.64	0.24	0.35	0.70
TUR057-SK	Dmm3	2.83	-0.82	0.25	0.39	0.04
TUR058-SA	Dmm3	2.69	-2.62	0.66	-0.62	0.31

Appendix D: Till drill core PCA Results

Sample_ID	Lithofacies	Alteration Elements, Partial Digest					
		PC-1	PC-2	PC-3	PC-4	PC-5	
TUR058-SC	Dmm3	-0.14	0.78	1.88	0.23	0.09	
TUR059-SA	Dmm3	0.33	-4.21	-0.12	-0.68	-0.85	
TUR059-SB	Dmm4	3.12	2.37	8.18	-2.99	-1.08	
TUR060-SA	Dmm3	1.46	-3.00	1.99	-1.00	-1.00	
TUR060-SB	Dmm3	4.23	0.54	0.88	-0.68	-0.07	
TUR060-SD	Dmm1	-1.13	-1.64	-0.07	-0.03	0.02	
TUR060-SE	Dmm3	2.89	1.51	1.64	0.00	-0.14	
TUR060-SF	Dmm3	4.21	2.35	-1.39	0.26	-0.04	
TUR061-SA	Dmm3	0.04	3.31	2.63	-1.11	-1.62	
TUR061-SB	Dmm3	2.05	1.15	1.90	-0.95	-0.98	
	Ni_p_ppm	-0.38	-0.38	0.65	0.25	0.11	
	Sc_p_ppm	0.47	0.36	-0.07	0.31	-0.33	
	Mo_p_ppm	0.69	-0.81	-0.16	-0.20	-0.01	
	Zn_p_ppm	-0.63	0.22	0.15	-0.39	-0.22	
	U_p_ppm	-0.67	-0.06	-0.66	0.15	0.14	
	V_p_ppm	0.51	0.67	0.10	-0.12	0.31	

Appendix E: Clay Mineralogy

Sample name	Quartz	Hematite	Muscovite	Orthoclase	Dickite	Albite	Dravite	Montmoril	Illite	Crandallite	Chlorite
TUR022-SA	22	NA	18	4	4	4	4	20	19	1	3
TUR022-SB	15	NA	25	5	4	3	3	13	26	1	4
TUR022-SC	24	NA	17	NA	4	4	4	24	18	1	3
TUR022-SD	22	1	NA	8	6	5	5	21	26	3	5
TUR021-SA	14	NA	27	4	3	3	3	12	28	1	4
TUR021-SB	13	NA	27	5	4	3	4	12	27	2	4
TUR021-SC	14	NA	26	5	4	4	3	11	26	2	4
TUR022-SE	13	NA	27	4	4	3	3	13	28	2	4
TUR022-SF	11	NA	26	7	3	4	4	13	26	1	4
TUR031-SA	12	NA	28	5	4	3	3	11	29	1	4
TUR031-SB	18	1	22	5	5	4	4	13	23	2	4
TUR031-SC	17	NA	23	5	4	3	3	13	25	2	4
TUR031-SD	18	1	23	5	4	4	4	15	23	1	4
TUR031-SF	13	NA	25	8	5	3	3	11	24	2	5
TUR032-SA	15	NA	25	6	5	3	3	10	26	1	4
TUR032-SB	18	NA	24	5	3	3	4	14	24	1	3
TUR032-SC	13	NA	25	5	4	5	4	12	24	2	4
TUR034-SA	17	NA	24	4	4	4	4	14	25	1	4
TUR034-SD	14	NA	25	6	4	3	3	13	26	1	4
TUR038-SA	11	NA	28	5	4	3	3	10	29	2	5
TUR039-SA	7	NA	27	18	4	4	4	6	19	3	6
TUR039-SB	11	NA	28	5	3	3	3	10	29	1	4
TUR039-SC	13	NA	27	4	4	3	3	12	28	1	4
TUR041-SA	11	NA	27	6	4	3	3	10	29	2	5
TUR041-SB	13	NA	28	5	3	3	3	12	28	1	4
TUR042-SA	14	NA	26	6	4	3	3	12	27	1	4
TUR042-SB	15	NA	26	5	4	3	3	13	26	1	4
TUR042-SC	17	NA	23	5	3	3	4	13	27	1	4
TUR042-SD	16	NA	25	6	4	3	3	12	25	1	4
TUR043-SA	14	NA	26	6	4	3	3	12	27	1	4
TUR043-SB	14	NA	25	5	5	3	3	14	26	1	4
TUR054-SA	10	NA	29	5	4	3	3	10	30	2	5
TUR054-SB	11	NA	29	4	4	3	4	13	27	1	4

All values %

Appendix E: Clay Mineralogy

Sample name	Quartz	Hematite	Muscovite	Orthoclase	Dickite	Albite	Dravite	Montmoril	Illite	Crandallite	Chlorite
TUR057-SK	10	NA	29	5	4	3	3	10	30	1	5
TUR054-SE	11	NA	28	5	4	3	3	11	29	1	5
TUR057-SA	14	NA	26	5	4	3	4	12	26	1	4
TUR057-SB	14	NA	26	5	4	3	3	12	27	1	4
TUR057-SC	15	NA	24	6	3	4	3	13	26	1	4
TUR057-SE	14	1	24	7	5	3	4	13	23	2	5
TUR057-SF	15	NA	25	4	4	3	3	12	26	1	4
TUR057-SG	16	NA	25	4	4	3	3	13	26	1	4
TUR057-SH	14	NA	25	6	4	3	3	12	26	1	4
TUR057-SI	11	NA	NA	10	6	3	5	13	40	2	9
TUR057-SJ	11	NA	28	5	4	3	3	11	29	1	5
MR-S007	7	NA	29	10	3	7	3	4	31	1	5
MR-S011	6	NA	31	7	6	5	3	5	27	1	8
MR-S013	6	NA	31	8	5	5	4	6	27	1	7
MR-S014	6	NA	31	11	3	6	2	4	29	1	5
MR-S034	9	NA	26	10	3	7	2	5	31	1	5
MR-S012	13	NA	27	7	2	5	3	5	32	1	4
MR-S032	11	NA	27	8	3	6	2	5	32	1	5
MR-S033	11	NA	NA	11	4	7	4	5	50	1	9
AB-S206	19	1	NA	8	5	9	3	8	42	1	6
MR-S015	10	NA	25	9	3	7	2	5	33	1	4

Appendix F: Till drill core alteration index values

Sample_ID	Lithofacies	Easting	Northing	Z	AI1	AI2	AI3	AI4
TUR020-SA	Dmm3	548870.8	7135474.2	-175.22	0.945	0.343	0.362	0.278
TUR021-SA	Dmm3	548891.4	7135508.7	-182.31	0.947	0.383	0.350	0.299
TUR021-SB	Dmm2	548891.9	7135508.4	-176.26	0.959	0.345	0.313	0.260
TUR021-SC	Dmm3	548891.3	7135508.7	-183.54	0.942	0.327	0.358	0.287
TUR022-SA	Dmm3	548908.1	7135515.1	-182.47	0.947	0.356	0.342	0.266
TUR022-SB	Dmm3	548908.4	7135514.9	-178.93	0.948	0.348	0.341	0.276
TUR022-SC	Dmm2	548908.6	7135514.8	-175.85	0.959	0.353	0.327	0.277
TUR022-SD	Dmm1	548908.9	7135514.6	-172.40	0.934	0.414	0.635	0.567
TUR022-SE	Dmm3	548908.5	7135514.9	-177.40	0.951	0.330	0.383	0.274
TUR022-SF	Dmm1	548908.7	7135514.7	-174.42	0.922	0.282	0.386	0.331
TUR024-SA	Dmm3	548837.7	7135464.7	-181.56	0.947	0.362	0.350	0.290
TUR025-SA	Dmm3	548853.2	7135464.7	-180.58	0.947	0.364	0.347	0.304
TUR029-SA	Dmm3	548656.1	7135825.5	-177.80	0.950	0.364	0.357	0.283
TUR031-SA	Dmm3	548665.9	7135874.1	-182.59	0.946	0.358	0.355	0.311
TUR031-SB	Dmm1	548665.5	7135873.2	-171.40	0.946	0.344	0.384	0.327
TUR031-SC	Dmm3	548665.7	7135873.6	-177.14	0.937	0.279	0.338	0.301
TUR031-SD	Dmm1	548665.6	7135873.4	-174.17	0.941	0.322	0.400	0.271
TUR031-SF	Dmm1	548665.4	7135872.9	-168.39	0.940	0.321	0.392	0.241
TUR032-SA	Dmm3	548911.1	7135490.1	-178.58	0.949	0.356	0.327	0.298
TUR032-SB	Dmm2	548910.2	7135490.8	-173.84	0.958	0.337	0.342	0.277
TUR032-SC	Dmm3	548911.7	7135489.7	-181.53	0.922	0.280	0.345	0.240
TUR034-SA	Dmm3	548884.0	7135447.3	-184.95	0.946	0.304	0.343	0.286
TUR034-SB	Dmm3	548882.0	7135448.7	-175.83	0.940	0.293	0.347	0.282
TUR035-SA	Dmm3	549040.6	7135710.4	-182.97	0.936	0.334	0.349	0.271
TUR035-SB	Dmm3	549040.4	7135709.9	-176.97	0.944	0.330	0.404	0.265
TUR036-SA	Dmm3	548862.0	7135460.2	-182.14	0.948	0.330	0.339	0.301
TUR038-SA	Dmm3	548933.8	7135399.9	-180.42	0.951	0.345	0.348	0.314
TUR039-SA	Dmm1	548928.1	7135431.0	-173.62	0.985	0.664	0.423	0.456
TUR039-SB	Dmm3	548928.3	7135430.9	-174.48	0.946	0.333	0.360	0.291
TUR039-SC	Dmm3	548929.8	7135429.9	-181.71	0.939	0.305	0.360	0.268
TUR040-SA	Dmm3	548950.4	7135459.6	-186.10	0.951	0.380	0.344	0.273
TUR041-SA	Dmm3	548939.4	7135456.9	-183.58	0.951	0.386	0.350	0.274
TUR041-SB	Dmm2	548939.3	7135458.2	-178.06	0.961	0.338	0.306	0.287
TUR042-SA	Dmm3	548983.3	7135400.5	-182.02	0.952	0.360	0.335	0.312
TUR042-SB	Dmm3	548979.7	7135402.9	-176.89	0.954	0.343	0.335	0.278
TUR042-SC	Dmm2	548973.9	7135406.7	-168.60	0.959	0.327	0.318	0.275
TUR042-SD	Dmm2	548976.3	7135405.1	-172.00	0.933	0.274	0.342	0.287
TUR043-SA	Dmm3	548924.8	7135365.7	-181.81	0.952	0.359	0.330	0.278
TUR043-SB	Dmm3	548917.2	7135371.6	-171.04	0.933	0.318	0.353	0.277
TUR044-SA	Dmm3	548760.5	7135323.1	-177.79	0.953	0.351	0.273	0.253
TUR044-SB	Dmm3	548757.7	7135325.5	-173.76	0.948	0.353	0.382	0.272
TUR045B-SA	Dmm3	549095.8	7135462.9	-175.31	0.952	0.346	0.406	0.268
TUR045B-SB	Dmm2	549091.6	7135466.4	-169.26	0.958	0.333	0.335	0.276
TUR045B-SC	Dmm3	549093.1	7135465.1	-171.35	0.928	0.239	0.457	0.241
TUR046-SA	Dmm3	549471.3	7135559.7	-177.61	0.951	0.337	0.338	0.271
TUR046-SB	Dmm3	549471.8	7135559.3	-180.96	0.925	0.254	0.344	0.260

Appendix F: Till drill core alteration index values

Sample_ID	Lithofacies	Easting	Northing	Z	AI1	AI2	AI3	AI4
TUR046-SC	Dmm3	549470.6	7135560.2	-172.38	0.939	0.268	0.365	0.218
TUR047-SA	Dmm3	549316.5	7135552.6	-180.80	0.944	0.333	0.341	0.270
TUR047-SB	Dmm2	549316.9	7135552.2	-174.87	0.950	0.345	0.341	0.252
TUR048-SA	Dmm3	549013.7	7135478.2	-178.74	0.954	0.314	0.300	0.228
TUR048-SB	Dmm2	549012.9	7135478.9	-172.79	0.962	0.330	0.296	0.272
TUR048-SC	Dmm2	549012.5	7135479.2	-169.86	0.958	0.340	0.276	0.245
TUR049-SA	Dmm3	548698.3	7135356.4	-178.21	0.949	0.351	0.365	0.272
TUR049-SB	Dmm1	548697.6	7135357.0	-173.15	0.959	0.432	0.550	0.596
TUR049-SC	Dmm4	548698.9	7135355.9	-182.32	0.920	0.326	0.350	0.197
TUR050-SA	Dmm3	549038.5	7135531.1	-175.59	0.952	0.357	0.347	0.263
TUR050-SB	Dmm1	549037.9	7135531.5	-171.84	0.939	0.345	0.400	0.271
TUR050-SC	Dmm3	549039.0	7135530.6	-179.65	0.940	0.276	0.291	0.264
TUR051-SA	Dmm3	548736.7	7135324.0	-177.94	0.940	0.340	0.364	0.277
TUR051-SB	Dmm3	548736.1	7135324.4	-173.80	0.951	0.340	0.384	0.317
TUR052-SA	Dmm3	548775.4	7135355.2	-180.08	0.949	0.361	0.355	0.268
TUR052-SB	Dmm3	548774.5	7135355.9	-173.36	0.940	0.337	0.338	0.229
TUR053-SA	Dmm3	548656.7	7135385.8	-177.65	0.936	0.353	0.348	0.305
TUR053-SB	Dmm3	548656.2	7135386.2	-174.46	0.943	0.338	0.349	0.266
TUR053-SC	Dmm1	548656.0	7135386.4	-172.35	0.946	0.366	0.468	0.435
TUR054-SA	Dmm3	548958.5	7135421.7	-176.20	0.950	0.341	0.361	0.286
TUR054-SB	Dmm2	548957.7	7135422.3	-170.24	0.950	0.362	0.327	0.265
TUR054-SE	Dmm2	548957.6	7135422.5	-169.13	0.952	0.294	0.319	0.260
TUR055-SA	Dmm3	548735.4	7135388.4	-173.95	0.945	0.356	0.269	0.253
TUR056-SA	Dmm3	548814.8	7135382.2	-181.14	0.947	0.361	0.351	0.270
TUR056-SB	Dmm3	548813.9	7135382.9	-174.65	0.946	0.360	0.339	0.279
TUR057-SA	Dmm3	548854.8	7135411.0	-181.77	0.949	0.322	0.338	0.260
TUR057-SB	Dmm3	548854.3	7135411.4	-177.83	0.950	0.367	0.349	0.283
TUR057-SC	Dmm3	548853.7	7135411.9	-173.78	0.936	0.333	0.347	0.247
TUR057-SE	Dmm1	548853.4	7135412.2	-171.27	0.942	0.391	0.474	0.287
TUR057-SF	Dmm3	548854.6	7135411.1	-180.24	0.952	0.327	0.359	0.284
TUR057-SG	Dmm3	548854.3	7135411.4	-178.17	0.951	0.345	0.355	0.248
TUR057-SH	Dmm3	548854.0	7135411.6	-175.78	0.951	0.342	0.362	0.260
TUR057-SI	Dmm3	548853.9	7135411.8	-174.70	0.948	0.322	0.366	0.249
TUR057-SJ	Dmm3	548853.6	7135412.0	-172.85	0.941	0.310	0.372	0.240
TUR057-SK	Dmm3	548853.5	7135412.1	-171.85	0.940	0.323	0.351	0.249
TUR058-SA	Dmm3	548794.8	7135400.4	-174.60	0.948	0.294	0.343	0.241
TUR058-SC	Dmm3	548795.0	7135400.3	-175.56	0.937	0.282	0.352	0.245
TUR059-SA	Dmm3	548835.6	7135430.0	-174.85	0.937	0.353	0.347	0.281
TUR059-SB	Dmm4	548836.9	7135428.9	-184.27	0.866	0.217	0.321	0.125
TUR060-SA	Dmm3	548896.3	7135825.7	-183.78	0.926	0.343	0.346	0.233
TUR060-SB	Dmm3	548893.8	7135827.8	-179.13	0.950	0.316	0.348	0.213
TUR060-SD	Dmm1	548891.2	7135830.0	-174.29	0.948	0.380	0.360	0.290
TUR060-SE	Dmm3	548892.1	7135829.2	-176.03	0.937	0.307	0.351	0.217
TUR060-SF	Dmm3	548894.9	7135826.8	-181.30	0.952	0.314	0.347	0.245
TUR061-SA	Dmm3	549378.5	7135747.9	-175.35	0.950	0.345	0.310	0.212
TUR061-SB	Dmm3	549377.4	7135748.8	-171.32	0.943	0.349	0.310	0.214

Appendix G: Surficial sample alteration index values

Sample_ID	Easting	Northing	Elevation	AI1	AI2	AI3	AI4
12-MR-S007A	548883	7135524	184	0.793	0.088	0.356	0.164
12-MR-S008A	548749	7135902	182	0.804	0.088	0.391	0.124
12-MR-S009A	548860	7135750	188	0.777	0.079	0.377	0.137
12-MR-S010A	548867	7135606	185	0.804	0.114	0.393	0.100
12-MR-S011A	549007	7135443	185	0.822	0.155	0.491	0.056
12-MR-S012A	548487	7135764	181	0.797	0.097	0.438	0.102
12-MR-S013A	548655	7135658	182	0.847	0.175	0.491	0.065
12-MR-S014A	548766	7135614	182	0.816	0.121	0.401	0.094
12-MR-S015A	548872	7135530	184	0.803	0.113	0.429	0.104
12-MR-S016A	548367	7135390	183	0.796	0.099	0.400	0.111
12-MR-S017A	548576	7135384	188	0.805	0.116	0.412	0.090
12-MR-S018A	548677	7135414	186	0.803	0.101	0.397	0.086
12-MR-S019A	548671	7135411	185	0.811	0.099	0.405	0.100
12-MR-S020A	548790	7135380	187	0.792	0.090	0.433	0.103
12-MR-S021A	548496	7135052	184	0.815	0.121	0.383	0.086
12-MR-S022A	548741	7135230	185	0.803	0.086	0.364	0.122
12-MR-S023A	548888	7135355	183	0.833	0.145	0.381	0.074
12-MR-S024A	548970	7134797	183	0.821	0.099	0.399	0.099
12-MR-S025A	548987	7134998	186	0.814	0.097	0.394	0.103
12-MR-S026A	548984	7135087	184	0.841	0.179	0.432	0.109
12-MR-S027A	548988	7135321	185	0.802	0.102	0.382	0.091
12-MR-S028A	549000	7135383	188	0.806	0.107	0.406	0.079
12-MR-S029A	549560	7135077	185	0.804	0.108	0.441	0.124
12-MR-S030A	549369	7135219	185	0.806	0.115	0.388	0.095
12-MR-S031A	549364	7135221	188	0.836	0.164	0.412	0.089
12-MR-S032A	549281	7135269	188	0.802	0.107	0.399	0.118
12-MR-S033A	549178	7135329	188	0.809	0.098	0.392	0.110
12-MR-S034A	549058	7135416	187	0.813	0.122	0.418	0.120
12-MR-S035A	549658	7135466	187	0.782	0.088	0.358	0.144
12-MR-S036A	549455	7135477	187	0.806	0.100	0.361	0.100
12-MR-S038A	549348	7135481	186	0.802	0.105	0.400	0.107
12-MR-S039A	549225	7135497	184	0.807	0.109	0.350	0.065
12-MR-S040A	547387	7137120	188	0.845	0.172	0.399	0.127
12-MR-S041A	547384	7136918	186	0.818	0.111	0.369	0.088
12-MR-S042A	547540	7136556	189	0.796	0.091	0.345	0.078
12-MR-S043A	547559	7136353	187	0.797	0.107	0.349	0.078
12-MR-S044A	547541	7136142	187	0.806	0.096	0.361	0.070
12-MR-S045A	547619	7135955	186	0.803	0.095	0.349	0.073
12-MR-S045A_D	547619	7135955	186	0.802	0.099	0.346	0.073
12-MR-S046A	547667	7135761	185	0.838	0.234	0.373	0.049
12-MR-S047A	547685	7135563	193	0.836	0.140	0.399	0.117
12-MR-S048A	547735	7135305	190	0.826	0.138	0.359	0.065
12-MR-S049A	547769	7135102	192	0.800	0.101	0.350	0.130
12-MR-S050A	547794	7134925	191	0.806	0.103	0.364	0.152
12-MR-S051A	547782	7134720	192	0.820	0.142	0.370	0.116
12-MR-S052A	548416	7134882	185	0.822	0.132	0.389	0.113

Appendix G: Surficial sample alteration index values

Sample_ID	Easting	Northing	Elevation	AI1	AI2	AI3	AI4
12-MR-S053A	548280	7135092	186	0.800	0.101	0.371	0.123
12-MR-S053A_D	548280	7135092	186	0.802	0.104	0.367	0.128
12-MR-S060A	545868	7142011	183	0.772	0.060	0.350	0.113
12-MR-S060A_D	545868	7142011	183	0.775	0.062	0.359	0.116
12-MR-S061A	545707	7140213	194	0.788	0.087	0.343	0.100
12-MR-S063A	545218	7138789	195	0.796	0.087	0.374	0.102
12-MR-S069A	548073	7138776	181	0.788	0.080	0.327	0.148
12-MR-S070A	548391	7137678	182	0.800	0.101	0.359	0.114
12-MR-S071A	548486	7137172	183	0.798	0.100	0.379	0.109
12-MR-S072A	548724	7136335	180	0.788	0.096	0.360	0.126
12-MR-S076A	546614	7134937	183	0.797	0.098	0.349	0.100
12-MR-S077A	547039	7134275	184	0.806	0.117	0.367	0.112
12-MR-S078A	548117	7133355	190	0.854	0.171	0.364	0.102
12-MR-S079A	548491	7133010	192	0.804	0.091	0.373	0.096
12-MR-S080A	548491	7133013	191	0.782	0.083	0.355	0.134
12-MR-S086A	549535	7135930	183	0.808	0.112	0.393	0.112
12-MR-S087A	549360	7136239	181	0.793	0.073	0.361	0.111
12-TH-S103A	543595	7140534	176	0.761	0.056	0.364	0.120
12-TH-S104A	543867	7138669	187	0.774	0.084	0.413	0.099
12-TH-S105A	543286	7138217	191	0.797	0.079	0.332	0.103
12-TH-S106A	542995	7137514	199	0.806	0.088	0.368	0.127
12-TH-S107A	543001	7137508	201	0.780	0.063	0.338	0.145
12-TH-S110A	543104	7136699	208	0.790	0.078	0.364	0.116
12-TH-S111A	543141	7135952	200	0.779	0.079	0.375	0.164
12-TH-S112A	543525	7135090	194	0.805	0.085	0.366	0.117
12-TH-S113A	543870	7134409	189	0.793	0.092	0.340	0.138
12-TH-S114A	543878	7134403	190	0.799	0.092	0.371	0.147
12-TH-S116A	542012	7136862	199	0.782	0.057	0.333	0.098
12-TH-S117A	541837	7138154	191	0.815	0.110	0.393	0.067
12-TH-S190A	550145	7134180	171	0.807	0.111	0.396	0.078
12-TH-S191A	550794	7134829	166	0.854	0.144	0.360	0.058
12-TH-S192A	550767	7135633	173	0.810	0.122	0.391	0.054
12-TH-S193A	550606	7136603	178	0.805	0.105	0.384	0.072
12-TH-S194A	550554	7137500	180	0.796	0.105	0.405	0.092
12-TH-S195A	550554	7137500	180	0.804	0.111	0.399	0.096
13-AB-244A	545393	7136377	183	0.804	0.087	0.301	0.119
13-AB-245A	545871	7136388	183	0.813	0.097	0.256	0.111
13-AB-246A	545644	7136733	183	0.815	0.097	0.289	0.113
13-AB-246A_D	545644	7136733	183	0.815	0.096	0.295	0.114
13-AB-247A	545330	7137015	184	0.790	0.077	0.312	0.128
13-AB-248A	545330	7137015	184	0.790	0.070	0.275	0.121
13-AB-249A	544674	7136023	187	0.820	0.100	0.283	0.113
13-AB-250A	546057	7138248	188	0.775	0.073	0.335	0.094
13-AB-252A	546770	7137877	185	0.787	0.108	0.299	0.118
13-AB-253A	547274	7139335	190	0.797	0.071	0.288	0.112

Appendix G: Surficial sample alteration index values

Sample_ID	Easting	Northing	Elevation	AI1	AI2	AI3	AI4
13-AB-254A	547274	7139335	190	0.798	0.107	0.300	0.132
13-AB-S199A	549563	7134642	178	0.797	0.103	0.343	0.087
13-AB-S200A	548005	7135190	185	0.809	0.097	0.298	0.091
13-AB-S201A	547928	7135473	185	0.819	0.094	0.319	0.075
13-AB-S202A	547372	7135439	183	0.811	0.127	0.306	0.092
13-AB-S203A	548024	7135696	185	0.840	0.151	0.332	0.074
13-AB-S204A	547979	7136015	185	0.839	0.146	0.320	0.080
13-AB-S205A	547899	7136324	185	0.836	0.134	0.321	0.158
13-AB-S206A	548298	7135911	184	0.797	0.094	0.354	0.094
13-AB-S207A	548626	7135837	184	0.792	0.091	0.330	0.094
13-AB-S209A	548771	7135683	184	0.833	0.151	0.376	0.074
13-AB-S210A	549050	7135598	184	0.795	0.086	0.304	0.115
13-AB-S210A_D	549050	7135598	184	0.794	0.078	0.294	0.119
13-AB-S211A	549393	7135816	182	0.787	0.082	0.323	0.126
13-AB-S212A	549359	7136064	182	0.814	0.104	0.337	0.095
13-AB-S213A	548955	7136193	185	0.788	0.077	0.313	0.116
13-AB-S214A	548724	7136133	184	0.834	0.122	0.331	0.082
13-AB-S215A	548551	7136009	180	0.808	0.105	0.356	0.104
13-AB-S216A	549075	7135893	182	0.773	0.089	0.338	0.127
13-AB-S217A	548890	7135857	179	0.783	0.109	0.320	0.110
13-AB-S218A	548760	7135896	180	0.785	0.111	0.315	0.109
13-AB-S228A	548414	7136662	181	0.817	0.144	0.346	0.153
13-AB-S229A	548986	7136679	185	0.813	0.119	0.318	0.108
13-AB-S230A	549466	7136639	182	0.819	0.120	0.289	0.111
13-AB-S231A	549827	7136412	176	0.811	0.126	0.367	0.167
13-AB-S232A	549430	7137183	184	0.786	0.137	0.347	0.159
13-AB-S234A	548982	7137169	185	0.809	0.112	0.316	0.109
13-AB-S235A	548956	7137674	184	0.811	0.146	0.438	0.065
13-AB-S236A	549482	7137692	183	0.798	0.104	0.337	0.088
13-AB-S237A	549973	7137187	183	0.834	0.160	0.297	0.121
13-AB-S239A	549792	7138749	181	0.830	0.125	0.330	0.074
13-AB-S240A	548918	7139639	176	0.785	0.105	0.357	0.125